NOVEL CONDUCTING POLYMERIC MATERIALS:

1. FLUOROALKYLATED POLYTHIOPHENES

2. STACKED OLIGOTHIOPHENES AS MODELS FOR THE INTERCHAIN CHARGE TRANSFER IN CONDUCTING POLYMERS

A Dissertation

Presented to

The Academic Faculty

By

Ling Li

In Partial Fulfillment

Of the Requirements for the Degree

Doctor of Philosophy in the

School of Chemistry and Biochemistry

Georgia Institute of Technology

July 2004

NOVEL CONDUCTING POLYMERIC MATERIALS:

1. FLUOROALKYLATED POLYTHIOPHENES

2. STACKED OLIGOTHIOPHENES AS MODELS FOR THE INTERCHAIN CHARGE TRANSFER IN CONDUCTING POLYMERS

Approved by:

Dr. David M. Collard, Chairman

Dr. Laren M. Tolbert

Dr. C. P. Wong

Dr. Mohan Srinivasarao

Dr. Marcus Weck

July 6. 2004

To My Dad, Mom and My Brother

ACKNOWLEGEMENT

First of all, I would like to thank my dad and my younger brother, for encouraging and helping me to fulfill my dream through all these years. Especially, I would like to thank my mom, who passed away when I was in high school, for all the precious characters she gave to me at my early age and for her bless from the heaven.

I would like to thank my research advisor Dr. David M. Collard for his guidance and encouragement. I sincerely appreciate what I learn from him in these years, his enthusiasm to chemistry, his hard work to research and his dedication to science. I would also like to thank my committee members, Dr. Laren M. Tolbert, Dr. C. P. Wong, Dr. Mohan Srinivasarao and Dr. Marcus Weck for their time and advices.

I also would like to thank Dr. Amyn S. Teja, Mr. Shutaro Kurosawa, Mr. Karl E. Counts and Dr. Tomek Wasowicz, for the successful collaboration.

I would like to thank all the Collard's group members, current and past, Fouad Salhi, Glen Brizius, Xiaoyong Hong, Sahar Javanmard, Genara Andrade, Michael Hibbs, Marian Vargas, Susi Coons, Jeffery Capadona, Kurt Knoblock, Shannon Watt, David Noga and Jenny Raynor for their help and advice.

I would like to thank for Dr**.** Janusz Kowalik**,** Hongmin Ma, Wenyu Huang and Yangyang Sun for their useful discussions and help.

TABLE OF CONTENTS

LIST OF TABLES

LIST OF FIGURES

LIST OF ABREVIATIONS

δ	chemical shift
ε	extinction coefficient
ϕ	quantum yield
J	coupling constant
d	doublet
t	triplet
m	multiplet
s	singlet
λ_{max}	wavelength maximum
mp	melting point
dppp	diphenylphosphinopropane
ppm	parts per million
$scCO_2$	supercritical carbon dioxide
Hz	hertz
DP	degree of polymerization
RT	room temperature

CV	cyclic voltammetry
IR	infrared spectroscopy
LC	liquid crystal
GC	gas chromatography
NMR	nuclear magnetic resonance spectroscopy
DSC	differential scanning calorimetry
TGA	thermal gravimetric analysis
DPV	differential pulse voltammetry
TEM	transmission electron microscopy
ESR	electron spin resonance spectrocopy
FET	field effect transistor
TFT	thin film transistor
LED	light emitting diode
NLO	nonlinear optics
NIR	near infrared
SCE	saturated calomel electrode
ITO	indium tin oxide
DMF	*N, N*-dimethylformamide
THF	tetrahydrofuran
DME	ethylene glycol dimethyl ether
NBS	N-bromosuccinimide
LDA	lithium diisopropylamine
TTF	tetrathiafulvalene

PPV	poly(phenylene vinylene)
PPE	poly(phenylene ethylynene)
PAT	poly(3-alkylthiophene)
HOMO	highest occupied molecular orbital
LUMO	lowest unoccupied molecular orbital
OFET	organic field effect transistor
PPHF	pyridinium poly(hydrogen fluoride)
HRMS	high resolution mass spectroscopy
HPLC	high performance liquid chromatography
UV-vis	ultra-violet/visible spectroscopy
Freon-113	1,1,2-trichloro-1,2,2-trifluoroethane
TMEDA	*N, N, N', N'*-tetramethylethylenediamine

SUMMARY

Polythiophenes have great potential as semiconductors for use in organic field effect transistors and light emitting diodes. Recent research has been focused on the design, synthesis and characterization of fluorinated polythiophenes and oligothiophenes. Various fluoroalkyl side chains have been introduced to induce polymer self-assembly, to control the electronic properties of the conjugated backbone, and to modify the solubility of the polymer in supercritical CO_2.

This work led to the preparation of poly(3-(perfluorooctyl)thiophene), which is one of only a few examples of n-dopable polythiophenes, and is the first supercritical CO_2-soluble conducting polymer. An alternating copolymer consisting of 3-perfluoroakyl and 3-alkylthiophene units has been synthesized. This polymer, with alternating electron-donating and withdrawing substituents, has a high quantum yield for fluorescence in solution relative to the two homopolymers, and strong fluorescence in solid state. Based on the study on its nanocrystals, the unusual photophyiscs may be due to the formation of the supramolecular structure with hexagonal packing.

A novel thiophene monomer, 3-(1,1-difluorooctyl)thiophene, was prepared to further tune the electronic structure of polythiophenes by changing the fluorination pattern of side chains, while retaining solubility in organic solvents by virtue of the

hydrocarbon side chain.. α-Hexyl-ω-perfluorohexylsexithiophene was synthesized to make a novel amphiphilic material for use in TFTs.

Models for interchain charge transfer in doped conducting polymers were also developed. Stacked and unstacked conjugated oligomers have been synthesized as models for conducting polymers. The bis(radical cation) form and the dication-neutral form of compounds in which conjugated oligomers are held in a stacked arrangement are shown to coexist and in equilibrium with each other. The coexistence of these two forms further suggests that both may serve as charge carriers. Interconversion between these forms by disproportionation mimics a possible mechanism for the interchain charge migration in doped conjugated polymers.

CHAPTER I

INTRODUCTION

Conjugated polymers

The electrical conductivity of conjugated polymers was first discovered for doped polyacetylene in 1977.[1,2,3] In 2000, the Nobel Prize in Chemistry was awarded to Alan J. Heeger, Alan G. MacDiarmid and Hideki Shirakawa for the initial discovery and further development of conductive polymers. After thirty years of maturation, the study of conjugated polymers and oligomers is a flourishing branch of materials science with many opportunities for applications in electronic and photonics. Extensive studies have been made of the synthesis, properties and applications of a wide variety of conjugated polymers, including polyacetylene, polypyrrole, polythiophene, polyphenylene, poly(phenylenev vinylene) (PPV), poly(thienylene vinylene), poly(phenylene ethylynene) (PPE), polyaniline, Table 1.1.[4] At the same time, various chemical structure modifications have been made to improve solubility, processibility, and morphology to achieve better performance in a variety of applications.

Conjugated polymers are characterized by an extended π-conjugated system along which charge carriers can be delocalized. In most cases, conjugated polymers have alternating single and double bonds. The degeneration of the molecular orbital of double

bonds gives a HOMO band and a LUMO band, as an analogue of the valence band and the conduction band of the inorganic semiconductors. The energy difference between two these bands is called the bandgap. The neutral conjugated polymers are usually semiconductors. Chemical or electrochemical oxidation (p-doping) introduces holes onto the conjugated backbone; reduction (n-doping) adds electrons on it. After doping, the electrical conductivity by mobility of either holes or electrons increases dramatically, and the doped conjugated polymers behave as conductors.

Table 1.1 Structure, name, bandgap and conductivity of the common conjugated

structure	polymer	π–π* bandgap (eV)	condcutivity (s/cm)
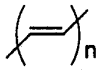	polyacetylene	1.5	10^3 - 1.7x10^5
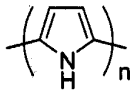	polypyrrole	3.1	10^2 - 7.5x10^3
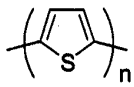	polythiophene	2.0	10-10^3
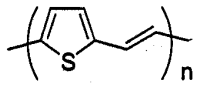	poly(thienylene vinylene)	1.6	40
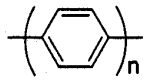	poly(*para*-phenylene)	3.0	10^2 -10^3
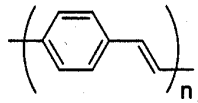	poly(*p*-phenylene vinylene)	2.5	3-5x10^3
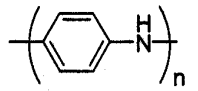	polyaniline	3.2	0-200

Compared with the traditional inorganic semiconductors, conjugated polymers have a number of advantages. As organic polymeric materials, conjugated polymers might be processed from solution or the melt to give a large area polymer film; they are also flexible and with low density which are distinct advantages compared to the brittle and heavy inorganic materials. Moreover, there are a lot of possibilities to modify the chemical structures of conjugated polymers to tune the physical properties.

Conjugated polymers have been applied to many areas. In the neutral state, conjugated polymers are utilized as semiconductors in electronic devices such as light emitting diodes (LED),[5] field effect transistors (FET),[6,7] nonlinear optical (NLO) devices, photovoltaic cells, solar cells, chemical, biochemical and thermal sensors. In the doped state, conjugated polymers are used as electrostatic dissipation materials, electromagnetic shielding materials and electronic conductors. In addition, the reversible switching between neutral and doped states leads to the electrochromic devices, battery electrodes and biosensors.

Orientation and chain packing of conjugated polymers

The orientation and packing of conjugated backbones significantly affect the physical properties of conducting polymers, and become very important issues in the achieving better performance in electronic and photonic devices.

A high degree of molecular order leads to a planar backbone with a long conjugation length, which facilitates the delocalization of the charge carriers along the polymer backbone. Optimal chain packing enhances communication between conjugated chains via π-π interactions, allowing for conduction in the second dimension, Figure 1.1.[8]

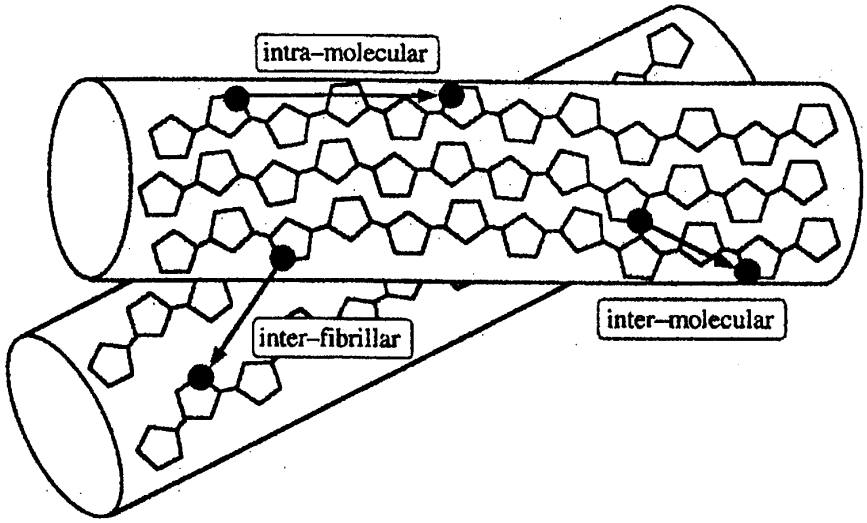

Figure 1.1 Orientation and packing effect on the charge transfer in films of conjugated polymers. (from ref. 8)

The orientation and efficient chain packing of conjugated polymer backbones are in determining the performance of organic semiconductors in field effect transistors. A good example of this is the effect of regioregularity in poly(3-alkylthiophene)s. Regioregular poly(3-hexylthiphene), forms a highly ordered lamellar structure with an efficient π-π stacking between chains, which gives high charge mobility and on/off ratio for OFET devices relative to the regiorandom analogues,[9,10] Figure 1.2.[11]

Various approaches have been used to enhance chain orientation and packing in conjugated polymers. Mechanical stretching, Langmuir-Blodgett deposition[12] and layer-by-layer self-assembly[13] have been used to enhance the crystallinity and molecular orientation. Conjugated polymers and tubules have been made with templates such as nanopores in polymeric membranes and nanochannels of mesoporous zeolites.[14,15,16]

Other approaches to order conjugated polymers include polymerization of polyacetylene in a nematic liquid crystal media. The self-organizing liquid crystal matrixes have also been used to make highly orientated poly(*p*-phenylene vinylene).[17] Liquid crystalline conjugated polymers have also been made by chemically linking liquid crystalline mesogens to conjugated backbones such as PPV.[18]

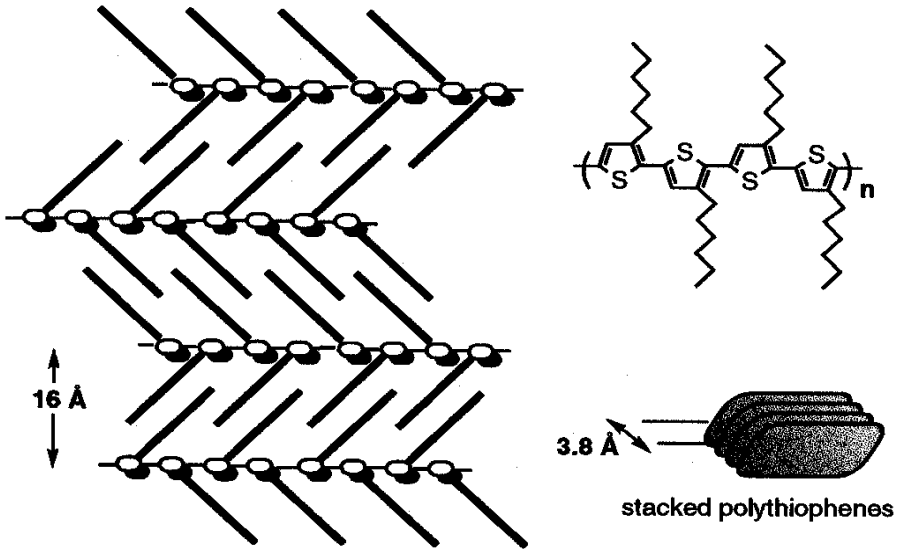

Figure 1.2 Self-assembling structure of regioregular poly(3-hexylthiophene)s. (from ref. 10)

Polythiophenes

Polythiophene is insoluble in organic solvents.[19,20] Installation of alkyl chains at the 3-position gives poly(3-alkylthiophene)s. Alkyl chains longer than butyl renders poly(3-alkylthiophene)s soluble in common organic solvents at room temperature,[21]

which allows them to be solution-processed into films which exhibit reasonably high electrical conductivities after doping. There are three types of linkages between α-positions of thiophene rings: head-to-tail (HT), head-to-head (HH) and tail-to-tail (TT). A head-to-tail linkage is the connection of the 2-position of one ring and the 5-position of the adjacent one. Head-to-head and tail-to-tail linkages are both symmetric couplings, by 2, 2'-linkage or 5, 5'-linkage, respectively. The structurally irregular polymers (regiorandom) have a shorter conjugation length due to the twist of adjacent thiophene rings with unfavorable HH couplings, Figure 1.3.

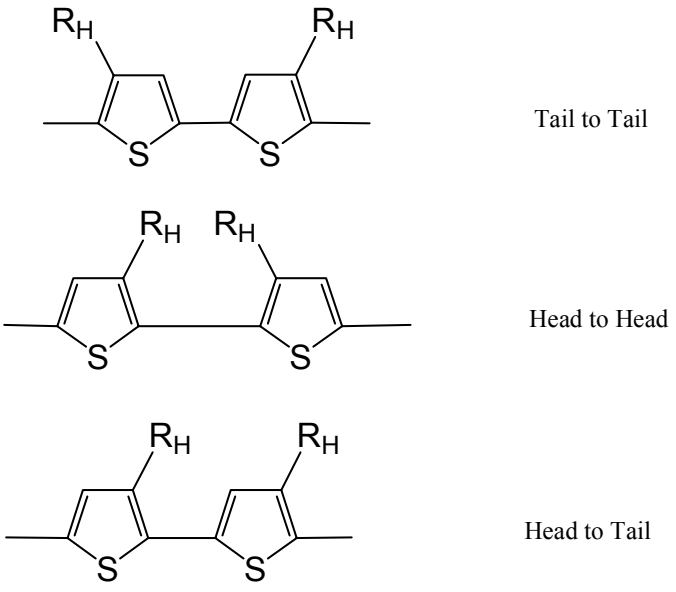

Figure 1.3. Different linkage patterns for adjacent 3-alkylthiophene rings.

Regioregular HT poly(3-alkylthiophene)s have a longer conjugation length and a more planar backbone than regiorandom ones, which gives a lower bandgap, a lower oxidation potential and a higher electrical conductivity. Detailed structural analysis indicates that regioregular HT poly(3-alkylthiophene)s have a 2-D self-assembling structure, with the interdigitated alkyl chain packing, and the conjugated backbone stacking at a distance of 3.8Å This highly ordered self-assembling structure strongly influences the electronic properties and the performance of devices, such as the charge mobility and the on/off ratio in FETs.

There are various methods to polymerize 3-alkylthiophenes. The chemical ($FeCl_3$, AsF_5) or electrochemical oxidation gives regiorandom polymers, although it has been reported that a high percentage of HT couplings can be achieved by controlling the polymerization conditions.[22] To make highly regioregular poly(3-alkylthiophene)s several organometallic coupling reactions have been developed. The most well-recognized methods are based on catalytic coupling of metallothienylhalides. The first method was reported in 1992,[23] which starts with the selective deprotonation of 2-bromo-3-alkylthiophene with LDA, transmetallation with $MgBr_2.Et_2O$, and coupling with $Ni(dppp)Cl_2$. Another method[24] uses 2,5-dibromo-3-alkylthiophene as starting materials, after lithiation, transmetallated with methylmagnesium bromide, followed by the coupling. Most recently, zinc reagents have been generated by transmetllation with $ZnCl_2$,[25] although it was previously reported that the activated zinc converts 2,5-dibromo-3-alkylthiophenes to a mixture of metallated isomers which are in equilibrium and undergo regioregular polymerization with $Ni(dppp)Cl_2$.[26] Stille coupling[27] and Suzuki coupling[28] have also been applied to prepare regioregular homopolymers and oligomers.

Copolymerization is a general approach to expand the range of properties of polymers and to create self-assembling supramolecular structures. In addition to the variation of comonomers, the copolymer microstructure (random, alternating, block, graft) also plays a large role on the properties. Regioregular polythiophenes are copolymerized with non-conductive polymers such as polystyrene, polymethacrylate to form di- and triblock copolymers, which show nanowire morphologies.[29] On the other hand, polythiophenes have been copolymerized with other conjugated polymers to tune the physical properties. Random copolymers of thiophenes include copolymers with pyrrole,[30] fluorene,[31, 32] quinoxaline,[33] thiazole[34] units to tune the electronic properties. 3-Alkylthiophenes have also been copolymerized with other substituted thiophenes (e.g., alkyl,[35] alkoxyl,[36] semifluoroalkyl,[37] oligo(ethylene glycol),[38,39] and ionic side chains.[40])

Fluoropolymers and n-type organic semiconductors

Semifluoroalkyl side chains have been attached to a variety of polymers to provide materials with unusual properties which arise as a consequence of the hydrophobicity, rigidity, thermal stability, chemical and oxidative resistance, and self-organization of perfluoroalkyl chains.[41] Since fluoroalkyl compounds are miscible with CO_2, the solubility of fluoropolymers in supercritical CO_2 has been explored, as a "green" method to process polymers with an environmental-benign solvent.

Semifluoroalkyl side chains have also been introduced to conjugated polymers, specifically polythiophenes, to induce the highly ordered solid state structure, which will enhance the hole mobility in p-type organic field effect transistors. 3-Semifluoroalkylthiophenes have been synthesized, with a hydrocarbon linker between the

thiophene ring and the fluoroalkyl chain. This hydrocarbon linker insolates the electron-withdrawing effect of the fluoroalkyl chain and keeps the oxidation potential low enough to allow the oxidative polymerization. A family of poly(3-semifluoroalkylthiophene)s with various linker lengths and fluoroalkyl chain lengths has been prepared in regioregular and regiorandom versions.[42] Some of the regioregular poly(3-semifluoroalkylthiophene)s show liquid crystallinity.[43] Alkyl/semifluoroalkyl thiophene alternating copolymers have been made, which show highly ordered double layer solid state structure.[37]

The important aspect for a successful implementation of organic semiconductors in microelectronic switching and memory devices is the availability of p-type (hole carrier) as well as n-type (electron carrier) semiconducting materials to enable important logic elements such as p-n junction diodes, bipolar transistors, and complementary circuits. Currently, the most advanced OFETs are based on pentacence, and oligo- or polythiophenes p-type semiconductors. In contrast to organic p-type semiconductors, n-type semiconductors remained less developed for a long time. This was partly due to the lack of electron-poor conjugated polymers, but also because of theoretical arguments which predict a lower stability of the n-conducting radical anionic polymers under ambient conditions.[44]

The fluoroalkyl group is a very strong electron-withdrawing group, so it should stabilize the radical anion in the conjugated system. Therefore, perfluoroalkyl substitution is an effective way to prepare the n-type organic semiconductors. Bao and coworkers prepared hexadecafluorinated copper phthaalocyanine and demonstrated it as an air-stable n-channel transistor.[45] Katz and coworkers reported high electron mobilities (>0.1

$cm^2\ V^{-1}s^{-1}$) and excellent on/off current ratio (> 10^5) for the fluoroalkyl-substituted naphthalenebisimide even in the presence of air.[46] Recently, the attention was moved to fluorinated oligothiophenes, whose hydrocarbon analogues are known as the excellent p-type semiconductors with the high hole mobility.[47,48] Tetradecafluorosexithiophene was synthesized as the first perfluorinated oligothiophene and the X-ray structure suggests the high electron mobility along π-π stacking direction.[49] α,ω-Diperfluorohexylsexithiophene was prepared as the first n-type oligothiophene-based semiconductor.[50,51] A homologous family of fluorocarbon-substituted thiophene oligomers were made and demonstrate the high electron mobility.[52] Besides α,ω-substitution, β,β'-di(perfluorohexyl)-substituted thiophene oligomers were also synthesized.[53] Most recently, a new polythiophene-fluorobenzene semiconductor family has been synthesized. The perfluorobenzene terminated tetrathiophene shows the highest electron mobility (0.08 $cm^2V^{-1}s^{-1}$) reported in the thiophene series.[54]

Interchain charge transfer mechanism in doped conjugated polymers

The polaron/bipolaron model for charge carriers in doped conjugated polymers serves to explain the observed paramagnetism at low levels of doping and diamagnetism at higher doping levels in materials with non-degenerate ground states, Figure 1.4. The polaronic versus bipolaronic nature of the charge carriers and their possible interconversion at intermediate doping levels remains a subject of discussion.[55,56] The creation of a spin-less bipolaron (B^{2+}) from two polarons ($P^{+\cdot}$) is driven by the energy difference of these two species and the balance between electron-phonon and electron-

electron interactions. In theory, both of these species could coexist in the case where the polaron and bipolaron formation energies become comparable.[57,58]

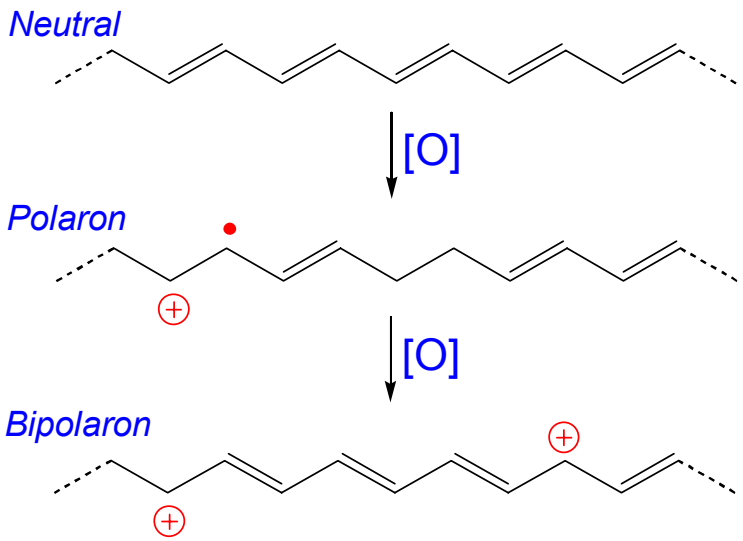

Figure 1.4. Polaron and biplaron models for doped conjugated polymers.

Lots of well-defined oligomeric compounds have been used as models to study the nature of the charge carriers in conjugated polymers. The first oxidation of the oligomers generates the monocation radicals, with two subgap electronic transitions and an ESR signal. The second oxidation gives the corresponding dications, which show only one subgap transition and no ESR signal.[59,60,61] Thus, mono(radical cations) have been

proposed as model polarons, and dication as bipolarons. Theoretical calculations agree with those results.[62,63] However, the studies on oxidized conjugated polymers show two strong subgap transitions, with the absence of or a very weak ESR signal.[64,65,66,67] Therefore, the charge carriers in doped conjugated polymers cannot be just simply addressed as either only the polaron or only bipolaron.

Extensive studies of π-conjugated oligomers have shown the monocation radicals can form π-dimers in solution at high concentrations, low temperatures or in poor solvents. This is a general finding for many conjugated oligomers, including oligothiophenes,[68,69,70,71,72,73] thienylenevinylene oligomers,[74] oligopyrroles,[75,76] mixed thiophene-pyrrole oligomers,[77] and oligo(p-phenylenevinylenes).[78] These π-dimers show two subgap absorptions, which is characteristic to monocation radicals. However, these π-dimers are also ESR silent, which is more like dications. The discovery and characterization of π-dimers provide a further understanding of the charge carrier nature in doped conjugated polymers.

Recently in some conjugated systems, such as diphenyloligoenes,[79] end-capped bithiophenes and bipyroles,[80,81] monocation radicals form σ-dimers instead of π-dimers. σ-Dimers have also been used to explain the weak ESR signal and the hysteresis between charging and discharging of conjugated polymers.

The dications of long oligothiophenes (nT, n≥12) are spinless and have two subgap absorptions, the same as polythiophenes.[82] This behavior has been explained as two polarons are located on the same chain, but further apart from each other. The decrease of Coulomb repulsion outweighs the energy cost to create a bipolaron. It has also been found the radical cations of 12T disproportionate into neutral oligomers and

dications. The similar disproportionation reaction was also observed for tetrathiafulvalene derivatives (TTF), in which dissolution of the salt of monocation radicals only gives the neutral and the dicationic states.[83]

Scope of work

Many efforts are focused on developing novel materials for various applications. At the same time, development of a better understanding of charge carriers nature and conduction mechanisms will lead to the rational design of new organic semiconductor materials.

In this thesis, we use perfluoroalkylation to tune the electronic and potonic properties of the oligo- and polythiophenes, and prepare novel n-type organic semiconductors and highly fluorescent materials. Perfluoroalkyl groups are directly attached to the thiophene rings without a hydrocarbon linker, in which the electron-withdrawing nature of fluorocarbon strongly affects the aromatic rings. 3-(Perfluoroalkyl)thiophenes have been made. The regioregular and regiorandom poly(3-(perfluoroalkyl)thiophene)s were prepared and their electronic properties were characterized. Solubility of the polymers in supercritical CO_2 was also studied.

The perfluoroalkyl group is an electron-withdrawing group, and the alkyl group is an electron-donating group. The alternating electron acceptor and donor arrangement will provide a pull-push electronic structure, and give rise to materials with interesting photonic properties. Regioregular perfluoroalkyl/alkyl thiophene alternating copolymers have been synthesized. Their photophysical properties are reported.

Besides the electron donor and acceptor interactions, the rigidity and immisciblity of fluorocarbons versus hydrocarbons in perfluoroalkyl/alkyl thiophene alternating copolymers is considered. The amphiphilicity of these polymers by virtue of the microphase separation of fluorocarbons and hydrocarbons promotes self-assembling structures. Self-aggregation of the alternating copolymers in solution has been studied through photophysical characterization.

Fluoropolymers are usually not soluble in normal organic solvents. To maintain the electron-withdrawing nature of fluorocarbons as well as to make materials processable in common solvents, 3-(1,1-difluoroalkyl)thiophene monomers were made and polymerized. The electronic properties of the polymer were characterized.

In order to extend studies of amphiphilic conjugated polymers further, we have also prepared α-hexyl-ω-(perfluorohexyl)sexithiophene.

In another direction, this work also develops further understanding of the charge carriers and the interchain charge transfer mechanism in doped conjugated polymers. Oliogoarenes covalently linked through a paracyclophane core were prepared as a model of two adjacent conjugated backbones stacking through π-π interaction in the solid state. The electrochemistry, photophysics and ESR have been used to study the nature of charge carriers and the inter-chain charge transfer mechanism.

References

1. Shirakawa, H.; Louis, E. J.; McDiarmid, A. G.; Chiang, C. K.; Heeger, A. J. *J. Chem. Soc., Chem. Commun.* **1977**, 578.

2. Chiang, C. K.; Fincher Jr., C. R.; Park, Y. W.; Heeger, A. J.; Shirakawa, H.; Louis, E. J.; Gau, S. C.; McDiamid, A. G. *Phys. Rev. Lett*. **1977**, *39*, 1098.

3. Chiang, C. K.; Park, Y. W.; Heeger, A. T.; Shirakawa, H.; Louis, E. J.; McDiamid, A. G. *J. Chem. Phy*. **1978**, *69*, 5098.

4. Skotheim, T. A.; Elsenbaumer, R. L.; Reynolds, J. R.; Eds. *Handbook of Conducting polymers* Mercel Dekker: New York, 1998.

5. Burroughes, J. H.; Bradley, D. C. C.; Brown, A. R.; MacKay, M. K.; Friend, R. H.; Burn, P. L. *Nature* **1990**, *347*, 539.

6. Garnier, F.; Horowitz, G.; Peng, X.; Fichou, D. *Adv. Mater*. **1990**, *2*, 592.

7. Garnier, F.; Hajlaoi, R.; Yassar, A.; Srivastava, P. *Science* **1994**, *265*, 1684.

8. Hotta, S.; Ito, K. In Handbook of Oligo- and Polythiophenes, Fichou, D. Ed.; Wiley-VCH: Weinheim; 1999, p45.

9. Bao, Z.; Dodabalapur, A.; Lovinger, A. J. *Appl. Phys. Lett.* **1996**, *69*, 4108.

10. Sirringhaus, H.; Brown, P. J.; Friend, R. H.; Nielsen, M. M.; Bechgaard, K.; Langeveld-Voss, B. M. M.; Spiering, A. J. H.; Jassen, R. A. J.; Meijer, E. W.; Herwig, P.; de Leeuw, D. M. *Nature* **1999**, *401*, 685.

11. Fichou, D.; Eds. *Handbook of Oligo- and Polythiophenes* Wo;Wiley-VCH: Weinheim, 1999.

12. Ando, M.; Watanabe, Y.; Iyoda, T.; Honda, K.; Shimidzu, T. *Thin Solid Films* **1989**, *179*, 225.

13. Ferreira, M.; Rubner, M. F. *Macromolecules* **1995**, *28*, 7107.

14. Martin, R. C. *Science* **1994**, *266*, 1961.

15. Wu, C. G.; Bein, T. *Science* **1994**, *264*, 1757.

16. Wu, C. G.; Bein, T. *Science* **1994**, *266*, 1013.

17. Smith, R. C.; Fisher, W. M.; Gin, D. L. *J. Am. Chem. Soc*. **1997**, *119*, 4092.

18. Akagi, K.; Katayama, S.; Ito, M.; Shirakawa, H.; Araya, K. *Synth. Metals* **1989**, *28*, D51.

19. Yamamoto, T.; Sanechika, K.; Yamamoto, A. *J. Polym. Sci. Polym., Lett. Ed.* **1980**, *18*, 9.

20. Lin, J. W. P.; Dudek, L. P. *J. Poly. Sci., Polym. Chem. Ed*. **1980**, *18*, 2869.

21. Miller, G. G.; Elsenbaumer, R. L. *J. Chem. Soc., Chem. Commun.* **1986**, *15*, 169.

22. Amou, S.; Haba, O.; Shirato, K.; Hayakawa, T.; Ueda, M.; Takuchi, K.; Osai, M. *J. Polym. Sci. A: Polym. Chem.* **1999**, *37*, 143.

23. McCullough, R. D.; Lowe, R. D. *J. Chem. Soc., Chem. Commun.* **1992**, 70.

24. Loewe, R. S.; Khersonsky, S. M.; McCullough, R. D. *Adv. Mater.* **1999**, *11*, 250.

25. Liu, J.; McCullough, R. D. *Macromolecules* **2002**, *35*, 9882.

26. Che, T. A.; Rieke, R. D. *J. Am. Chem. Soc*. **1992**, *114*, 10087.

27. McCullough, R. D.; Ewbank, P. C.; Loewe, R. S. *J. Am. Chem. Soc*. **1997**, *119*, 633 .

28. Bidan, G.; De Nicola, A.; Enee, V.; Guillerez, S. *Chem. Mater*. **1998**, *10*, 1052.

29. Liu, J.; Sheina, E.; Kowalewski, T.; McCullough, R. D. *Angew. Chem. Int. Ed*. **2002**, *41*, 329.

30. Czerwinski, W.; Wrzeszcz, G.; Kania, K.; Rabek, J. F.; Linden, L. A. *J. Mat. Sci*. **2000**, *35*, 2305.

31. Beaupre, S.; Leclerc, M. *Adv. Funct. Mater*. **2002**, *12*, 192.

32. Charas, A.; Morgado, J.; Martinbo, J. M. G.; Alcacer, L.; Cacilli. F. *Synth. Met.* **2002**, *127*, 251 .

33. Yamamoto, T.; Zhou, Z.; Kanbara, T.; Shimura, M,; Kizu, K.; Maruyama, T.; Nakamura, Y.; Fukuda, T.; Lee, B.; Ooba, N.; Tomaru, S.; Kurihara, T.; Kaino, T.; Kubota, K.; Sasaki, S. *J. Am. Chem. Soc*. **1996**, *118*, 10389.

34. Yamamoto, T.; Arai, M.; Kokubo, H.; Sasaki, S. *Macromolecules*, **2003**, *36*, 7986.

35. McCullough, R. D.; Jayaraman, M. *J. Chem. Soc., Chem. Commun*. **1995**, 135.

36. Iraqi, A.; Clark, D.; Jones, R.; Krier, A. *Synth. Met*. **1999**, *102*, 1220.

37. Hong, X.; Tyson, J. C.; Collard, D. M. *Macromolecules* **2000**, *33*, 3502.

38. Bjornholm, T.; Hassenkam, T.; Greve, D. R.; McCullough, R. D.; Jayaraman, M.; Savoy, S. M.; Jones, C. E.; McDevitt, J. T. *Adv. Mater*. **1999**, *11*, 1218.

39. Reitzel, N.; Greve, D. R.; Kjaer, K.; Howes, P. B.; Jayaraman, M.; Savoy, S.; McCullough, R. D.; McDevitt, J. T.; Bjornholm, T. *J. Am. Chem. Soc.* **2000**, *122*, 5788.

40. Stokes, K. K.; Heuze, K.; McCullough, R. D. *Macromolecules* **2003**, *36*, 7114.

41. Schmiegel, W. W. *Chemistry of Organic Fluorine Compounds II: A Critical Review.*

42. Hong, X.; Tyson, J. C.; Middlecoff, J. S.; Collard, D. M. *Macromolecules* **1999**, *9*, 2155.

43. Hong, X. M.; Collard, D. M. *Macromolecules* **2000**, *33*, 3502.

44. Wurthner, F. *Angew. Chem., Int. Ed.* **2001**, *40*, 1037.

45. Bao, Z.; Lovinger, A. J.; Brown, J. *J. Am. Chem. Soc.* **1998**, *120*, 207.

46. Katz, H. E.; Lovinger, A. J.; Kloc, C.; Siegrist, T.; Lin, Y. Y.; Dodabalapur, A. *Nature* **2000**, *404*, 478.

47. Garnier, F. *Acc. Chem. Res*. **1999**, *32*, 209.

48. Dodabalapur, A.; Torsi, L.; Katz, H. E. *Science* **1995**, *268*, 270.

49. Sakamoto, Y.; Komatsu, S.; Suzuki, T. *J. Am. Chem. Soc*. **2001**, *123*, 4643.

50. Facchetti, A.; Deng, Y.; Wang, A.; Koide, Y.; Sirringhaus, H.; Marks, T. J.; Friend, R. H. *Angew. Chem., Int. Ed.* **2000**, *39*, 4547.

51. Marks, T. J.; Facchetti, A.; Sirringhaus, H.; Friend, R. H. *WO Patent* 0209201, **2002.**

52. Facchetti, A.; Mushrush, M.; Katz, H. E.; Marks, T. J. *Adv. Mater*. **2003**, *15*, 33.

53. Facchetti, A.; Marks, T. J. *Polym. Prep*. **2002**, *43*, 734.

54. Facchetti, A.; Yoon, M-H.; Stern, C. L.; Katz, H. E.; Marks, T. J. *Angew. Chem., Int. Ed.* **2003**, *42*, 3900.

55. Furukawa, Y. *J. Phys. Chem.* **1996**, *100*, 15644.

56. Tol, A. J. W. *Chem. Phy*. **1996**, *208*, 73.

57. Nowak, M. J.; Rughooputh, S. D. D. V.; Hotta, S.; Heeger, A. J. *Macromolecules*, **1987**, *20*, 965.

58. Colaneri, N.; Nowak, M.; Spiegel, D.; Hotta, S.; Heeger, A. J. *Phys. Rev. B*, **1987**, *36*, 7964.

59. Fichou, D.; Xu, B.; Horowitz, G.; Garnier, F. *Synth. Met*. **1991**, *41-43*, 463.

60. Fichou, D.; Horowitz, G.; Garnier, F. *Synth. Met*. **1990**, *39*, 125.

61. Fichou, D.; Horowitz, G.; Xu, B.; Garnier, F. *Synth. Met*. **1990**, *39*, 243.

62. Cornil, J.; Bredas, *Adv. Mater*. **1995**, *7*, 295.

63. Cornil, J.; Beljonne, D.; Bredas, J. L. *J. Chem. Phys.* **1995**, *103*, 842.

64. Su, W. P.; Schrieffer, J. R.; Heeger, A. J. *Phys. Rev. Lett*. **1979**, *42*, 1698.

65. Fesser, K.; Bishop, A. R.; Campbell, D. K. *Phys. Rev. B* **1983**, *27*, 4804.

66. Bredas, A. J.; Street, G. B. *Acc. Chem. Res*. **1985**, *18*, 309.

67. Patil, O.A.; Heeger, A. J.; Wudl, F. *Chem. Rev*. **1988**, *88*, 183.

68. Hill, M. G.; Mann, K. R.; Miller, L. L.; Peneau, J. F. *J. Am. Chem. Soc.* **1992**, *114*, 2728.

69. Yu, Y.; Gunic, E.; Zinger, B.; Miller, L. L. *J. Am. Chem. Soc.* **1996**, *118*, 1013.

70. Baüerle, P.; Segelbacher, U.; Maier, A.; Mehring, M. *J. Am. Chem. Soc.* **1993**, *115*, 10217.

71. Baüerle, P.; Segelbacher, U.; Gaudl, K. U.; Huttenlocher, D.; Mehring, M. *Angew. Chem., Int. Ed*. **1993**, *32*, 76.

72. Zotti, G.; Schiavon, G.; Berlin, A.; Pagani, G. *Chem. Mater.* **1993**, *5*, 430.

73. Hapiot, P.; Audebert, P.; Monnier, K.; Pernaut, J. M.; Garcia, P. *Chem. Mater*. **1994**, *6*, 1549.

74. Apperloo, J. J.; Raimundo, J. M.; Frere, P.; Roncali, J.; Janssen, R. A. J. *Chem. Eur. J.* **2000**, *6*, 1698.

75. van Haare, J. A. E. H.; Groenendaal, L.; Havinga, E. E; Janssen, R. A. J.; Meijer, E. W. *Angew. Chem., Int. Ed.* **1996**, *35*, 638.

76. van Haare, J. A. E. H.; van Boxtel, M.; Jassen, R. A. J. *Chem. Mater*. **1998**, *10*, 1166.

77. Prakka, J. P.; Jeevarajan, J. A.; Jeevarajan, A. S.; Kispert, L. D.; Cava, M. P. *Adv. Mater*. **1996**, *8*, 54.

78. Sakamoto, A.; Furukawa, Y.; Tasumi, M. *J. Phys. Chem. B* **1997**, *101*, 1726.

79. Smie, A.; Heinze, J. *Angew. Chem., Int. Ed*. **1997**, *36*, 363.

80. Tschuncky, P.; Heinze, J.; Smie, A.; Engelmann, G.; Kobmehl, G. *J. Electroanal. Chem.* **1997**, *433*, 223.

81. Merz, A.; Kronberger, J.; Dunsch, L.; Neudeck, A.; Petr, A.; Parkanyi, L. *Angew. Chem., Int. Ed.* **1999**, *38*, 1442.

82. van Haare, J. A. E. H.; Havinga, E. E.; van Dongen, J. L. J.; Janssen, R. A. J.; Cornil, J.; Bredas, J. L. *Chem. Eur. J.* **1998**, *4*, 1509

83. Frere, P.; Allain, M.; Elandaloussi, E. H.; Levillain, E.; Sauvage, F. X.; Riou, A.; Roncali, J. *Chem. Eur. J.* **2002**, *8*, 784

CHAPTER II

SYNTHESIS AND CHARACTERIZATION OF POLY(3-(PERFLUOROALKYL)THIOPHENE)S

Introduction

An important requirement for the successful implementation of organic semiconductors in microelectronic switching and memory devices is the availability of p-type as well as n-type semiconducting materials for the fabrication of important logic elements such as p-n junction diodes, bipolar transistors, and complementary circuits. Organic n-type conducting polymers remain less developed than p-dopable materials, partly due to the lack of electron-poor polymers. Polythiophene derivatives are normally amenable to p-doping (i.e., oxidation) and poly(3-alkylthiophene)s (PATs) only undergo reduction under extreme conditions.[1] Approaches to n-dopable oligothiophenes include preparation of polymers containing fused thiophene rings,[2] and the preparation of electron poor polythiophenes substituted with strong electron withdrawing groups (e.g., esters[3], nitriles[4]). However, the syntheses of polythiophenes bearing electron-withdrawing substituents are limited by the high oxidation potential of the monomers and by the reactivity of the substituents. In addition, steric hindrance between substituents disrupts conjugation along the polymer chain.

Hong and Collard have recently described the thermochromism,[5] liquid crystallinity[6] and solid state assembly[7] of poly(3-semifluoroalkylthiophene)s which arise from the amphiphilicity of the semifluoroalkyl side chains. In each case, a short alkyl spacer was used to separate the conjugated polymer backbone from the electron withdrawing effect of the fluorine atoms.[8] The direct attachment[9] of perfluoroalkyl substituents to the backbone would provide an opportunity to influence the electronic structure of the π-system, with the potential to prepare n-dopable materials. Previous reports of perfluoroalkyl-substituted polythiophenes are limited to a preliminary report of the p-doping of poly(3-trifluoromethylthiophene),[10] and studies of the n-channel conductivity of fluoroalkyl substituted oligothiophenes.[11,12]

Fluoroalkyl substituents also present the opportunity to impart solubility to conjugated polymers in supercritical carbon dioxide ($scCO_2$), an environmentally benign solvent explored for use in numerous reactions and processes. The electrooxidative polymerization of pyrrole and aniline in $scCO_2$ was recently reported.[13] Prior to this report, a number of groups had reported the oxidation of these monomers in $scCO_2$ using a chemical oxidant (typically iron(III) triflate)[14] in an attempt to prepare new conducting composites.[15] However, none of these studies reports the formation of $scCO_2$-soluble conjugated polymers. Given the fluorophilicity of $scCO_2$,[16] we reasoned that substitution of a conjugated polymer with fluoroalkyl groups would provide $scCO_2$-soluble materials. The combination of small size, electron withdrawing nature, and $scCO_2$-philicity of perfluoroalkyl groups led us to investigate poly(3-(perfluoroalkyl)thiophene)s as analogs of the widely studied PATs.[17]

In a direct perfluoroalkylation of thiophenes, 2-isomers are obtained as the main products.[18,19] There are two examples of the preparation of 3-perfluoroalkylthiophene. One is the reaction of 3-halogenothiophene, perfluoroalkyl iodide and copper-bronze in DMF, which gives 3-perfluoroalkyl thiophene in the yield of 17-50%.[20] This method was reported to give a small amount of 2-isomers. The other one is the reaction of 2,5-substituted-thiophene with bis(heptafluorobutyryl) peroxide in Freon-113, followed by the deprotection, which gives 3-perfluoroalkylthiophene in the yield around 20%.[21] Recently, an ICSM conference proceeding described the synthesis with this method, the thermal and spectroscopic characteristics of poly(3-(perfluorohexyl)thiophene), and the formation of the stable monolayers.[22]

Here we report an efficient synthesis and polymerization of 3-perfluoroalkylthiophenes, and the characterization of the electrochemistry, photophysics and the solubility in supercritical CO_2.

Experimental

General methods

All reagents were obtained from commercial sources and used without further purification unless stated otherwise. Tetrahydrofuran (THF) and diethyl ether was dried over sodium benzophenone ketyl prior to distillation under nitrogen. Methylene chloride (CH_2Cl_2) was dried over calcium hydride prior to distillation under nitrogen. Column chromatography was performed on silica gel (40 mesh, 60Å, Baker). Thin layer chromatography was performed on 3×5 cm plates of silica gel (0.2 mm thick, 60 F_{254}) on an aluminum support (EM Separations). All ^1H NMR spectra were collected on a Varian

Gemini 300 MHz instrument using $CDCl_3$ as the solvent unless otherwise specified. Chemical shifts are reported relative to tetramethylsilane. ^{13}C NMR spectra were obtained at 75.5 MHz. All ^{19}F NMR spectra were collected on a Bruker DSX 400 MHz instrument using $CDCl_3$ as the solvent unless otherwise specified. Chemical shifts are reported relative to trifluoromethane. IR analysis was performed on a Nicolet 520 FTIR spectrometer. UV-vis analysis was performed with a Perkin-Elmer Lambda 19 spectrometer. Fluorescence spectra were collected with a Spex Fluorolog Fluometer 1681 0.22m Spectrometer. Electron ionization or chemical ionization mass spectra was performed using a VG Analytical 70-SE instrument with a L-250J Data System Analyzer.

Polymer films were spin coated onto glass slides or ITO glass slides using a Specialty Coating System P-6000 spin coater.

Electrochemical experiments were performed using a BAS 100B electrochemical analyzer in three-electrode cell equipped with a 2.0 mm^2 gold or platinum or graphite disk working electrode, a platinum wire counter electrode, and a saturated calomel electrode (SCE).

Synthesis

3-Iodothiophene (1). 3-Bromothiophene (48.9 g, 30.0 mmol) was added to a solution of copper iodide (85.7 g, 45.0 mmol) in pyridine (115 mL). After stirring for 24 h at 140 ^oC the mixture was cooled to 70 ^oC. H_2O (115 mL) and concentrated HCl (115 mL) were added. The mixture was stirred for 30 min at room temperature. Steam distillation afforded a mixture which separated into two layers. The organic phase was washed with 100 mL 5% $NaHCO_3$, 100 mL 5% $Na_2S_2O_3$, 100 mL H_2O and dried over

$CaCl_2$. After filtration, the product was purified by fractional distillation under vacuum to give **1** (27.72g, 44%), as a colorless liquid. – ^{1}H NMR (300 MHz, $CDCl_3$): δ 7.25 (m, J = 5.6, 2.2, 1 H, C5-H), 7.22 (m, J = 3.3, 2.2, 1 H, C4-H), 6.99 (m, J =5.6, 2.2, 1 H, C2-H). IR (NaCl): 3105, 1482, 1353, 1195, 1083, 873, 844, 786, 762 cm^{-1}. MS (EI): M^+ = 210.

3-(Perfluorooctyl)thiophene (2).[20] 3-Iodothiophene (4.38 g, 21.0 mmol) was added to a well-stirred suspension of copper-bronze powder (4.27 g, 67.0 mmol) in dry DMF (25 mL), followed by perfluorooctyl iodide (13.7 g, 25.0 mmol) and the mixture was heated under N_2 for 24 h at 120 to130 ^oC. After cooling and filtration of the solid, the liquid was poured into chilled aqueous HCl (crushed ice ~ 75 g; concentrated HCl 75 mL). The layers were separated and the aqueous solution was extracted with hexane. The combined organic extracts were washed with 100 mL 5% $Na_2S_2O_3$, 100 mL H_2O and dried over $MgSO_4$. The solvent was removed under reduced pressure and the product was purified by column chromatography (silica/hexane) to give **2** (8.35 g, 80%), as a yellow liquid. – ^{1}H NMR (300 MHz, $CDCl_3$): δ 7.71 (m, J_{H-H} = 4.0, 1.6 Hz, 1 H, C2-H), 7.43 (m, J_{H-H} = 5.2, 3.1 Hz, J_{H-F} = 1.7 Hz, 1H, C4-H), 7.24 (m, J_{H-H} = 5.9, 1.6 Hz, 1H, C5-H). ^{19}F NMR (400 MHz, $CDCl_3$, reference: $CFCl_3$) δ = -82.3 (t, 3F, J = 10.7 Hz, -C$\underline{F}_3$), -108.6 (t, 2F, J =13.7 Hz, Th-C$\underline{F}_2$-), -122.9 (m, 2F), -123.4 (m, 4F), -123.6 (m, 2F), -124.1 (m, 2F), -127.6 (m, 2F). IR (NaCl): 2973 (sp^2 C-H str), 1209 (C-F str) cm^{-1}. HRMS (EI): Calculated for $C_{12}H_3F_{17}S$, 501.96840; Found, 501.97284; Δ = 9 ppm.

3-(Perfluorohexyl)thiophene (3). The title compound was prepared from 3-iodothiophene (9.80 g, 46.7 mmol) and perfluorohexyl iodide (24.9 g, 56.0 mmol) according to the procedure described for the synthesis of **2** (14.6 g, 78%) as a yellow liquid. – ^{1}H NMR (300 MHz, $CDCl_3$): δ 7.71 (m, J_{H-H} = 4.0, 1.6 Hz, 1 H, C2-H), 7.43 (m,

$J_{H\text{-}H}$ = 5.9, 1.6 Hz, $J_{H\text{-}F}$ = 1.7 Hz, 1H, C4-H), 7.24 (m, $J_{H\text{-}H}$ = 5.9, 1.6 Hz, 1H, C5-H). ^{19}F NMR (400 MHz, $CDCl_3$, reference: $CFCl_3$) δ -82.3 (t, 3F, J = 10.7 Hz, -C$\underline{F}_3$), -108.6 (t, 2F, J =13.7 Hz, Th-C$\underline{F}_2$-), -122.9 (m, 2F), -123.4 (m, 2F), -124.1 (m, 2F), -127.6 (m, 2F). IR (NaCl): 2973 (sp^2 C-H str), 1209 (C-F str) cm^{-1}. MS (EI): M^+ = 402.

2-Bromo-4-(perfluorooctyl)thiophene (4). A solution of 3-(perfluorooctyl)thiophene (9.00 g, 17.9 mmol) and NBS (6.38 g, 35.6 mmol) in 50 mL acetic acid was heated for 24 h at 115 °C, the mixture was cooled and poured into H_2O (100 mL) and extracted with Et_2O (3 × 100 mL). The combined organic phases were washed with 10% NaOH (3 × 50 mL), 100 mL water and dried over Na_2SO_4. The solvent was removed under reduced pressure and the residue was recrystallized from methanol to give **4** (7.40 g, 71%), as a flake golden solid, mp = 56-58 °C. – ^{1}H NMR (300 MHz, $CDCl_3$): δ 7.62 (m, $J_{H\text{-}H}$ = 1.6, $J_{H\text{-}F}$ = 1.7, 1H, C2-H), 7.19 (m, $J_{H\text{-}H}$ = 1.6, $J_{H\text{-}F}$ = 1.7, 1 H, C4-H). ^{19}F NMR (400 MHz, $CDCl_3$, reference: $CFCl_3$) δ = -82.3 (t, 3F, J = 10.7 Hz, -C$\underline{F}_3$), -107.5 (t, 2F, J =13.7 Hz, Th-C$\underline{F}_2$-), -122.8 (m, 2F), -123.2 (m, 4F), -123.5 (m, 2F), -124.0 (m, 2F), -127.6 (m, 2F). IR (NaCl): 2973 (sp^2 C-H str), 1209 (C-F str) cm^{-1}. HRMS(EI): Calculated for $C_{12}H_2BrF_{17}S$, 579.87891; Found, 579.88391; Δ = 9 ppm.

2-Bromo-4-(perfluorohexyl)thiophene (5). The title compound was prepared from 3-(perfluorohexyl)thiophene (10.9 g, 27.0 mmol) and NBS (12.0 g, 67.5 mmol) according to the procedure described for the synthesis of **4**.The crude product was purified by vacuum fractional distillation to give **5** (8.42 g, 65%), as a yellow liquid. – ^{1}H NMR (300 MHz, $CDCl_3$): δ = 7.62 (m, $J_{H\text{-}H}$ = 1.6, $J_{H\text{-}F}$ = 1.7, 1H, C2-H), 7.19 (m, $J_{H\text{-}H}$ = 1.6, $J_{H\text{-}F}$ = 1.7, 1 H, C4-H). ^{19}F NMR (400 MHz, $CDCl_3$, reference: $CFCl_3$) δ -82.3 (t, 3F, J = 10.7 Hz, -C$\underline{F}_3$), -107.5 (t, 2F, J =13.7 Hz, Th-C$\underline{F}_2$-), -122.8 (m, 2F), -123.2 (m, 2F), -

124.0 (m, 2F), -127.6 (m, 2F). IR: 2973 (sp^2 C-H str), 1209 (C-F str) cm^{-1}. MS (EI): M^+ = 480.

Poly(3-(perfluorooctyl)thiophene) (PF8T). Monomer **2** was polymerized according to the methods described by McCullough[23] for the polymerization of 3-alkyl-2-bromothiophenes. Dry diisopropylamine (1.23 ml, 8.80 mmol) and freshly distilled THF 80 mL were added into a dry Schlenk flask. 2.5 M n-butyllithium (3.67 mL, 8.80 mmol) was added into the mixture at room temperature. The mixture was cooled to -40 ^oC and stirred for 40 min. The reaction mixture containing LDA was then cooled to -78 ^oC, and 2-bromo-4-(perfluorooctyl)thiophene (4.66 g, 8.00 mmol) was added. The mixture was stirred for 40 min at -40 ^oC. The mixture was cooled to -60 ^oC, $MgBr_2.Et_2O$ (2.27 g, 8.80 mmol) was added, and the reaction was stirred at -60 ^oC for 20 min. The reaction was warmed to -40 ^oC and stirred for 15 min. The mixture was allowed to slowly warm to -5 ^oC and 0.5 mol % $Ni(dppp)Cl_2$ (44 mg, 0.080 mmol) was added. The mixture was allowed to warm to room temperature overnight (18 h). The mixture was poured into MeOH (300 mL), and the resulting precipitate was filtered and washed with MeOH, H_2O, MeOH again. The solid was then dried under vacuum to afford a deep brown solid. (1.20g, 30% crude yield). Removal of oligomers and impurities was achieved by subjecting the solid to sequential extractions in a Soxhlet extractor with MeOH, acetone, followed with chloroform and perfluorohexane. The chloroform and perfluorohexane fraction were characterized. – ^1H NMR (300 MHz, $CDCl_3$): δ 7.47. ^{19}F NMR (400 MHz, $CDCl_3$, reference: $CFCl_3$) δ -83.1 (m, 3F, $-CF_3$), -104.7 (m, 2F, α-CF_2), -122.9 (m, 2F, -β-CF_2), -123.2 (m, 2F, CF_2), -123.7 (m, 2F, CF_2), -123.8 (m, 2F, CF_2), -124.6 (m, 2F, CF_2), -128.2 (m, 2F, CF_2). IR (NaCl): 2980 (C-H str), 1205 (C-F str), 1148 cm^{-1}.

Poly(3-(perfluorohexyl)thiophene) (PF6T). The title polymer was prepared from monomer **5** (4.80 g, 10.0 mmol) according to the procedure described for the synthesis of **PF8T**. – ^{1}H NMR (300 MHz, $CDCl_3$): δ 7.47. ^{19}F NMR (400 MHz, $CDCl_3$, reference: $CFCl_3$) δ -83.1 (m, 3F, -CF_3), -104.7 (m, 2F, α-CF_2), -122.8 (m, 2F, -β-CF_2), -123.5 (m, 2F, CF_2), -124.6 (m, 2F, CF_2), -128.0 (m, 2F, CF_2). IR (NaCl): 2980 (C-H str), 1205 (C-F str), 1148 cm^{-1}.

3,4'-Bis(perfluorooctyl)-2,2'-bithiophene (6). A solution of LDA (3.68 mL, 5.52 mmol, 1.5 M in cyclohexane) was added dropwise into a Schlenk flask containing 30 mL dry Et_2O and 3-(perfluorooctyl)thiophene (2.01 g, 4.00 mmol) at -70 °C, After 45 min, $ZnCl_2$ (8.24 mL, 8.24 mmol, 1.0 M in Et_2O) was added. The reaction mixture was allowed to warm to room temperature, and stirred for 1 h. A solution of tetrakis(triphenylphosphine)palladium(0) (0.32 g, 0.28 mmol) and 2-bromo-4-(perfluorooctyl)thiophene (2.32 g, 4.00 mmol) in 10 mL of Et_2O was added. The reaction mixture was heated at reflux overnight and poured into 100 mL H_2O. The aqueous layer was extracted with Et_2O (3 × 100 mL). The combined organic extracts were washed with brine (100 mL) and dried over $MgSO_4$. After removal of the solvent, the residue was purified by column chromatography on silica with petroleum ether to afford **6** as a white wax solid (0.70g, 18%). – ^{1}H NMR (300 MHz, $CDCl_3$): δ 7.79 (m, 1 H), 7.46 (d, 1 H, J = 5.5), 7.23 (m, 1H), 6.95 (d, 1H, J = 5.5). ^{19}F NMR (400 MHz, $CDCl_3$, reference: $CFCl_3$) δ -82.3 (m, 6F, -CF_3), -104.0 (t, 2F, J =13.7, Th-3-α-CF_2-), -108.4 (t, 2F, J =12.2, Th-3'-α-CF_2-), -122.3 (m, 2F, -β-CF_2-), -122.8 (m, 2F, -β'-CF_2-), -123.1 (m, 2F), -123.4 (m, 4F), -123.5 (m, 4F), -124.2 (m, 4F), -127.6 (m, 4F). IR (NaCl): 2970 (sp^2 C-H, str), 1210

(C-F, str) cm^{-1}. HRMS (FAB): Calculated for $C_{24}H_4F_{34}S_2$, 1001.90231; Found, 1001.91643; Δ = 14 ppm.

Results and Discussion

Synthesis of 3-(perfluoroalkyl)thiophenes

3-Alkylthiophenes can be made in high yields by Kumada coupling, in which 3-bromothiophene is treated with alkyl Grignard reagents in the presence of Ni(II) catalyst. The same route cannot be used to prepare 3-perfluoroalkylthiophenes because perfluorinated Grignard reagents possess anomalous reactivity. Direct perfluoroalkylation of thiophene itself gives 2-substituted isomers as the major product.[18,19] Copper-bronze catalyzed perfluoroalkylation of 3-bromothiophene with perfluoroalkyl iodide gives a mixture of 3- and 2-isomers of perfluoroalkyl thiophene.[20] It was reported the 3-trifluoromethylthiophene, along with the 3-difluoromethyl analog,[24] can be isolated at low yield (17%), but the regioisomers with longer perfluoroalkyl chains are inseparable. The reaction of 2,5-substituted-thiophene with bis(perfluoroalkylryl) peroxide in Freon-113, followed by the deprotection, which gives 3-(perfluoroalkyl)thiophene in the yield around 20%.[21]

Instead of using 3-bromothiophene, copper-bronze catalyzed couplings of 3-iodothiophene and perfluoroalkyl iodides in dry DMF under N_2 give 3-(perfluoroalkyl)thiophene without 2-regioisomers (<1% by GC) in high yields (~80%). Optimization of the reaction conditions led us to use 20% excess of perfluoroalkyl iodide, a dry N_2 atmosphere, dry solvent and fresh copper-bronze. 3-(Perfluorooctyl)thiophene and 3-(perfluorohexyl)thiophene were prepared in multigram scales. 3-

(Perfluorobutyl)thiophene cannot be made by this method due to the low boiling point of perfluorobutyl iodide, Figure 2.1.

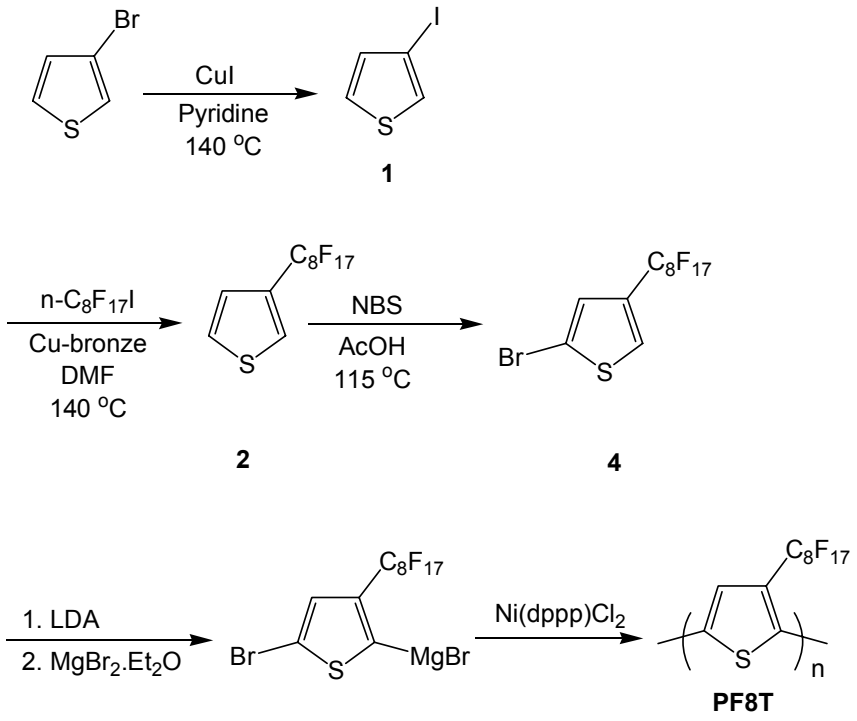

Figure 2.1. Synthesis of monomer **4** and polymerization.

Bromination of 3-(perfluroalkyl)thiophenes

Bromination of 3-substituted thiophenes is an electrophilic substitution. Since the electron-donating alkyl groups activate the aromatic thiophene rings, it is easy to brominate 3-alkylthiophenes under mild conditions (e.g., NBS or Br_2 as a source of

electrophilic bromine; $CHCl_3$ or DMF as solvent, at room temperature in 3 h). In the case of thiophenes, the α-positions (2- and 5-positions) are more reactive than the β-positions (3- and 4-positions). Furthermore, the alkyl groups direct the electrophilic substitution to the ortho position. Thus, the electrophilic bromination of 3-alkylthiophenes proceeds selectively at the 2-position (ortho position) instead of 5-position (i.e., meta to the alkyl group). However, this selectivity is very subtle. It is very easy to be over brominated to give the dibromo compounds, which can be avoided by carefully controlling the reaction conditions (e.g., low temperature, dark, stoichiometry.)

Perfluoroalkyl groups are very strong electron-withdrawing substituents, which deactivate the aromatic thiophene rings and hinder the electrophilic bromination under such mild conditions. Harsh conditions were required to push the bromination of 3-(perfluoroalkyl)thiophenes to the completion (e.g., 2~3 eq. of NBS, AcOH as solvent, reflux overnight). Since the thiophenes are deactivated, over bromination does not occur.

Perfluoroalkyl groups are meta- directing for electrophilic substitutions. In contrast to bromination of 3-alkylthiophenes, the electrophilic bromination of 3-(perfluoroalkyl)thiophenes processes selectively at the 5-position (i.e., the meta position) instead of the 2-position (i.e., ortho position), Figure 2.1.

H-F coupling in ^{1}H NMR of 3-(perfluoroalkyl)thiophenes and derivatives

^{1}H NMR spectra of 3-(perfluoroalkyl)thiophene and its brominated derivative show long distance (four-bond H-C-C-C-F) ^{1}H-^{19}F coupling, Figure 2.2.

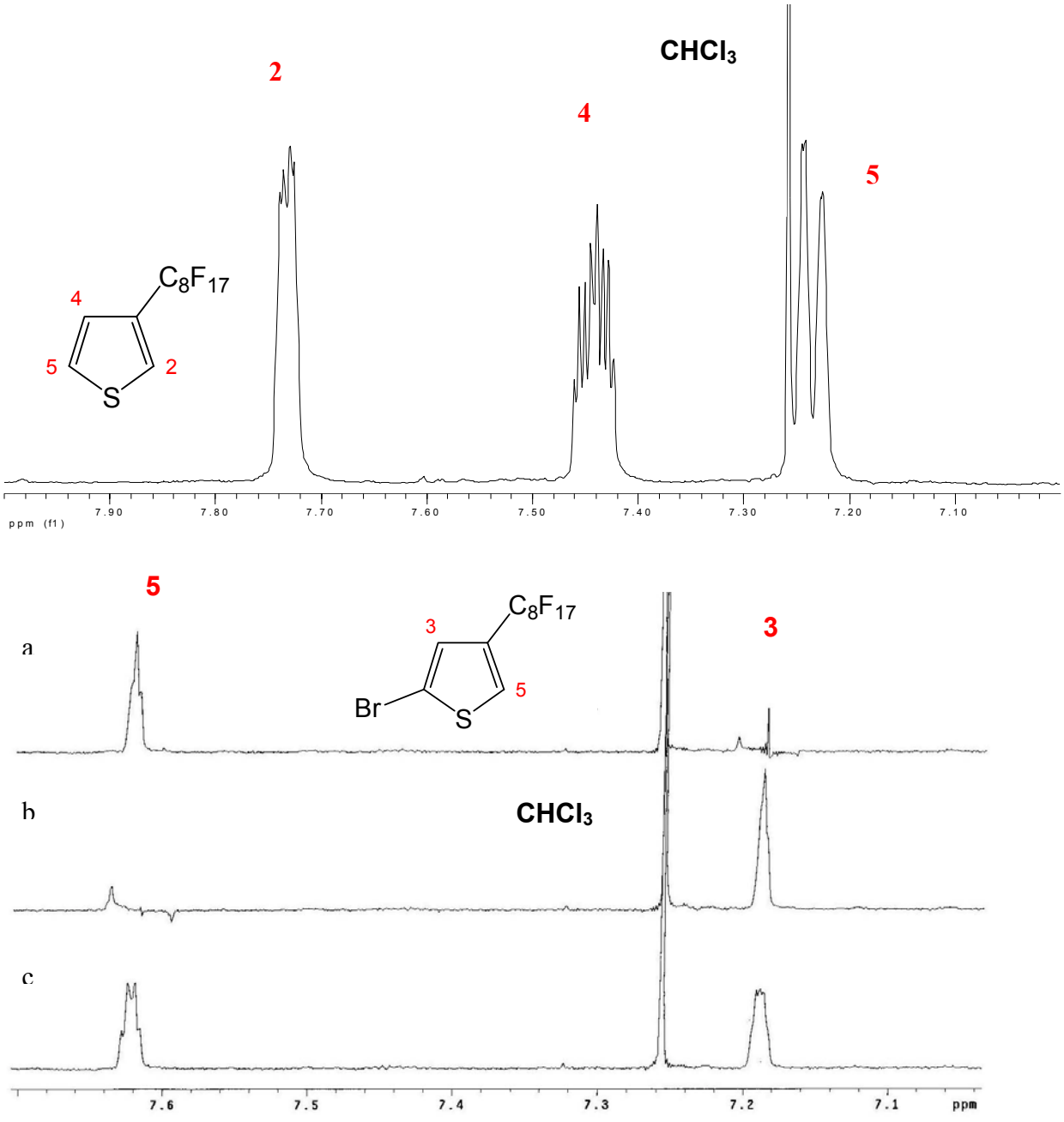

Figure 2.2. ^{1}H-NMR spectrum of 3-(perfluorooctyl)thiophene (top), 300 MHz, $CDCl_3$; ^{1}H-NMR spectra of 2-bromo-4-(perfluorooctyl)thiophene (bottom, c), 300 MHz, $CDCl_3$; Decoupling at 7.19 ppm (bottom, a); Decoupling at 7.62 ppm (bottom, b).

Protons at 4- and 2-positions of 3-(perfluorooctyl)thiophene both show more complicated splitting patterns than the doublet-doublet, common to other 3-substituted thiophenes. This is especially true for the proton at the 4-position which appears as a pattern of ten peaks. Thus, besides the ^{1}H-^{1}H coupling to give a doublet-doublet, each peak should be spilt further into a triplet due to the coupling with two identical ^{19}F nuclei three carbons away (i.e., H-C-C-C-F). This should result in a doublet of doublet of triplet (ddt). Since the meta ^{1}H-^{1}H coupling constant ($J_{H-H} = 3.1$) is about twice of the ^{1}H-^{19}F coupling constant ($J_{H-F} = 1.6$), there are two peaks overlapping to other peaks. This explains only ten peaks with the ratio of 1 : 2 : 2 (i.e., 1+1) : 2 : 1 : 1 : 2 : 2 (i.e.,1+1) : 2 : 1 observed, instead of twelve (ddt), Figure 2.3.

Proton decoupling experiments were used to determine splitting of these proton NMR signals for 2-bromo-4-(perfluorooctyl)thiophene. ^{1}H NMR shows a broad quartet for both proton 3 and 5. Decoupling of proton 5 results in the pattern of proton 3 becoming a triplet, because of coupling with two fluorines (H-C-C-C-F). If there was no H-F coupling, the decoupling experiment should have only given a sharp singlet for proton 3. Proton 3 gives the same result when decoupling proton 5, Figure 2.2. However, H-F coupling is not apparent in the ^{19}F NMR spectra, Figure 2.4. This is because the resolution of spectra is different from ^{1}H NMR to ^{19}F NMR.

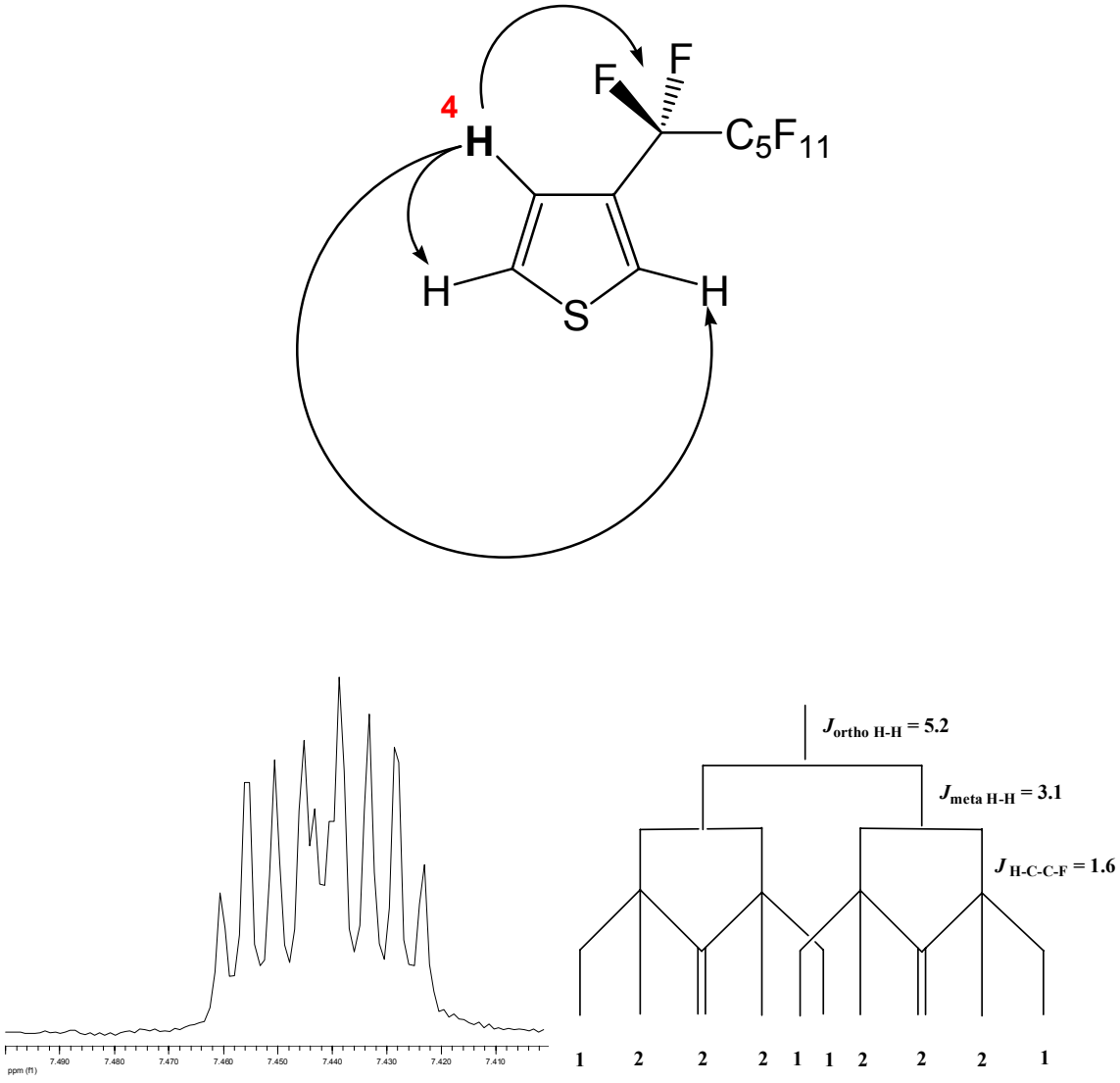

Figure 2.3. Coupling pattern for proton 4 of 3-(perfluorooctyl)thiophene.

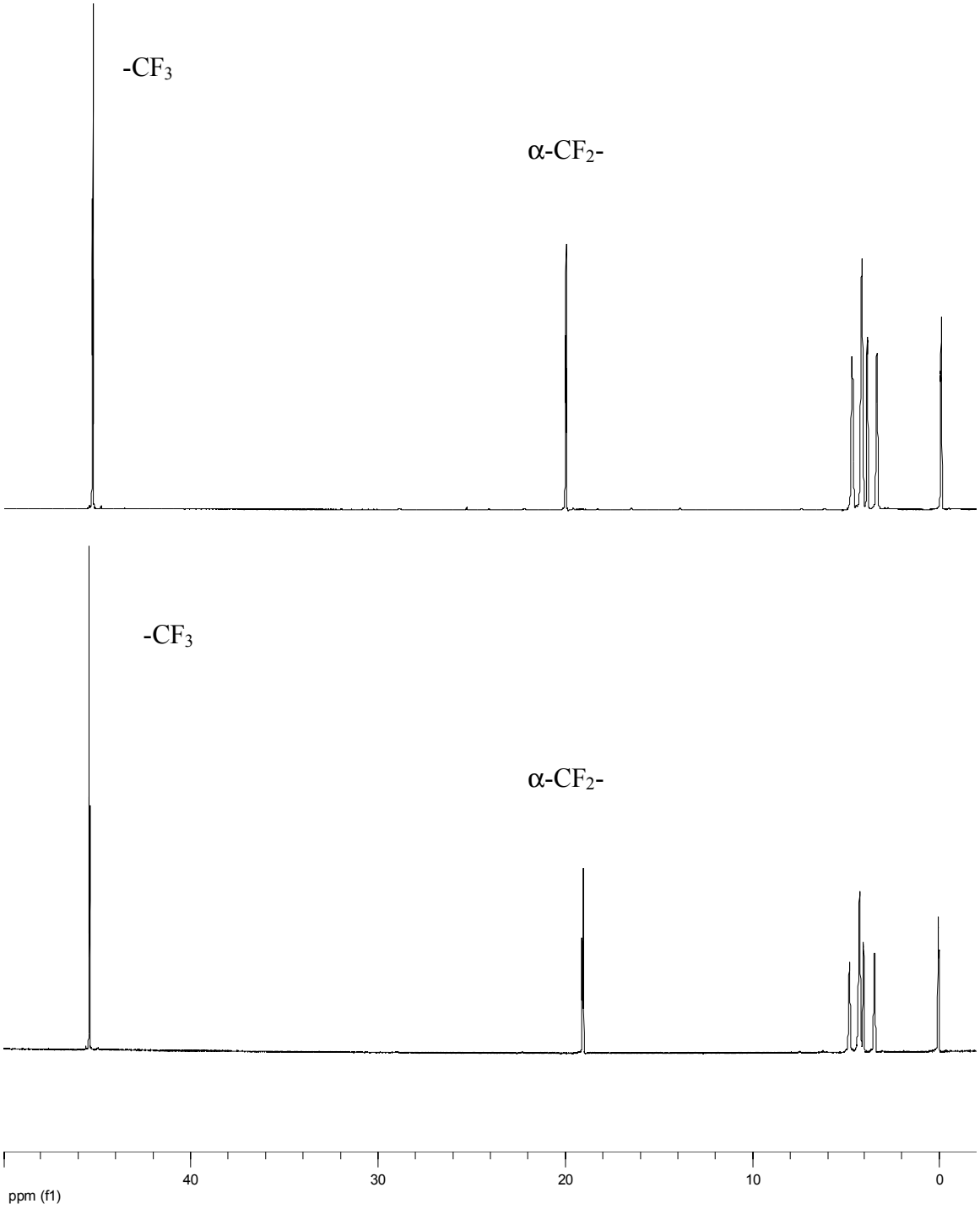

Figure 2.4. ^{19}F-NMR spectrum of 3-(perfluorooctyl)thiophene (top), 400 MHz, $CDCl_3$; ^{19}F-NMR spectrum of 2-bromo-4-(perfluorooctyl)thiophene (bottom), 400 MHz, $CDCl_3$. Reference to trifluoromethylbenzene

Polymerization and polymer NMR spectra

Attempts to polymerize 3-(perfluorooctyl)thiophene by chemical oxidation with $FeCl_3$ in $CHCl_3$ did not yield any polymer. However, an organometallic arene-coupling method did afford polymer. Treatment of 2-bromo-4-perfluorooctylthiophene with fresh LDA followed by addition of D_2O resulted in 2-deuterio-4-(perfluorooctyl)thiophene. This result indicates that α-lithiation is very efficient and regioselective.

Polymerization of 2-bromo-4-(perfluorooctyl)thiophene to form regioregular PF8T was performed using McCullough's method for the polymerization of 2-bromo-3-alkylthiophenes to afford regioregular (i.e., head-to-tail) PATs. Lithiation of 2-bromo-4-perfluorooctylthiophene with LDA, followed by the transmetallation with $MgBr_2.Et_2O$, gives the Grignard reagent. The $Ni(dppp)Cl_2$-catalyzed coupling reaction followed by precipitation yields the crude polymer. The polymer was fractionated by successive extraction in a Soxhlet extractor with MeOH, acetone, hexane, $CHCl_3$ and perfluorohexane. The perfluorohexane fraction (polymer, PF8T) and $CHCl_3$ fraction (oligomer) were further characterized.

^1H NMR and ^{19}F NMR spectroscopies were used to characterize the microstructure of PF8T. The ^1H NMR spectrum of the perfluorohexane-soluble fraction (PF8T) shows a singlet at δ 7.47 ppm for the proton on the 4-position of the repeat unit, and small peaks corresponding to the end groups and penultimate structural units of the polymer chains. Compared to the spectrum of 3-(perfluorooctyl)thiophene, the disappearance of protons at 2- and 5-positions indicates the perfluorohexane fraction (PF8T) has a reasonable high molecular weight, Figure 2.5.

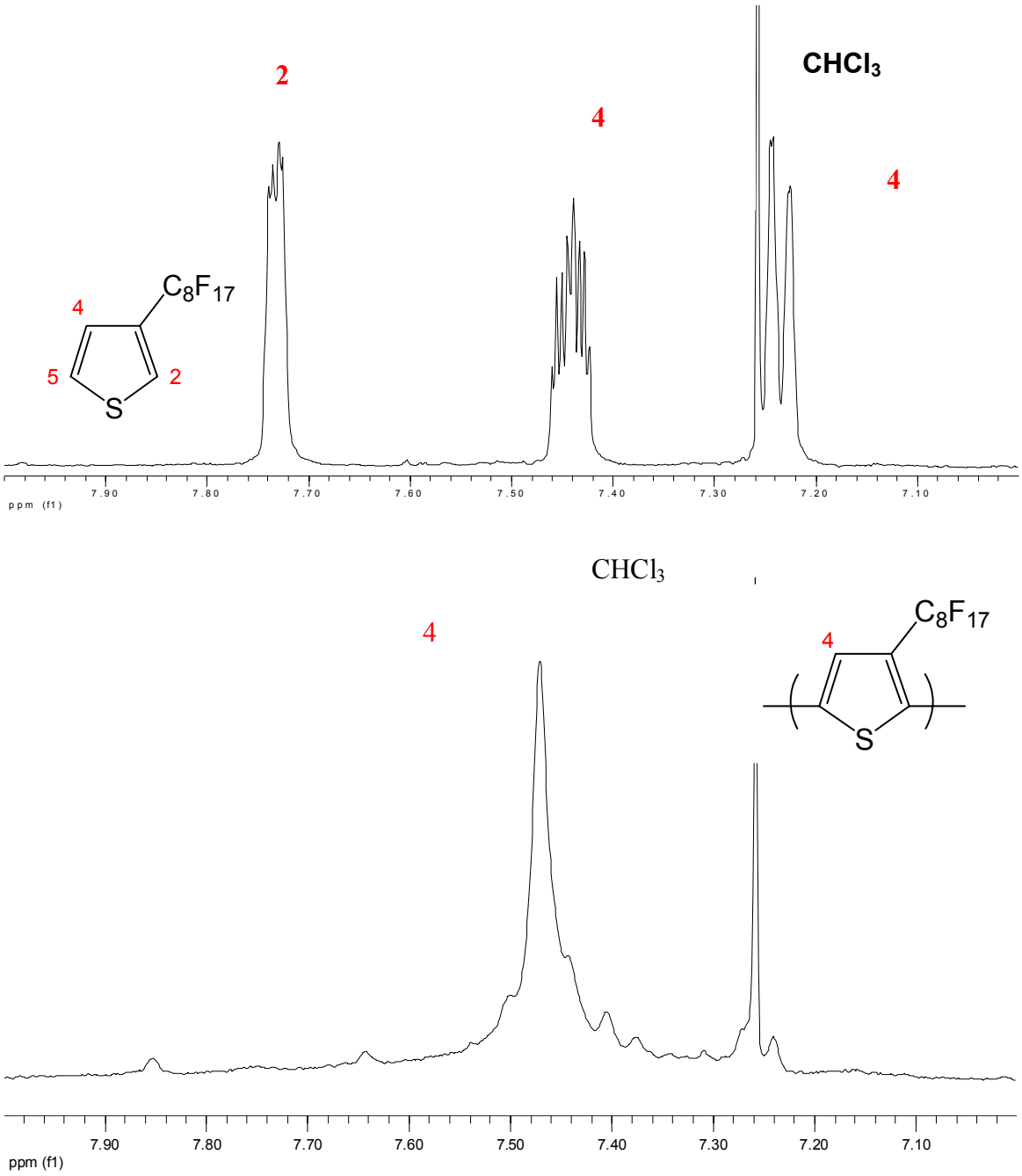

Figure 2.5. ^{1}H-NMR spectrum of 3-(perfluorooctyl)thiophene (top), 300MHz, in 1:1 Freon-113 and $CDCl_3$;^{1}H-NMR spectrum of poly(3-(perfluorooctyl)thiophene) (bottom), 300MHz, in 1:1 Freon-113 and $CDCl_3$

^{19}F NMR spectroscopy of PF8T shows eight peaks for eight different types of fluorines on the side chain, Figure 2.6. The peak for the α-difluoromethylene of the side chains give rise to a slightly broadened signal at -104.7 ppm (chemical shifts are given relative to $CFCl_3$) which is similar to the chemical shift for the α-CF_2 of the perfluoroalkyl group on the C-3 position of dimer **6** (-104.0 ppm). The chemical shift of the α-CF_2 unit in the 4'-position of **6** (-108.4 ppm) allows us to assign a small peak at -109.0 ppm in the spectrum of the polymer to end groups. ^{19}F NMR spectroscopy of the $CHCl_3$-solution fraction indicates that this extract is an oligomer, which displays a larger contribution from end groups at around at -109.0 ppm. Other peaks in this region might arise from the α-CF_2 unit of the penultimate repeat units, other types of end groups, and non-regioregular diads (i.e., head-to-head, head-to-tail), Figure 2.7. Based on the ^{1}H and ^{19}F NMR spectra we estimate $M_n = 65x10^3$ g/mol and the head-to-tail regioregularity as >86%.

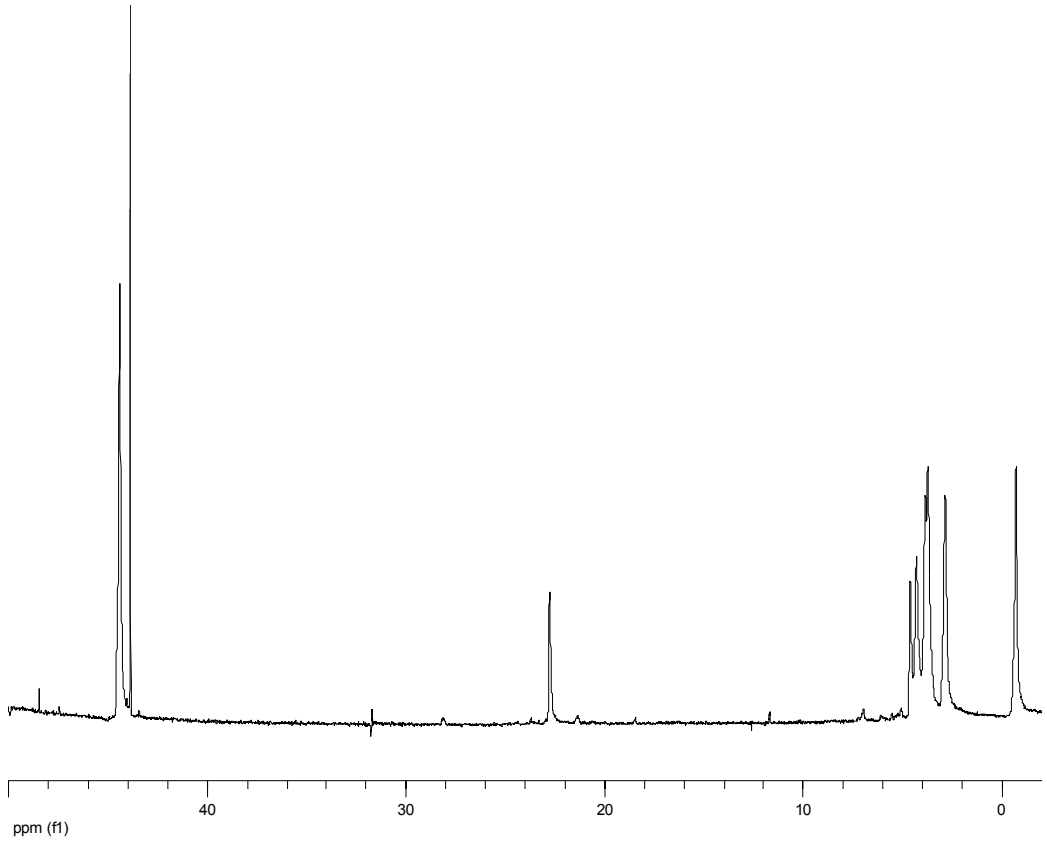

Figure 2.6. ^{19}F-NMR spectrum of poly(3-(perfluorooctyl)thiophene) 400 MHz, in 1:1 Freon-113 and $CDCl_3$, reference to trifluoromethylbenzene.

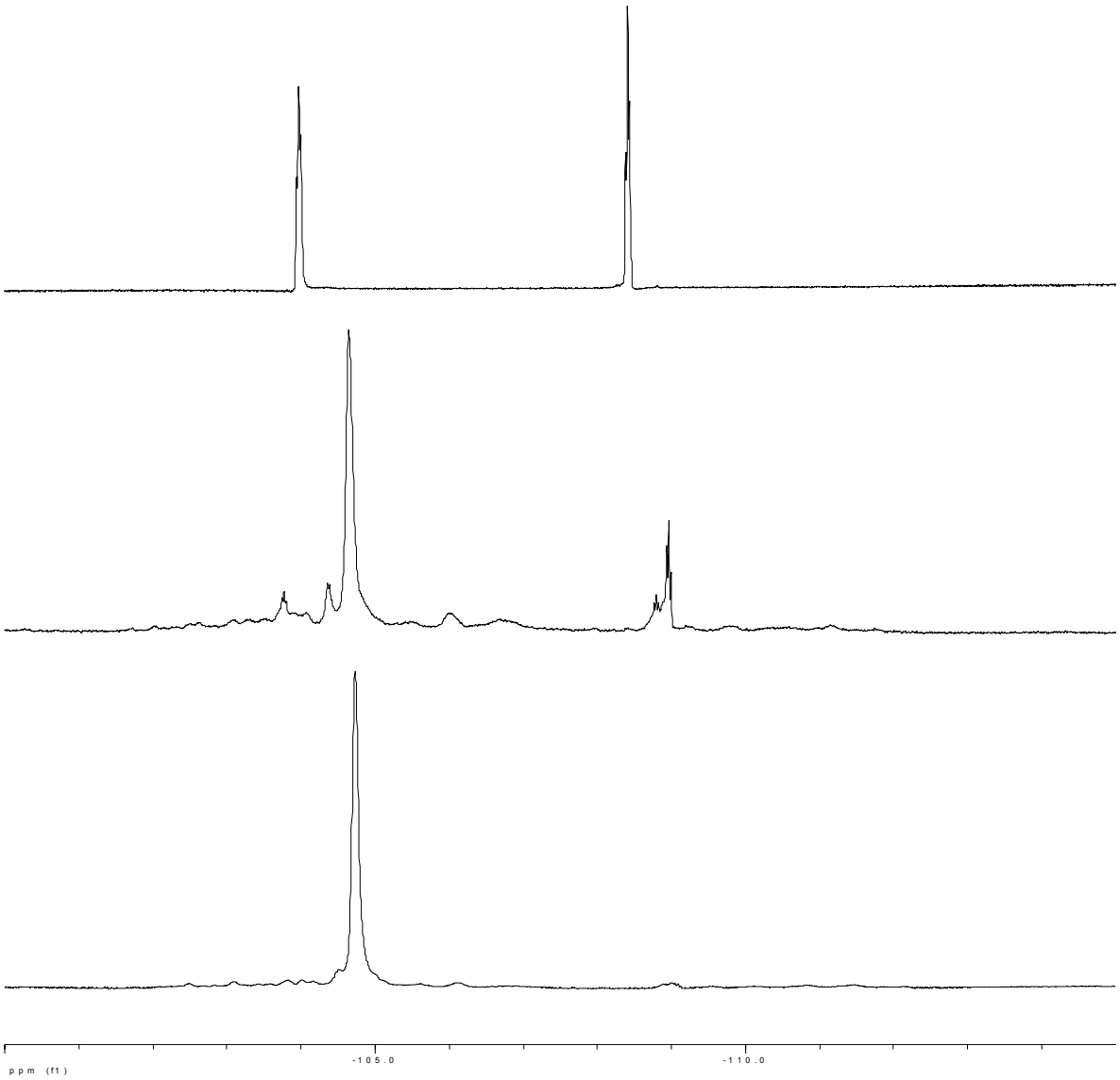

Figure 2.7. ^{19}F-NMR spectra of α-difluoromethylene (-100 to –115 ppm), 400 MHz, 1:1 Freon-11and $CDCl_3$ of dimer, **6**, (top); of $CHCl_3$ fraction, oligomer, (middle); of perfluorohexane fraction, **PF8T**, (bottom).

Electrochemistry

In order to lower the oxidation potential and thereby enable oxidative polymerization, as well as to get end group information for the homopolymer, 3,4'-

bis(perfluorooctyl)-2,2'-bithiophene, 6, was prepared by the $Pd(PPh_3)_4$ catalyzed coupling reaction of 2-metallated-3-perfluorooctylthiophene and 2-bromo-4-perfluorooctylthiophene, Figure 2.8.

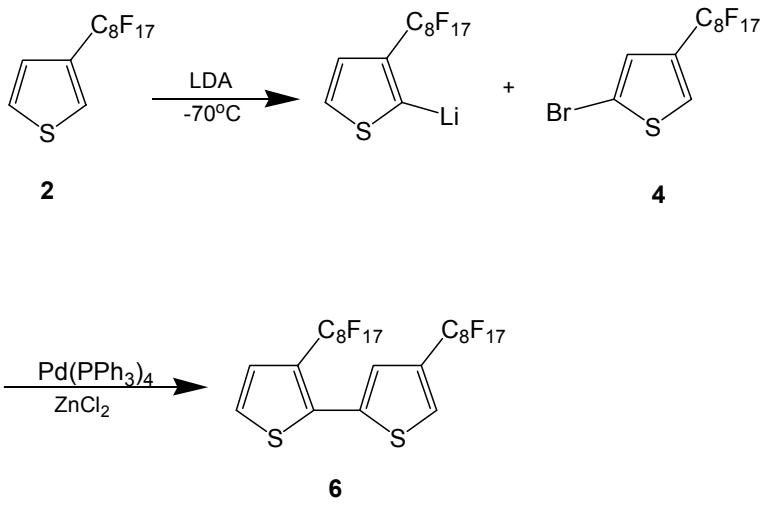

Figure 2.8. Synthesis of dimer **6**.

The ^{19}F NMR of the bithiophene shows two triplets for the α-difluoromethylene of the side chains, which indicates that the α-difluoromethylene of the side chains is sensitive to the connection of adjacent thiophene ring, Figure 2.9.

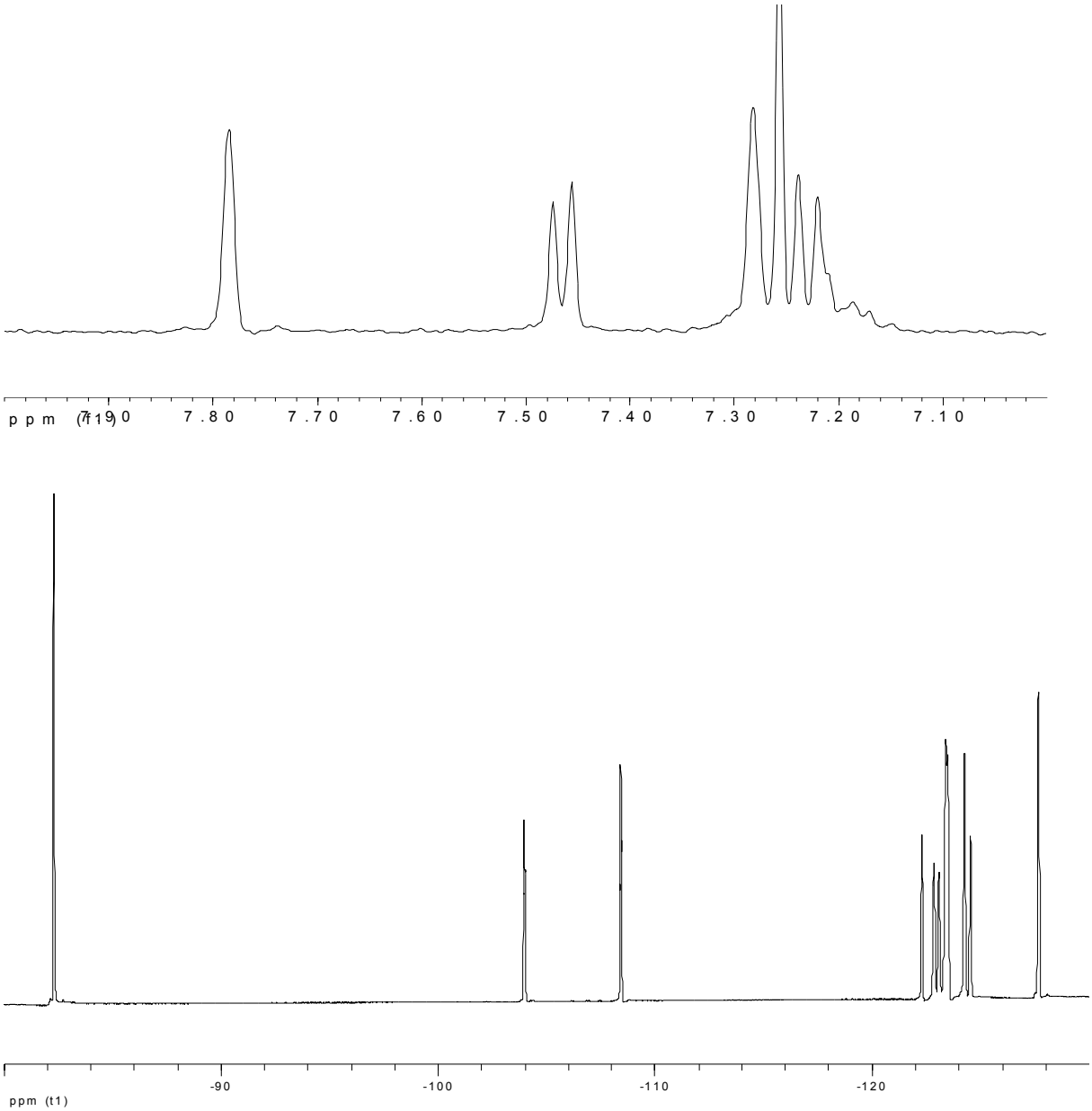

Figure 2.9. ^{1}H-NMR spectrum of dimer, **6** (top), 300MHz, in $CDCl_3$; ^{19}F-NMR spectrum of dimer, **6** (bottom), 300MHz, in $CDCl_3$.

Cyclic voltammetry (CV) of 3-(perfluorooctyl)thiophene (1.0 mM in 0.1 M Bu_4NPF_6/CH_2Cl_2, Au working electrode) shows an irreversible oxidation peak at +2.05 V

(versus SCE) without deposition of a polymer film. The high oxidation potential of the monomer is consistent with the electron withdrawing effect of the perfluoroalkyl substituent (for comparison, 3-octylthiophene undergoes oxidation at +1.84 V). Dimer **6** undergoes irreversible oxidation with a peak potential of +1.75 V. Electrochemical polymerization of **6** was performed potentiostatically (1.0 mM, +1.80 V on a carbon electrode) to afford PF8T' as a redox-active electrochromic film on the electrode surface. The cyclic voltammetry of this film in monomer-free electrolyte shows an oxidation peak at +1.19 V, approximately 250 mV higher than that of PH8T deposited under similar conditions. The CV also shows a sharp reversible peaks, corresponding to reversible n-doping at -1.18 V, Figure 2.10. For comparison, bis(perfluoroalkyl)oligothiophenes,[11] with a lower degree of substitution than PF8T, have more negative reduction potentials, and poly(3-methylthiophene) undergoes reduction at ca. -2.5 V versus SCE. Cyclic voltammetry of a dip-coated film of chemically-prepared PF8T shows similar redox activity as electrochemically prepared films, Figure 2.11.

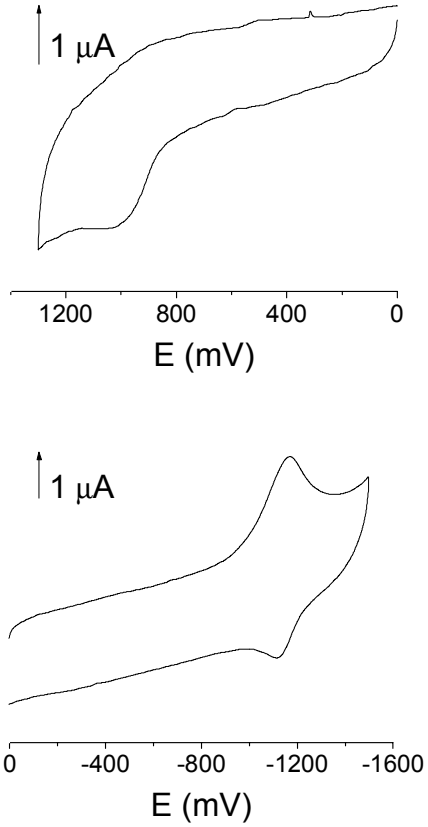

Figure 2.10. Cyclic voltammetry of electrochemically prepared **P8FT'**onto an electrode surface (0.1 M Bu_4NPF_6/CH_2Cl_2, carbon working electrode): top, 0 to +1300 mV; bottom, 0 to -1500 mV.

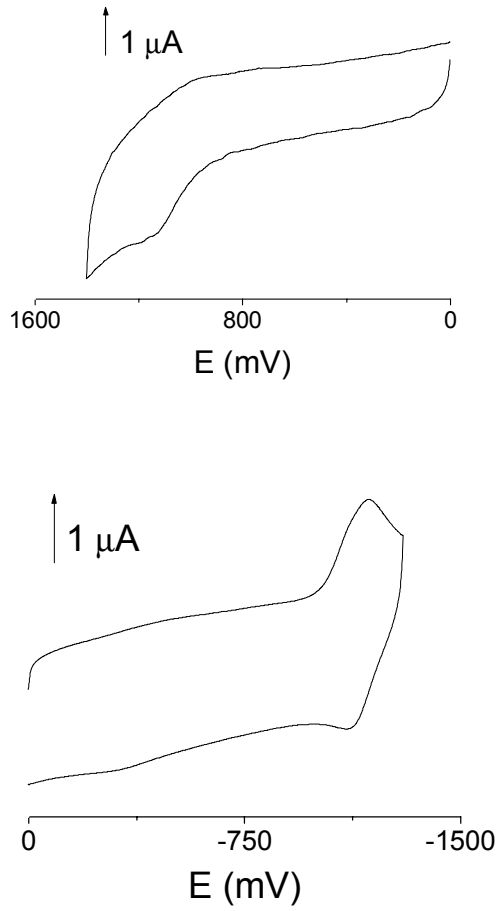

Figure 2.11. Cyclic voltammetry of chemically prepared **P8FT** dip-coated onto an electrode surface (0.1 M Bu_4NPF_6/CH_2Cl_2, carbon working electrode): top: 0 to +1300 mV; bottom, 0 to -1500 mV.

Bulk electrolysis of dimer, **6** (5.0 mM in 0.1 M Bu_4NPF_6/CH_2Cl_2, ITO glass as working electrode) at +1.80 V (dimer **6**, E_{ox} = + 1.75 V) deposits a yellow-green film. This neutral state film absorbs at 311 nm. Doping experiment was done with the same film on ITO glass in a solution only with electrolyte (0.1 M Bu_4NPF_6/CH_2Cl_2). Bulk electrolysis of the film at –1300 mV changes the color of the film from yellow-green to brown. The doped state film has two major absorptions, 351 nm and 453 nm, both of them red shifted relative to the neutral state film, Figure 2.12. This electrochromism indicates the twisted polymer backbone of PF8T can be planarized upon doping, since the doped polythiophene backbone takes more quinoid form, similar to the photoexcited state.

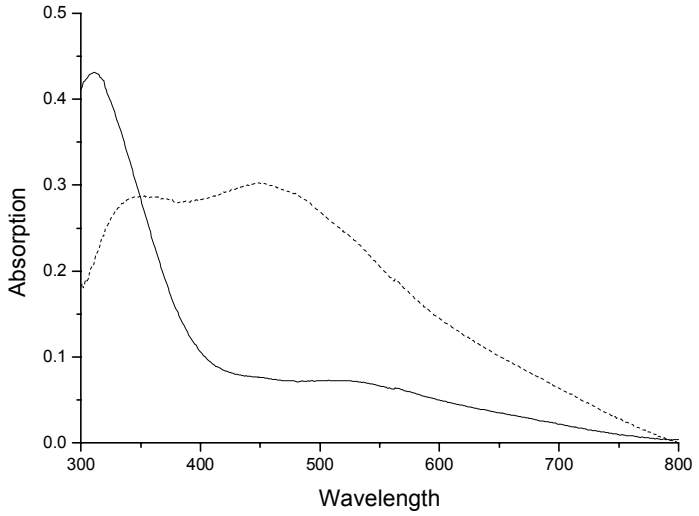

Figure 2.12. UV-vis absorption spectra of electrochemically deposited **PF8T** film: neutral state (—); doped state, -1500 mV (---).

Photophysics

The conjugation length of poly(3-alkylthiophene)s can be assessed from the absorption maximum in the electronic spectrum. Whereas regioregular (i.e., head-to-tail) poly(3-octylthiophene), PH8T, displays a maximum at 442 nm in $CHCl_3$/Freon-113 solution, the absorbance maximum of PF8T appears at 328 nm (i.e., blue shifted by 114 nm), Figure 2.13. This blue shift could arise from a particularly low molecular weight, thereby limiting the conjugation length; electronic effects of the substituents; or disruption of conjugation arising from twisting around the backbone. We have already determined that the degree of polymerization of this sample is high enough so as not to limit the extent of conjugation. In addition, the electronic effect of perfluoroalkyl substituents on the absorption spectra of arenes is relatively small (e.g., for 3-(perfluorooctyl)thiophene, **2**, the λ_{max} is at 229 nm; for the alkyl analog 3-octylthiophene, it is at 235 nm). Thus, we ascribe the anomalously low absorption maximum of PF8T to the effect of twisting around the backbone. Fluorine (van der Waals radius, r = 1.35Å) is slightly larger than hydrogen (r = 1.2Å). In addition, the fluoroalkyl substituents on these polymers may be more bulky than alkyl chains because the fluorocarbon chains form a helical low energy conformation. It is apparent that the difference in size of the side chains is sufficiently large to cause twisting of the conjugated backbone of PF8T due to steric interactions between the perfluoroalkyl substituents and the adjacent repeat unit.

PF8T exhibits green fluorescence (λ_{max} = 512 nm) in solution with a maximum blue-shifted by 58 nm relative to PH8T (570 nm), Figure 2.13. Accordingly, PF8T shows a Stokes shift of ca. 1.4 eV (186 nm) compared to only 0.6 eV (126 nm) for PH8T. This suggests that there is a large difference in the conformation of the polymer backbone

between the ground state and the excited state of the fluorinated polymer. We explain this observation on the basis of the planarization of the backbone in the excited state which has more quinoid character than the benzenoid form of the ground state. Thus, the effect of twisting due to steric interactions in the ground state is relatively weak and it is overcome in the excited state by formation of the quinoid form, Figure 2.13.

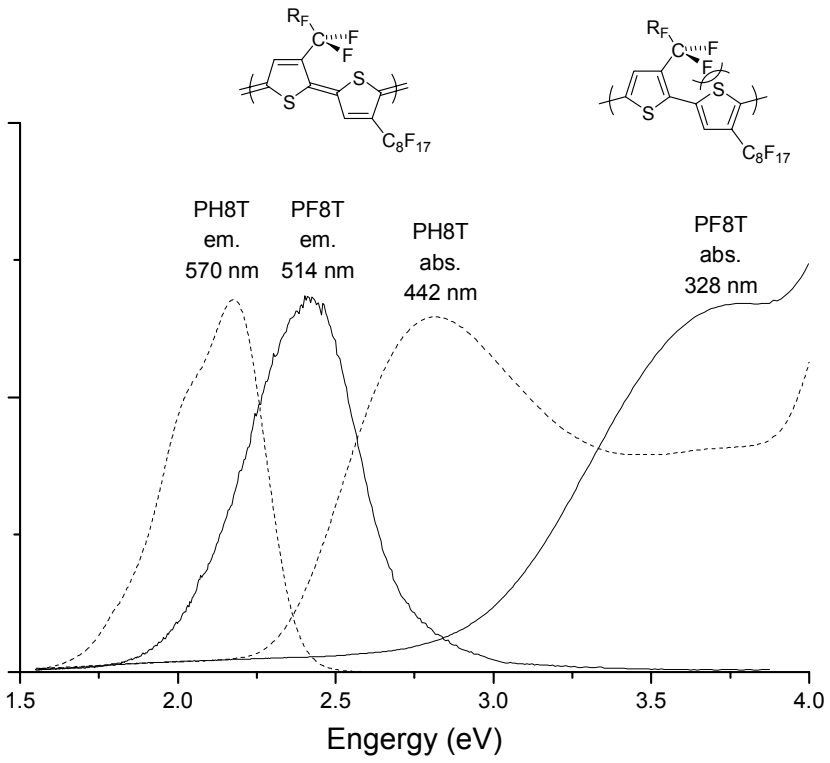

Figure 2.13. Absorption and emission spectra of **PF8T** solution (—) (0.1 mM in 1:1 $CHCl_3$/Freon-113) displaying a low $_{max}$ due to a twisted benzenoid ground state and emission from a more planar quinoid excited state, resulting in a large Stokes shift. Spectra of **PH8T** (----) provided for comparison.

The absorption maximum (336 nm) and fluorescence maximum (508 nm) of a thin film of PF8T are also both blue-shifted relative to PH8T, Figure 2.14. This suggests PF8T still takes a twisted conformation in solid state, relative to the planar backbone in films of PH8T.

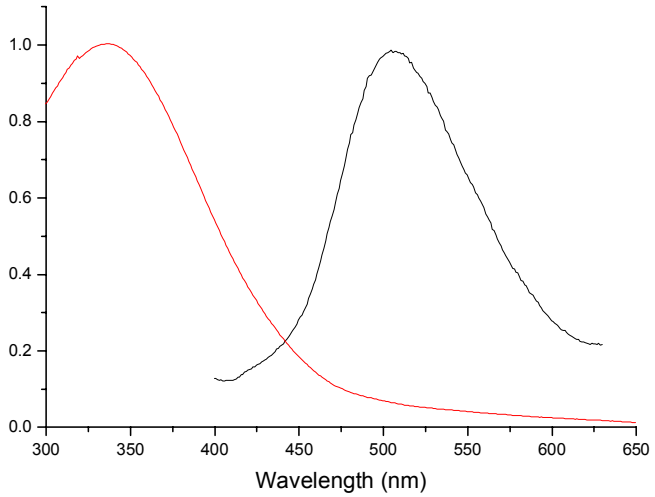

Figure 2.14. Absorption and emission spectra of spin-coated **PF8T** films.

Solubility in supercritical CO_2

The solubility of PF8T in $scCO_2$ was established by placing a sample into a stainless steel cell equiped with quartz windows and a magnetic stir bar.[25] UV-visible spectra were measured at 50 ^{o}C at various pressures. At 1500 psi the polymer starts to dissolve, giving rise to a peak with λ_{max} of 310 nm. As the pressure is increased, the

absorption becomes greater, corresponding to a more concentrated solution, and there is a small (ca. 10 nm) blue shift in the absorbance maximum. The concentration of the solution increases with increasing pressure up to 2400 psi, Figure 2.15.

Fluorescence spectra were also collected at 50 ^{o}C at these pressures. The fluorescence intensity is first increased with the increase of pressure up to 1800 psi. At the higher pressure conditions, supercritical CO_2 dissolves more PF8T and the concentration is high enough to start to quench the fluorescence of the polymer. So the fluorescence intensity is decreased above 1800 psi, and the quenching effect levels off at even higher pressure (e.g. 2400 psi.), Figure 2.15.

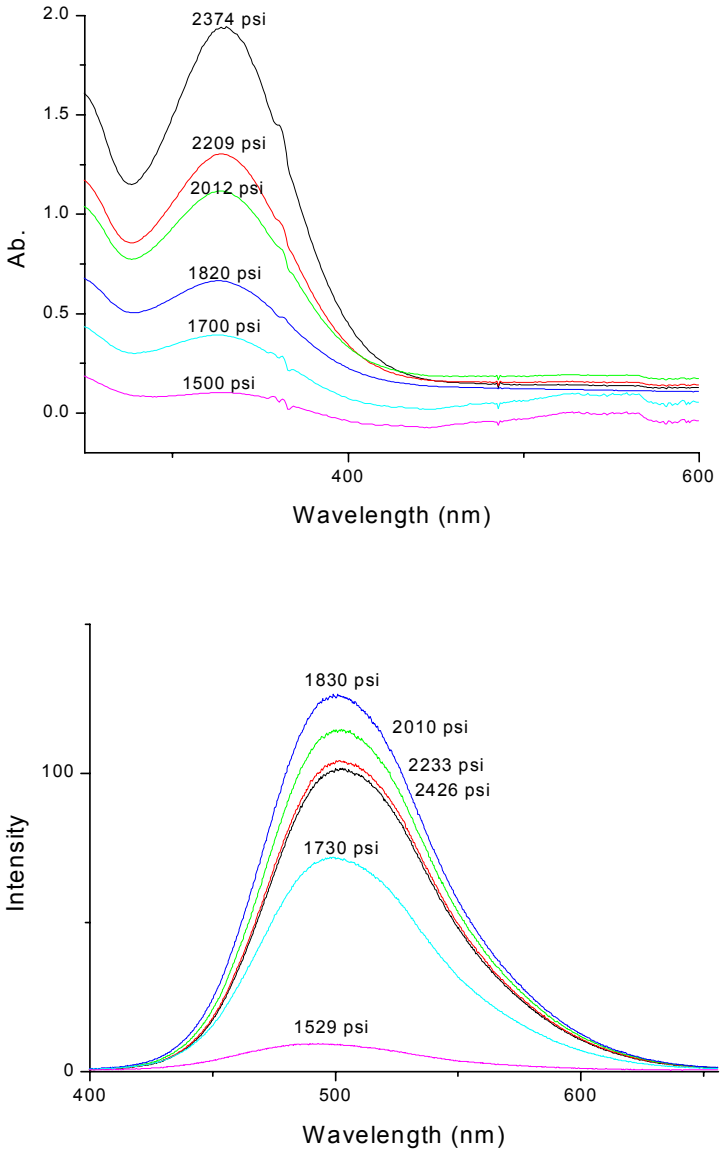

Figure 2.15. Absorption and emission spectra **PF8T** in $scCO_2$ (50 °C), with the increasing of pressure.

Conclusion

In conclusion, we have shown that poly(3-(perfluorooctyl)thiophene) can be prepared by organometallic coupling. The unique combination of features of the perfluoroalkyl side chains affords a material which undergoes reversible reduction, displays a large Stokes shift, and which is soluble in $scCO_2$. This combination of properties will allow for new opportunities in the development of new functional materials and processing of conjugated polymers.

References

1. Crooks, R. M.; Chyan, O. M. R.; Wrighton, M. S. *Chem. Mater*. **1989**, *1*, 2.

2. Lee, K.; Sotzing, G. *Macromolecules* **2001**, *34*, 5746.

3. Pomerantz, M.; Cheng, Y.; Kasim, R. K.; Elsenbaumer, R. L. *J. Mater. Chem*. **1999**, *9*, 2155.

4. Greve, D. R.; Apperloo, J. J.; Janssen, A. J. *Eur. J. Org. Chem.* **2001**, 3437.

5. Hong, X.; Tyson, J. C.; Middlecoff, J. S.; Collard, D. M. *Macromolecules* **1999**, *32*, 4232.

6. Hong, X. M.; Collard, D. M. *Macromolecules* **2000**, *33*, 6916.

7. Hong, X.; Tyson, J. C.; Collard, D. M. *Macromolecules* **2000**, *33*, 3502.

8. Robitaille, L.; Leclerc, M. *Macromolecules* **1994**, *27*, 1847.

9. Leclerc, M.; Robitaille, M.; Bergeron, J. Y.; Callender, C. L. *Polym. Prep. (Am. Chem. Soc., Div. Polym. Chem.)* **1994**, *35(1)*, 305.

10. Ritter, S. K.; Noftle, R. E.; Ward, A. E. *Chem. Mater.* **1993**, *5*, 752.

11. a) Facchetti, A.; Deng, Y.; Wang, A.; Koide, Y.; Sirringhaus, H.; Marks, T. J.; Friend, R. H. *Angew. Chem., Int. Ed.* **2000**, *39*, 4547. b) Facchetti, A.; Mushrush, M.; Katz, H. E.; Marks, T. J. *Adv. Mater.* **2003**, *15*, 33

12. Sakamoto, Y.; Komatsu, S.; Suzuki, T. *J. Am. Chem. Soc.* **2001**, *123*, 4643.

13. Anderson, P. E.; Badlani, R. N.; Mayer, J.; Mabrouk, P. A. *J. Am. Chem. Soc.* **2002**, *124*, 10284.

14. a) Kerton, F. M.; Lawless, G. A.; Armes, S. P. *J. Mater. Chem.* **1997**, 7, 1965. b) DeSimone, J. M.; Ni, Y. US Patent 5 855 819, **1999.**

15. a) Tang, M.; Wen, T.-Y.; Du, T.-B.; Chen, Y.-P. *Eur. Polym. J.* **2003**, 39, 151. b) Fu, Y.; Palo, D. R.; Erkey, C.; Weiss, R. A. *Macromolecules* **1997,** 30, 7611.

16. DeSimone, J. M.; Guan, Z.; Elsbernd, C. S. *Science* **1992**, *257*, 945.

17. McCullough, R. D. *Adv. Mater.* **1998**, *10*, 93.

18. Cowell, A. B.; Tamborski, C. *J. Fluorine Chem*. **1981**, *17*, 3672.

19. Umemoto, T.; Kuriu, Y.; Shuyama, H. *Chem. Lett*. **1981**,1633.

20. Leroy, J.; Rubinstein, M.; Wakselman, C. *J. Fluorine Chem*. **1985**, *27*, 291.

21. Yoshida, M.; Yoshida, T.; Kamigata, N.; Kobayashi, M. *Bull. Chem. Soc. Jpn.* **1988**, *61*, 3549.

22. Endo, T.; Takeoka, Y.; Rikukawa, M.; Sanui, K. *Synth. Met*. **2003**, *135*, 333.

23. a) McCullough, R. D.; Lowe, R. D.; Jayaraman, M.; Anderson, D. L. *J. Org. Chem.* **1993**, *58*, 904. b) McCullough, R. D.; Tristram-Nagle, S.; Williams, S. P.; Lowe, R. D.; Jayaraman, M. *J. Am. Chem. Soc.* **1993**, *115*, 4910.

24. Noftle, R. E.; Odian, M. A.; Ritter, S. K. *J. Fluorine Chem.* **1995**, *71*, 177.

25. Kazarian, S. G.; Vincent, M. F.; Eckert, C. A. *Rev. Sci. Instrum.* **1996**, *67*, 1586.

CHAPTER III

SYNTHESIS AND CHARACTERIZATION OF REGIOREGULAR ALTRENATING ALKYL/PERFLUOROALKYL-SUBSTITUTED POLYTHIOPHENE

Introduction

Semifluoroalkyl side chains have been attached to a wide variety of polymers to provide materials with unusual properties which arise as a consequence of the hydrophobicity, rigidity, thermal stability, chemical and oxidative resistance, and self-organization of perfluoroalkyl chains.[1] Following earlier reports on the synthesis and polymerization of 3-(semifluoroalkyl)thiophene, [2] Hong and Collard have reported that semifluoroalkyl side chains allow for control over the supramolecular organization of conjugated polymers.[3,4,5] Control of supramolecular packing of conjugated chains is expected to have profound effects on their properties and the efficiency of devices incorporating these materials (e.g., LEDs and FETs).[6,7,8] The immiscibility of the hydrocarbon and fluorocarbon segments in the side chains of poly(3-semifluoroalkylthiophene)s provided materials which display liquid crystallinity[3,5] and highly ordered and oriented solid state structures.[4] These studies made use of side chains in which an alkyl spacer insulates the electron-withdrawing influence of the fluoroalkyl segment from the conjugated backbone. The influence of direct attachment of

perfluoroalkyl side chains on the electronic structure of conjugated oligothiophenes and polythiophenes has only been reported recently.[9,10] The fluoroalkyl substituents raise the oxidation potential of monomers, oligomers[11,12] and polymers[9,10] relative to the alkyl-substituted analogs. In addition, the electron-withdrawing nature of the side chains renders oligo- and polythiophenes n-dopable. Most recently, we have described the solubility of poly(3-(perfluorooctyl)thiophene) in supercritical CO_2 by virtue of their CO_2-philic side chains.[10]

Copolymerization is a general approach to expand the range of properties of polymers and to create self-assembling supramolecular structures. In addition to the variation of the comonomers used, the microstructure (random, alternating, block, graft) also plays a large role in determining the properties of the copolymer. Thus, random copolymers have been prepared from thiophene and a number of other arenes (e.g., pyrrole,[13] fluorene,[14, 15] quinoxaline,[16] thiazole[17]) to provide materials with tunable electronic properties. Extensive research on poly(3-alkylthiophene)s has led to the preparation of copolymers of 3-alkylthiophenes with other substituted thiophenes such as those with alkyl,[18] alkoxyl,[19] oligo(ethylene glycol),[20] ionic[21] side chains.

Block[22] and alternating copolymer[23] microstructures with thiophenes have attracted less attention. Both of these approaches offer opportunities to prepare well-defined materials with electron rich and electron poor segments in the backbone with potential use in electronic and optoelectronic applications. For most of the electroluminescent conjugated polymers reported in literature, the hole injection/transport is more favorable than the electron injection/transport because of the high electron richness of the conjugated backbone. To achieve performance of devices incorporating

these materials, it is desirable to design and synthesize polymers in which there is a balance between rates of injection of electrons and holes, as well as enhance the charge-transporting ability. The regioregular alternating copolymer of 3-dodecyl and 3-cyanothiophenes[24] has been synthesized, but does not show significant difference in its photophysics from poly(3-dodecylthiophene). Poly(3-methoxy-4'-cyano-2,2'-bithiophene)[25, 26] has also been made and the push-pull electronic structure has been proposed as the molecular quantum well to confine charge carriers.

Here we report the preparation and characterization of a regioregular alternating copolymer consisting of 3-octylthiophene and 3-(perfluorooctyl)thiophene units (PT-H8-*alt*-F8) and the homologues. The properties are compared to those of the regioregular homopolymers: poly(3-octylthiophene), PT-H8, and poly(3-(perfluorooctyl)thiophene), PT-F8. This illustrates the use of perfluorinated substituents to tune the electronic structure of polythiophenes, and provides a material which is highly fluorescent in solid state.

Experimental

General methods

All reagents were obtained from commercial sources and used without further purification unless stated otherwise. Tetrahydrofuran (THF) and diethyl ether was dried over sodium benzophenone ketyl prior to distillation under nitrogen. Methylene chloride was dried over calcium hydride prior to distillation under nitrogen. Column chromatography was performed on silica gel (40 mesh, 60Å, Baker). Thin layer chromatography was performed on 3×5 cm plates of silica gel (0.2 mm thick, 60 F_{254})

on an aluminum support (EM Separations). All ^{1}H NMR spectra were collected on a Varian Gemini 300 MHz instrument using $CDCl_3$ as the solvent unless otherwise specified. Chemical shifts are reported relative to internal tetramethylsilane. ^{13}C NMR spectra were obtained at 75.5 MHz. IR analysis was performed on a Nicolet 520 FTIR spectrometer. UV-vis analysis was performed with a Perkin-Elmer Lambda 19 spectrometer. Fluorescence spectra were collected with a Spex Fluorolog Fluometer 1681 0.22m Spectrometer. Electron ionization or chemical ionization mass spectra was performed using a VG Analytical 70-SE instrument with a L-250J Data System Analyzer.

Polymer films were spin coated onto glass slides or ITO glass slides using a Specialty Coating System P-6000 spin coater.

Electrochemical experiments were performed using a BAS 100B electrochemical analyzer in three-electrode cell equipped with a 2.0 mm^2 gold, platinum or graphite disk working electrode, a platinum wire counter electrode, and a saturated calomel electrode (SCE).

3-(Perfluorooctyl)thiophene (**2**), 3-(perfluorohexyl)thiophene (**3**), 2-bromo-4-(perfluorooctyl)thiophene (**4**) and 2-bromo-4-(perfluorohexyl)thiophene (**5**) were synthesized following the methods we reported previously.[10]

Synthesis

[1',3'-(2',2'-Dimethylpropylene)]-3-octyl-2-thienylboronate (7). A mixture of magnesium (50.0 mmol, 1.22 g) in dry THF (45 mL) was heated to maintain a gentle reflux. 2-Bromo-3-octylthiophene (9.08 g, 33.0 mmol) was added and the mixture was kept at reflux for 3 h. The resulting solution was cooled and transferred via a cannula to a

solution of trimethyl boronate (130 mmol, 14.6 mL) in dry THF (45 mL) at –78 °C. The mixture was allowed to warm to room temperature and stirred overnight. The reaction mixture was poured into 10% HCl (45 mL) and extracted with Et_2O (3 × 100 mL). The combined extracts were dried over Na_2SO_4 and molecular sieves (4Å) in the presence of 2,2-dimethyl-1,3-propanediol (3.45 g, 33.0 mmol). The solvent was removed using a rotary evaporator to provide 9.65 g of a yellow liquid contaminated by white crystals. This crude product was dissolved in hexanes and filtered. The solvent was removed and the crude product was heated under vacuum for 1 day at 140 °C to remove 3-octylthiophene to give **7**. (8.33 g, 82%), as a viscous yellow liquid. – ^{1}H NMR (300 MHz, $CDCl_3$): δ 7.42 (d, J = 4.7, 1 H), 6.99 (d, J = 4.7, 1 H), 3.75 (s, 4 H), 2.86 (m, 2 H), 1.55 (m, 2 H), 1.27 (m, 10 H), 1.02 (s, 6 H), 0.88 (m, 3 H). ^{13}C NMR (300 MHz, $CDCl_3$): δ 153.3, 130.7, 130.2, 72.5, 32.3, 32.1, 30.6, 30.4, 30.0, 29.8, 29.6, 23.1, 22.3, 14.5; IR (NaCl): 3118, 2961, 2933, 1530, 1488, 1298, 1123, 751, 646 cm^{-1}. MS (EI): M^+ = 276.

[1',3'-(2',2'-Dimethylpropylene)]-3-dodecyl-2-thienylboronate (8). The title compound was prepared according to the procedure described for the synthesis of **7**. Treatment of 2-bromo-3-dodecylthiophene (4.97 g, 15.0 mmol) with magnesium (0.58 g, 24.2 mmol) followed by trimethyl boronate (7.10 mL, 63.0 mmol) gave **8** (90%), as a viscous yellow liquid. – ^{1}H NMR (300 MHz, $CDCl_3$): δ 7.42 (d, J = 4.7, 1 H), 6.99 (d, J = 4.7, 1 H), 3.75 (s, 4 H), 2.86 (m, 2 H), 1.55 (m, 2 H), 1.27 (m, 18 H), 1.02 (s, 6 H), 0.88 (m, 3 H). ^{13}C NMR (300 MHz, $CDCl_3$): δ 153.3, 130.7, 130.2, 72.5, 32.3, 32.1, 30.0, 29.8, 29.6, 23.1, 22.3, 14.5. IR (NaCl): 3118, 2961, 2933, 1530, 1488, 1298, 1123, 751, 646 cm^{-1}. MS (EI): M^+ = 332.

[1',3'-(2',2'-Dimethylpropylene)]-3-hexyl-2-thienylboronate (9). The title compound was prepared according to the procedure described for the synthesis of **7**. Treatment of 2-bromo-3-hexylthiophene (12.30 g, 50.0 mmol) with magnesium (1.84 g, 75.8 mmol) followed by trimethyl boronate (18.6 mL, 195 mmol) gave **9** (80%), as a viscousk yellow liquid. – ^{1}H NMR (300 MHz, $CDCl_3$): δ 7.42 (d, *J* = 4.7, 1 H), 6.99 (d, *J* = 4.7, 1 H), 3.75 (s, 4 H), 2.86 (m, 2 H), 1.55 (m, 2 H), 1.27 (m, 6H), 1.02 (s, 6 H), 0.88 (m, 3 H). ^{13}C NMR (300 MHz, $CDCl_3$): δ 153.3, 130.7, 130.2, 72.5, 32.3, 32.1, 30.3, 29.4, 23.0, 22.3, 14.5. IR (NaCl): 3118, 2961, 2933, 1530, 1488, 1298, 1123, 751, 646 cm^{-1}. MS (EI): M^{+} = 248.

4'-Perfluorooctyl-3-octyl-[2,2']-bithiophene (10). N_2 was bubbled through a solution of 2-bromo-4-(perfluorooctyl)thiophene (4.64 mmol, 2.70 g) in DME (60 mL) for 10 min. $Pd(PPh_3)_4$ (0.139 mmol, 0.161 g) was added and the mixture was stirred for 10 min at room temperature. [1',3'-(2',2'-Dimethylpropylene)]-3-octyl-2-thienylboronate, (5.10 mmol, 1.86 g) and 13 mL 1M $NaHCO_3$ were added and the mixture was heated to reflux overnight with vigorous stirring. The reaction mixture was poured into H_2O (100 mL) and extracted with Et_2O (3 × 100 mL).The combined organic extracts were dried over Na_2SO_4, the solvent was removed on a rotary evaporator and the residue was heated under vacuum for 1 day at 140 ^{o}C to remove 3-octylthiophene. The crude product was purified by column chromatography (silica gel/hexane) to give **10** (2.91 g, 90%), as a colorless liquid. – ^{1}H NMR (300 MHz, $CDCl_3$): δ 7.66 (s, 1 H), 7.23 (d, *J* =5.8, 1 H), 7.18 (s, 1 H), 6.95 (d, *J* =5.8, 1 H), 2.72 (t, *J* =8.1, 2 H), 1.60 (m, 2 H), 1.27 (m, 10H), 0.86 (m, 3 H). ^{13}C-NMR (300 MHz, $CDCl_3$): δ 141.3, 139.5, 130.3, 128.0,

125.2, 124.0, 32.0, 30.8, 29.7, 29.6, 29.5, 29.3, 23.7, 14.2. IR (NaCl): 3118 (C-H, sp^3), 2973, 2855 (C-H, sp^2), 1467, 1237, 1209 (C-F), 707 cm^{-1}. MS (EI): $M^+ = 696$.

4'-Perfluorooctyl-3-dodecyl-[2,2']-bithiophene (11). The title compound was prepared according to the procedure described for the synthesis of **10**. Reaction of 2-bromo-4-perfluorooctylthiophene (2.70 g, 4.64 mmol) and [1',3'-(2',2'-dimethylpropylene)]-3-dodecyl-2-thienylboronate, (1.86 g, 5.10 mmol) gave **11** (74%), as a colorless liquid. – ^{1}H NMR (300 MHz, $CDCl_3$): δ 7.66 (s, 1 H), 7.23 (d, *J* =5.8, 1 H), 7.18 (s, 1 H), 6.95 (d, *J* =5.8, 1 H), 2.72 (t, *J* =8.1, 2 H), 1.60 (m, 2 H), 1.27 (m, 18H), 0.86 (m, 3 H). ^{13}C NMR (300 MHz, $CDCl_3$): δ 141.3, 139.5, 130.3, 128.0, 125.2, 124.0, 32.3, 30.0, 29.7, 29.6, 29.3, 23.1, 14.5. IR (NaCl): 3118 (C-H, sp^3), 2973, 2855 (C-H, sp^2), 1467, 1237, 1209 (C-F), 707 cm^{-1}. MS (EI): $M^+ = 752$.

4'-Perfluorohexyl-3-dodecyl-[2,2']-bithiophene (12). The title compound was prepared according to the procedure described for the synthesis of **10**. Reaction of 2-bromo-4-perfluorohexylthiophene (9.28 g, 19.3 mmol) and [1',3'-(2',2'-dimethylpropylene)]-3-dodecyl-2-thienylboronate, (8.43 g, 23.2 mmol) gave **12** (75%), as a colorless liquid. – ^{1}H NMR (300 MHz, $CDCl_3$): δ 7.66 (s, 1 H), 7.23 (d, *J* =5.8, 1 H), 7.18 (s, 1 H), 6.95 (d, *J* =5.8, 1 H), 2.72 (t, *J* =8.1, 2 H), 1.60 (m, 2 H), 1.27 (m, 18H), 0.86 (m, 3 H). ^{13}C-NMR (300 MHz, $CDCl_3$): δ 141.3, 139.5, 130.3, 128.0, 125.2, 124.0, 32.3, 30.0, 29.7, 29.6, 29.3, 23.1, 14.5. IR (NaCl): 3118 (C-H, sp^3), 2973, 2855 (C-H, sp^2), 1467, 1237, 1209 (C-F), 707 cm^{-1}. MS (EI): $M^+ = 652$.

4'-Perfluorohexyl-3-hexyl-[2,2']-bithiophene (13). The title compound was prepared according to the procedure described for the synthesis of **10**. Reaction of 2-bromo-4-perfluorohexylthiophene (4.80 g, 10.0 mmol) and [1',3'-(2',2'-

dimethylpropylene)]-3-hexyl-2-thienylboronate (3.36 g, 12.0 mmol) gave **13** (80%), as a colorless liquid. – ^{1}H NMR (300 MHz, $CDCl_3$): δ 7.66 (s, 1 H), 7.23 (d, *J* =5.8, 1 H), 7.18 (s, 1 H), 6.95 (d, *J* =5.8, 1 H), 2.72 (t, *J* =8.1, 2 H), 1.60 (m, 2 H), 1.27 (m, 6H), 0.86 (m, 3 H). ^{13}C NMR (300 MHz, $CDCl_3$): δ 141.3, 139.5, 130.3, 128.0, 125.2, 124.0, 32.3, 30.3, 29.4, 23.0, 14.5. IR (NaCl): 3118 (C-H, sp^3), 2973, 2855 (C-H, sp^2), 1467, 1237, 1209 (C-F), 707 cm^{-1}. MS (EI): M^+ = 568.

2-Bromo-4'-perfluorooctyl-3-octyl-[2,2']-bithiophene (14). A mixture of 4'-perfluorooctyl-3-octyl-[2,2']-bithiophene (1.10 g, 1.58 mmol) and NBS (0.338 g, 1.90 mmol) in DMF (5 mL) was stirred at room temperature overnight. The reaction mixture was poured into water (10 mL) and extracted with petroleum ether (3 × 20 mL). The combined extracts were dried over Na_2SO_4 and the solvent was removed using a rotary evaporator. The crude product was purified by column chromatography (silica gel/petroleum ether) to give **14** (0.88 g, 72%), as a colorless liquid. – ^{1}H NMR (300 MHz, $CDCl_3$): δ 7.67 (s, 1 H), 7.12 (s, 1 H), 6.91 (s, 1 H), 2.64 (t, *J* =8.1, 2 H), 1.60 (m, 2 H), 1.27 (m, 10H), 0.86 (m, 3 H). IR (NaCl): 3118, 2973, 2933, 2861, 1466, 1262, 1209, 1163, 908, 715, 657 cm^{-1}. HRMS (EI): 773.99153 (observed), 773.99183 (calculated), Δ = 0.4 ppm.

2-Bromo-4'-perfluorooctyl-3-dodecyl-[2,2']-bithiophene (15). The title compound was prepared according to the procedure described for the synthesis of **14**. Reaction of 4'-perfluorooctyl-3-dodecyl-[2,2']-bithiophene (0.552 g, 1.00 mmol) and NBS (0.214 g, 1.20 mmol) gave **15** (80%), as a colorless liquid. – ^{1}H NMR (300 MHz, $CDCl_3$): δ 7.67 (s, 1 H), 7.12 (s, 1 H), 6.91 (s, 1 H), 2.64 (t, *J* =8.1, 2 H), 1.60 (m, 2 H),

1.27 (m, 18H), 0.86 (m, 3 H). IR (NaCl): 3118, 2973, 2933, 2861, 1466, 1262, 1209, 1163, 908, 715, 657 cm^{-1}. MS (EI): M^+ = 830.

2-Bromo-4'-perfluorohexyl-3-dodecyl-[2,2']-bithiophene (16). The title compound was prepared f according to the procedure described for the synthesis of **14**. Reaction of 4'-perfluorohexyl-3-dodecyl-[2,2']-bithiophene (13.3 g, 20.3 mmol) and NBS (3.59 g, 20.3 mmol) gave **16** (75%), as a colorless liquid. – ^{1}H NMR (300 MHz, $CDCl_3$): δ = 7.67 (s, 1 H), 7.12 (s, 1 H), 6.91 (s, 1 H), 2.64 (t, *J* =8.1, 2 H), 1.60 (m, 2 H), 1.27 (m, 18H), 0.86 (m, 3 H). IR (NaCl): 3118, 2973, 2933, 2861, 1466, 1262, 1209, 1163, 908, 715, 657 cm^{-1}. HRMS (EI): 730.06032 (observed), 730.06082 (calculated), Δ = 0.7 ppm.

2-Bromo-4'-perfluorohexyl-3-hexyl-[2,2']-bithiophene (17). The title compound was prepared according to the procedure described for the synthesis of **14**. Reaction of 4'-perfluorohexyl-3-hexyl-[2,2']-bithiophene (0.606 g, 1.00 mmol) and NBS (0.214 g, 1.20 mmol) gave **17** (80%), as a colorless liquid. – ^{1}H NMR (300 MHz, $CDCl_3$): δ = 7.67 (s, 1 H), 7.12 (s, 1 H), 6.91 (s, 1 H), 2.64 (t, *J* =8.1, 2 H), 1.60 (m, 2 H), 1.27 (m, 6H), 0.86 (m, 3 H). IR (NaCl): 3118, 2973, 2933, 2861, 1466, 1262, 1209, 1163, 908, 715, 657 cm^{-1}. MS (EI): M^+ = 646.

Poly(4'-Perfluorooctyl-3-octyl-[2,2']-bithiophene) (PT-H8-*alt*-F8). Into a dry Shlenk flask was placed a solution of dry diisopropylamine (0.86 mL, 6.1 mmol) in freshly distilled THF (35 mL). A solution of n-butyllithium (2.5 M in hexane, 2.55 mL, 6.13 mmol) was added at room temperature. The mixture was cooled to -40 °C and stirred for 40 min. The fresh LDA was then cooled to -78 °C, and 2-bromo-4'-perfluoroctyl-3-octyl-[2,2']-bithiophene (4.32 g, 5.57 mmol) was added. The mixture was stirred for 40

min at –40 °C, then cooled to -60 °C, $MgBr_2.Et_2O$ (1.58 g, 6.13 mmol) was added, and the reaction was stirred at - 60 °C. After 20 min, the reaction was then warmed to - 40 °C and stirred for another 15 min. The reaction mixture was allowed to slowly warm to - 5 °C. At - 5 °C, 0.5 mol % $Ni(dppp)Cl_2$ (16.6 mg, 0.0310 mmol) was added. The mixture was allowed to warm to room temperature and stirred overnight. The solution was poured into MeOH (300 mL), and the resulting precipitate was filtered and washed with MeOH (100 mL), H_2O (100 mL) and MeOH (100 mL) again. The solid was dried under vacuum to give a deep red solid (1.20 g, 31%). Removal of oligomers and impurities was achieved by subjecting the solid to extractions in a Soxhlet extractor with MeOH and acetone, followed by hexane, chloroform, THF and chlorobenzene. The hexane, chloroform, and chlorobenzene fractions were characterized.

Poly(4'-Perfluorohexyl-3-dodecyl-[2,2']-bithiophene) (PT-H12-*alt*-F6). The title polymer was prepared according to the procedure described for the synthesis of **PT-H8-*alt*-F8**. Polymerization of 2-bromo-4'-perfluorohexyl-3-dodecyl-[2,2']-bithiophene (8.74 g, 11.4 mmol) gave **PT-H12-*alt*-F6** as a deep red solid (35%).

3,3'-Diperfluorooctyl-3'',3'''-dioctyl-[2',5]-[5',5'']-[2''-5''']-tetrathiophene (18). *Method A: Oxidation.* A solution of 4'-perfluorooctyl-3-octyl-[2,2']-bithiophene (1.21 g, 1.74 mmol) in 8 mL $CHCl_3$ was added via syringe to a solution of anhydrous $FeCl_3$ (1.13 g, 6.95 mmol) in $CHCl_3$ (2 ml) in a 25 mL two neck round-bottom flask with argon. The mixture was stirred under argon for 24 h and aqueous HCl (10%, 20 mL) was added. The mixture was extracted with hexane (3 × 30 mL), and the combined extracts were washed with H_2O (100 mL). The crude product was purified by column chromatography (silica gel/hexane) to give **18** (0.76 g, 63%), as a red solid.

Method B: Organometallic coupling: n-BuLi (2.5 M in hexane, 0.13 mL, 0.32 mmol) was added to a solution of 2-bromo-4'-perfluorooctyl-3-octyl-[2,2']-bithiophene (0.18 g, 0.23 mmol) in dry Et_2O (10 mL) uder argon at -78°C. The mixture was stirred at -78°C for 1 h, $ZnCl_2$ (65 mg, 0.48 mmol) was added, and the mixture was warmed to room temperature and stirred for 1 h. A solution of $Pd(PPh_3)_4$ (19 mg, 0.016 mmol) and another portion of 2-bromo-4'-perfluorooctyl-3-octyl-[2,2']-bithiophene (0.18 g, 0.23 mmol) in 10 mL dry Et_2O was added and the mixture was heated at reflux overnight. The mixture was poured into H_2O (100 mL) and extracted with Et_2O (3 × 100 mL). The extract was washed with brine (100 mL) and dried over anhydrous $MgSO_4$. The crude product was purified by column chromatography (silica/hexane) to give **18** (0.27 g, 84%), as a red solid. – ^{1}H NMR (300 MHz, $CDCl_3$): δ 7.71 (s, 1 H), 7.23 (s, 1 H), 7.08 (s, 1 H), 2.75 (t, *J* =8.1, 2 H), 1.60 (m, 2 H), 1.27 (m, 10H), 0.86 (m, 3 H). ^{13}C-NMR (300 MHz, $CDCl_3$): δ 141.3, 139.5, 130.3, 128.0, 125.2, 124.0, 32.1, 30.7, 29.5, 29.3, 29.0, 28.6, 23.0, 14.4. IR (NaCl): 2926, 2856, 1249, 1214, 1151, 674. MS (FAB): M^+ = 1390.

2-Bromo-5'-tributylstannyl-4'-perfluorohexyl-3-dodecyl-[2,2']-bithiophene (19). n-BuLi (2.5 M in hexane, 0.72 mL, 1.8 mmol) was added to diisopropyl amine (0.25 mL, 1.8 mmol) in 10 mL dry THF at –70°C under argon and the mixture was stirred for 20 min. 2-Bromo-4'-perfluorohexyl-3-dodecyl-[2,2']-bithiophene (1.10 g, 1.5 mmol) was added and the mixture was stirred for 1 h at –70°C. Tributyltin chloride (0.45 mL, 1.65 mmol) was added and the mixture was slowly warmed to room temperature and then stirred overnight. The reaction mixture was diluted with 50 mL of Et_2O and washed with H_2O (3 × 50 mL). The organic solution was dried over anhydrous $MgSO_4$ and was filtered through a 5 cm plug of silica gel. Removal of the solvent gave **19** (1.53 g, 100%),

as a colorless liquid. – ^{1}H NMR (300 MHz, $CDCl_3$): δ 7.15 (t, 1 H, *J* =1.4), 6.80 (s, 1 H), 2.57 (t, 2 H, *J* =7.8), 1.60-1.34 (m, 8 H), 1.32-0.93 (m, 30 H), 0.89-0.69 (m, 12 H).

Results and Discussion

Synthesis

4'-Perfluorooctyl-3-octyl-[2,2']-bithiophene **10**, Figure 3.1, was prepared by Suzuki coupling of 2-bromo-4-perfluorooctylthiophene, **3,**[9] and [1',3'-(2',2'-dimethylpropylene)]-3-octyl-2-thienylboronate, **7**,[27] which were both prepared according to literature procedures. Bromination of **10** with *N*-bromosuccinimide in DMF at room temperature resulted in regioselective bromination of the α-thienyl position of the electron-rich alkyl-substituted thiophene rings to give **14**, Figure 3.6. The perfluoroalkyl-substituted ring of **10** resists bromination even under relatively harsh conditions, because the perfluoroalkylation deactivates the aromatic thiophene ring. Other homologues were prepared with the same route.

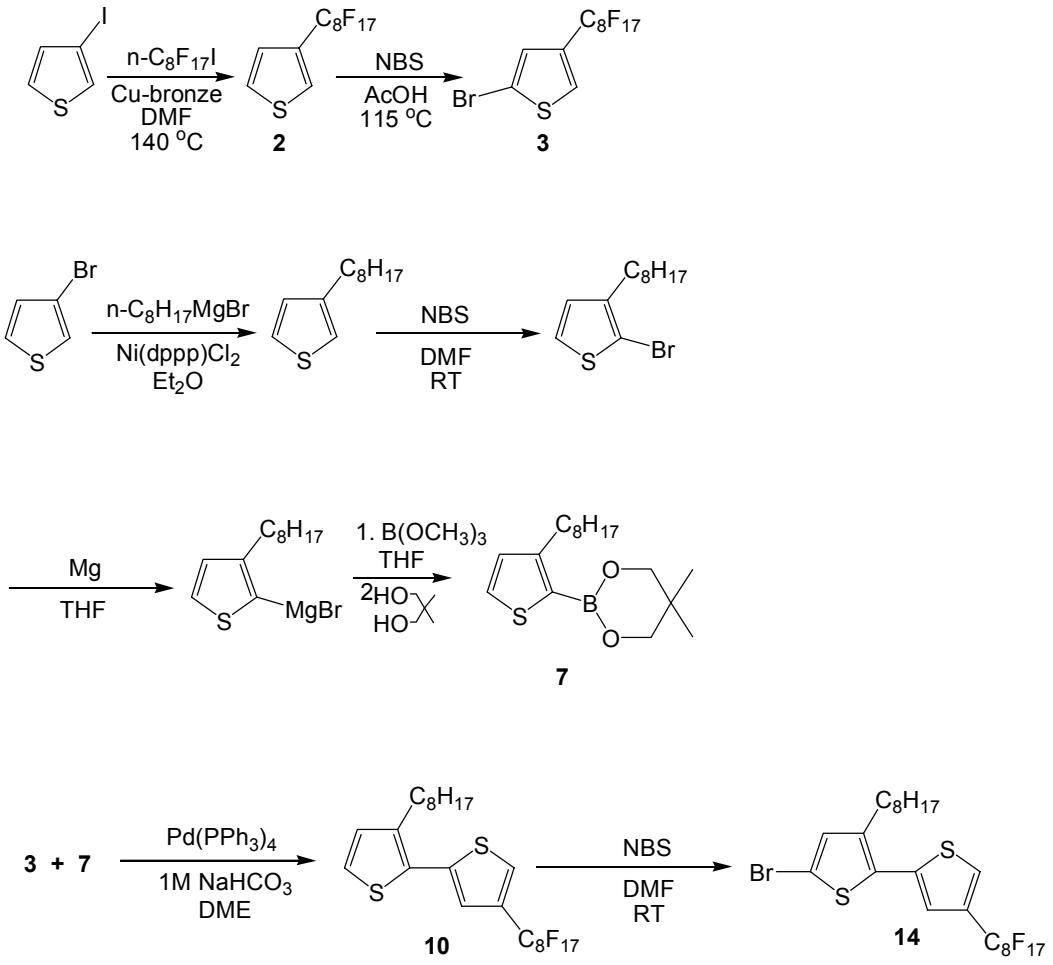

Figure 3.1. Synthesis of monomers.

Chemical Polymerization

Polymerization of **14** to form the regioregular alternating copolymer PT-H8-*alt*-F8 was performed using McCullough's method for the preparation of regioregular PATs,[28] Figure 3.2. Lithiation of **14** with LDA, transmetallation with $MgBr_2$. Et_2O and treatment with a catalytic amount of Ni(II) resulted in a red solution. Addition of

methanol to the reaction mixture resulted in precipitation of polymer which was fractionated by successive extraction in a Soxhlet extractor with MeOH, acetone, hexane and $CHCl_3$. The $CHCl_3$ fraction (PT-H8-*alt*-F8) was characterized further.

We also attempted other organometallic coupling reactions to make the alternating copolymer. Since the 5-bromo-bithienyl-5'-boronate could not be made, Suzuki coupling method could not go further. Although the 5-bromo-5'-bithienyl stannyl reagent was made by lithiation, followed by reaction with tributyltin chloride, the polymerization via Stille coupling reaction only gave short oligomers in high yield, based on ^{1}H-NMR of the major fraction, Figure 3.2.

^{1}H NMR spectroscopy was used to characterize the structure of PT-H8-*alt*-F8. A singlet at δ7.21 ppm is assigned to β-proton on the fluoroalkyl substituted thiophene ring, and a singlet at δ7.08 ppm corresponds to the β-proton on the alkyl-substituted ring. The sharpness of these peaks, and lack of other peaks, indicates formation of a highly regioregular (i. e., head-to-tail), and therefore alternating, copolymer structure. Comparison of the intensities of these peaks with those of signals arising from the terminal groups at δ7.69 and 7.01 ppm (the α and β protons on terminal perfluoroalkyl substituted thiophene rings), and 6.91 ppm (the β proton on terminal alkyl substituted thiophene ring) indicates that the polymer has a number-average molecular weight greater than 1.4×10^4 g/mol, corresponding to a degree of polymerization ≥20 (i.e., ≥40 thiophene rings per chain). A triplet at 2.78 ppm is assigned to α-methylene group of alkyl side chain. The absence of additional peaks in this region further indicates that the polymer is highly regioregular,[29] Figure 3.3.

McCullough method

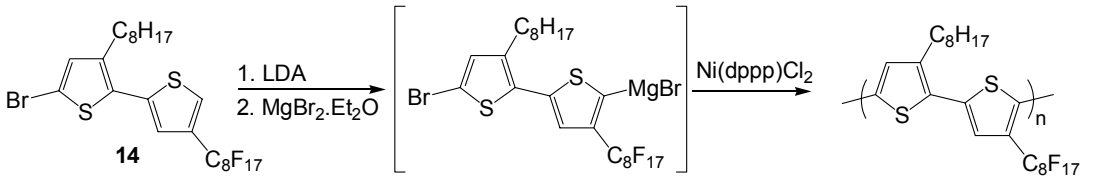

PT-H8-*alt*-F8

Suzuki coupling

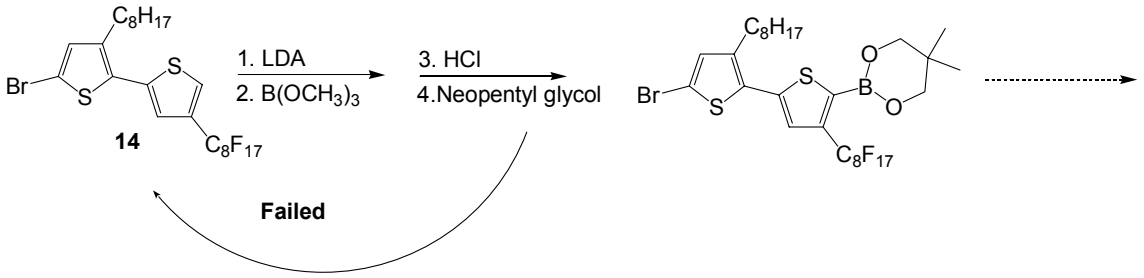

Stille coupling

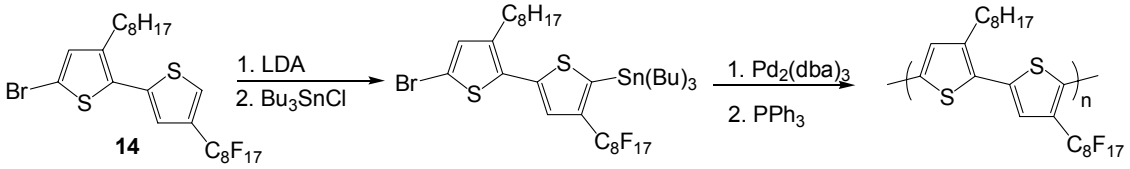

PT-H8-*alt*-F8

Figure 3.2. Polymerizations.

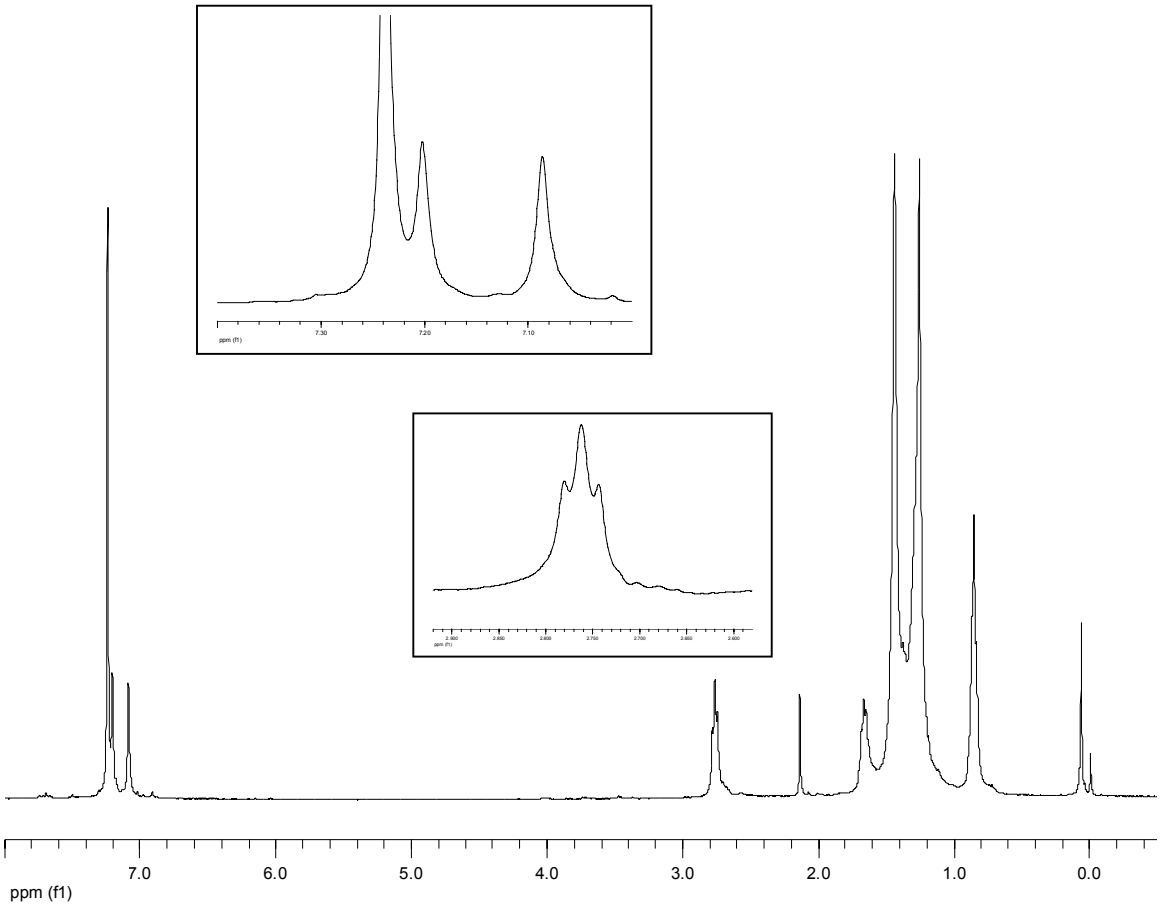

Figure 3.3. ^{1}H-NMR spectrum of **PT-H8-*alt*-F8**, 400 MHz, 55°C, in $CDCl_3$.

Attempt to make random and block copolymers

In order to explore a wider variety of copolymer microstructures, we also attempted to prepare the random copolymer by oxidative polymerization of an 1:1 mixture of 3-(perfluorooctyl)thiophene and 3-octylthiophene by treatment with $FeCl_3$ in $CHCl_3$, Figure 3.4. The resulting polymer was precipitated from methanol. Fractionation afforded a deep red $CHCl_3$-soluble polymer. The ^1H NMR spectrum of the polymer prepared in this manner shows a broad singlet at δ6.90, which is typical of the β-proton on the poly(3-alkylthiophene) backbone. Several peaks slightly shifted from this peak (Figure 3.5.) indicate the polymer has a regiorandom linkage of 3-alkylthiophenes, which is expected for the oxidative polymerization. Small peaks appear at δ7.53 corresponding to the proton in the 4-position of a 3-(perfluoroalkyl)thiophene unit, which appears as a singlet at δ7.47 for PT-F8. and δ7.70 ppm (typical for the proton in the 5-position of a 3-perfluoroalkyl-substituted thiophene ring) arise from 3-(perfluorooctyl)thiophene end groups. The integrations of these peaks relative to those for the alkylthiophene units indicate that the material prepared in this manner is a relatively low molecular weight poly(3-octylthiophene) (DP ~ 44) bearing 3-(perfluorooctyl)thiophene rings at each end, Figure 3.5. Termination of the chains with 3-(perfluorooctyl)thiophene units arises from its electron-poor nature. Once the fluoroalkylated ring is incorporated onto the end of a growing conjugated chain, the radical cation generated by further oxidation will localize on segment of electron-rich alkylthiophene rings rather than at the termini. Since there is little radical cation character on the end groups, the polymerization is thereby terminated. An attempt was made to prepare a block copolymer of 3-perfluoroalkylthiophenes and 3-alkylthiophenes using McCullough method. 2-Bromo-4-perfluorooctylthiophene was

lithiated (LDA), Ni(dppp)Cl_2 was added and the mixture was stirred for 3 h. Separately, 2-bromo-3-octylthiophene was also pre-polymerized for 3 h. Two pre-polymerized solutions were combined and more catalyst was added. NMR of the resulting high molecular weight polymer indicates this polymer is a typical regioregular poly(3-alkylthiophene). This may be due to anomalous reactivity of the perfluoroalkyl-substituted Grignard reagent such that is not polymerized, Figure 3.4.

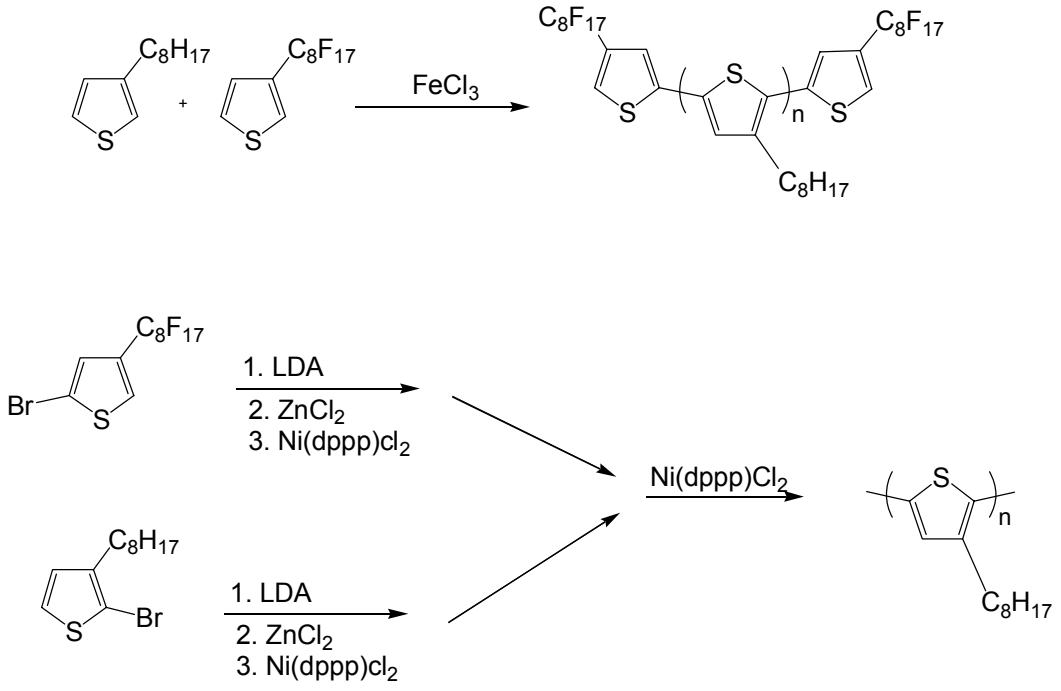

Figure 3.4. Attempt to make the random and block copolymers.

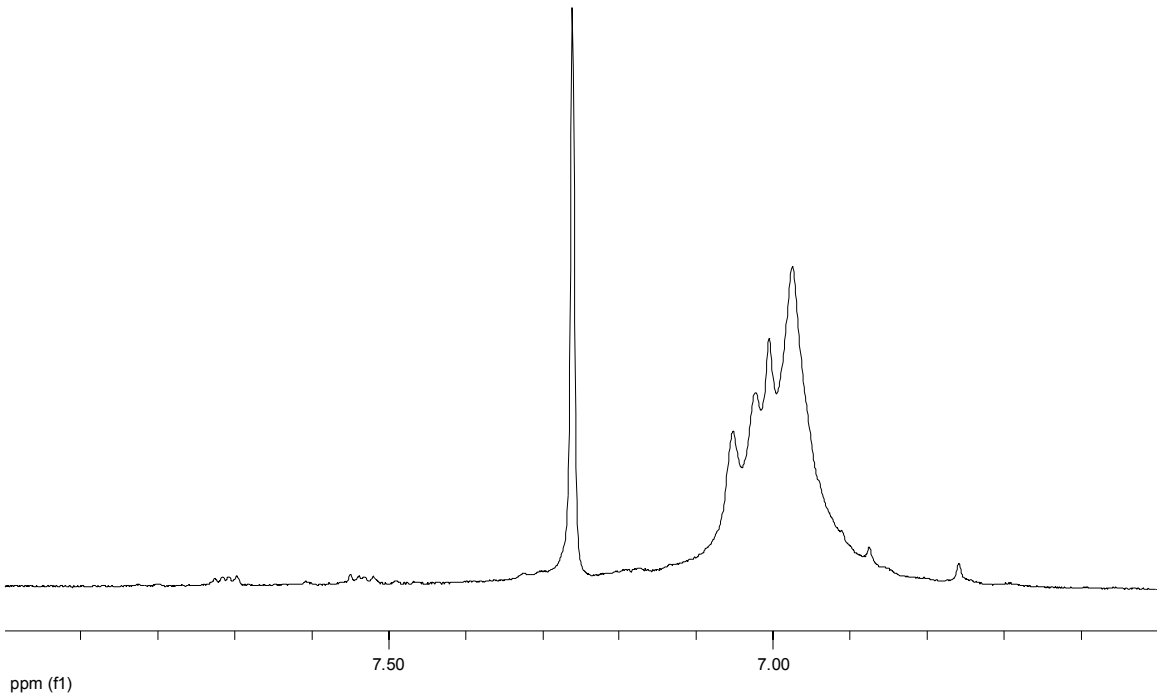

Figure 3.5. ^{1}H-NMR spectrum of oligo(3-octylthiophene) with the terminal 3-(perfluorooctyl)thiophenes, 300 MHz, in $CDCl_3$.

Oxidative polymerization

We also attempted to oxidatively polymerize dimer **10**. This dimer has a lower oxidation potential than either of the substituted monothiophenes. Bulk electrolysis (+1.60 V versus SCE) resulted in the formation of a violet species which diffused from the electrode surface. No film was deposited, even after long electrolysis time. Chemical oxidation of the dimer **10** with $FeCl_3$ also failed to afford polymer. The major product obtained by this procedure was the tetrathiophene **18**, Figure 3.6. This product arises as a consequence of localization of the radical cation on the electron-rich ring of the dimer (i.e., the alkyl substituted ring) and coupling of two dimers via the 5-positions. While the

tetrathiophene **18** is subject to further oxidation under the oxidative conditions, the resulting radical cation is localized on the central thiophene rings. The localization of the unpaired electron density on the interior of the four-ring system and the presence of perfluoroalkyl substituents ortho to the unsubstituted α-thienyl positions on the terminal rings, hinders further coupling reactions.

We also purposely synthesized the tetrathiophene **18**, for comparison with the product of the oxidation of **10**. The first attempt was to use traditional Grignard chemistry, which is hindered because the according Grignard reagent cannot be made through the reaction of magnesium with bithienyl bromide. The second attempt was to use n-BuLi to perform a metal-halogen exchange, followed by the transmetallation with $MgBr_2.Et_2O$. The Ni(II) catalysed coupling reaction did not give any product. This indicates that either the generation of the Grignard reagent, or the transmetllation is unsuccessful. Finally, we changed the transmetallation agent to $ZnCl_2$. The Pd(0) catalysed reaction gives the tetrathiophene **18** in high yield. Structure analysis proves both methods, oxidation and organometallic coupling, give the same product, Figure 3.6.

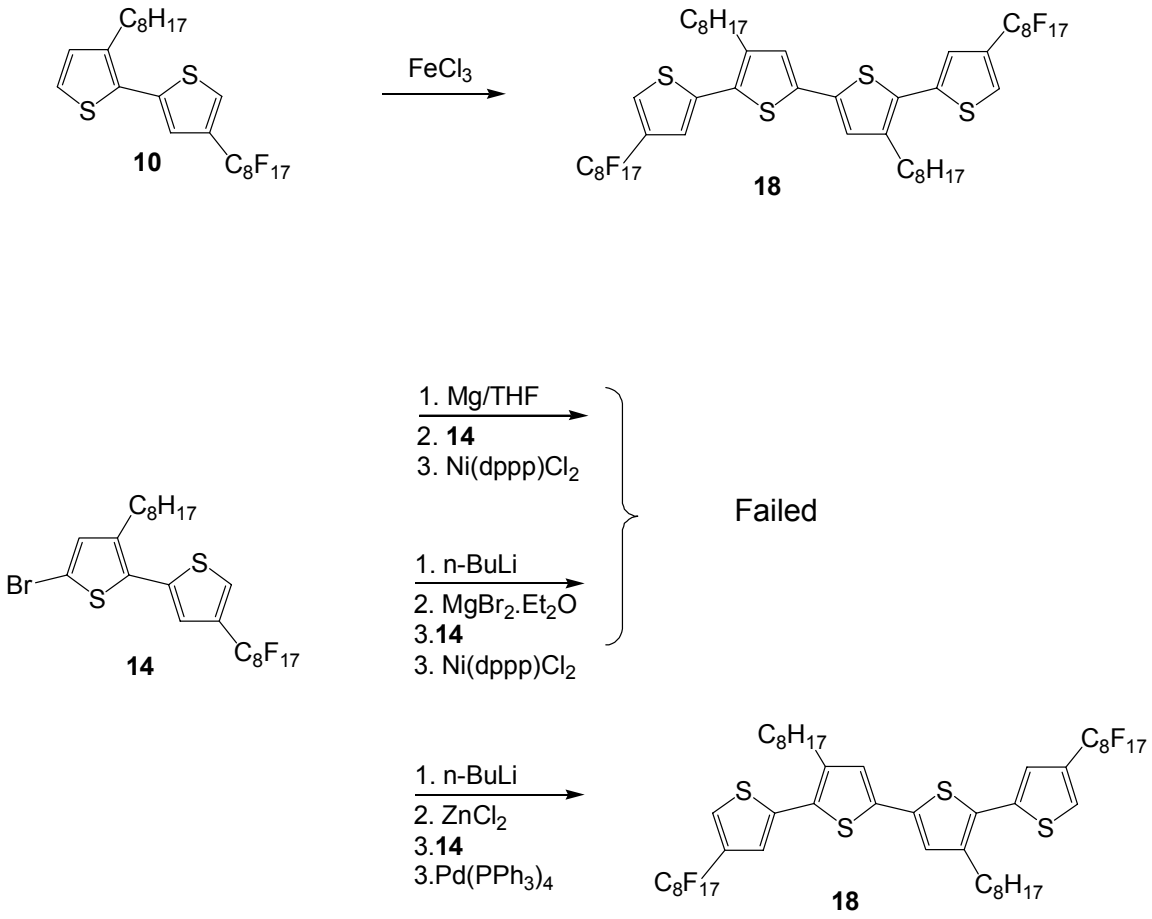

Figure 3.6. Attempt of oxidative polymerization.

Electrochemistry

Cyclic voltammetry of dimer **10** shows an irreversible oxidation at +1.51 V. Multiple potential cycles between 0.00 V and + 1.60 V did not result in growth of a film on the electrode surface. Bulk electrolysis (+1.60 V vs SCE) also did not result in film deposition. Cyclic voltammetry of the dip-coated film of PT-H8-*alt*-F8 shows a reversible oxidation peak at +1.07 V and an irreversible reduction peak at –2.30 V.

The electrochemistry of other monomers, dimers and polymers were also characterized by cyclic voltammetry. In the case of both thiophenes and bithiophenes, fluoroalkyl substitution increases the oxidation potential by over 200 mV relative to the alkyl analog. The same trend is observed for the polymers: Increasing the density of fluoroalkyl substituents on the polythiophene backbone leads to a higher oxidation potential and a less negative reduction potential. PT-H8-*alt*-F8 undergoes oxidation at +1070 mV versus SCE, compared to +940 mV for the alkyl-substituted homopolymer, and +1190 mV for the perfluoroalkyl homopolymer, Table 3.1. Thus, the oxidation potential of the alternating polymer falls between those of the two homopolymers. In addition to the electron withdrawing nature of the perfluoroalkyl substituents, the twisting effect of steric interactions between the α-fluorine atoms of the side chain and the sulfur atom of the adjacent thiophene ring may also contribute to the higher oxidation potential of the fluoroalkyl analogs.

PT-H8-*alt*-F8 undergoes reduction at -2300 mV versus SCE, compared to -1180 mV for the perfluoroalkyl homopolymer, Table 3.1. The alkyl-substituted homopolymer cannot be reduced under normal conditions. Thus, the electron-withdrawing nature of perfluoroalkyl chain can stablize negative charges on the polythiophene backbone. A

higher density of perfluoroalkyl substitution makes the reduced polythiophene more accessible, resulting a lower reduction potential of the substituted polythiophenes.

Table 3.1. Redox behavior of alkyl and perfluoroalkyl thiophenes, bithiophenes and polythiophenes.

monomer [a]		polymer [b]		
	oxidation *E* (V)		oxidation *E* (V)	reduction *E* (V)
T-H8	+1.84	PT-H8	+0.94	NA
T-F8	+2.05	PT-F8	+1.19	-1.18
T-F8/T-F8	+1.75			
10, T-H8/T-H8	+1.51	PT-H8-*alt*-F8	+1.07	-2.30

[a] 10^{-5} M, gold electrode, 100 mV/s, 0.1 M Bu_4NPF_6 in CH_2Cl_2. [b] regioregular polymer films dip-coated on a carbon electrode, 100 mV/s, 0.1 M Bu_4NPF_6 in CH_2Cl_2.

Electronic spectra in solution

UV-vis and fluorescence spectroscopy was used to further characterize the electronic structure of PT-H8-*alt*-F8, with comparisons to spectra of the two homopolymers PT-H8 and PT-F8. A solution of PT-H8-*alt*-F8 in chloroform gives an absorption maximum at 384 nm, and yellow emission with maximum intensity at 547 nm, Figure 3.7.

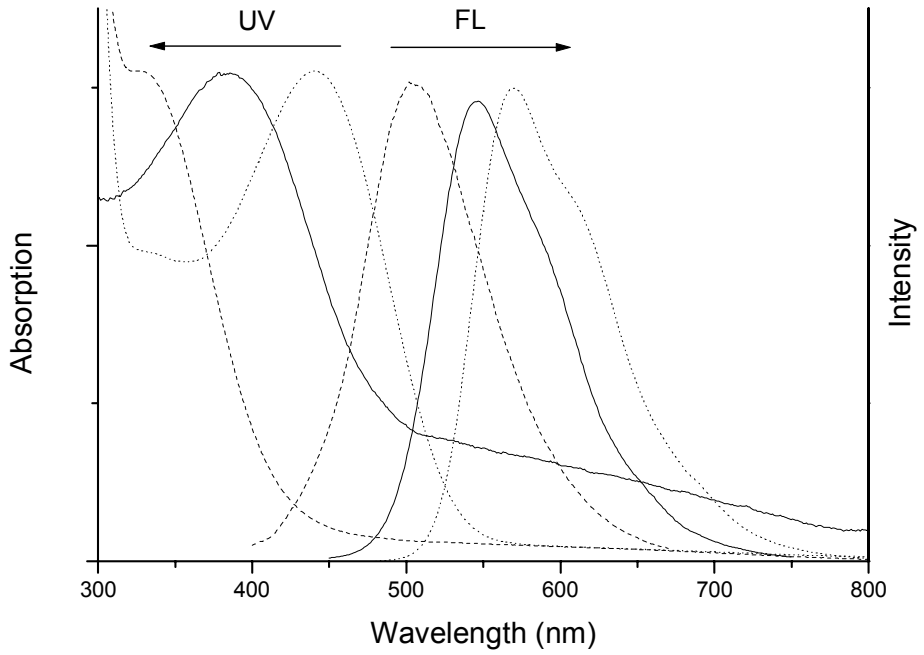

Figure 3.7. UV-vis and fluorescence spectra (normalized) of **PT-F8** (----), **PT-H8-*alt*-F8** (—) and **PT-H8** (….) in 10^{-5} M solution in chloroform.

These values for the alternating copolymer are between those of the two homopolymers, Table 3.2. From PT-H8, to PT-H8-*alt*-F8, to PT-F8, the density of the fluoroalkyl substitution is increasing, which leads to a consistent blue shifting of absorption (PT-H8 441 nm, to PT-H8-*alt*-F8 384 nm, to PT-F8 326 nm), a continuous blue shifting of emission (PT-H8 570 nm, to PT-H8-*alt*-F8 547 nm, to PT-F8 504 nm), and a continuous increasing of the Stoke's shift (PT-H8 129 nm, to PT-H8-*alt*-F8 163 nm, to PT-F8 178 nm).

Table 3.2. UV-vis absorption and emission spectra

	Solution [a]			Film [b]				
	abs. λ_{max} (nm)	fluor. λ_{max} (nm)	Stoke's shift (nm)	abs. λ_{max} (nm)	fluor. λ_{max} (nm)	Stoke's shift (nm)	band gap [c] (eV)	abs. $\Delta\lambda_{max}$ [d] (nm)
PT-T8	441	570	129	515	-	-	1.83	74
PT-H8-*alt*-F8	384	547	163	456	612	156	2.07	72
PT-F8	326	504	178	338	505	167	2.52	12

[a] $CHCl_3$ solution. [b] spin-coated solid film. [c] calculated from onset of UV-vis spectra. [d] $\Delta\lambda_{max} = \lambda_{max}(film) - \lambda_{max}(solution)$

Thus, the photophysical properties of polythiophenes in solution can be tuned by varying the degree of fluoroalkyl substitution. We ascribe the systematic changes in absorption, emission, and Stoke's shift to the steric influence of perfluoroalkyl groups. Steric interactions between the perfluoroalkyl substituents and the adjacent repeat units leads to the twisting of the backbone and a reduction in the conjugation length.[9] The decrease in conjugation in the ground states becomes more apparent with more perfluoroalkyl substituents. This explains the dramatic decrease in the wavelength of the absorption band with more perlfluoroalkyl substituents. In the excited states, although the polythiophene backbones take more planar quinoid form, the twisting effect of substituents still exists. This is why the emission is still affected by the degree of perfluoroalkyl substitution, although this effect is not as dramatic as the absorption. The Stoke's shift arises from the difference in the conformation of the polymer backbone

between the ground state and the excited state. The increase of the Stoke's shift with the increase in density of perfluoroalkyl substituent can be explained by the argument that the twisting effect has a larger influence on absorption than emission and that this twisting effect can be overcome in the excited state by formation of the quinoid form.

Solutions of the alternating copolymer (PT-H8-*alt*-F8) show much brighter fluorescence than the two homopolymers (PT-F8 and PT-H8), Figure 3.8. The quantum yields of the polymers were calibrated against Coumarin 500. The quantum yield of the alternating copolymer PT-H8-*alt*-F8, $\phi = 0.31$, is three times that of the two homopolymers (PT-F8, $\phi = 0.10$; and PT-H8, $\phi = 0.11$). This enhancement of the quantum yield arises from the electronic structure of the copolymer PT-H8-*alt*-F8, which has an alternating sequence of electron-rich and electron-poor thiophene rings. The two adjacent thiophene rings have an alternating electron donor and acceptor electronic structure which gives an intrinsic dipole for every repeating unit. The quantum yield for fluorescence is proportional to the square of the change in dipole moment between the ground and excited states. Polyarenes such as polythiophene adopt a more planar quinoidic conformation upon photoexcitation to the excited state, relative to the twisted conformation of the ground state. In the case of two homopolymers, there is no intrinsic dipole, so there is no significant dipole change upon excitation. In the case of the alternating copolymer, upon photoexcitation the planarization and corresponding increase in a longer conjugation length results in a change in dipole between the ground state and the excited state, resulting in the enhanced quantum yield of the alternating copolymer relative to the homopolymers. In other examples of conjugated polymers with both electron donor and acceptor segments, other than the enhancement of quantum yield, the

control of bandgaps,[30] the NLO properties[31] and the performance of OLEDs[32] have been explored. The same enhancement of the quantum yield has not been investigated in detail.

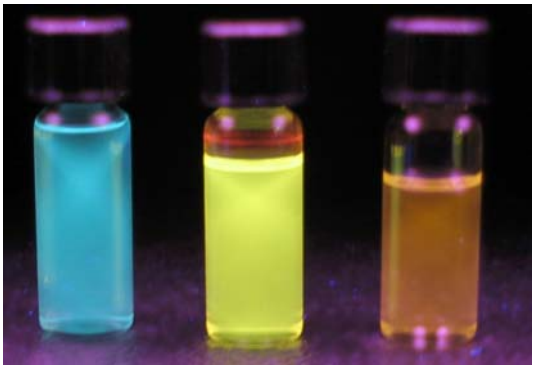

Figure 3.8. Fluorescence of solution of polymers upon irradiation at 365 nm Left to right: **PT-F8**, **PT-H8-*alt*-F8** and **PT-H8** (10^{-4} M solution in chloroform).

Electronic spectra of the solid-state

UV-vis and fluorescence spectroscopies were also used to investigate the photophysics of solid films of the polymers, Table 3.2. Spin-coated films of PT-H8-*alt*-F8 absorb at λ_{max}= 456 nm. PF8T absorbs at λ_{max}=338 nm and PH8T absorbs at λ_{max}= 515 nm, Figure 3.9. Again, the data of the solid state alternating copolymer fit between that of the two homopolymers and the absorption of the solid state polythiophenes also can be tuned by varying the density of fluoroalkyl substituents. With more

perfluoroalkylation, the polythiophene backbone is more twisted due to steric interactions between the fluorine atoms of the side chain and the sulphur on the adjacent thiophene ring. The more twisted polymer backbone leads to a blue-shifted absorption.

The difference in the wavelength for the absorption for solutions and solid films of conjugated polymers is often ascribed to the assembly of conjugated backbones in an ordered solid-state structure. The enhanced planarity of the backbone in the solid state accounts for a large observed red shift relative to the solution spectra. A large shift (72-74 nm) is observed for the alkyl-substituted homopolymer, PT-H8, and alternating copolymer, PT-H8-*alt*-F8, but only a small shift (12 nm) is observed for the fluoroalkyl homopolymer, PT-F8. Again, this suggests that the steric influence of the fluoroalkyl groups causes twisting of the polymer backbone and that the films are largely disordered, resulting in a low conjugation length. PT-H8 forms a highly ordered lamellar structure in the solid-state by virtue of side chain interdigitation and backbone π-π interactions, leading to a large red shift in absorption for polymer films relative to solutions. The same large red shift is also observed in PT-H8-*alt*-F8. X-ray diffraction of the alternating copolymer films, PT-H8-*alt*-F8, indicates there is an ordered solid-state structure, the pattern different from that of the lamellar structure of PT-H8. More work is needed to determine the structure of the alternating copolymer, but whatever it is, the ordered solid-state structure leads to the planarization of the backbone leading to a longer conjugation length.

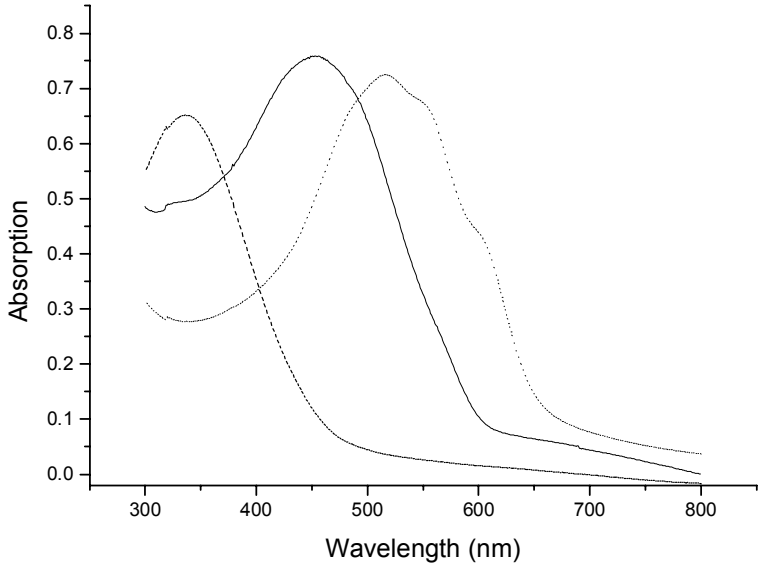

Figure 3.9. UV-vis spectra of the spin-coated film of **PT-F8** (----), **PT-H8-*alt*-F8** (—) and **PT-H8** (….).

More importantly, the alternating copolymer PT-H8-*alt*-F8 displays strong fluorescence in the red (λ_{max}= 612 nm), whereas PT-F8 emits green fluorescence at λ_{max}=505 nm, Figure 3.10.

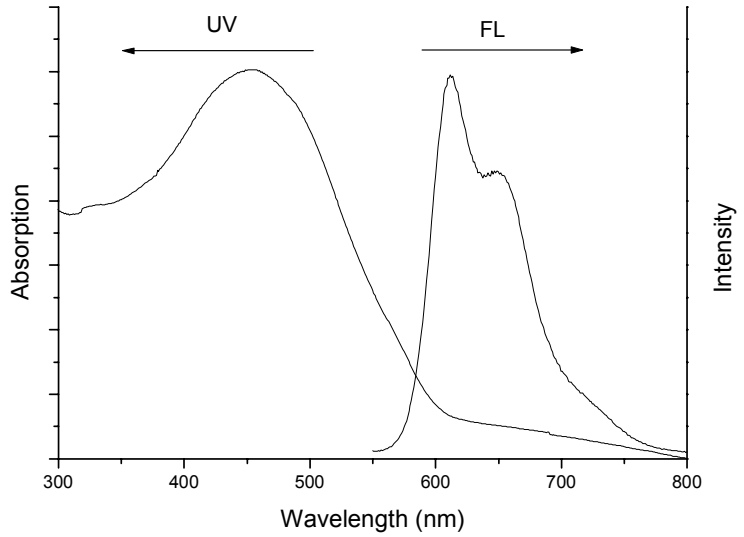

Figure 3.10. UV-vis and fluorescence spectra of spin-coated film of **PT-H8-*alt*-F8.**

In the case of the alkyl homopolymer PT-H8, the lamellar self-assembling structure in solid state quenches the fluorescence emission by energy transfer to another stacked segment through non-rediative relaxation. The strong red fluorescence of films of the alternating copolymer again suggests that this polymer assembles into a superamolecular structure other than the lamellar structure. It may be also due to the intrinsic dipole. The fluorescence from films of PT-H8-*alt*-F8 is stable under ambient conditions; the bright fluorescence is retained after more than six months, Figure 3.11.

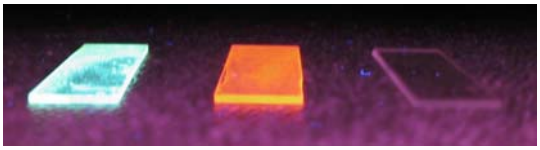

Figure 3.11. Fluorescence of polymer films upon irradiation at 365 nm, from left to right of spin-coated films: **PT-F8**, **PT-H8-*alt*-F8** and **PT-H8.**

With more fluoroalkyl substitution, the bandgap of polythiophene increases. For PT-H8 the badgap is 1.83 eV. With 50% replacement of the alkyl substituents with fluoroalkyl chains (PT-H8-*alt*-F8) the alternating copolymer has a bandgap of 2.07 eV, and for the wholly fluoroalkyl substituted polymer (PT-F8) it increases further to 2.52 eV, Figure 3.9. The 3-perfluoroalkylation has the effect of reducing both the HOMO and LUMO energies of polythiophenes, relative to poly(3-alkylthiophene)s, due to the electron-withdrawing nature of perfluoroalkyl groups. However, the 3-perfluoroalkylation has less effect on LUMO energies, and significantly decreases the HOMO energies, which enlarges the bandgap of polythiophenes. The similar trend has also been observed in the perfluoroalkyl-substituted oligothiophenes.[33]

Thermal anaysis

DSC studies of hexane, chloroform, chlorobenzene fractions of PT-H8-*alt*-F8 all show a double melting behaviour upon heating and a single crystallization peak upon cooling, Figure 3.12. This double melting behaviour may be explained by the presence of

a solid state to liquid crystalline or solid-solid transition. All the transition temperatures increase from the hexane to chloroform and chlorobenzene fractions, Table 3.3. The chlorobenzene fraction has the highest molecular weight and the hexane fraction has the lowest. It is expected that all of the transition temperatures increase when the molecular weight increases.

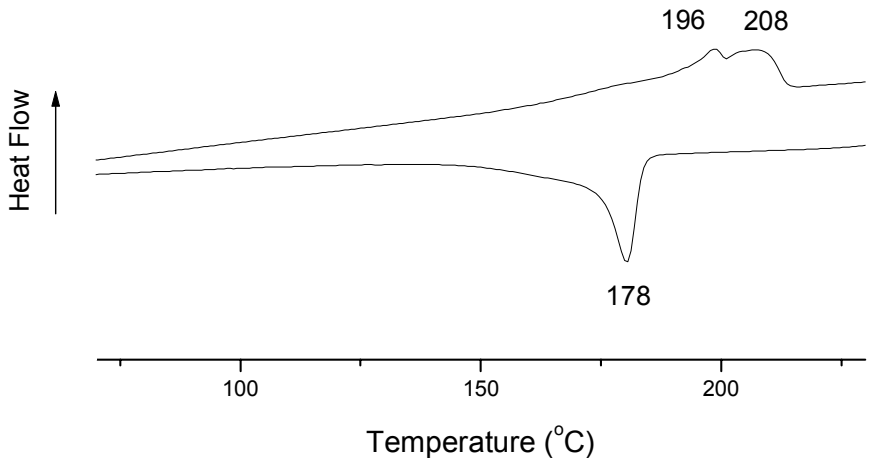

Figure 3.12. DSC of **PT-H8-*alt*-F8** ($CHCl_3$ fraction), 25-250°C, 20°C/min, N_2.

Table 3.3. Thermal transitions of different fractions.			
	1st transition (°C)	2nd transition (°C)	Crystallization (°C)
Hexane Frac.	152	166	142
$CHCl_3$ Frac.	196	208	178
Cl-Ph Frac.	208	214	176

X-ray diffraction

The X-ray diffraction of regioregular alternating semifluoroalkyl/alkyl-substituted polythiophenes shows a highly-ordered bilayer lamellar structure. This indicates that the immiscibility of hydrocarbon and fluorocarbon chains drives the assembly of the polymer into a bilayer structure, in contrast to the monolayer lamellar structure of regioregular poly(3-alkylthiophene) homopolymers.[5] We expected the same bilayer structure for the alternating fluoroalkyl/alkyl-substituted polythiophenes.

However, the powder X-ray diffraction of the alternating perfluorooctyl/octyl-substituted polythiophenes, PT-H8-*alt*-F8, shows two reflections at low angles, the first of which corresponds to a distance of 26.2Å, Figure 3.13. The regioregular poly(3-octylthiophene) assembles into a lamellar structure with a spacing of 20.8Å, so the expected bilayer lamellar structure should have a spacing of 41.6Å. Thus, the experimental data for PT-H8-*alt*-F8 does not fit either the monolayer or bilayer lamellar structure. In addition, the broadness of the second reflection ($2\theta = 6.81^{\circ}$) is inconsistent with the regular lamellar structure of regioregular poly(3-alkylthiophene)s. In addition, there are two wide-angle peaks. One is located near $2\theta = 24.0^{\circ}$, identified as the interstack chain-to-chain distance of 3.7Å, and the other one at $2\theta = 18.3^{\circ}$ (4.8Å), which may correspond the side chain packing.[34]

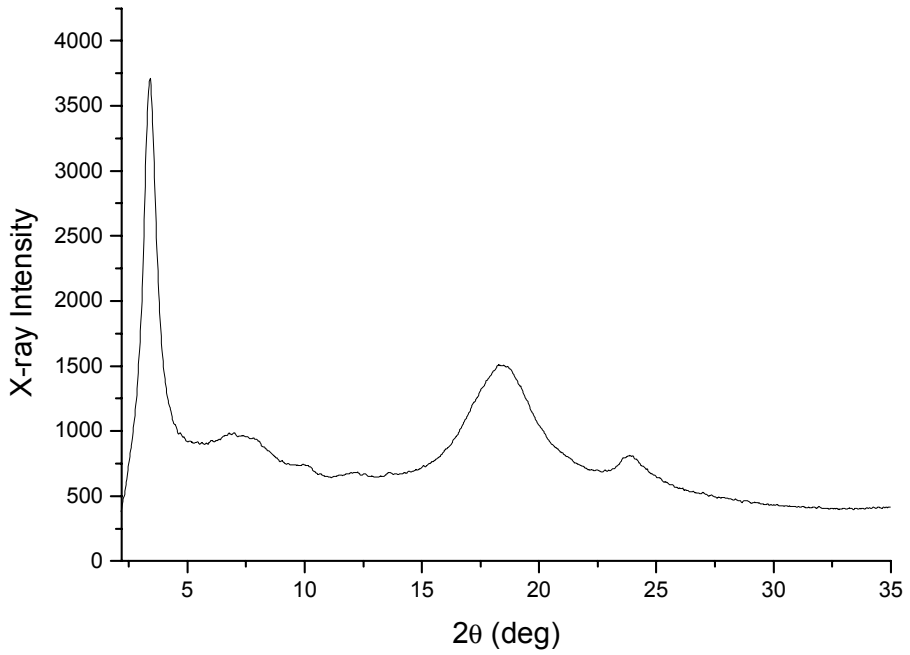

Figure 3.13. Powder X-ray diffraction of **PT-H8-*alt*-F8**.

In addition to the immiscibility of hydrocarbon and fluorocarbon side chains, the backbone of the perfluoroalkyl substituted copolymer is twisted and there are electron rich and poor units along the polymer chains. These might combine to give a more complicated structure, which is still under investigation. The non-lamellar assembling structure should contribute the unusual photophysics of PT-H8-*alt*-F8.

Conclusion

In conclusion, the photophysics and electrochemistry of polythiophenes bearing weakly electron-donating alkyl, and inductively electron-withdrawing perfluoroalkyl groups allows us to tune the electronic structure of the conjugated backbone. The alternating copolymer displays absorption and emission maxima between those of homopolymers composed of the individual structural units. The combination of the alternating electron-rich and electron-poor units, together with a small twisting influence of the perfluoroalkyl group, provides a material which displays enhanced solution-phase fluorescence, and strong solid-state fluorescence which is absent for the wholly alkyl analogue.

References

1. Recent examples include: (a) poly(methyl methacrylate)s: Johansson, G.; Percec, V.; Ungar, G.; Zhou, J. P. *Macromolecules* **1996**, *29*, 646. Hwang, H. S.; Heo, J. Y.; Jin, S. H.; Cho, D.; chang, T.; Lim, K. T. *Polymer* **2003**, *44*, 5153 (b) ionenes, Wang, J.; Ober, C. K. *Macromolecules* **1997**, 30, 7560; (c) norbornenes: Tran, H. V.; Hung, R. J.; Chiba, T.; Yamada, S.; Mrozek, T.; Hsieh, Y. T.; Chambers, C. R.; Osborn, B. P.; Trinque, B. C.; Pinnow, M. J.; MacDonald, S. A.; Willson, C. G.; Sanders, D. P.; Connor, E. F.; Grubbs, R. H.; Conley, W. *Macromolecules* **2002**, *35*, 6539. (d) styrene-butadiene: Ren, Y.; Lodge, T. P.; Hillmyer, M. A. *Macromolecules* **2001**, *34*, 4780. and (e) styrene-isoprene block copolymers: Hayakawa, T.; Wang, J.; Xiang, M.; Li, X.; Ueda, M.; Ober, C. K.; Genzer, J.; Sivaniah, E.; Kramer, E. J.; Fisher, D. A. *Macromolecules* **2000**, *33*, 8012.

2. Büchner, W.; Garreau, R.; Lemaire, M.; Roncali, J.; Garnier, F. *J. Electroanal. Chem. Interfacial Electrochem.* **1990**, *277*, 355; Büchner, W.; Garreau, R.; Roncali, J.; Lemaire, M. *J. Fluorine Chem.* **1992**, *59*, 301; Robitaille, L.; Leclerc, M. *Macromolecules* **1994**, *27*, 1847; Leclerc, M.; Robitaille, L.; Bergeron, J.Y.; Callender, C.L. *Polym. Prepr.* **1994**, *35(1)*, 305.

3. Hong, X.; Tyson, J. C.; Middlecoff, J. S.; Collard, D. M. *Macromolecules* **1999**, *32*, 4232.

4. Hong, X. M.; Collard, D. M. *Macromolecules* **2000**, *33*, 3502.

5. Hong, X.; Tyson, J. C.; Collard, D. M. *Macromolecules* **2000**, *33*, 6916.

6. Cornil, J.; Beljonne, D.; Calbert, J.; Brédas, J. L. *Adv. Mater.* **2001**, *13*, 1053.

7. Hajlaoui, R.; Fichou, D.; Horowitz, G.; Nessakh, B.; Constant, M.; Garnier, F. *Adv. Mater.* **1997**, *9*, 557.

8. Garnier, F.; Horowitz, G.; Fichou, D.; Yassar, A. *Synth. Metals* **1996**, *81*, 163.

9. Endo, T.; Takeoka, Y.; Rikukawa, M.; Sanui, K. *Synth. Metals* **2003**, *135*, 333.

10. Li, L.; Counts, K. E.; Kurosawa, S.; Teja, A. S.; Collard, D. M. *Adv. Mater.* **2004**, *16*, 180.

11. Facchetti, A.; Deng, Y.; Wang, A.; Koide, Y.; Sirringhaus, H.; Marks, T. J.; Friend, R. H. *Angew. Chem., Int. Ed.* **2000**, *39*, 4547.

12. Facchetti, A.; Mushrush, M.; Katz, H. E.; Marks, T. J. *Adv. Mater.* **2003**, *15*, 33.

13. Czerwinski, W.; Wrzeszcz, G.; Kania, K.; Rabek, J. F.; Linden, L. A. *J. Mat. Sci*. **2000**, *35*, 2305.

14. Beaupre, S.; Leclerc, M. *Adv. Funct. Mater*. **2002**, *12*, 192.

15. Charas, A.; Morgado, J.; Martinbo, J. M. G.; Alcacer, L.; Cacilli, F. *Synth. Metals* **2002**, *127*, 251.

16. Yamamoto, T.; Zhou, Z.; Kanbara, T.; Shimura, M.; Kizu, K.; Maruyama, T.; Nakamura, Y.; Fukuda, T.; Lee, B.; Ooba, N.; Tomaru, S.; Kurihara, T.; Kaino, T.; Kubota, K.; Sasaki, S. *J. Am. Chem. Soc*. **1996**, *118*, 10389.

17. Yamamoto, T.; Arai, M.; Kokubo, H.; Sasaki, S. *Macromolecules* **2003**, *36*, 7986.

18. McCullough, R. D.; Jayaraman, M. *J. Chem. Soc., Chem. Commun*. **1995**, 135.

19. Iraqi, A.; Clark, D.; Jones, D.; Krier, A. *Synth. Metals* **1999**, *102*, 1220.

20. Bjornholm, T.; Hassenkam, T.; Greve, D. R.; McCullough, R. D.; Jayaraman, M.; Savoy, S. M.; Jones, C. E.; McDevitt, J. T. *Adv. Mater*. **1999**, *11*, 1218. Reitzel, N.; Greve, D. R.; Kjaer, K.; Howes, P. B.; Jayaraman, M.; Savoy, S.; McCullough, R. D.; McDevitt, J. T.; Bjornholm, T. *J. Am. Chem. Soc.* **2000**, *122*, 5788.

21. Stokes, K. K.; Heuze, K.; McCullough, R. D. *Macromolecules* **2003**, *36*, 7114.

22. Liu, J.; Sheina, E.; Kowalewski, T.; McCullough, R. D. *Angew. Chem,. Int. Ed*. **2002**, *41*, 329; Henze, O.; Feast, W. J. *J. Mater. Chem*. **2003**, *13*, 1274. Francois, B.; Olinga, T. *Synth. Metals* **1993**, *57*, 3489

23. Kowalik, J.; Tolbert, L. M.; Narayan, S.; Abhiraman, A. S. *Macromolecules* **2001**, *34*, 5471. Demadrille, R.; Divisia-Blohorn, B.; Zagorska, M.; Quillard, S.; Rannou, P.; Travers, J. P.; Pron, A. *New J. Chem*. **2003**, *27*, 1479. Era, M.; Yoneda, S.; Sano, T.; Noto, M. *Thin Solid Films* **2003**, *438-439*, 322

24. Greve, D. R.; Apperloo, J. J.; Janssen, R. A. J. *Eur. J. Org. Chem*. **2001**, 3437.

25. Demanze, F.; Yassar, A.; Garnier, F. *Macromolecules* **1996**, *29*, 4267.

26. Demanze,F.; Yassar, A.; Garnier, F. *Synth. Metals* **1996**, *78*, 143.

27. Bidan, G.; De Nicola, A.; Enee, V.; Guillerez, S. *Chem. Mater*. **1998**, *10*, 1052.

28. McCullough, R. D.; Tristram-Nagle, S.; Williams, S. P.; Lowe, R. D.; Jayaraman, M.; *J. Am. Chem. Soc.* **1993**, *115*, 4910.

29. McCullough, R. D.; Lowe, R. D.; Jayaraman, M.; Anderson, D. L. *J. Org. Chem*. **1993**, *58*, 904. Chen, T. A.; Wu, X.; Rieke, R. D. *J. Am. Chem. Soc.* **1995**, *117*, 233

30. Dhanabalan, A.; van Duren, J. K. J.; van Hal, P. A.; van Dongen, J. L. J.; Janssen, R. A. J. *Adv. Funct. Mater.* **2001**, *11*, 255.

31. Zhan, X.; Liu, Y.; Zhu, D.; Huang, W.; Gong, Q. *Chem. Mater.* **2001**, *13*, 1540.

32. Paik, K. L.; Baek, N. S.; Kim, H. K.; Lee, J. H.; Lee, Y. *Macromolecules* **2002**, *35*, 6728. Huang, F.; Wu, H.; Wang, D.; Yang, W.; Cao, Y. *Chem. Mater*. **2004**, *16*, 708. Chen, Y.; Sheu, R. B.; Wu, T. Y. *J. Polym. Sci. Part A: Polym. Chem*. **2003**, *41*, 725

33. Facchetti, A.; Marks, T. J. *Polym. Prep.* **2002**, *43*, 734

34. Prosa, T. J.; Minokur, M. J.; McCullough, R. D. *Macromolecules* **1996**, *29*, 3654.

CHAPTER IV

HEXAGONAL AGGREGATION OF JANUS POLYTHIOPHENES IN SOLUTION

Introduction

Polythiophenes and other conjugated polymers have attracted attentions because of their electronic and photonic properties.[1,2,3] The π-conjugated electronic structure of these polymers facilitates the delocalization of the charge carriers upon doping and imparts high charge mobility. This delocalized electronic structure also leads to characteristic strong absorptions, and emissions, in most cases in the UV-vis region. Since the original unsubstituted conjugated polymers are not solution- or melt-processable, flexible side chains are attached to improve processibility. In addition to solubility and fusibility, the attachment of various substituents can modify other physical properties of conjugated polymers, and lead phenomena which are not observed in the original unsubstituted polymers.[4]

Chromism

Intriguing chromisms (color changes) are found in some functionalized conjugated polymers upon changing the temperature, the solvent, the pressure and the electrolyte, namely, thermochromism,[5] solvatochromism,[6] piezochromism[7] and ionochromism.[8,9,10] Photochromism can be achieved by photochemically inducing side

chain disordering or ordering.[3,11] The complexation between binding sites in the side chains and biochemical targets (e.g., lock and key interactions, host-guest interactions, etc.) could lead to significant color changes, termed affinity chromism.[12,13,14,15] Beside the absorption property, the emission characteristics of conjugated polymers can also be modified through external stimuli[16,17,18] which could be used to make fluorescent sensors.[19,20,21]

These interesting chromic effects were first explained as a transition between a planar (longer conjugation length) to a non-planar (shorter conjugation length) conformation of the conjugated backbone. In conjugated polymers, the strong correlation between the electronic structure and the backbone conformation leads to a consistent shift in absorption spectra upon changing the backbone conformation.[22] Extensive studies of the chromic polythiophene derivatives[23] suggest that steric interactions control the chromic transitions. These chromic effects are controlled by a delicate balance between repulsive intrachain steric interactions and attractive interchain (or intrachain, through chain folding) interactions. The interchain stacking interaction forces the polymer chains into a more rigid conformation to form planar assemblies. These assemblies can be disassembled by a twisting of the backbone which is caused by the steric interactions of side chain substitutents.[24] The presence of an isosbestic point in UV-vis spectra, in response to the change in solvent or temperature, is observed in some regioregular conjugated polymers.[25] The planar conformation of well-defined conjugated macromlecules becomes the "twiston" conformation without any intermediate state, Figure 4.1.A. Only two conformations involved in the transition explains the isosbestic point in the absorption spectra. On the other hand, a continuous blue shift of the

absorption maximum takes place upon heating solutions or films of most of non-regioregular conjugated polymers.[26] The less ordered polymers (non-regioregular) twist locally along the backbone and form continuous less conjugated segments, Figure 4.1.B. The continuous conformation changes leads to a continuous blue shift in absorption spectra.

However, it was also suggested that the formation of small aggregates or nonocrystallites could facilitate some interchain interactions (e.g. π-π interactions) which lead to the chromic changes,[36,27] Figure 4.1.C.

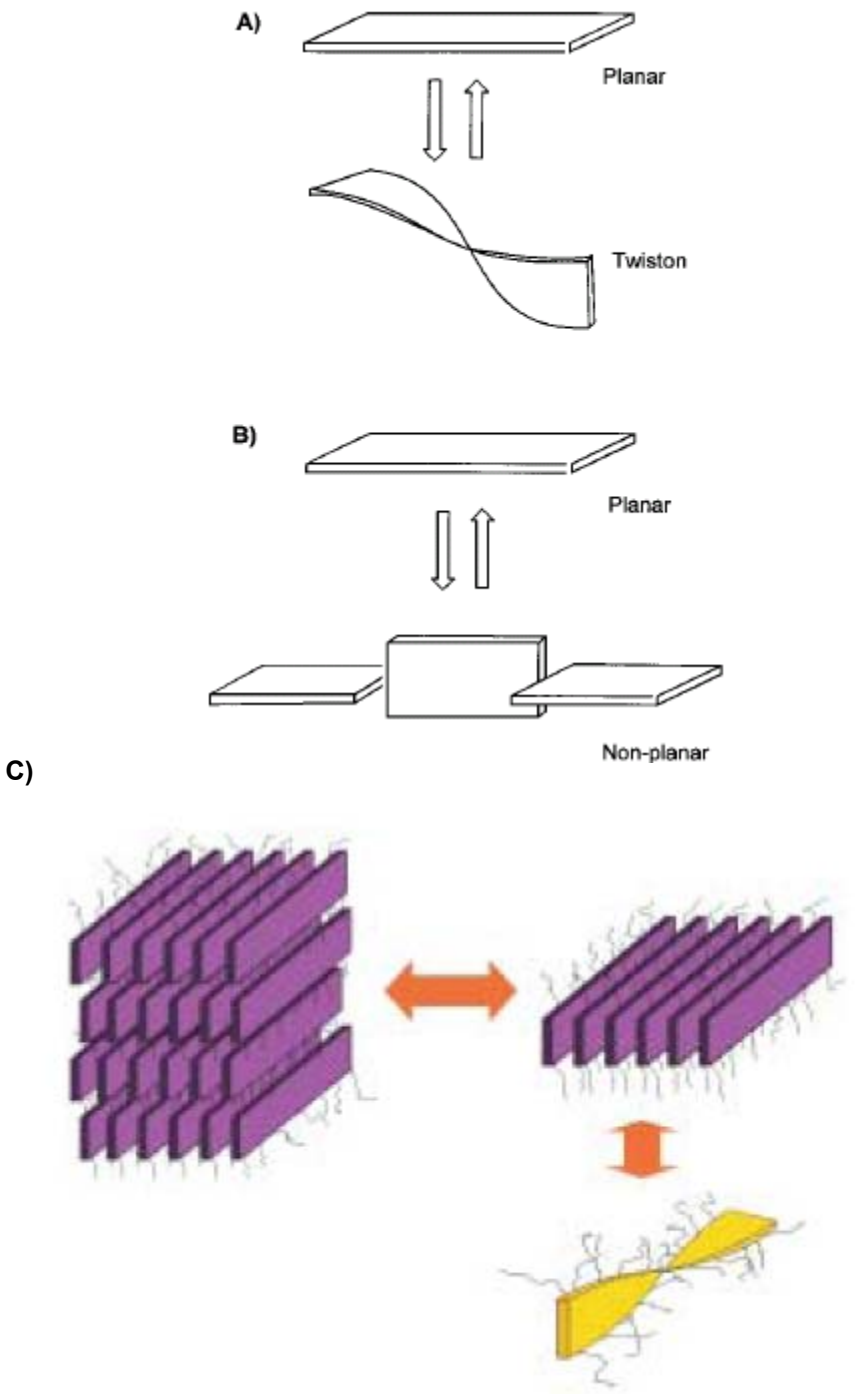

Figure. 4.1. Planar-to-non-planar conformational transitions in functionalized conjugated polymers (ref. 3 and 24.)

Aggregation of polythiophenes

The organization of conjugated polymer chains into supramolecular structures lead to control the chain conformation and interchain interaction, thereby providing a very important contribution to their electronic and optical properties. There are extensive studies of the aggregation of a variety of conjugated polymers in solution.[28] These aggregates assemble in solution upon cooling or adding poor solvents, and they usually show the similar photophysical properties as those in the solid state. In the case of polythiophenes, most of studies only address this aggregation using indirect evidences, such as the shifting of the absorption peak, or the intensity changes of the fluorescent emission.[29,30,31,32,33] Only a few of studies describe the morphologies of the aggregates, although some models have been proposed without direct structural evidence.[34,35] Recently, a study of an amphiphilic polythiophene included electron diffraction patterns of the platelets which indicated a hexagonal lattice. However, the details of the suprastruture of the assemblies were not described.[36]

Self-assembly of conjugated polymers

Conjugated polymer chains are rigid rodlike and these chains can be used as the rod component to make the rod-coil block copolymers. This approach has built up various supramolecular structures with conjugated polymer segments. Their nanoscale morphologies include lamellar, spherical, cylindrical and vesicular structures with tunable optical and electronic properties.[37,38,39,40,41,42]

Another approach is to introduce various sustituents as the side chains onto conjugated backbones. Specifically, in the case of polythiophenes, the regioregular poly(3-alkylthiophene)s have a rigid backbone and the flexible alkyl side chains. Similar

to the rod-coil block copolymer, although in a very different length scale, the brush-like polymer forms an ordered lamellar structure in solid state. To enlarge the difference between the backbone and side chains, and thereby form even more ordered structures, hydrophilic side chains (e.g. oligo(ethylene glycol),[43] ionic[44]) have been installed onto the polythiophene backbone. Most of these polymers are still lamellar, except one recent study claiming a hexagonal assembly.[36] Hong and Collard also attached the fluorophilic side chains onto the polythiophene backbone,[45] which lead to liquid crystallinity[46] and highly ordered bilayer structures.[47]

Here we report the solution photophysical characterization of solutions of regioregular alternating copolymers, poly(4'-perfluorooctyl-3-octyl-[2,2']-bithiophene) (**PT-H8-*alt*-F8**) and poly(4'-perfluorohexyl-3-dodecyl-[2,2']-bithiophene) (**PT-H12-*alt*-F6**). The thermochromism and solvatochromism of the polymer solutions were studied and compared with other polythiophenes by both absorption and emission spectroscopies. The morphology and the structure of the aggregated nano-size crystals formed in solution were explored with TEM.

Experimental

General methods

The regioregular alternating copolymers consisting of (perfluoroalkyl)thiohene and alkylthiophene units, namely, poly(4'-perfluorohexyl-3-dodecyl-[2,2']-bithiophene) (**PT-H12-*alt*-F6**) and poly(4'-perfluorooctyl-3-octyl-[2,2']-bithiophene) (**PT-H8-*alt*-F8**), were synthesized following the methods described in Chapter III.

3-Alkylthiophenes were prepared by Kumada-coupling, which is a Ni(dppp)Cl_2 catalyzed reaction of 3-bromothiophene and alkyl Gringard reagents.

Poly(3-(4,4,5,5,6,6,7,7,8,8,9,9,9-tridecafluorononyl)-4'-nonyl-2,2'-bithiophene, **PT-H3F6-*alt*-H9**, was synthesized by Hong and Collard.[47]

UV-vis analysis was performed with a Perkin-Elmer Lambda 19 spectrometer. Fluorescence spectra were collected with a Spex Fluorolog Fluometer 1681 0.22m Spectrometer.

TEM images and diffraction patterns were collected in a JEDL 100C TEM (100KV) equipment. samples were prepared by placing a drop of the solution on carbon-coated Cu grids and allowed to dry in air.

Results and Discussion

"Shoulder" in the solution UV-vis spectrum

When comparing the UV-vis absorption spectra of poly(3-octylthiophene) (**PT-H8**) and poly(3-(perfluorooctyl)thiophene) (**PT-F8**) with the alternating copolymer poly(4'-perfluorooctyl-3-octyl-[2,2']-bithiophene) (**PT-H8-*alt*-F8**), besides a shift of the absorption peak, the absorption spectra of the copolymer has a distinct shoulder starting at around 500 nm. This shoulder is absent in the spectra of the two homopolymers, **PT-H8** and **PT-F8**. The homopolymers both have a sharp cut-off in the absorption spectrum, which is typical for the contribution of a single species, Figure 4.2.

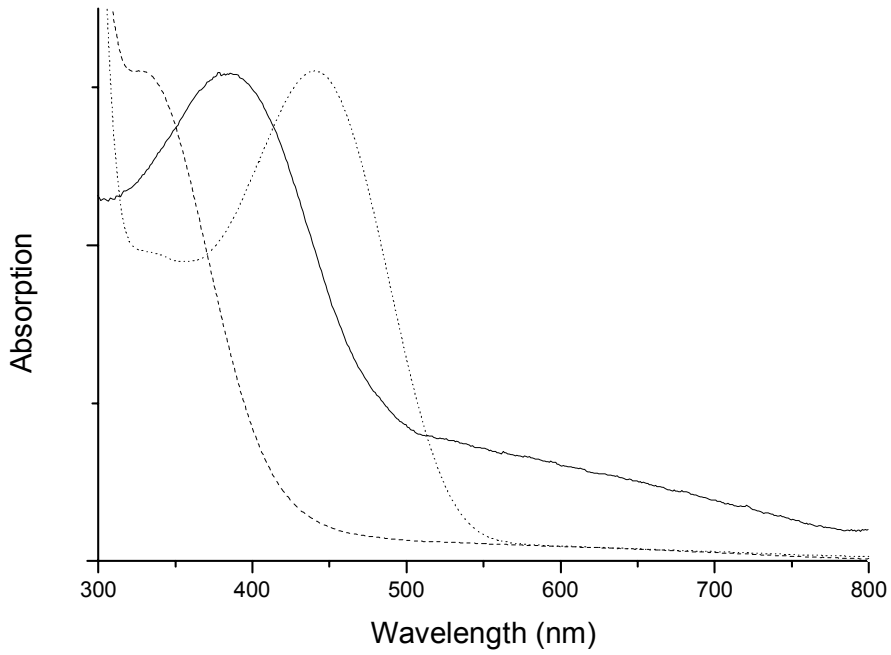

Figure 4.2. UV-vis spectra (normalized) of **PT-F8** (----), **PT-H8-*alt*-F8** (—) and **PT-H8** (….) in 10^{-5} M solution in chloroform.

We reason that this absorption at higher wavelength is due to another species. The spin-coated films of **PT-H8-*alt*-F8** absorb at a maximum of 456 nm. It suggests the shoulder starting around 500 nm in the solution spectrum could be contributed by the solid-state-like aggregates in solution, Figure 4.3. Those aggregates should have the similar photophysical properties with the solid state polymers.

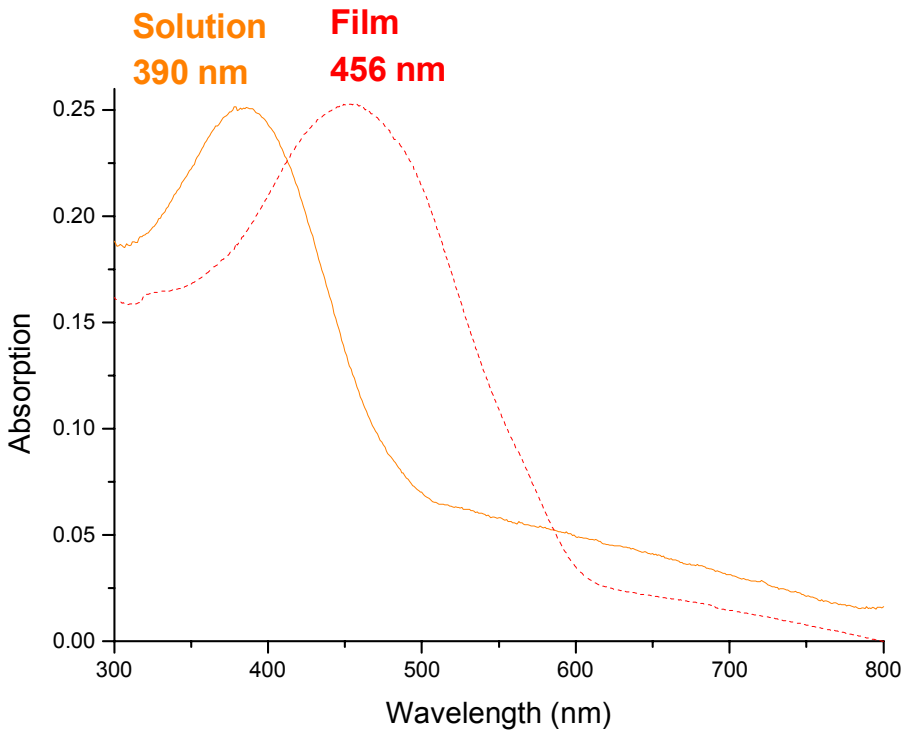

Figure 4.3. UV-vis spectra (normalized) of **PT-H8-*alt*-F8**: spin-coated film (----) and 10^{-5} M solution in chloroform (—)

Fluorescence of the aggregates

To provide further evidence for the presence of aggregates of **PT-H8-*alt*-F8** formed in solution, we observed the solid-state-like emission in the fluorescence spectra of solutions. The alternating copolymer solution emits yellow fluorescence with the maximum at 547 nm which is excited at the solution absorption maximum of 390 nm. The polymer film emits red fluorescence with maximum at 612 nm and a shoulder at 649 nm when excited at the film absorption maximum 456 nm, Figure 4.4.

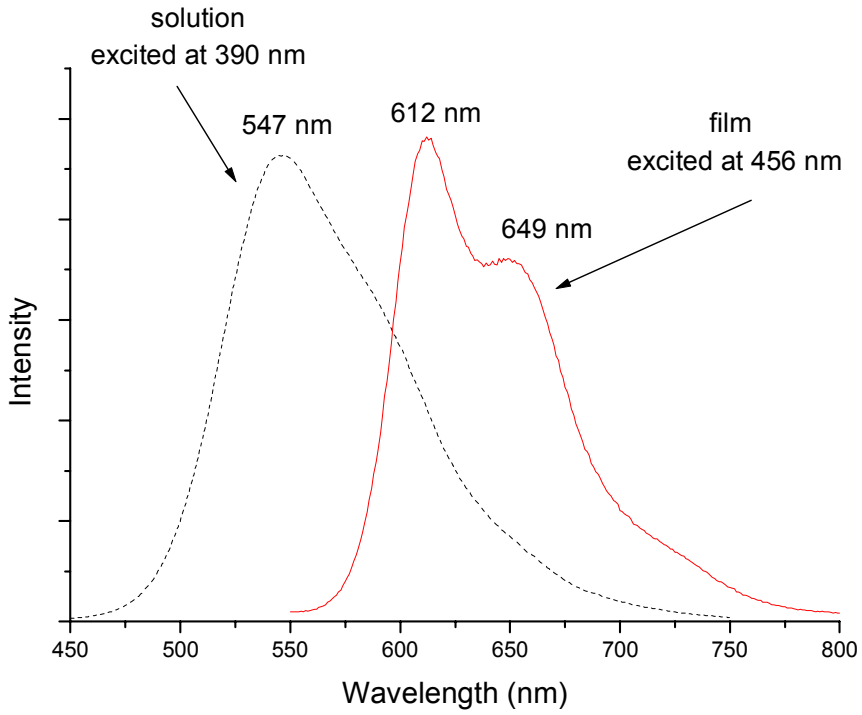

Figure 4.4. Emission spectra (normalized) of **PT-H8-*alt*-F8**: 10^{-5} M solution in chloroform (----), excited at 390 nm and spin-coated film (—).

If no aggregates are formed in solution, changing the excitation wavelength to the red direction (toward the shoulder ~500 nm) should provide the same emission spectra since there was only one species. However, the solution emission shows the significant changes upon changing the excitation wavelength, Figure 4.5. With the excitation at 480 nm, there is a new peak at the maximum of 600 nm, which is similar with the emission of the solid state. Further shifting the excitation to longer wavelengths increases the relative strength of this contribution for the emission of the solution state. These results suggest the existence of the aggregates which have very similar photophyisical properties to those

of the polymer films. The absorption of the aggregates is dominant in the shoulder region, so the emission spectra excited at 500 nm should show the characteristics of the emission of aggregates.

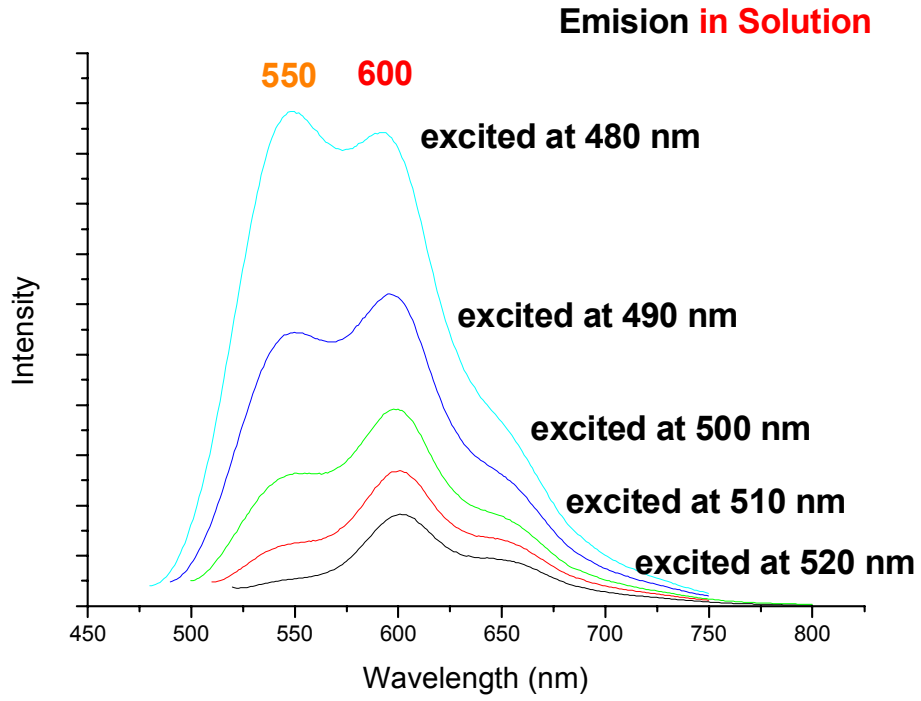

Figure 4.5. Emission spectra of **PT-H8-*alt*-F8**, 10^{-5} M solution in chloroform, excited at various wavelength (from 480 nm to 520 nm)

Thermochromism in solution

The process of self-assembly in solution to form aggregates is an equilibrium process which can be controlled by external stimuli. Thermochromism of the polymer solution in both UV-vis and fluorescence spectra suggests the existence of such an equilibrium.

The UV-vis absorption spectra of solutions were collected at different temperatures. At high temperature (60 °C), the shoulder almost disappears and the spectrum has a sharp cut-off, consistent with the absorption of a single species, the pure solution state. With the decrease of temperature, a shoulder at ~500 nm grows with a concomitant decrease in the intensity of the absorption at 390 nm. This suggests the formation of polymer aggregates upon cooling solution. An isosbestic point at 420 nm indicates there are only two states of the polymer which are in equilibrium with each other in solution, the pure solution state and the aggregation state, Figure 4.6. The presence of an isosbestic point and absence of a continuous shift of the absorption peak indicates that there is no intermediate conformation change between the twisted conformation in solution state and the planar conformation in aggregation state.

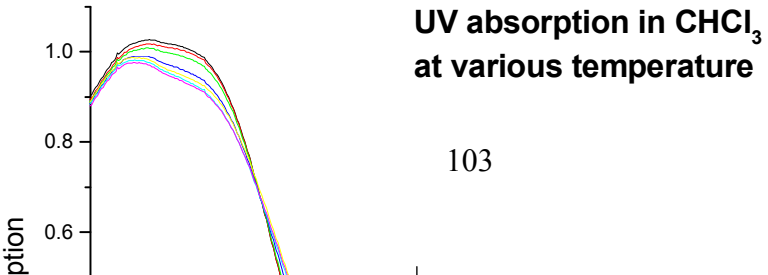

Figure 4.6. UV-vis spectra of **PT-H8-*alt*-F8**, 10^{-5} M solution in chloroform at every10 °C from 0°C to 60°C.

The thermochromism in solution has also been shown with fluorescence experiments. The polymer solution was excited at 390 nm, the absorption maximum of the solution state. With the decrease of temperature, a shoulder at 600 nm appears in the emission spectra, Figure 4.7. This indicates the formation of aggregates. Although the solid state absorbs at a maximum at 456 nm, it still has the absorption at 390 nm, Figure 4.3. When the solution with aggregates was excited at 390 nm, both the solution state and the aggregation state emit strongly. The solution state has a stronger absorption to give a peak, and the aggregation state has a weaker absorption contributes to form a shoulder.

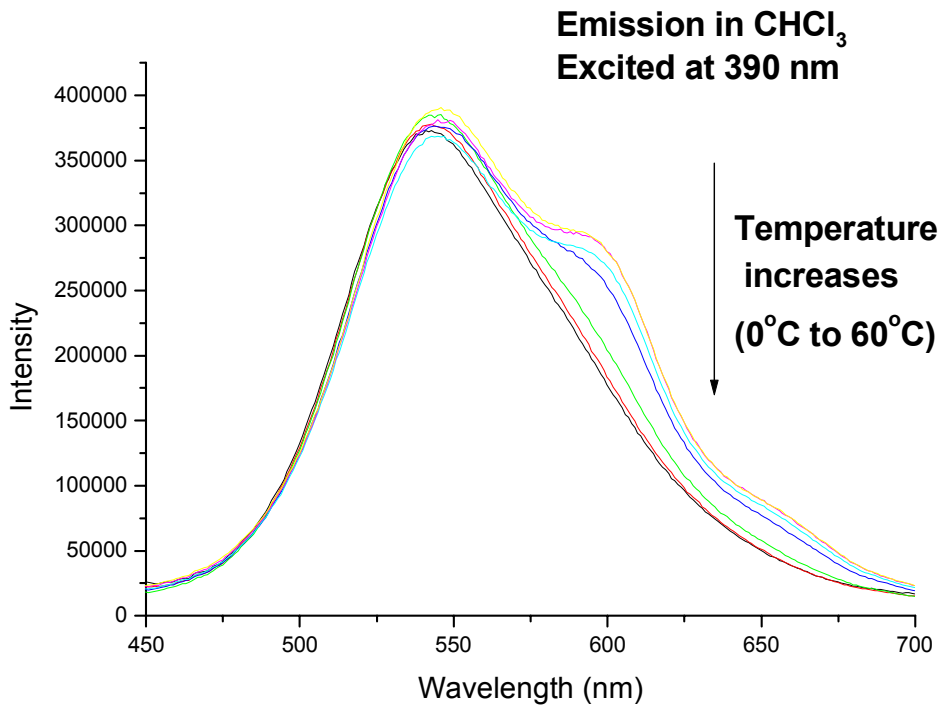

Figure 4.7. Fluorescence emission spectra of **PT-H8-*alt*-F8**, excited at 390 nm, 10^{-5} M solution in chloroform at every 10 °C from 0 °C to 60 °C.

The polymer solution was also excited at 500 nm where only the aggregation state has an absorption contribution. At higher temperature (e.g., 50-60 °C), there is no emission at 600 nm. This again indicates that there is no aggregation at the higher temperature. Between 50 °C and 40 °C, the solid-state-like emission turns on as aggregates are formed. The intensity of this emission increases further at lower temperatures, Figure 4.8. These emission experiments at various temperatures further prove the existence of the aggregation state and also gives the details for the aggregation process.

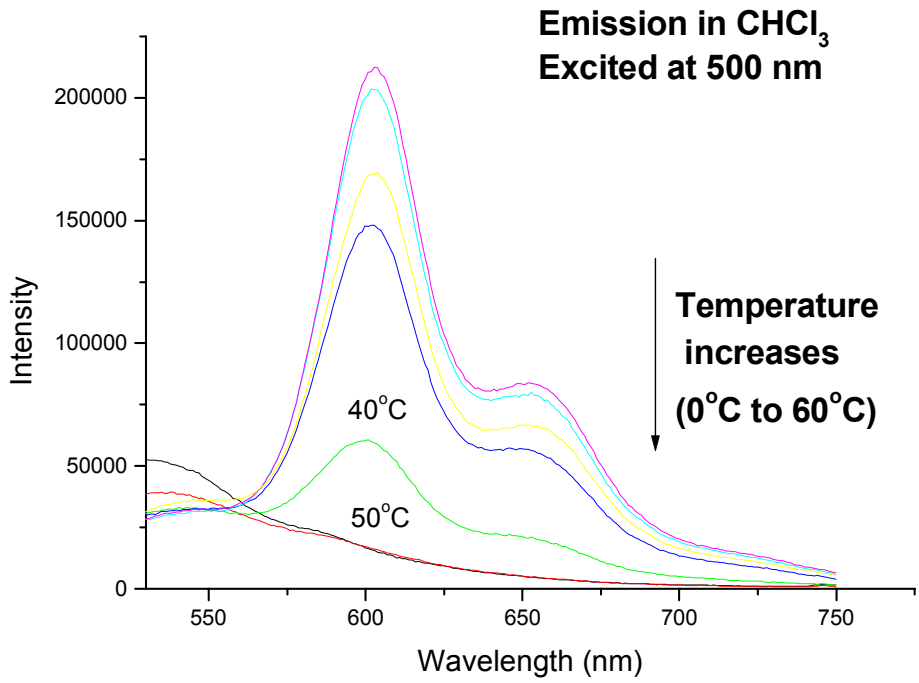

Figure 4.8. Fluorescence emission spectra of **PT-H8-*alt*-F8**, excited at 500 nm, 10^{-5} M solution in chloroform at every 10 °C from 0 °C to 60 °C.

Solvatochromism upon addition of methanol

The equilibrium between the solution state and the aggregation state can also be controlled by addition of a poor solvent.

The UV-vis absorption spectra of the solution were collected with the addition of MeOH. With more MeOH, the shoulder at ~500 nm increases in intenisty with a decrease in the absorption at 390 nm. This suggests the gradual formation of polymeric aggregates in solution upon addition of a poor solvent. As in the case of

thermochromism, an isosbestic point at 451 nm indicates there are only two states of the polymer which are in equilibrium with each other in solution, Figure 4.9.

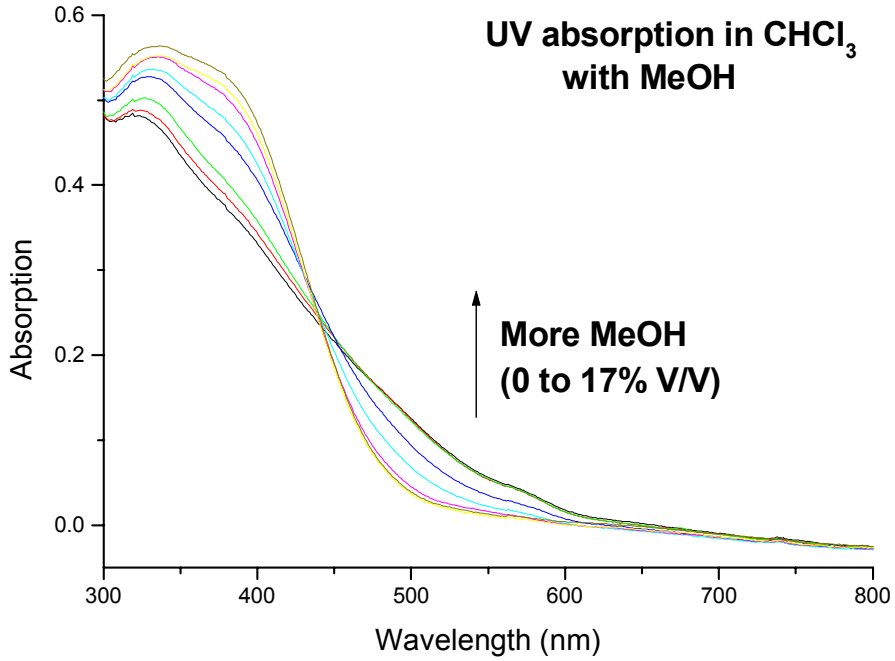

Figure 4.9. UV-vis spectra (normalized to the same concentration) of **PT-H8-*alt*-F8**, 10^{-5} M solution in chloroform by addition of every 2.4% (V/V) of MeOH from 0 to 17%.

The solvatochromism in solution is also demonstrated by the fluorescence experiments. The polymer solution was excited at 390 nm. Upon addition of more MeOH, the shoulder at 600 nm appears and becomes more and more evident in the

emission spectra, and finally competes with the emission from the solution state, Figure 4.10. This suggests more and more aggregates form upon addition of MeOH. The polymer solution was also excited at 500 nm. All the spectra were collected at room temperature and the aggregates already start to form in pure $CHCl_3$. So even without MeOH, the solid-state-like emission was observed. With more and more MeOH, the emission intensity increases due to the formation of even more aggregates, Figure 4.11.

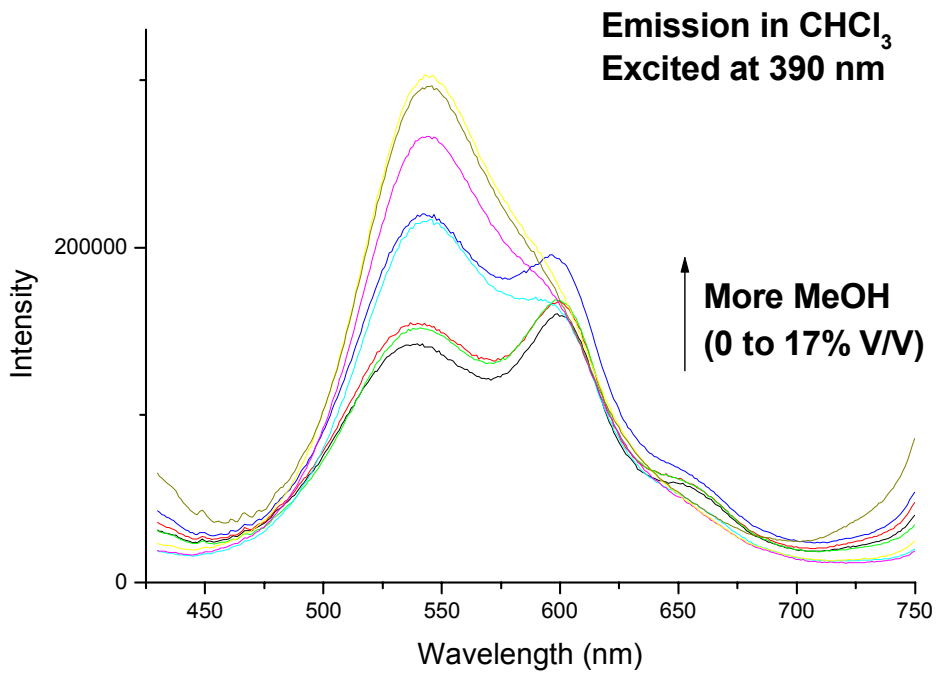

Figure 4.10. Fluorescence spectra of **PT-H8-*alt*-F8**, excited at 390 nm, 10^{-5} M solution in chloroform by addition of every 2.4% (V/V) of MeOH from 0 to 17%.

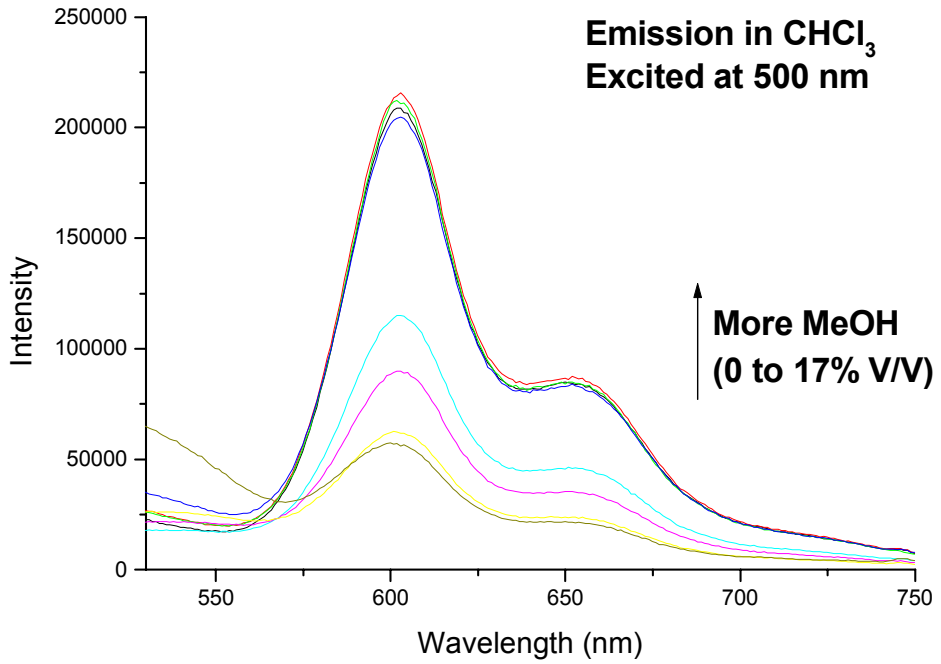

Figure 4.11. Fluorescence spectra of **PT-H8-*alt*-F8**, excited at 500 nm, 10^{-5} M solution in chloroform by addition of every 2.4% (V/V) of MeOH from 0 to 17%.

Solvatochromism in fluorophilic solvent

The alternating copolymer, **PT-H8-*alt*-F8**, is amphiphilic with both fluoroalkyl chains and alkyl chains. Thus, the fluorophlilic solvents (e.g., Freon-113) might also influence the conformation the amphiphilic polymer backbone. UV-vis absorption spectra of the polymer were collected in different solvents: pure $CHCl_3$, pure Freon-113 and mixtures of the two, Figure 4.12. The $CHCl_3$ solution absorbs at a maximum of 396 nm (ε = 6300 $M^{-1}cm^{-1}$). This is the highest value of λ_{max} recorded in this selection of solvents, corresponding to the longest conjugation length, in other words, a most planar

backbone. With the fluorophilic solvent, Freon-113, the solution is a blue shifted to 376 nm (ε = 6900 $M^{-1}cm^{-1}$). This suggests that the fluorophilic solvent makes the fluoroalkyl chain disordered and twists the conjugated backbone. Interestingly, the mixture solvent solution has the lowest absorption at 343 nm (ε = 21000 $M^{-1}cm^{-1}$). This might be due to the disordering of both alkyl chain and fluoroalkyl chain.

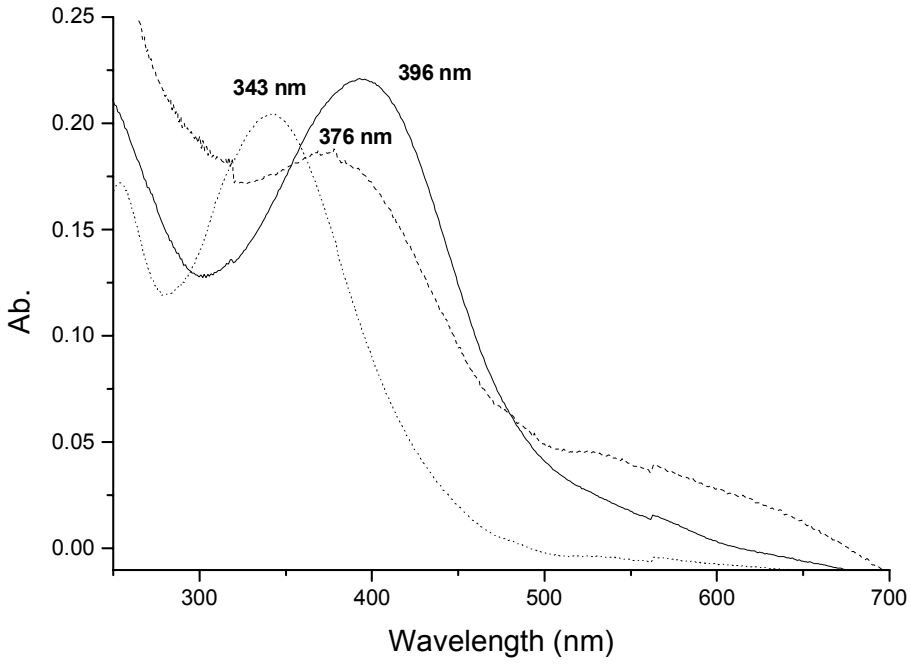

Figure 4.12. UV-vis spectra (normalized) of **PT-H8-*alt*-F8**, 10^{-5} M solution in Freon-113 (----), $CHCl_3$ (—) and 1:1 Freon-113/$CHCl_3$ (….)

Contribution of intra-molecular interaction

Although polythiophenes have a relative rigid backbone, these chains still can fold, if the chains are long enough. Thus, intra-molecular interaction can also contribute to the aggregation in solution.

A 100 μM solution of PT-H8-*alt*-F8 in $CHCl_3$ was diluted by a factor of ten and one hundred. The UV-vis spectra of all these solutions were collected and normalized to the same absorbance at λ_{max}. Even for the 1 μM solution, the aggregation band (shoulder around 500 nm) still exists, Figure 4.13. It indicates the aggregation has the contribution from the intra-molecular interaction by folding.

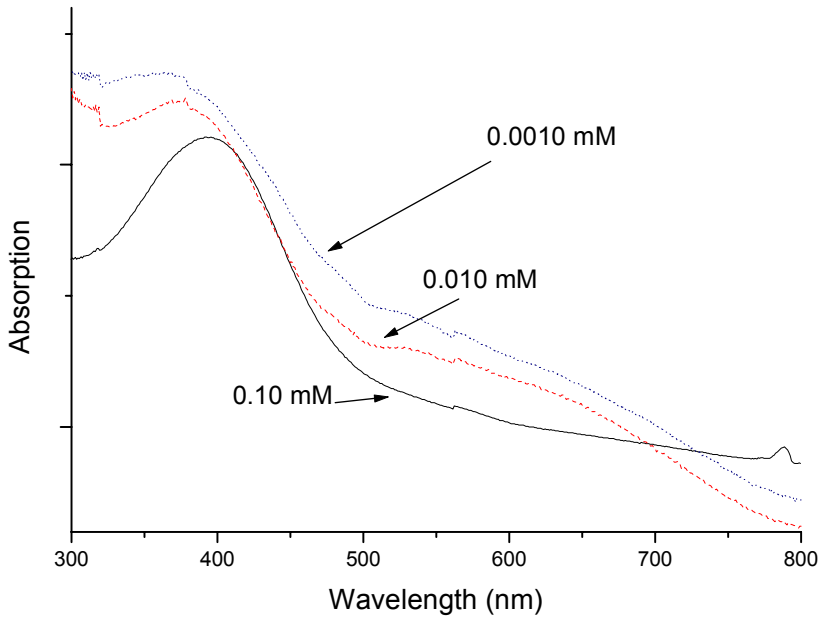

Figure 4.13. UV-vis spectra (normalized) of **PT-H8-*alt*-F8**, 0.10 mM (—), 0.010 mM (- - -) and 0.0010 mM (….) solution in $CHCl_3$

To further prove the existence of aggregation in dilute solutions (e.g., 1 μM), the fluorescence spectra were collected at different excitation wavelengths. As expected, these show a typical solution state emission upon the excitation at the maximum absorption at 390 nm. With the excitation in the range of the aggregation band from 480 nm to 520 nm, the profile of emission spectra gradually changes from the solution emission to the solid-state-like emission, Figure 4.14. The evolution of emission spectra confirms the existence of the aggregation in highly dilute solution. Thus, the aggregation of the alternating copolymer in solution is the result of both intermolecular and intramolecular interaction.

A.

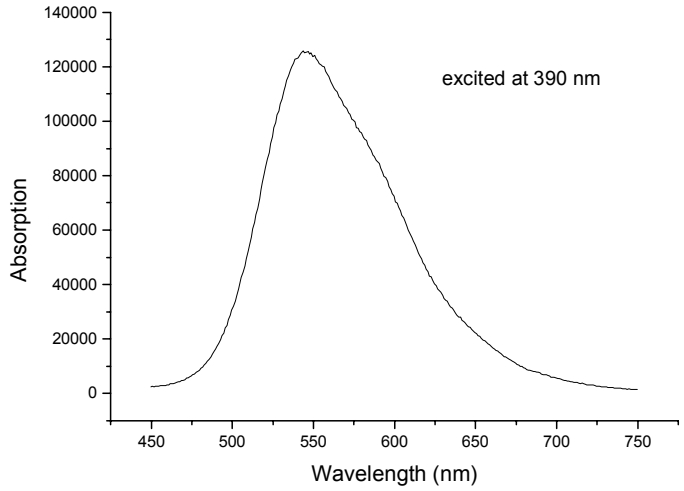

B.

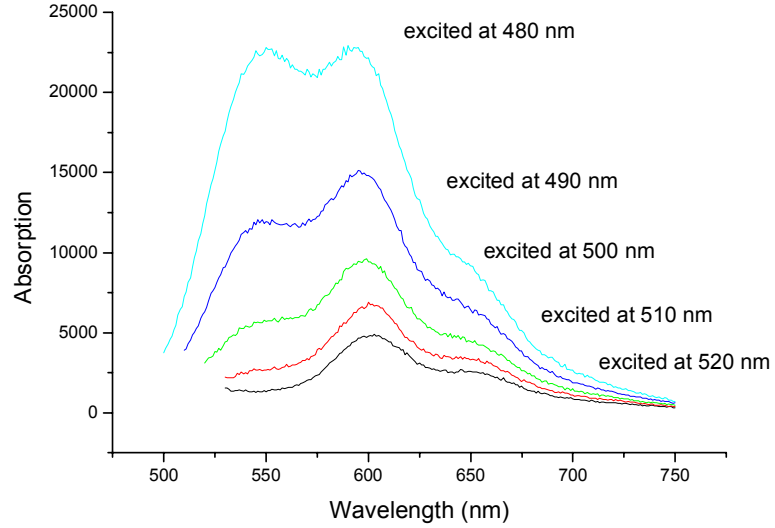

Figure 4.14. (A): Fluorescence spectra of **PT-H8-*alt*-F8**, excited at 390 nm, 10^{-6} M solution in chloroform; (B): Emission spectra of **PT-H8-*alt*-F8**, 10^{-6} M solution in chloroform, excited at various wavelength (from 480 nm to 520 nm)

On the other hand, with a shorter chain length, **PT-H8-*alt*-F8** oligomers should have less chance to aggregate with an intramolecular interaction by folding. The crude PT-H8-*alt*-F8 was fractionated with Soxhlet extractor and the extraction gave several fractions. The hexane fraction of PT-H8-*alt*-F8, which is the oligomer, was used to explore this further. The $CHCl_3$ solution of oligomers shows the similar thermochromism and solvatochromism as PT-H8-*alt*-F8. In the thermochromism study, the solid-state-like emission turns on between 20 °C and 30 °C which is lower than the polymer turn-on temperature (40-50 °C), Figure 4.15. This arises because the oligomer has less contribution from intramolecular assembling and requires less energy (lower temperature) to disassemble. The solvatochromism experiments show the same result. The oligomers do not aggregate at room temperature and they only start to aggregate with 8% of MeOH, Figure 4.16. In the case of polymers, even without addition of MeOH, polymers are partially aggregated in $CHCl_3$.

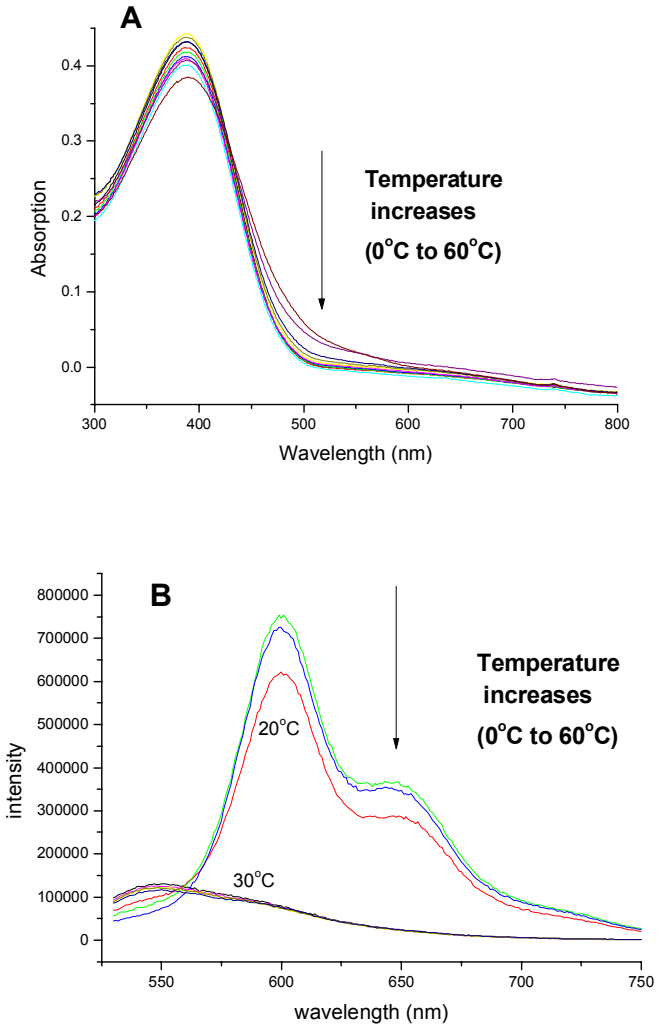

Figure 4.15. (A): UV-vis spectra of **PT-H8-*alt*-F8** oligomer, 10^{-5} M solution in chloroform at every 10 °C from 0 °C to 60 °C; (B): Fluorescence emission spectra of **PT-H8-*alt*-F8** oligomer, excited at 500 nm, 10^{-5} M solution in chloroform at every 10 °C from 0 °C to 60 °C.

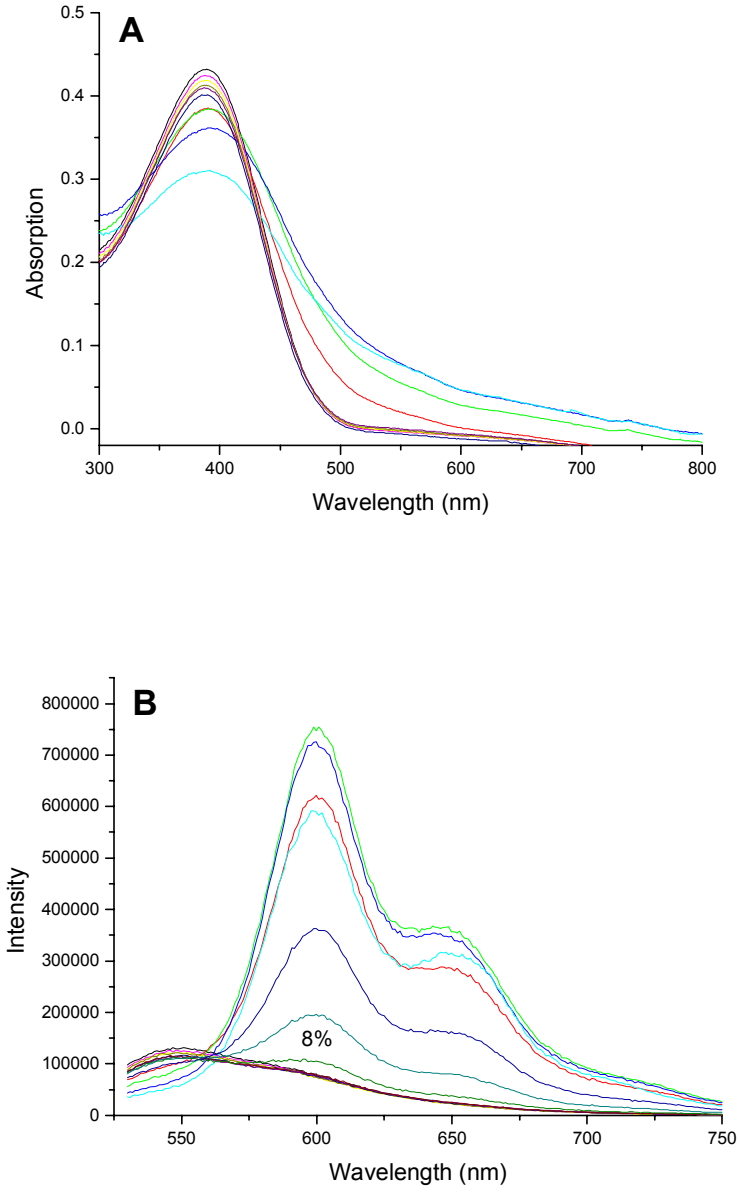

Figure 4.16. (A): UV-vis spectra (normalized to the same concentration) of **OligoT-H8-*alt*-F8**, 10^{-5} M solution in chloroform by addition of every 2.4% (V/V) of MeOH from 0 to 24%; (B): Fluorescence spectra of **OligoT-H8-*alt*-F8**, excited at 500 nm, 10^{-5} M solution in chloroform by addition of every 2.4% (V/V) of MeOH from 0 to 24%.

Exploring the origin of polymer aggregation

There are three structure characteristics of PT-H8-*alt*-F8 which could induce the aggregation: (I), the incompatibility of rigid backbone and flexible side chains; (II), the amphiphilicity of the polymer by virtue of the fluoroalkyl and alkyl substituents; (III), electron donor-acceptor interactions between alkyl-substituted electron rich rings and perfluoroalkyl-substituted electron poor rings. Control experiments were performed to identify which factor may induce this aggregation.

UV-vis and fluorescence spectra of $CHCl_3$ solution of regioregular poly(3-octylthiophene), **PT-H8**, were collected at various temperatures and upon addition of MeOH. **PT-H8** does not show either thermochromism or solvatochromism in solution and no solid-state-like emission was turned on, Figure 4.17. This result suggests the aggregation does not arise solely from the incompatibility of the backbone and side chains.

The same experiments were performed to an alternating copolymer with alkylthiophene and semifluoroalkylthiophene units, **PT-H3F6-*alt*-H9**. This copolymer is amphiphilic by virtue of the fluoroalkyl and alkyl chains. However, the hydrocarbon linker of the semifluoroalkyl chains insulates the electron withdrawing effect of fluoroalkyl chains from the polythiophene backbone. All of the thiophene rings are electron-rich. **PT-H3F6-*alt*-H9** does not have the electron donor-acceptor structrue. The UV-vis and fluorescence spectra were collected under various temperatures or upon addition of MeOH. **PT-H3F6-*alt*-H9** does not show either thermochromism or solvatochromism in solution, and no solid-state-like emission was observed, Figure 4.18.

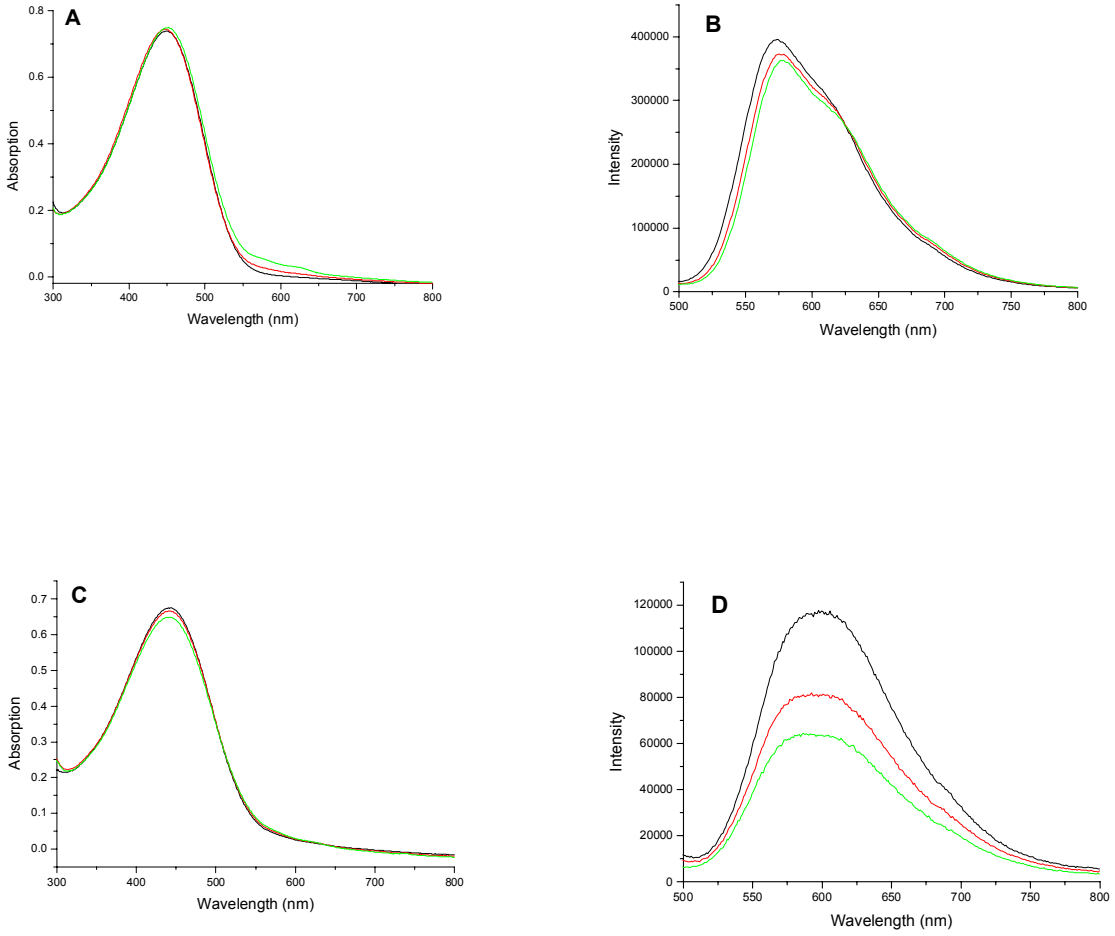

Figure 4.17. (A): UV-vis spectra of **PT-H8**, 10^{-5} M solution in chloroform at every 30 °C from 0 °C to 60 °C; (B): Fluorescence emission spectra of **PT-H8**, excited at 449 nm, 10^{-5} M solution in chloroform at every 30 °C from 0 °C to 60 °C; (C): UV-vis spectra (normalized to the same concentration) of PT-H8, 10^{-5} M solution in chloroform by addition of every 8% (V/V) of MeOH from 0 to 16%; (D): Fluorescence spectra of PT-H8, excited at 449 nm, 10^{-5} M solution in chloroform by addition of every 8% (V/V) of MeOH from 0 to 16%.

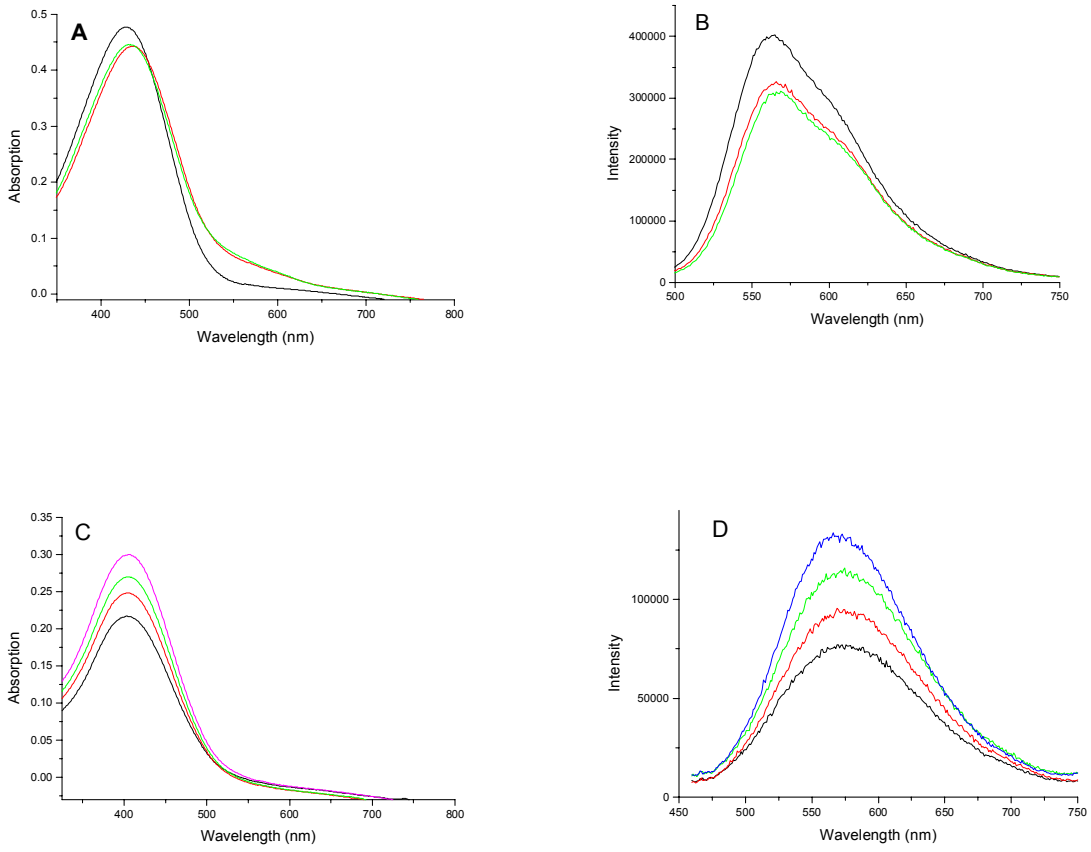

Figure 4.18. (A): UV-vis spectra of **PT-H3F6-*alt*-H9**, 10^{-5} M solution in chloroform at every 30 °C from 0 °C to 60 °C; (B): Fluorescence emission spectra of **PT-H3F6-*alt*-H9**, excited at 434 nm, 10^{-5} M solution in chloroform at every 30 °C from 0 °C to 60 °C; (C): UV-vis spectra (normalized to the same concentration) of **PT-H3F6-*alt*-H9**, 10^{-5} M solution in chloroform by addition of every 8% (V/V) of MeOH from 0 to 24%; (D): Fluorescence spectra o **PT-H3F6-*alt*-H9**, excited at 434 nm, 10^{-5} M solution in chloroform by addition of every 8% (V/V) of MeOH from 0 to 24%.

Combing these two control experiments, we reason that the electron donor-acceptor interaction is a key factor to induce self-assembly and to turn on the solid-state-like emission, although the amphiphilicity of fluoroalkyl and alkyl chains and the incompatibility of rigid backbone and flexible side chains might also contribute to the aggregation.

Nano-size crystals

The solid-like emission from solution of **PT-H12-*alt*-F6** changes upon cooling or addition of poor solvent in a similar manner as **PT-H8-*alt*-F8**. However, while a $CHCl_3$ solution of **PT-H12-*alt*-F6** containing 17% MeOH remains homogeneous, it shows red fluorescence (600 nm), the same as the red emission of polymer films. A solution of **PT-H12-*alt*-F6** in $CHCl_3$ displays the yellow fluorescence (547 nm). This indicates the formation of the aggrgation, the nano-size crystals, in solution, Figure 4.19.

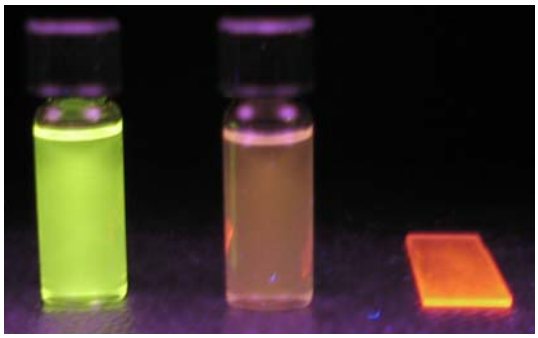

Figure 4.19. Fluorescence of **PT-H12-*alt*-F6** upon irradiation at 365 nm Left to right: 10^{-4} M solution in $CHCl_3$, nano-size crytals (10^{-4} M solution in $CHCl_3$ with 17% MeOH) and the film.

Transmission electron microscopy (TEM) carried out on samples evaporated from 83:17 $CHCl_3$/MeOH solution of the polymer. These images reveal the formation of platelets with an average dimension of 200 nm, Figure 4.20. Selected area electron diffraction of the platelets shows a diffraction pattern typical for single crystals, while other aggregates show polycrystalline diffraction. The diffraction pattern of single crystals indicates a hexagonal lattice, which is unexpected based on the lamellar packing of regioregular poly(3-alkylthiophene) homopolymers, Figure 4.21. However, the mode of packing of the polymer chains cannot be elucidated from the electron diffraction data alone, and further investigation is required.

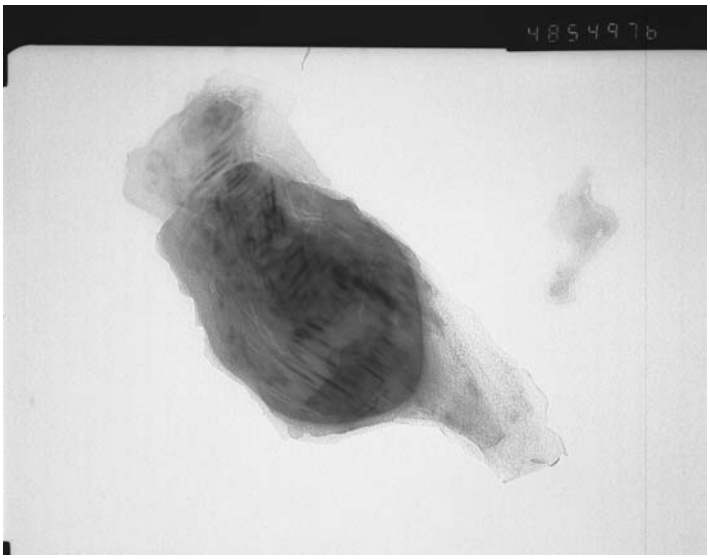

Figure 4.20. TEM image of nano-size crystals of **PT-H12-*alt*-F6**.

Figure 4.21. Selected area electron diffraction of nano-size crystals of **PT-H12-*alt*-F6**.

Proposed supramolecular structure

The aggregation state of **PT-H12-*alt*-F6** is the intermediate state between the solution state and solid state. The structure study of these nanocrystals could give some hints on the aggregation process from solution to films. The electron diffraction pattern with hexagonal lattice suggests the formation of an unusual supramolecular structure of nano-size crystals. Most X-ray diffraction studies on regioregular poly(3-substituted thiophene)s show a lamellar assembly in films, which leads to non-radiative relaxation of exicted state and shut off the fluorescence in solid state.

In the case of **PT-H12-*alt*-F6**, the combination of the electron donor-acceptor interactions, the amphiphilicity of the fluoroalkyl and alkyl substituents and the incompatibility of rigid backbone and flexible side chains, could induce a hexagonal

packing of polythiophene chains. This might be explained by the packing shown in Figure 4.22. This non-lamellar packing may explain the unusual strong fluorescence of this polymer in the solid state, although more study is still needed.

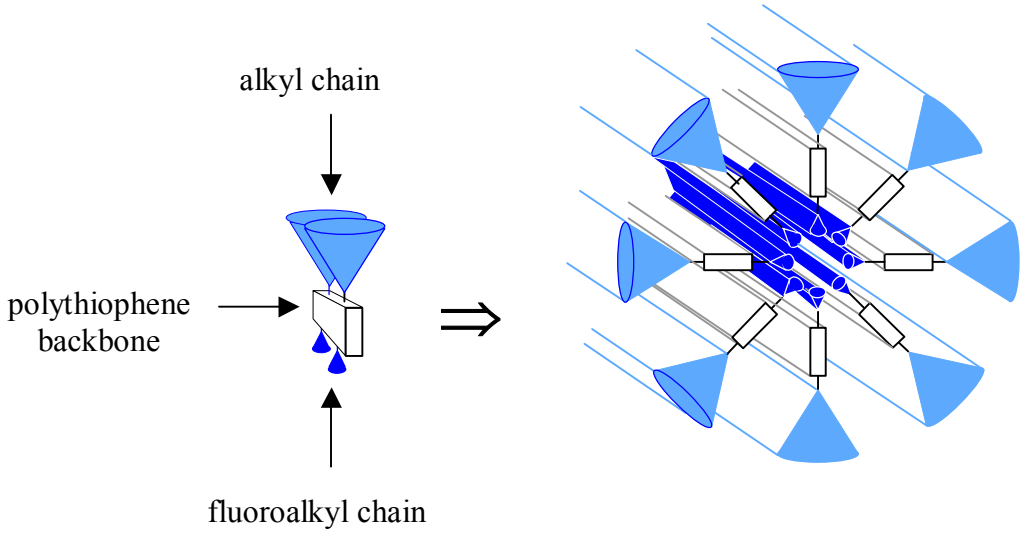

Figure 4.22. Proposed supramolecular structure.

Conclusions

The alternating fluoroalkyl/alkyl-subsituted polythiophene copolymers have a chemical structure which combines electron donor-acceptor interactions, the amphiphilicity of the fluoroalkyl and alkyl substituents, twisting of the backbone and the incompatibility of rigid backbone and flexible side chains, which leads both the

thermochromism and solvatochromism in solution in both absorption and emission. The chromic phenomena are attributed to non-lamella packing of chains in the aggregation-state of nano-size crystals, which show a hexagonal lattice in electron diffraction pattern. It may explain its unusually strong fluorescence in solid state.

References

1. *Handbook of Conducting Polymers*, 2nd ed. (Eds: Skotheim, T.; Reynolds, R. L.; Elsenbaumer, R. L.), Marcel Dekker, New York **1997**.

2. McCullough, R. D. *Adv. Mater*. **1998**, *10*, 93.

3. Leclerc, M.; Faid, K. *Adv. Mater*. **1997**, *9*, 1087.

4. Garnier, F. *Angew. Chem. Int. Ed.* **1989**, *28*, 513.

5. Examples include: (a) polythiophene derivatives: Robitaille, L.; Leclerk, M. *Macromolecules* **1994**, *27*, 1847; Sandstedt, C. A.; Rieke, R. D.; Eckhardt, C. J. *Chem. Mater.* **1995**, *7*, 1057; Ng, S. C.; Miao, P. *Macromolecules* **1999**, *32*, 5313. Yamamoto, T.; Komarudin, D.; Arai, M.; Lee, B. L.; Suganuma, H.; Asakawa, N.; Inoue, Y.; Kubota, K.; Sasaki, S.; Fukuda, T.; Matsuda, H. *J. Am Chem. Soc.* **1998**, *120*, 2047. (b) polysilane derivatives: Miller, R. D.; Michl, J. *Chem. Rev.* **1989**, *89*, 1359; Yuan, C. H.; West, R. *Macromolecules* **1994**, *27*, 629. (c) polydiacetylene derivatives: Chu, B.; Xu, R. *Acc. Chem. Res.* **1991**, *24*, 384; Jonas, U.; Shah, K.; Norvez, S.; Charych, D. H. *J. Am. Chem. Soc.* **1999**, *121*, 4580; (d) poly(alkyldithiazole)s: Conzalez-Ronda, L.; Martin, D. C.; Nanos, J. I.; Politis, J. K.; Curtis, M. D. *Macromolecules* **1999**, *32*, 4558. (e) polyanilines: Norris, I. D.; Kane-Maguire, L. A. P.; Wallace, G. G. *Macromolecules* **1998**, *31*, 6529. (f) oligo(*m*-phenylene ethynylene)s: Nelson, J. C.; Saven, J. G.; Moore, J. S.; Wolynes, P. G. *Science* **1997**, *277*, 1793; Prince, R. B.; Saven, J. G.; Wolynes, P. G.; Moore, J. S. *J. Am. Chem. Soc*. **1999**, *121*, 3114.

6. Leclerc, M.; Faid, K. in Handbook of Conducting Polymers, 2nd ed. (Eds: Skotheim, T.; Reynolds, R. L.; Elsenbaumer, R. L.), Marcel Dekker, New York **1997**, p. 695.

7. Song, K.; Miller, R. D.; Wallraff, G. M.; Rabolt, J. F. *Macromlecules* **1992**, *25*, 3629.

8. Yuan, C. H.; West, R. *Chem. Commun*. **1997**, 1825.

9. Marsella, M. J.; Newland, R. J.; Carroll, P. J.; Swager, T. M. *J. Am. Chem. Soc.* **1995**, *117*, 9842.

10. McCullough, R. D.; Ewband, P. C.; Loewe, R. S. *J. Am. Chem. Soc.* **1997**, *119*, 633.

11. Levesque, I.; Leclerc, M. *Macromolecules* **1997**, *30*, 4347.

12. Ahlers, M.; Muller, W.; Reichert, A.; Ringsdorf, H.; Venzmer, J. *Angew. Chem., Int. Ed*. **1990**, *29*, 1209.

13. Charych, D. H.; Nagy, J. O.; Spevak, W.; Bednarski, M. D. *Science* **1993**, *261*, 585

14. Okada, S. Y.; Peng, S.; Spevak, W.; Charych, D. *Acc. Chem. Res*. **1998**, *31*, 229

15. Faid, K.; Leclerc, M. *J. Am. Chem. Soc.* **1998**, *120*, 5274

16. Levesque, I.; Leclerc, M. *Chem. Mater*. **1996**, *8*, 2843.

17. Zhou, Q.; Swager, T. M. *J. Am. Chem. Soc.* **1995**, *117*, 12593.

18. Swager, T. M. *Acc. Chem. Res*. **1998**, *31*, 201.

19. Wang, B.; Wasielewski, M. R. *J. Am. Chem. Soc*. **1997**, *119*, 12.

20. Kimura, M.; Horai, T.; Hanabusa, K.; Shirai, H. *Adv. Mater*. **1998**, *10*, 459.

21. Yang, J. S.; Swager, T. M. *J. Am. Chem. Soc*. **1998**, *120*, 5321.

22. Bredas, J. L.; Street, G. B.; Themans, B.; Andre, J. M. *J. Chem. Phys*. **1985**, *83*, 1323.

23. Examples include: (a) regioregular poly(3-alkylthiophene)s: Zerbi, G.; Chirerichetti, B.; Inganas, O. *J. Chem. Phys.* **1991**, *94*, 4646. (b) poly(3-alkylthiothiophene)s: Wu, X.; Chen, T. A.; Rieke, R. D. *Macromolecules* **1996**, *29*, 7671. (c) poly(3-alkoxy-4methylthiophene)s: Faid, K.; Frechette, M.; Ranger, M.; Mazerolle, L.; Levesque, I.; Leclerc, M.; Chen, T. A.; Rieke, R. D. *Chem. Mater*. **1995**, *7*, 1390. (d) poly(3,3'-dialkyl-2,2'-bithiophene)s: Garreau, S.; Leclerc, M.; Errien, N.; Louarn, G. *Macromolecules* **2003**, *36*, 692. (e) poly(3,3'-dialkylthio-2,2'-bithiophene)s: Raymond, F.; DiCesae, N.; Belletete, M.; Durocher, G.; Leclerc, M. *Adv. Mater*. **1998**, *10*, 599. Apperloo, J. J.; Janssen, R. A. J.; Malenfant, P. R. L.; Frechet, J. M. J. *Macromolecules* **2000**, *33*, 7038.

24. Leclerc, M.; Ho, H-A. *Synlett.* **2004**, *2*, 380.

25. Roux, C.; Leclerc, M. *Chem. Mater*. **1994**, *6*, 620.

26. Wenz, G.; Muller, M. A.; Schmidt, M.; Wegner, G. *Macromolecules* **1984**, *17*, 837.

27. Politis, J. K.; Somoza, F. B. Jr.; Kampf, J. W.; Curtis, M. D.; Gonzalez Ronda, L.; Martin, D. C. *Chem. Mater.* **1999**, *11*, 2274.

28. Harlev, E.; Wudl, F. In *Conjugated Polymers and Related Materials. The Interconnection of Chemical and Electronic Structures;* Salaneck, W. R.; Lundstrom, I.; Ranby, B. Eds.; Proceedings of the 81st Nobel Symposium; Oxford University Press: Oxford, England, 1993; p 139.

29. Nilsson, K. P. R.; Andersson, M. R.; Inganas, O. *Synth. Metals* **2003**, *135-136*, 291.

30. Zhang, Z. B.; Fujiki, M.; Montonaga, M.; Nakashima, H.; Torimitsu, K.; Tang, H. Z. *Macromolecules* **2002**, *35*, 941.

31. Apperloo, J. J.; Janssen, R. A. J.; Malenfant, P. R. L.; Frechet, J. M. J. *J. Am. Chem. Soc.* **2001**, *123*, 6916.

32. Iarossi, D.; Mucci, A.; Parenti, F.; Schenetti, L.; Seeber, R.; Zanardi, C.; Forni, A.; Tonelli, M. *Chem. Eur. J.* **2001**, *7*, 676.

33. Kim, B.; Chen, L.; Gong, J.; Osada, Y. *Macromolecules* **1999**, *32*, 3964.

34. Bolognesi, A.; Giacometti Schieroni, A.; Botta, C.; Marinelli, M.; Mendichi, R.; Rolandi, R.; Relini, A.; Inganas, O.; Theandher, M. *Synth. Metals*. **2003**, *139*, 303.

35. Kiriy, N.; Jahne, E.; Adler, H-J.; Schneider, M.; Kiriy, A.; Gorodyska, G.; Minko, S.; Jehnichen, D.; Simon, P.; Fokin, A. A.; Stamm, M. *Nano Lett*. **2003**, *3*, 707.

36. Brustolin, F.; Goldoni, F.; Meijer, E. W.; Sommerdijk, N. A. J. M. *Macromolecules* **2002**, *35*, 1054.

37. Jenekhe, S. A.; Chen, X. L. *Science* **1998**, *279*, 1903.

38. Jenekhe, S. A.; Chen, X. L. *Science* **1999**, *283*, 372.

39. Tew, G. N.; Pralle, M. U.; Stupp, S. I. *Angew. Chem., Int. Ed.* **2000**, *39*,517.

40. Wang, H.; Wang, H. H.; Urban, V. S.; Littrell, K. C.; Thiyagarajan, P.; Yu, L. *J. Am. Chem. Soc*. **2000**, *122*, 6855.

41. Leclere, P.; Calderone, A.; Marsitzky, D.; Francke, V.; Geerts, Y.; Mullen, K.; Bredas, J. L.; Lazzaroni, R. *Adv. Mater*. **2000**, *12*, 1042.

42. Liu, J.; Sheina, E.; Kowalewski, T.; McCullough, R. D. *Angew. Chem., Int. Ed*. **2002**, *41*, 329.

43. Bjornholm, T.; Hassenkam, T.; Greve, D. R.; McCullough, R. D.; Jayaraman, M.; Savoy, S. M.; Jones, C. E.; McDevitt, J. T. *Adv. Mater*. **1999**, *11*, 1218. Reitzel, N.; Greve, D. R.; Kjaer, K.; Howes, P. B.; Jayaraman, M.; Savoy, S.; McCullough, R. D.; McDevitt, J. T.; Bjornholm, T. *J. Am. Chem. Soc.* **2000**, *122*, 5788.

44. Stokes, K. K.; Heuze, K.; McCullough, R. D. *Macromolecules* **2003**, *36*, 7114.

45. Hong, X.; Tyson, J. C.; Middlecoff, J. S.; Collard, D. M. *Macromolecules* **1999**, *32*, 4232.

46. Hong, X. M.; Collard, D. M. *Macromolecules* **2000**, *33*, 3502.

47. Hong, X.; Tyson, J. C.; Collard, D. M. *Macromolecules* **2000**, *33*, 6916.

CHAPTER V

SYNTHESIS AND ELECTROCHEMISTRY OF POLY(3-(1,1-DIFLUOROOCTYL)THIOPHENE)

Introduction

The first preparation of unsubstituted polythiophene was reported in 1980.[1,2] Polythiophene itself is insoluble in common organic solvents. Installation of alkyl chains at the 3-position gives poly(3-alkylthiophene)s affords a soluble and processable analogue. The first synthesis of stable and soluble poly(3-alkylthiophene)s was reported by Elsenbaumer in 1985.[3] Alkyl chains longer than butyl render poly(3-alkylthiophene)s soluble in common organic solvents at room temperature,[4] which allows them to be solution-processed into films which exhibit reasonably high electrical conductivities after doping. Since the early 1990s, McCullough[5,6,7] and Rieke[8] developed methods to prepare the regioregular, head-to–tail coupled, poly(3-alkylthiophene)s. Detailed structural analysis indicates that regioregular HT poly(3-alkylthiophene)s assemble into 2-D solid-state structures, with interdigitated alkyl chain packing, and the conjugated backbone stacking at a distance of 3.8Å This highly ordered self-assembled structure strongly influences the electronic properties of the polymer and the performance of devices incorporating them, such as the charge mobility and the on/off ratio in FETs.

An important aspect for a successful implementation of organic semiconductors in microelectronic switching and memory devices is the availability of p-type (hole carrier) as well as n-type (electron carrier) semiconducting materials to enable important logic elements such as p-n junction diodes, bipolar transistors, and complementary circuits.[9] However, polythiophene derivatives are normally only amenable to p-doping (i.e., oxidation), and poly(3-alkylthiophene)s (PATs) only undergo reduction under extreme conditions.[10] Poly(3-alkylthiophene) has naturally an electron-rich conjugated backbone, which upon reduction leads to a high energy polymeric radical.

Perfluoroalkyl substitution is an effective way to prepare the n-type oligothiophenes. α,ω-Diperfluorohexylsexithiophene was prepared as the first n-type oligothiophene-based semiconductor.[11,12] A homologous family of fluorocarbon-substituted thiophene oligomers were made and demonstrate the high electron mobility.[13] Besides α,ω-substitution, β,β'-di(perfluorohexyl)-substituted thiophene oligomers were also synthesized.[14] Most recently, a new polythiophene-fluorobenzene semiconductor family has been synthesized. The perfluorobenzene terminated tetrathiophene shows the highest electron mobility (0.08 $cm^2V^{-1}s^{-1}$) reported in the thiophene series.[15] In addition, fluorine substituents also lower the reduction potential of thiophenes, tetradecafluorosexithiophene was synthesized as the first perfluorinated oligothiophene and the X-ray structure suggests the high electron mobility along π-π stacking direction.[16]

We recently reported the synthesis and characterization of regioregular HT poly(3-perfluorooctylthiophene), PT-F8.[17] PT-F8 is n-dopable and it is soluble in supercritical CO_2. However, while PT-F8 is soluble in fluorophilic solvents such as Freon, it is not soluble in common organic solvents, making it difficult to process this

polymer by traditional solution methods. PT-F8 has a twisted backbone and does not form an ordered solid state structure, which might lower the electron mobility.

Here we describe the design of a new polythiophene analogue, poly(3-(1,1-difluoroalkyl)thiophene), which combines the electronic characteristic of poly(3-(perfluoroalkyl)thiophene)s and with long hydrocarbon side chains characteristic of poly(3-alkylthiophene)s. This polymer still has the fluorocarbon directly attaching to the backbone, so it should retain the n-dopablility; on the other hand, the long alkyl chains might still facilitate formation of an ordered solid-state structure.

The monomer was prepared and polymerized electrochemically. The electrochemistry of the polymer was characterized.

Experimental

General methods

All reagents were obtained from commercial sources and used without further purification unless stated otherwise. Tetrahydrofuran (THF) and diethyl ether were dried over sodium benzophenone ketyl prior to distillation under nitrogen. Methylene chloride was dried over calcium hydride prior to distillation under nitrogen. Column chromatography was performed on silica gel (40 mesh, 60Å, Baker). Thin layer chromatography was performed on 3×5 cm plates of silica gel (0.2 mm thick, 60 F_{254}) on an aluminum support (EM Separations). All ^{1}H NMR spectra were collected on a Varian Gemini 300 MHz instrument using $CDCl_3$ as the solvent unless otherwise specified. Chemical shifts are reported relative to tetramethylsilane. ^{13}C NMR spectra were obtained at 75.5 MHz. IR analysis was performed on a Nicolet 520 FTIR

spectrometer. Electrochemical experiments were performed using a BAS 100B electrochemical analyzer in three-electrode cell equipped with a 2.0 mm^2 gold or platinum or graphite disk working electrode, a platinum wire counter electrode, and a saturated calomel electrode (SCE).

Synthesis

1-Thiophen-3-yl-octan-1-one (20). A mixture of thiophen-3-yl-boranediol (5.0 g, 39 mmol, $Pd(OAc)_2$ (0.26 g, 1.2 mmol) and tri(*para*-methoxylphenyl)phosphine (0.96 g, 2.7 mmol)) in 150 mL THF under N_2 was heated at 60 °C for 16 h. The resulting solution was poured into 200 mL ice/water and extracted with hexane (3 × 100 mL). The extract was stirred with 100 mL 10% NaOH for 4 h. The organic layer was separated, washed with H_2O (100 mL) and dried over Na_2SO_4. After removing the solvent, the crude product was purified by column chromatography (silica/50:1 hexane:ethyl acetate) to give **20** (5.40 g, 66%), as a white crystalline solid, mp = 28-30 °C. -^{1}H NMR (300 MHz, $CDCl_3$) δ 8.03 (dd, 1H, *J* = 3.2, 1.4 Hz), 7.54 (dd, 1H, *J* = 5.5, 1.4 Hz), 7.30 (dd, 1H, *J* = 5.5, 3.2 Hz), 2.86 (t, 2H, *J* = 7.3 Hz), 1.70 (m, 2H), 1.25 (m, 8H), 0.93 (t, 3H). IR (NaCl): 3105, 2947, 2927, 2848, 1677, 1460, 769 cm^{-1}. MS (EI): M^+ = 210.

2-(3-Thien-yl)-2-heptyl-1,3-dithiolane (21). BF_3.2HOAc (2.48 mL, 17.7 mmol) was added over 5 min to a mixture of 1-thiophen-3-yl-octan-1-one (3.37 g, 16.1 mmol) and ethane-1,2-dithiol (2.95 mL, 35.3 mmol) under N_2. The resulting solution was stirred vigorously for 20 min. The mixture was diluted with 250 mL hexane and washed with saturated aqueous $NaHCO_3$ (3 × 50 mL), followed by 15% NaOH (3 × 50 mL) and brine (3 × 50 mL). The organic layer was dried over Na_2SO_4 and concentrated to afford **21**

(4.01 g, 89%), as a yellow liquid. -^{1}H NMR (300 MHz, $CDCl_3$) δ 7.36 (dd, 1H, J = 3.2, 1.4 Hz), 7.26 (dd, 1H, J = 5.5, 3.2 Hz), 7.11 (dd, 1H, J = 5.5, 1.4 Hz), 3.32 (m, 4H), 2.27 (t, 2H), 1.22 (m, 10H), 0.93 (t, 3H). IR (NaCl): 3112, 2934, 2855, 1466, 1407, 1275, 1229, 841, 762, 657 cm^{-1}. MS (EI): M^+ = 286.

3-(1,1-Difluorooctyl)thiophene (22). $NOBF_4$ (5.00 g, 42.7 mmol) was placed in a pre-dried 250 mL plastic bottle (PP, NALGENE) with a magnetic stirrer under argon. Anhydrous CH_2Cl_2 (85 mL) and pyridinium poly(hydrogen fluoride) (PPHF) (17.7 mL, 70% HF content) were injected into the bottle and the reaction mixture was cooled to 0 °C. A solution of 2-(3-thien-yl)-2-heptyl-1,3-dithiolane (5.09 g, 17.8 mmol) in anhydrous CH_2Cl_2 (35 mL) was added dropwise over 5 min. The ice bath was removed and the reaction mixture was stirred for another 2 min before dilution with petroleum ether (200 mL) and transfer the mixture to a plastic (PP) separation funnel. The organic layer was removed and the dark bottom layer was extracted with 3:1 mixture of petroleum ether/CH_2Cl_2 (3 × 50 mL). The organic layers were combined and passed through a short plug of silica gel (5 cm). The filtrate was concentrated in vacuo to afford **22** (3.30 g, 80%), as a colorless liquid. -^{1}H NMR (300 MHz, $CDCl_3$) δ 7.45 (m, 1H), 7.34 (m, 1H), 7.12 (dd, 1H, J = 5.5, 1.4 Hz), 2.12 (m, 2H), 1.40 (m, 2H), 1.25 (m, 8H), 0.93 (t, 3H). IR (NaCl): 3105, 2927, 2848, 1460, 1209, 769 cm^{-1}. MS (EI): M^+ = 232.

Results and Discussion

Synthesis

1-Thiophen-3-yl-octan-1-one, **20**, was prepared in high yields by a palladium-catalyzed cross-coupling reaction of octanoic anhydride and 3-thienylboronic acid using a

modification of a method from the literature.[18] The treatment of 1-thiophen-3-yl-octan-1-one with ethane-1,2-dithiol gave 2-(3-thien-yl)-2-heptyl-1,3-dithiolane, **21**. The monomer, 3-(1,1-difluorooctyl)thiophene, **22**, was synthesized by the fluorination of **21** with $NOBF_4$ and PPHF. The fluorination step is very sensitive to the reaction time, the reaction vessel and the ratio of starting materials.[19] The optimized conditions, include as of a very short reaction time (e.g., 6 minutes, a longer time leads to decomposition), plastic vessels, and a 2.4:1 ratio of $NOBF_4$/dithiolane, gave the designed product, Figure 5.1.

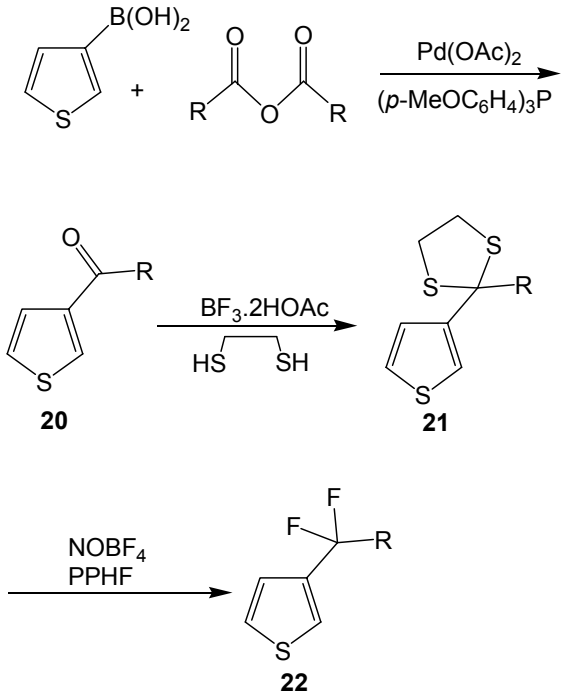

Figure 5.1. Synthesis of 3-1,1-difluoroalkylthiophene.

^{1}H-^{19}F coupling in ^{1}H NMR of 3-1,1-difluoroalkylthiophenes

As for the 3-(perfluoroalkyl)thiophenes, 3-(1,1-difluoroalkyl)thiophenes also show ^{1}H-^{19}F coupling in the ^{1}H NMR spectrum. Before the fluorination, the aromatic region in the ^{1}H NMR spectrum of 2-(3-thien-yl)-2-heptyl-1,3-dithiolane shows three doublet of doublets, each for one proton, which is typical for a 3-substituted thiophene, Figure 5.2. After the fluorination, 3-(1,1-difluoroalkyl)thiophenes show the same complex signals as seen in the aromatic region of 3-(perfluoroalkyl)thiophenes (Chapter II). Protons at the 4- and 2-positions of 3-(1,1-difluorooctyl)thiophene show more complicated splitting patterns than the doublet of doublets of the precursor. This is especially true for the proton at the 4-position which appears as a pattern of ten peaks, Figure 5.3. Thus, besides the ^{1}H-^{1}H coupling to give a doublet of doublets, each peak is spilt further into a triplet due to the coupling with two identical ^{19}F nuclei three carbons away (i. e., H-C-C-C-F). This should result in a doublet of doublet of triplets. (See detailed analysis in Chapter II). In addition to the complexity of the proton signals, the chemical shift of this signal to low field relative to the 3-octylthiophenes is also consistent with attachment of the fluorocarbon, a strong electron withdrawing group, to the thiophene ring.

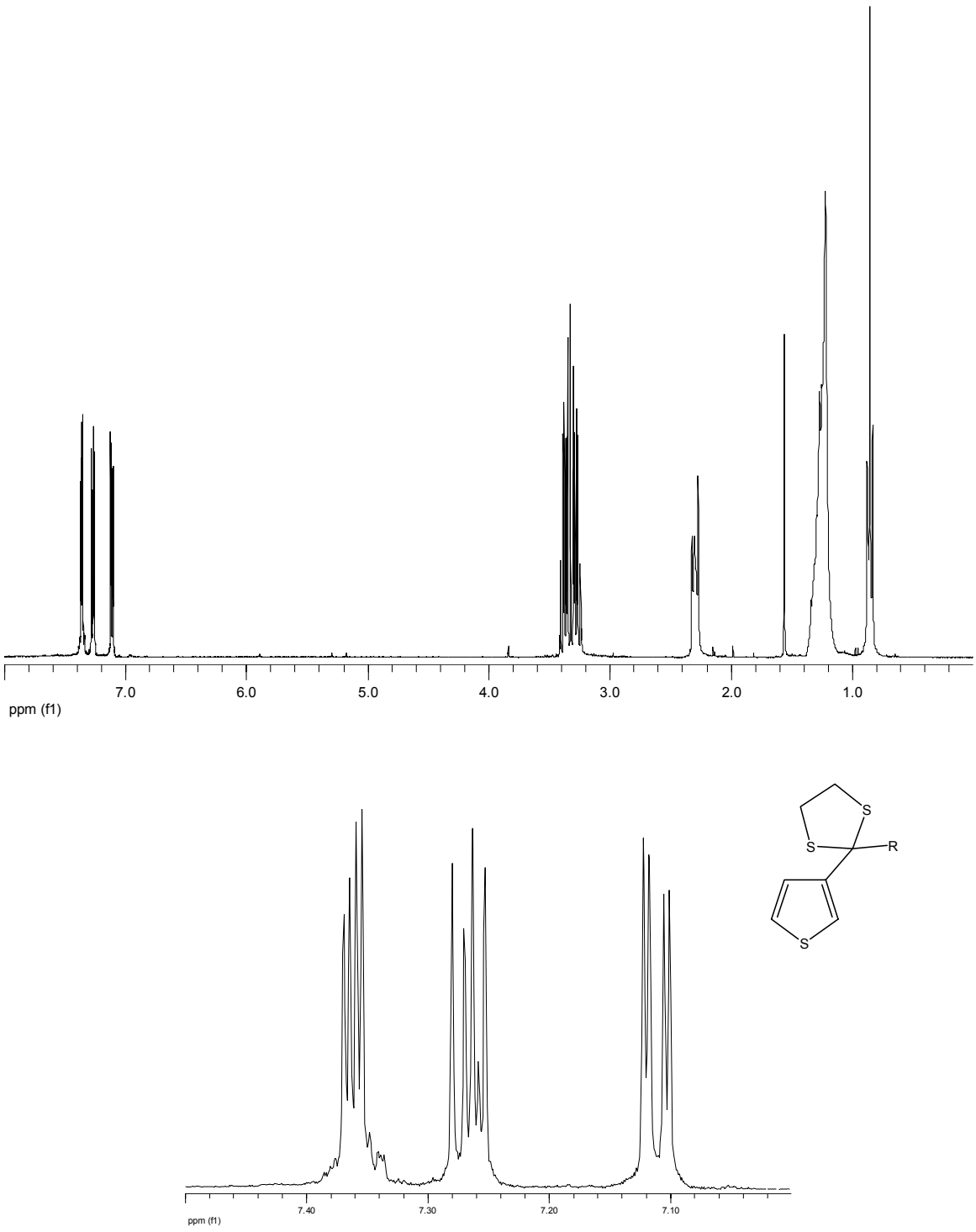

Figure 5.2. ^{1}H-NMR of 2-(3-thien-yl)-2-heptyl-1,3-dithiolane, **21**, 300 MHz, in $CDCl_3$.

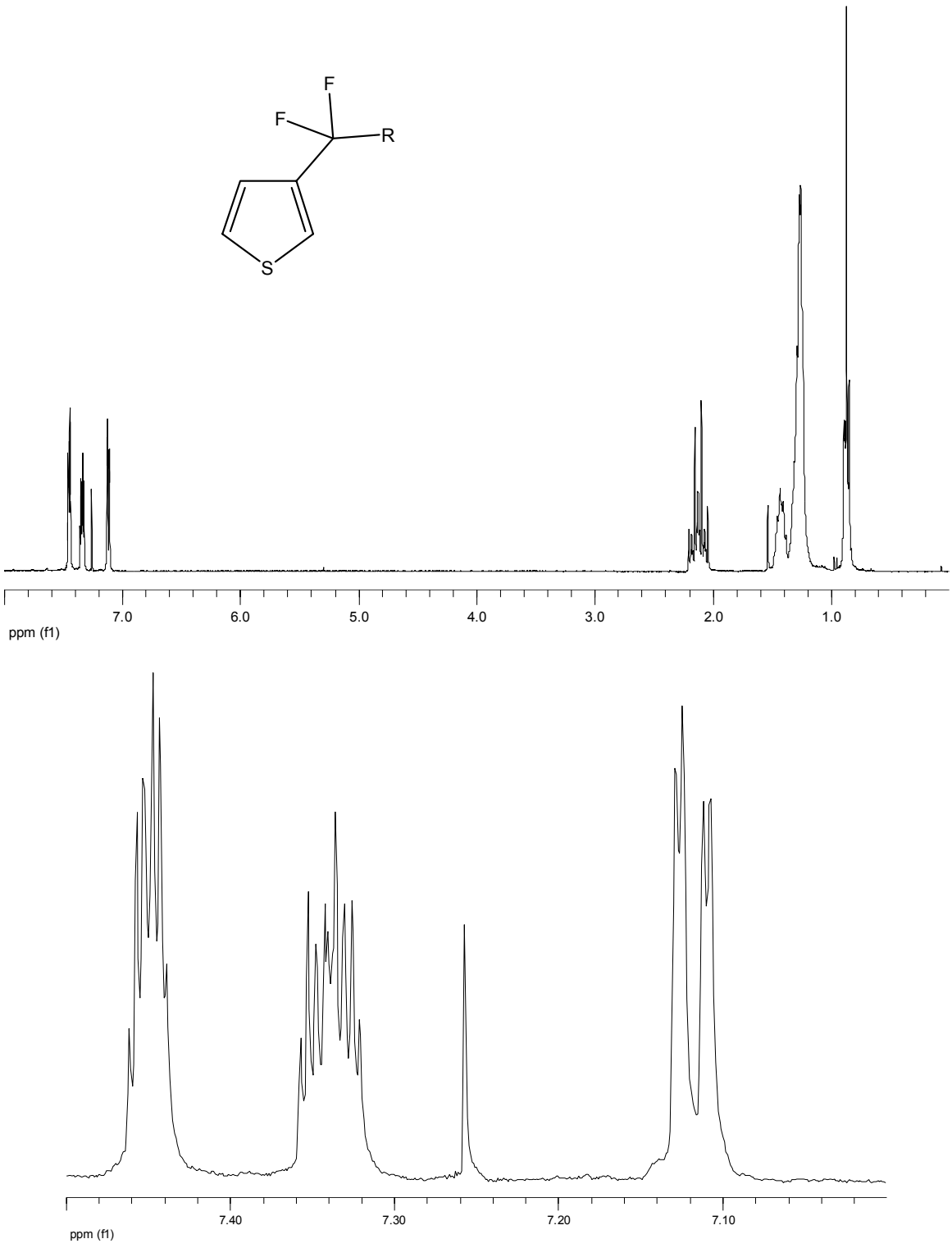

Figure 5.3. ^{1}H-NMR of 3-(1,1-difluorooctyl)thiophene, **22**, 300 MHz, in $CDCl_3$.

Electrochemical polymerization and electrochemistry

Cyclic voltammetry (CV) of 3-(1,1-difluorooctyl)thiophene (1.0 mM in 0.1 M Bu_4NPF_6/CH_2Cl_2, Au working electrode) shows an irreversible oxidation at + 1.98 V (versus SCE) without deposition of a polymer film, similar to the behavior of 3-(perfluorooctyl)thiophene. The high oxidation potential of the monomer is consistent with the electron withdrawing effect of the fluorocarbon (for comparison, 3-octylthiophene undergoes oxidation at + 1.84 V, 3-(perfluorooctyl)thiophene undergoes oxidation at + 2.05 V), Figure 5.4.

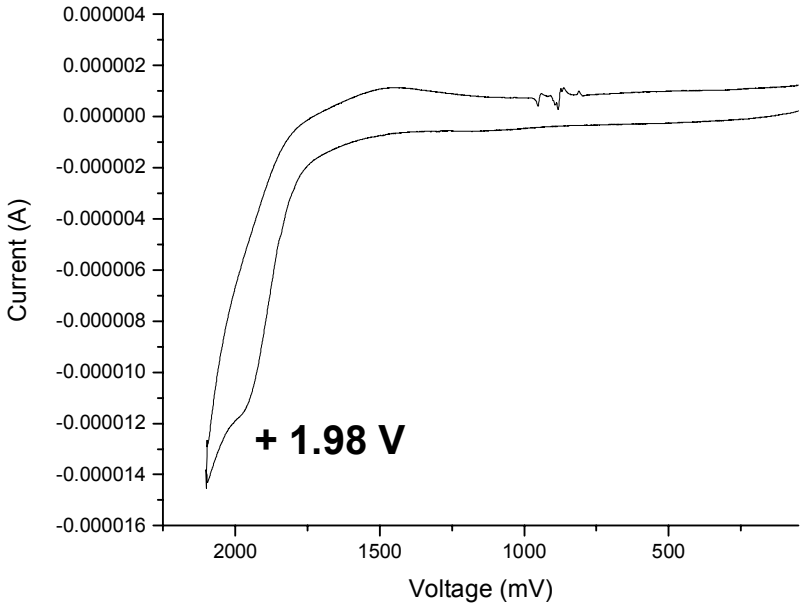

Figure 5.4. Cyclic voltammetry of 3-(1,1-difluorooctyl)thiophene, 1.0 mM in 0.1 M Bu_4NPF_6/CH_2Cl_2, Au working electrode, relative to SCE.

Electrochemical polymerization of 3-(1,1-difluorooctyl)thiophene was performed potentiostatically (1.0 mM, + 2.03 V on a carbon electrode) to afford poly(3-(1,1-difluorooctyl)thiophene) as a redox-active electrochromic film on the electrode surface. The CV of this film in monomer-free electrolyte solution shows an oxidation peak at + 1.01 V (Figure 5.5.) approximately 70 mV higher than that of PT-H8 and 180 mV lower than PT-F8 deposited under similar conditions. The CV also shows an irreversible peak corresponding to n-doping at - 1.44 V, Figure 5.6. For comparison, PT-F8, with a stronger electron withdrawing substituent than poly(3-(1,1-difluoroalkyl)thiophene) (PT-diFH8), has a less negative reduction potential (PT-F8, -1.18 V),[17] and poly(3-methyl-thiophene) undergoes reduction at ca. -2.5 V versus SCE.[1]

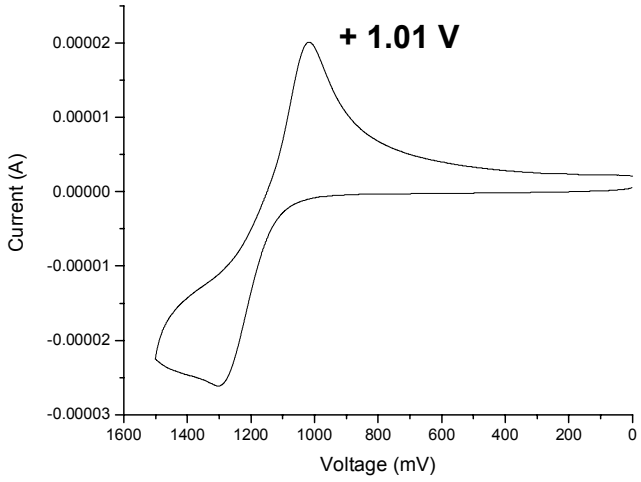

Figure 5.5. Cyclic voltammetry of electrochemically prepared poly(3-(1,1-difluorooctyl)thiophene) which is deposited on an electrode surface (0.1 M Bu_4NPF_6/CH_2Cl_2, carbon working electrode, relative to SCE), 0 to + 1500 mV, scan rate: 100 mV/s.

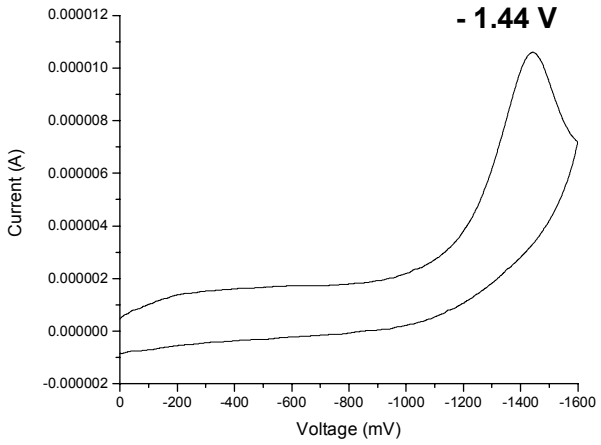

Figure 5.6. Cyclic voltammetry of electrochemically prepared poly(3-(1,1-difluorooctyl)thiophene) which is deposited on an electrode surface (0.1 M Bu_4NPF_6/CH_2Cl_2, carbon working electrode, relative SCE), 0 to - 1600 mV, scan rate: 100 mV/s.

To prove the redox behavior in Figures 5.5. and 5.6. are due to the polymer film deposited on the electrode surface, the cyclic voltammetry was performed at different scan rates. If the redox behavior was due to a species in solution, the redox behavior would be controlled by diffusion, and the peak currents of the redox waves would be proportional to the square root of the scan rate. The results of this experiment show that the peak currents of the redox waves are proportional to the scan rate (Figure 5.7), suggesting that the redox behavior is caused by the film attached on the electrode surface and not controlled by diffusion.

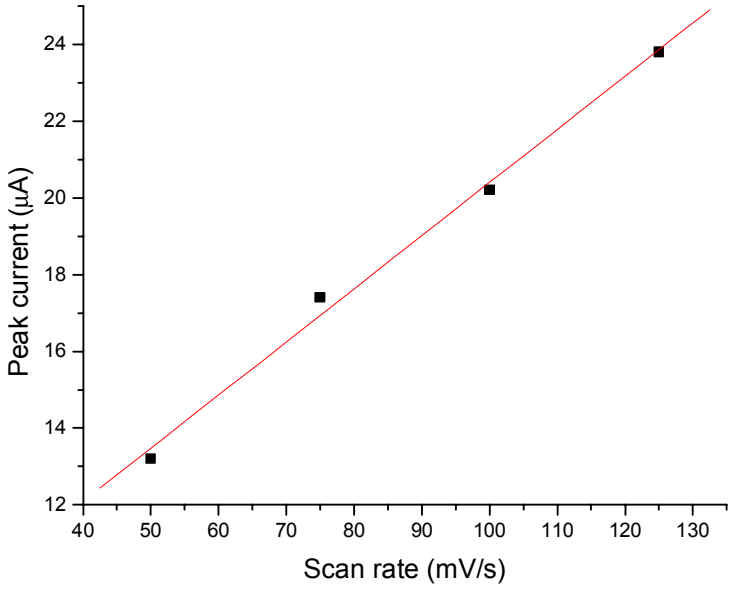

Figure 5.7. Plot of oxidation wave peak currents *v.s.* scan rate of the poly(3-(1,1-difluorooctyl)thiophene) film electrochemically deposited on the electrode surface (0.1 M Bu_4NPF_6/CH_2Cl_2, carbon working electrode, relative to SCE), 0 to + 1500 mV

The relative electronic effects of alkyl, perfluoroalkyl group and 1,1-difluoroalkyl groups are apparent the electrochemistry of the polymers. PT-F8 is the hardest to oxidize (+ 1.19 V) and PT-H8 is the easiest (+ 0.94 V). PT-diF-H8 has an oxidation potential between these values, at +1.01 V. PT-H8 cannot be reduced under normal conditions. With the fluorination of side chains, PT-diF-H8 can be reduced at – 1.44 V which is more negative than PT-F8 (- 1.18 V), Table 5.1. The electrochemistry of PT-diF-H8 indicates the strength of the electron withdrawing effect from the less fluorinated side chains can be used to tailor the electronic structure of polythiophenes, as an alternative of varying the density of fluoroalkylation as we described in Chapter III.

Table 5.1. Redox behavior of alkyl, perfluoroalkyl and 1,1-difluoroalkyl thiophenes and polythiophenes.

monomer [a]		polymer [b]		
	oxidation *E* (V)		oxidation *E* (V)	reduction *E* (V)
T-H8	+1.84	PT-H8	+0.94	NA
T-F8	+2.05	PT-F8	+1.19	-1.18
1,1-difluoro-T-H8	+1.98	PT-diFH8	+1.01	-1.44

[a] 10^{-5} M, gold electrode, 100 mV/s, 0.1 M Bu_4NPF_6 in CH_2Cl_2. [b] polymer films electrochemically deposited on a carbon electrode, 0.1 M Bu_4NPF_6 in CH_2Cl_2.

Conclusion

In conclusion, a novel thiophene monomer, 3-(1,1-difluorooctyl)thiophene, has been prepared in good yields. The monomer was electrochemically polymerized to give poly(3-(1,1-difluoroalkyl)thiophene). Electrochemistry of this polymer, relative to poly(3-octylthiophene) and poly(3-perfluorooctylthiophene), indicates the electronic structure of polythiophenes can be tuned by changing the fluorination pattern of side chains.

References

1. Yamamoto, T.; Sanechika, K.; Yamamoto, A. *J. Polym. Sci. Polym., Lett. Ed.* **1980**, *18*, 9.

2. Lin, J. W. P.; Dudek, L. P. *J. Poly. Sci., Polym. Chem. Ed*. **1980**, *18*, 2869.

3. Jen, K. Y.; Oboodi, R.; Elsenbaumer, R. L. *Polym. Mater. Sci. Eng*. **1985**, *53*, 79

4. Miller, G. G.; Elsenbaumer, R. L. *J. Chem. Soc., Chem. Commun.* **1986**, *15*, 169.

5. McCullough, R. D.; Lowe, R. D. *J. Chem. Soc., Chem. Commun.* **1992**, 70.

6. Loewe, R. S.; Khersonsky, S. M.; McCullough, R. D. *Adv. Mater.* **1999**, *11*, 250.

7. Liu, J.; McCullough, R. D. *Macromolecules* **2002**, *35*, 9882.

8. Che, T. A.; Rieke, R. D. *J. Am. Chem. Soc*. **1992**, *114*, 10087.

9. Wurthner, F. *Angew. Chem., Int. Ed.* **2001**, *40*, 1037.

10. Crooks, R. M.; Chyan, O. M. R.; Wrighton, M. S. *Chem. Mater*. **1989**, *1*, 2.

11. Facchetti, A.; Deng, Y.; Wang, A.; Koide, Y.; Sirringhaus, H.; Marks, T. J.; Friend, R. H. *Angew. Chem., Int. Ed.* **2000**, *39*, 4547.

12. Marks, T. J.; Facchetti, A.; Sirringhaus, H.; Friend, R. H. *WO Patent* 0209201, **2002**.

13. Facchetti, A.; Mushrush, M.; Katz, H. E.; Marks, T. J. *Adv. Mater*. **2003**, *15*, 33.

14. Facchetti, A.; Marks, T. J. *Polym. Prep*. **2002**, *43*, 734.

15. Facchetti, A.; Yoon, M-H.; Stern, C. L.; Katz, H. E.; Marks, T. J. *Angew. Chem., Int. Ed.* **2003**, *42*, 3900.

16. Sakamoto, Y.; Komatsu, S.; Suzuki, T. *J. Am. Chem. Soc*. **2001**, *123*, 4643.

17. Li, L.; Counts, K. E.; Kurosawa, S.; Teja, A. S.; Collard, D. M. *Adv. Mater*. **2004**, *16*, 180.

18. Gooben, L. J.; Ghosh, K. *Angew. Chem., Int. Ed*. **2001**, *40*, 3458.

19. Kiryanov, A. A.; Seed, A. J.; Sampson, P. *Tetrahedron* **2001**, *57*, 5757.

CHAPTER VI

SYNTHESIS AND CHARACTERIZATION OF α-HEXYL-ω-PERFLUOROHEXYL SEXITHIOPHENE

Introduction

Since the discovery of highly conductive polyacetylene in 1977, various of monomeric building blocks have been used to prepare conjugated polymers. However, due to statistical chain length distribution and interruption of the conjugated chain by defects, conjugated polymers are often disordered. Oligomers, which pack in well-defined crystalline arrays, are often used as models to explore the properties of polymers. They have also been used as semiconducting layers in devices such as thin film transistors (TFTs). Oligo- and polythiophenes have attracted great interest to make p-type TFTs. α,ω-Dialkyl substituted oligothiophenes,[1,2] together with pentacene, are the most promising p-type TFT materials. The enhancement of the charge mobility, relative to unsubstituted oligothiophenes, has been attributed to the close-packed self-assembled structures which is brought about by the alkyl groups in the α and ω positions.[2]

The development of n-type TFT materials with high mobility is also very important in order to fabricate complementary circuits. In contrast to organic p-type semiconductors, n-type semiconductors remained less developed for a long time. This

was partly due to the lack of electron-poor conjugated polymers, but also because of theoretical arguments which predict a lower stability of the n-conducting radical anionic polymers under ambient conditions.[3] Only few of n-type organic materials have been made, such as those containing perfluorophthalocyanine and naphthalene cores.[4,5,6] Most recently, α,ω-diperfluorohexyl-substituted oligothiphenes have been synthesized and characterized as the first n-type thiophene-based TFT material.[7,8,9]

The aromatic thiophene ring itself is electron-rich, so unsubstituted oligo- and polythiophenes are known to be p-type conductive materials. Intrinsically, oligothiophenes are p-type and this property is enhanced by the alkyl substituents, which are electron-donating. The perfluoroalkyl substitution converts the oligothiophenes from p-type to n-type. This is due to the strong electron-withdrawing effect of the fluoroalkyl group, which lowers the HOMO and LUMO energies and thereby facilitates electron injection. Insertion of a methylene group between the perfluorohexyl chain and the oligothiophene yields a material which is TFT-inactive.[10] This result confirms that the electron-withdrawing effect of fluoroalkyl chain plays the major role in p- to n-type conversion. In addition, fluoroalkyl substititution also contributes to the environmental stability of the n-channel conduction due to its ability to protect the film from contaminant penetration by inducing a the more favorable molecular packing.[11]

With the aim of achieving even better packing and higher electron mobility, we designed an amphiphilic sexithiophene, Figure 6.1. Here, we report an efficient synthesis of α-hexyl-ω-perfluorohexyl sexithiophene, and its physical properties.

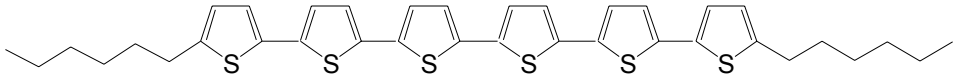

H_6-6T-H_6 (Ref. 2)

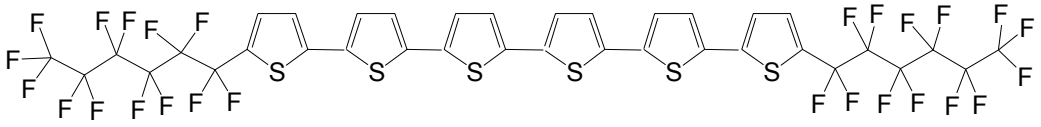

F_6-6T-F_6 (Ref. 7)

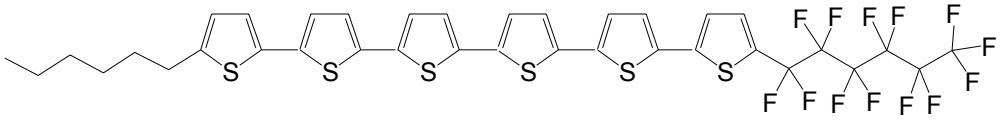

F_6-6T-H_6

Figure 6.1. Structures of α,ω-substituted sexithiophenes.

Experimental

General methods

All reagents were obtained from commercial sources and used without further purification unless stated otherwise. Tetrahydrofuran (THF) and diethyl ether were dried over sodium benzophenone ketyl prior to distillation under nitrogen. Methylene chloride was dried over calcium hydride prior to distillation under nitrogen. Column chromatography was performed on silica gel (40 mesh, 60Å, Baker). Thin layer

chromatography was performed on 3 × 5 cm plates of silica gel (0.2 mm thick, 60 F_{254}) on an aluminum support (EM Separations).

All ^{1}H NMR spectra were collected on a Varian Gemini 300 MHz instrument using $CDCl_3$ as the solvent unless otherwise specified. Chemical shifts are reported relative to tetramethylsilane. ^{13}C NMR spectra were obtained at 75.5 MHz. IR analysis was performed on a Nicolet 520 FTIR spectrometer. UV-vis analysis was performed with a Perkin-Elmer Lambda 19 spectrometer. Fluorescence spectra were collected with a Spex Fluorolog Fluometer 1681 0.22m Spectrometer. Electron ionization or chemical ionization mass spectra was performed using a VG Analytical 70-SE instrument with a L-250J Data System Analyzer. Matrix assisted laser desorption/ionization (MALDI) was performed using an Applied Biosystems with a 4700 Proteomics Analyzer. TGA analysis was performed on a Model 2050 TGA (TA instruments). DSC analysis was performed on a Model 2920 DSC (TA. Instruments).

Synthesis

2,2'-Bithiophene (23). A mixture of 2-bromothiophene (39.1 g, 0.240 mol) and magnesium filings (8.75 g, 0.360 mol) in 200 mL dry THF was heated to reflux for 3 h under N_2 and then cooled down to room temperature. The resulting Gringard reagent was transferred via canular into a solution of 2-bromothiophene (32.6 g, 0.200 mol) and $Ni(dppp)Cl_2$ (1.08 g, 2.00 mmol) in 150 mL dry THF under N_2 in an ice-bath. The reaction mixture was then heated at reflux overnight. After cooling to room temperature, the mixture was poured into 400 mL H_2O and extracted with Et_2O (3 × 150 mL). The solvent was removed under reduced pressure, and a vacuum distillation gave **23** (26.56 g,

80%), as a white solid, mp = 34 °C. – ^{1}H NMR (300 MHz, $CDCl_3$): δ 7.21 (dd, 2 H, C5-H, C5'-H, *J* = 5.1, 1.2), 7.18 (dd, 2 H, C3-H, C3'-H, *J* = 3.6, 1.2), 7.02 (dd, 2 H, C4-H, C4'-H, *J* = 5.1, 3.6).

5-Bromo-2,2'-bithiophene (24). A solution of NBS (17.8 g, 0.100 mol) in 35 mL DMF was added in dropwise to a solution of 2,2'-bithiophene (16.6 g, 0.10 mol) was dissolved in 150 mL DMF at 0°C. The reaction mixture was stirred overnight at room temperature, poured into H_2O (200 mL), and extracted with hexane (3 × 150 mL). The combined organic extracts were washed with 1% aqueous HCl (3 × 200 mL) and brine (150 mL). The solvent was removed under reduced pressure and the product was purified by column chromatography (silica/hexane) to give **24** (18.5 g, 76%), as a white solid, mp = 34 °C. – ^{1}H NMR (300 MHz, $CDCl_3$): δ 7.23 (dd, 1 H, C5'-H, *J* = 5.1, 1.2), 7.11 (dd, 1 H, C3'-H, *J* = 3.6, 1.2), 7.01 (dd, 1 H, C4'-H, *J* = 5.1, 3.6), 6.97 (d, 1 H, C4-H, *J* = 3.6), 6.91 (d, 1 H, C3-H, *J* = 3.6). ^{13}C NMR (300 MHz, $CDCl_3$): δ 139.1, 136.6, 130.8, 128.0, 125.1, 124.4, 124.1, 110.1.

2-Hexylthiophene (25). n-BuLi (2.5 M in hexane, 60.0 mL, 0.150 mol) was added dropwise into a solution of thiophene (15.1 g, 0.180 mol) in THF (150 mL) at –78 °C under N_2 and the mixture was stirred for 45 min. n-Hexyl bromide (21.1 mL, 0.150 mol) was added dropwise into the reaction mixture via syringe at - 78 °C and then the mixture was warmed to room temperature. After stirring for another 3 h, the reaction mixture was poured into H_2O (150 mL) and extracted with Et_2O (3 × 150 mL). The combined organic extracts were dried over anhydrous $MgSO_4$. The solvent was removed under reduced pressure and the product was purified by vacuum distillation to give **25** (23.2 g, 92%), as a colorless liquid. – ^{1}H NMR (300 MHz, $CDCl_3$): δ 7.10 (dd, 1 H, C5-

H, J = 5.1, 1.2), 6.91 (dd, 1 H, C4-H, J = 5.1, 3.6), 6.78 (ddt, 1 H, C3-H, J = 3.6, 1.2, 0.86), 2.82 (td, 2 H, α-CH_2-, J = 7.8, 0.86), 1.66 (m, 2 H, β-CH_2), 1.32 (m, 6 H), 0.88 (t, 3 H).

5-Hexyl-2,2'-2'',5'-terthiophene (26). n-BuLi (2.5 M in hexane, 7.20 mL, 18.0 mmol) and TMEDA (2.70 mL, 18.0 mmol) were added into a solution of 2-hexylthiophene (2.77 g, 16.5 mmol) in dry THF (45 mL) at – 70 °C under N_2. After stirring at - 70°C for 30 min, the reaction mixture was allowed to warm to room temperature. $ZnCl_2$ (1.0 M in Et_2O, 18.0 mL, 18.0 mmol) was added dropwise and after stirring at room temperature for 1 h, a solution of 5-bromo-2,2'-bithiophene (3.66 g, 15.0 mmol) and $Pd(PPh_3)_4$ (0.330 g, 0.286 mmol) in dry THF (10 mL) was added dropwise via syringe. The mixture was stirred at room temperature for 20 h and quenched with 5% aqueous HCl (100 mL). The mixture was extracted with Et_2O (3 × 100 mL) and the combined extracts were washed with H_2O (100 mL) and dried over anhydrous $MgSO_4$. After removing the solvent under reduced pressure, the product was purified by column chromatography (silica / 98:2 hexane/ethyl acetate) to give **26** (3.03 g, 60%), as a yellow powder solid, mp = 66-68 °C. – ^{1}H NMR (300 MHz, $CDCl_3$): δ 7.20 (dd, 1 H, C5''-H, J = 5.1, 1.1), 7.15 (dd, 1 H, C3''-H, J = 3.6, 1.1), 7.05 (d, 1 H, C4'-H, J = 3.8), 7.02 (dd, 1 H, C4''-H, J = 5.1, 3.6), 6.99 (d, 1 H, C3'-H, J = 4.0), 6.97 (d, 1 H, C3-H, J = 3.7), 6.68 (dt, 1 H, C4-H, J = 3.6. 0.90), 2.79 (td, 2 H, α-CH_2-, J = 7.9, 0.90), 1.68 (m, 2 H, β-CH_2), 1.32 (m, 6 H), 0.89 (t, 3 H). ^{13}C NMR (300 MHz, $CDCl_3$): δ 145.8, 137.5, 137.0, 135.7, 134.7, 128.0, 125.0, 124.5, 123.7, 123.5, 32.0, 30.3, 29.1, 23.0, 14.5. IR (KBr): 3072, 2954, 2921, 2855, 1512, 834, 801, 690 cm^{-1}. HRMS (EI): 332.07184 (observed), 332.07272 (calculated), Δ = 2.7 ppm.

5-Bromo-5''-hexyl-2,2'-2'',5'-terthiophene (27). A solution of NBS (1.49 g, 8.34 mmol) in $CHCl_3$ (20 mL) was added dropwise to a solution of 5-hexyl-2,2'-2'',5'-terthiophene (2.77 g, 8.34 mmol) in $CHCl_3$ (80 mL) at – 16 °C. The reaction mixture was slowly warmed to room temperature and stirred overnight. The mixture was poured into H_2O (100 mL) and extracted with CH_2Cl_2 (3 × 100 mL). The combined organic extracts were washed with brine (100 mL) and dried over anhydrous Na_2SO_4. The solvent was removed under reduced pressure and the product was purified by column chromatography (silica / 98:2 hexane/ethyl acetate) to give **27** (3.24 g, 95%), as a yellow powder solid, mp = 126 - 128 °C. – ^{1}H NMR (300 MHz, $CDCl_3$): δ 6.98 (m, 3 H, C3',4',3''-H), 6.96 (d, 1 H, C4''-H, *J* = 3.6), 6.89 (d, 1 H, C3-H, *J* = 3.6), 6.68 (dt, 1 H, C4-H, *J* = 3.6, 0.90), 2.79 (td, 2 H, α-CH_2-, *J* = 7.9, 0.90), 1.68 (m, 2 H, β-CH_2), 1.32 (m, 6 H), 0.89 (t, 3 H). ^{13}C NMR (300 MHz, $CDCl_3$): δ 146.2, 138.8, 134.5, 134.4, 130.7, 125.0, 124.6, 123.8, 123.7, 111.0, 32.0, 30.5, 29.0, 23.0, 14.5. IR (KBr): 3065, 2954, 2921, 2848, 1512, 1433, 854, 795, 466 cm^{-1}. MS (EI): M^+ = 410.

[1',3'-(2',2'-Dimethylpropylene)]-2-(5''-hexyl-2',5-2'',5'-terthienyl)boronate (28). n-BuLi (2.5 M in hexane, 0.58 mL, 1.4 mmol) was added dropwise to a solution of 5-bromo-5''-hexyl-2,2'-2'',5'-terthiophene (0.49 g, 1.2 mmol) in THF (25 mL) at – 30 °C under N_2. After stirring at - 30°C for 30 min, $B(OCH_3)_3$ (0.55 mL, 4.8 mmol) was added dropwise. The reaction mixture was slowly warmed to room temperature, stirred overnight, and then quenched with 10% aqueous HCl (30 mL). The mixture was extracted with Et_2O (3 × 100 mL) and neopentyl glycol (0.13 g, 1.2 mmol) and anhydrous $MgSO_4$ were added. Filtration followed by removal of the solvent under reduced pressure gave **28** (0.53 g, 100%), as a green powder solid, mp = 124 - 126 °C. – ^{1}H NMR (300

MHz, $CDCl_3$): δ 7.45 (d, 1 H, C3-H, *J* = 3.6), 7.19 (d, 1 H, C4-H, *J* = 3.6), 7.10 (d, 1 H, C3'-H, *J* = 3.8), 6.99 (d, 1 H, C4'-H, *J* = 3.8), 6.97 (d, 1 H, C3''-H, *J* = 3.6), 6.68 (dt, 1 H, C4''-H, *J* = 3.6. 0.90), 2.78 (td, 2 H, α-CH_2-, *J* = 7.9, 0.90), 1.68 (m, 2 H, β-CH_2), 1.32 (m, 6 H), 0.89 (t, 3 H). ^{13}C NMR (300 MHz, $CDCl_3$): δ 136.6, 125.0, 124.9, 123.8, 123.6, 72.7, 32.4, 31.9, 30.5, 29.1, 22.9, 22.3, 14.5. IR (KBr): 3223, 2960, 2934, 2861, 1493, 1460, 1328, 1308, 1275, 1242, 1117, 788, 657 cm^{-1}. HRMS (EI): 444.14417 (observed), 444.14228 (calculated), Δ = 4.3 ppm.

2-(Perfluorohexyl)thiophene (29). 2-Bromothiophene (7.56 g, 46.7 mmol) and perfluorohexyl iodide (25.0 g, 56.0 mmol) were added to a well-stirred suspension of copper bronze (9.48 g, 149 mmol) in dry DMF (60 mL). The mixture was heated at 120 to 130 °C under N_2. After 24 h, the reaction mixture was cooled to room temperature and filtered. The liquid was poured into ice cold aqueous HCl (200 mL concentrated HCl with 200 g ice) and extracted with hexane (4 × 50 mL). The combined organic extracts were washed with 5% aqueous $Na_2S_2O_3$ (200 mL) and H_2O (200 mL), and dried over anhydrous $MgSO_4$. The solvent was removed under reduced pressure and vacuum distillation gave **29** (15.20 g, 81%), as a colorless liquid. – ^{1}H NMR (300 MHz, $CDCl_3$): δ 7.60 (dd, 1 H, C5-H, *J* = 5.1, 1.2), 7.45 (m, 1 H, C4-H), 7.15 (m, 1 H, C3-H). ^{13}C NMR (300 MHz, $CDCl_3$): δ 130.4 (m), 130.2 (m), 127.4. MS (EI): M^+ = 488.

5-Perfluorohexyl-2,2'-2'',5'-terthiophene (30). n-BuLi (2.5 M in hexane, 6.90 mL, 17.3 mmol) and TMEDA (2.59 mL, 17.3 mmol) were added into a solution of 2-perfluorohexylthiophene (6.37 g, 15.8 mmol) in dry THF (45 mL) at – 70 °C under N_2. After stirring at – 70 °C for 30 min, the reaction mixture was allowed to warm to room temperature. $ZnCl_2$ (1.0 M in Et_2O, 17.3 mL, 17.3 mmol) was added dropwise. After

stirring at room temperature for 1 h, a solution of 5-bromo-2,2'-bithiophene (3.50 g, 14.4 mmol) and $Pd(PPh_3)_4$ (0.320 g, 0.277 mmol) in dry THF (10 mL) was added dropwise via syringe. The reaction mixture was stirred at room temperature for 20 h and quenched with 5% aqueous HCl (100 mL). The mixture was extracted with Et_2O (3 × 100 mL) and the combined extract was washed with H_2O (100 mL) and dried over anhydrous $MgSO_4$. After removing the solvent under reduced pressure, the product was purified by column chromatography (silica / 98:2 hexane/ethyl acetate) to give **30** (5.52 g, 68%), as a flake yellow solid, mp = 131-133 °C. – ^{1}H NMR (300 MHz, $CDCl_3$): δ 7.34 (d, 1 H, C4-H, *J* = 3.9), 7.26 (dd, 1 H, C5''-H, *J* = 5.1, 1.1), 7.21 (dd, 1 H, C3''-H, *J* = 3.6, 1.1), 7.16 (d, 1 H, C4'-H, *J* = 3.7), 7.15 (d, 1 H, C3-H, *J* = 3.8), 7.11 (d, 1 H, C3'-H, *J* = 3.7), 7.04 (dd, 1 H, C4-H, *J* = 5.1, 3.6). ^{13}C NMR (300 MHz, $CDCl_3$): δ 142.5, 138.3, 136.7, 134.0, 130.2 (m), 128.2, 126.1, 125.3, 124.7, 124.5, 123.6. IR (KBr): 1235, 1207, 1147, 795, 703 cm^{-1}. HRMS (EI): 565.94910 (observed), 565.95023 (calculated), Δ = 2.0 ppm.

5-Perfluorohexyl-5''-tributylstannyl-2,2'-2'',5'-terthiophene (31). n-BuLi (2.5 M in hexane, 1.32 mL, 3.30 mmol) was added dropwise into a solution of 5-perfluorohexyl-2,2'-2'',5'-terthiophene (1.70 g, 3.30 mmol) in THF (60 mL) at –30 °C under N_2. After stirring at –30 °C for 10 min, tributyltin chloride (0.93 mL, 3.30 mmol) was added dropwise. The reaction mixture was slowly warmed to room temperature and stirred for another 3 h. The mixture was partitioned between Et_2O (100 mL) and brine (150 mL) and the organic layer was dried over anhydrous Na_2SO_4. The solvent was removed under reduced pressure to give **31** (2.56 g, 100%), as a black viscous liquid. The product was used for the next step without further characterization or purification.

5-Bromo-5''-perfluorohexyl-2,2'-2'',5'-terthiophene (32). A solution of NBS (0.147 g, 0.827 mmol) in $CHCl_3$ (2 mL) was added dropwise to a solution of 5-perfluorohexyl-2,2'-2'',5'-terthiophene (0.468 g, 0.827 mmol) in $CHCl_3$ (10 mL) at – 16 °C. The reaction mixture was slowly warmed to room temperature and stirred overnight. The mixture was poured into H_2O (50 mL) and extracted with CH_2Cl_2 (3 × 50 mL). The combined organic extracts were washed with brine (50 mL) and dried over anhydrous Na_2SO_4. The solvent was removed under reduced pressure to give **32** (0.415 g, 78%), as a flake yellow solid, mp = 134-136 °C. – ^{1}H NMR (300 MHz, $CDCl_3$): δ 7.34 (d, 1 H, C4-H, *J* = 3.9), 7.15 (d, 1 H, C3-H, *J* = 3.6), 7.14 (d, 1 H, C4''-H, *J* = 3.7), 7.04 (d, 1 H, C3''-H, *J* = 3.8), 6.99 (d, 1 H, C4'-H, *J* = 3.7), 6.94 (d, 1 H, C3'-H, *J* = 3.6). ^{13}C NMR (300 MHz, $CDCl_3$): δ 131.4 (m), 131.0, 126.1, 124.9, 124.5, 123.7. IR (KBr): 1473, 1427, 1367, 1307, 1210 (C-F), 1150, 1084, 795, 716 cm^{-1}. HRMS (EI): 643.85969 (observed), 643.86074 (calculated), Δ = 1.6 ppm.

α-Hexyl-ω-perfluorohexyl-sexithiophene, F_6-6T-H_6 (33). *Method A, Stille coupling*: 5-Perfluorohexyl-5''-tributylstannyl-2,2'-2'',5'-terthiophene (2.56 g, 3.00 mmol) were dissolved in dry DMF (45 mL). 5-Bromo-5''-hexyl-2,2'-2'',5'-terthiophene (1.03 g, 2.50 mmol) and $Pd(PPh_3)_4$ (100 mg, 0.0865 mmol) was added under N_2. N_2 was bubbled through the reaction mixture for 10 min, which was then heated to 100 °C for 20 h. After cooling to room temperature, the mixture was poured into H_2O (100 mL) and filtered. The resulting solid was washed with saturated aqueous KF (150 mL), H_2O (100 mL), hexane (150 mL) and CH_2Cl_2 (100 mL). The solid was continuously washed with hot $CHCl_3$ with a Soxlet extractor to give a brown solid (1.88 g). MALDI analysis shows

this solid contains the product, **F_6-6T-H_6** (M^+ = 896.1) and α,ω-hexyl-sexithiophene, H_6-6T-H_6 (M^+ = 662.2) at 1:1 ratio. This byproduct could not be separated.

Method B, Suzuki coupling: N_2 was bubbled through of a solution 5-bromo-5''-perfluorohexyl-2,2'-2'',5'-terthiophene (0.415 g, 0.644 mmol) in DME (15 mL) for 10 min. $Pd(PPh_3)_4$ was added in and the mixture was stirred at room temperature for 10 min under N_2. [1',3'-(2',2'-Dimethylpropylene)]-2-(5''-hexyl-2',5-2'',5'-terthienyl)boronate (0.315 g, 0.708 mmol) and 1 N aqueous $NaHCO_3$ (2 mL) were added and the reaction mixture was heated at reflux with vigorous stirring overnight. After cooling to room temperature, the mixture was poured to H_2O (30 mL) and filtered. The resulting solid was washed with saturated aqueous H_2O (30 mL), hexane (60 mL) and CH_2Cl_2 (30 mL). The solid was continuously washed with hot $CHCl_3$ in a Soxlet extractor to give **33** (0.498 g, 86%), as an orange powder solid, mp = 322 °C. The product is insoluble in most of organic solvents, but it has a very subtle solubility in hot toluene. IR (KBr): 3059, 2967, 2934, 2861, 1473, 1440, 1242, 1210, 1150, 785, 709 cm^{-1}. HRMS (MALDI): 896.0077 (observed), 896.0073 (calculated), Δ = 0.45 ppm; Elemental analysis: $C_{36}H_{27}F_{13}S_6$ (with 0.96% H_2O) Calculated: C 47.19, H 3.18, F 26.96, S 20.90; Observed: C 47.19 H 2.74 F 27.28 S 20.73.

Results and Discussion

Synthesis

α-Hexyl-terthiophene **26** was prepared according to a literature.[2] Bromination with NBS gave α-bromo-ω-hexylterthiophene **27**. The boronic ester **28**, was synthesized by halogen-metal exchange, followed by the quenching with trimethyl borate, Figure 6.2.

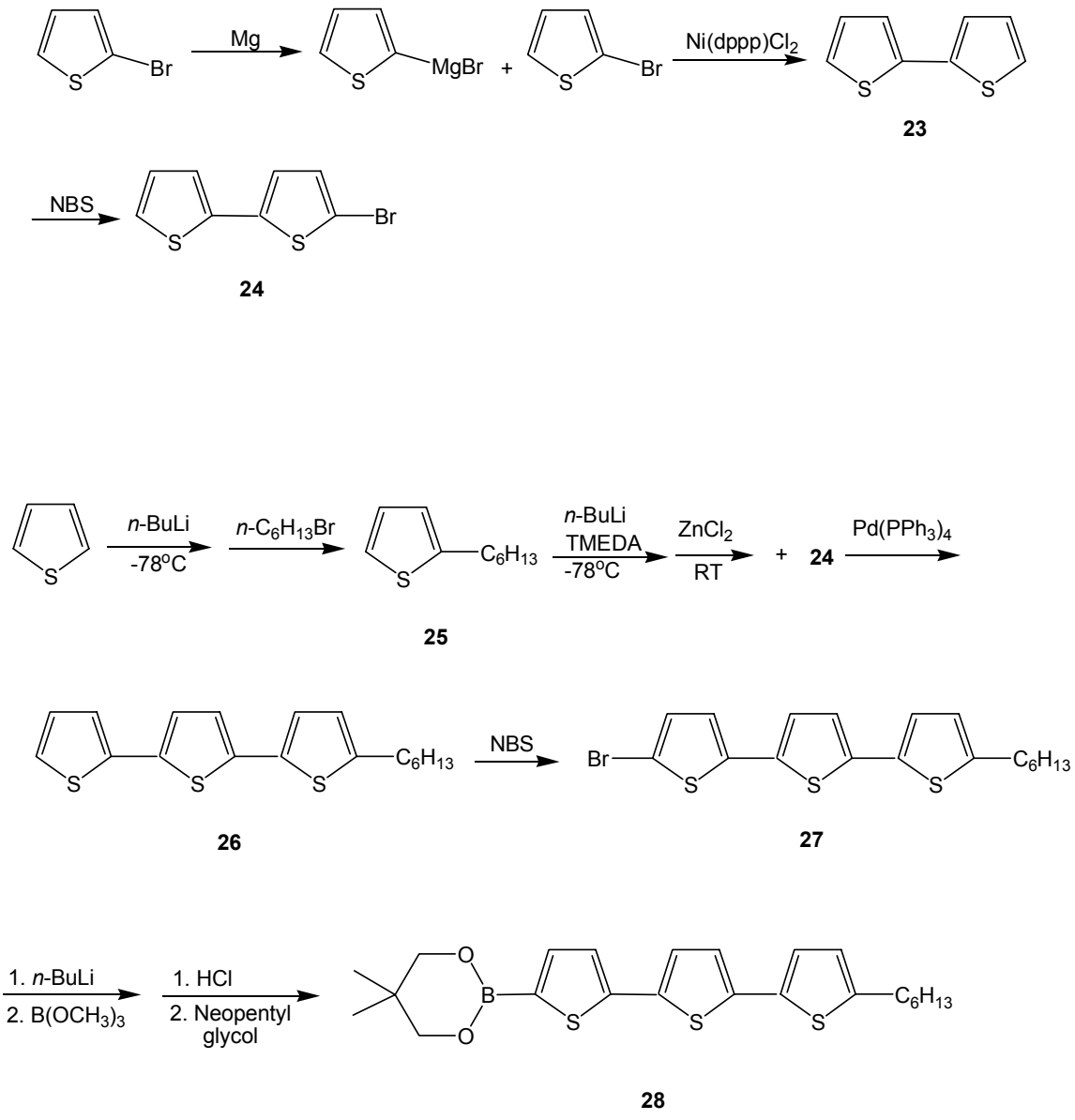

Figure 6.2. Synthesis of compounds **23**, **24**, **25**, **26**, **27**, **28**.

Copper-bronze catalyzed fluoroalkylation of 2-bromothiophene gave 2-(perfluorohexyl)thiophene, **29**. Lithiation of **29**, followed by transmetallation with $ZnCl_2$ and coupling with 2-bromobithiophene **24** gave α-(perfluorohexyl)terthiophne, **30**. α-Perfluorohexyl-terthienyl stannyl reagent, **31**, was prepared by lithiation of **30**, followed by reaction with tributyltin chloride. Bromination of **30** generated α-bromo-ω-(perfluorohexyl)terthiophene, **32**, Figure 6.3.

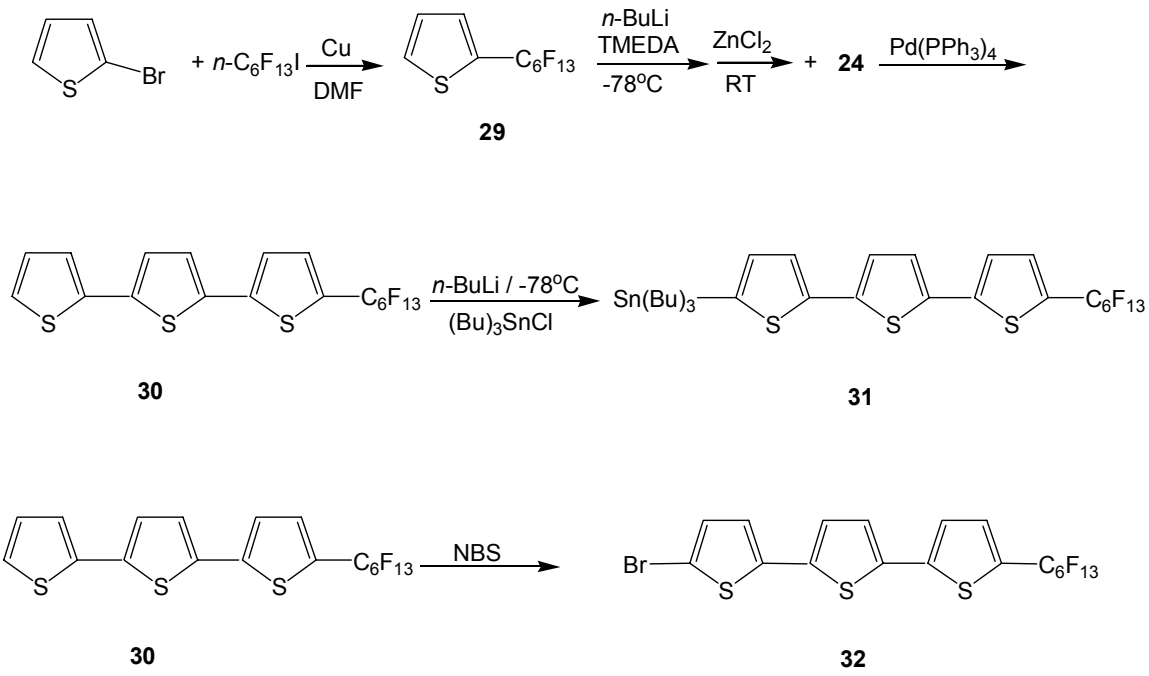

Figure 6.3. Synthesis of compounds **30**, **31**, **32**.

Two different organometallic cross couplings were used to make α-hexyl-ω-perfluorohexyl sexithiophene, **F_6-6T-H_6**. The Stille cross-coupling of **27** and **31** gave a mixture of α-hexyl-ω-(perfluorohexyl)sexithiophene (M^+ = 896.1) and α,ω-dihexyl-sexithiophene (M^+ = 662.2) at 1:1 ratio. Both the product and the side product are insoluble in most solvents and the dialkyl analogue could not be removed. Suzuki cross-coupling was also used to prepare α-hexyl-ω-perfluorohexyl sexithiophene, in which α-hexyl-terthienyl boronic ester **28** and α-bromo-ω-perfluorohexyl terthiophene **32** with Pd(0) under basic conditions, Figure 6.4. The identity of the product **F_6-6T-H_6** was confirmed by HRMS and used for further characterization.

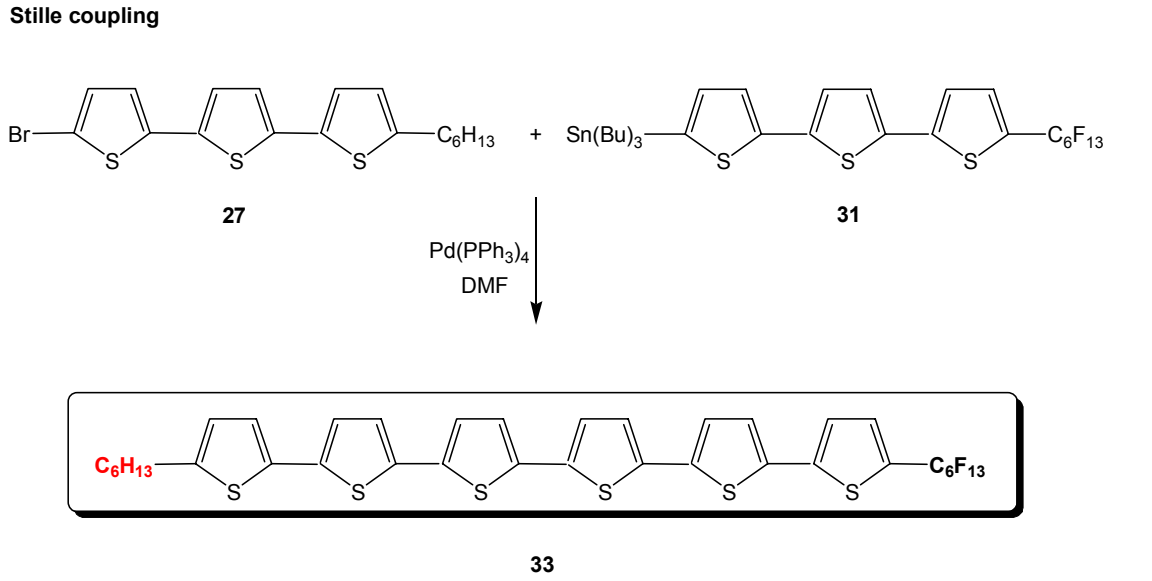

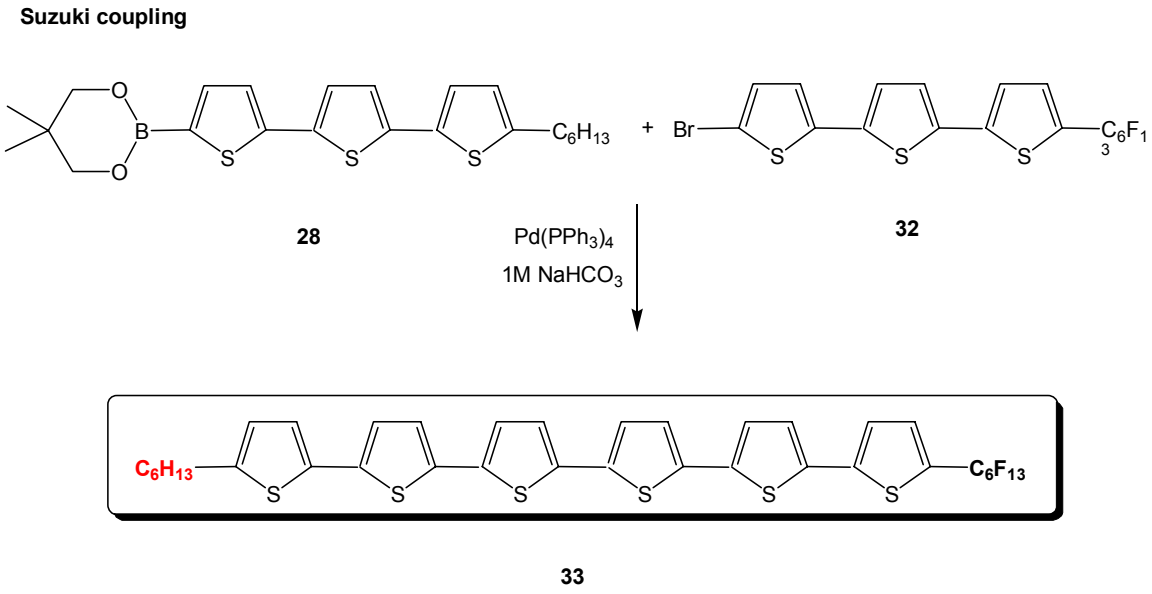

Figure 6.4. Synthesis of compound **33**.

^{1}H-NMR

α-Hexyl substituted oligothiphenes, **26**, **27**, **28**, show a long distance ^{1}H-^{1}H coupling (H-C-C-C-H) in the ^{1}H-NMR spectrum. The first methylene of the hexyl group appears as a triplet of doublet. Besides the large coupling (J = 7.8 Hz) with the adjacent methylene to give the triplet, the small coupling (J = 0.90 Hz) with the adjacent β-proton on the attached thiophene ring causes further splitting. Accordingly, in the aromatic region, that β-proton appears as a doublet of triplet. It first couples with another β-proton on the same thiophene ring (J = 3.6 Hz) to give a doublet, then the long distance coupling with the two identical protons on the α-methylene splits each peak to be a small triplet (J = 0.90 Hz), Figure 6.5, 6.6 and 6.7. Interestingly, the analogous β-alkyl substituted thiophenes do not show this long distance coupling.

In Chapters II and III, the ^{1}H-^{19}F long distance coupling (H-C-C-C-F) was observed in the ^{1}H NMR spectra of β-perfluoroalkyl substituted thiophene compounds. Here, a similar coupling was observed in the α-perfluoroalkyl substituted terthiophenes (30 and 32) leading to a broadened doublet or a doublet of triplet by virtue of coupling between to the proton 4 and the two identical fluorine nuclei, Figure 6.8 and 6.9.

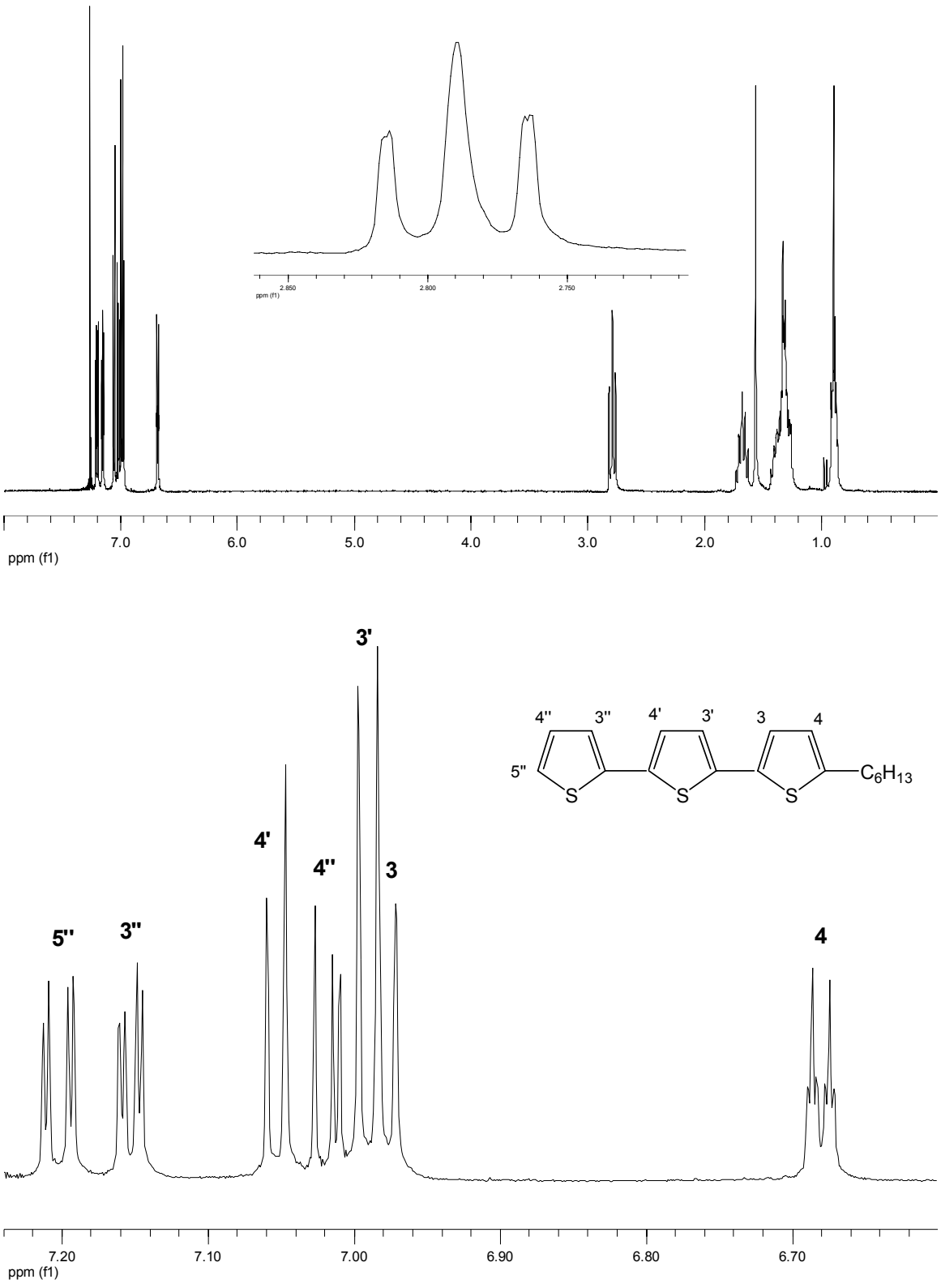

Figure 6.5. ^{1}H NMR spectrum (300 MHz, $CDCl_3$) of **26**.

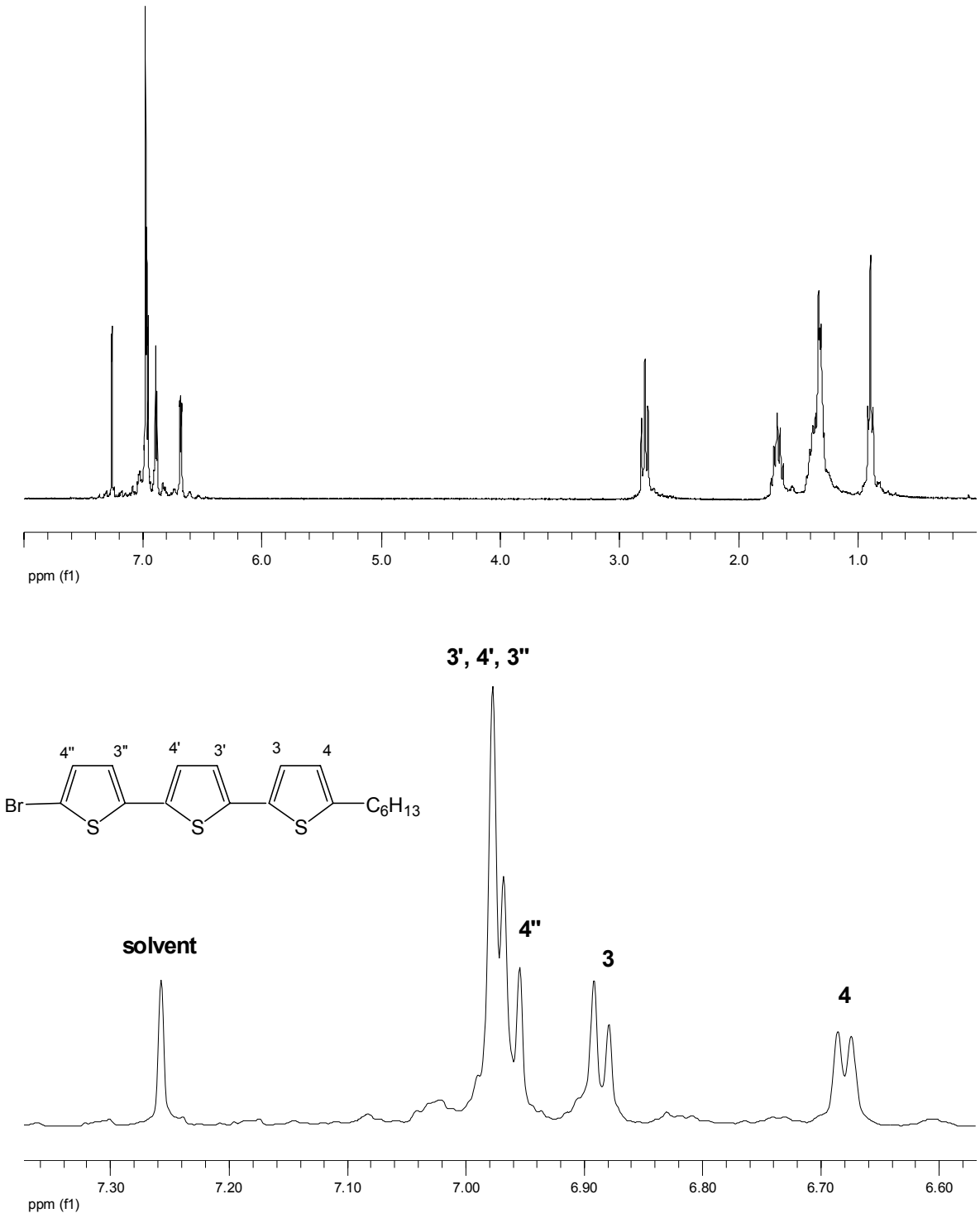

Figure 6.6. ^{1}H NMR spectrum (300 MHz, $CDCl_3$) of **27**.

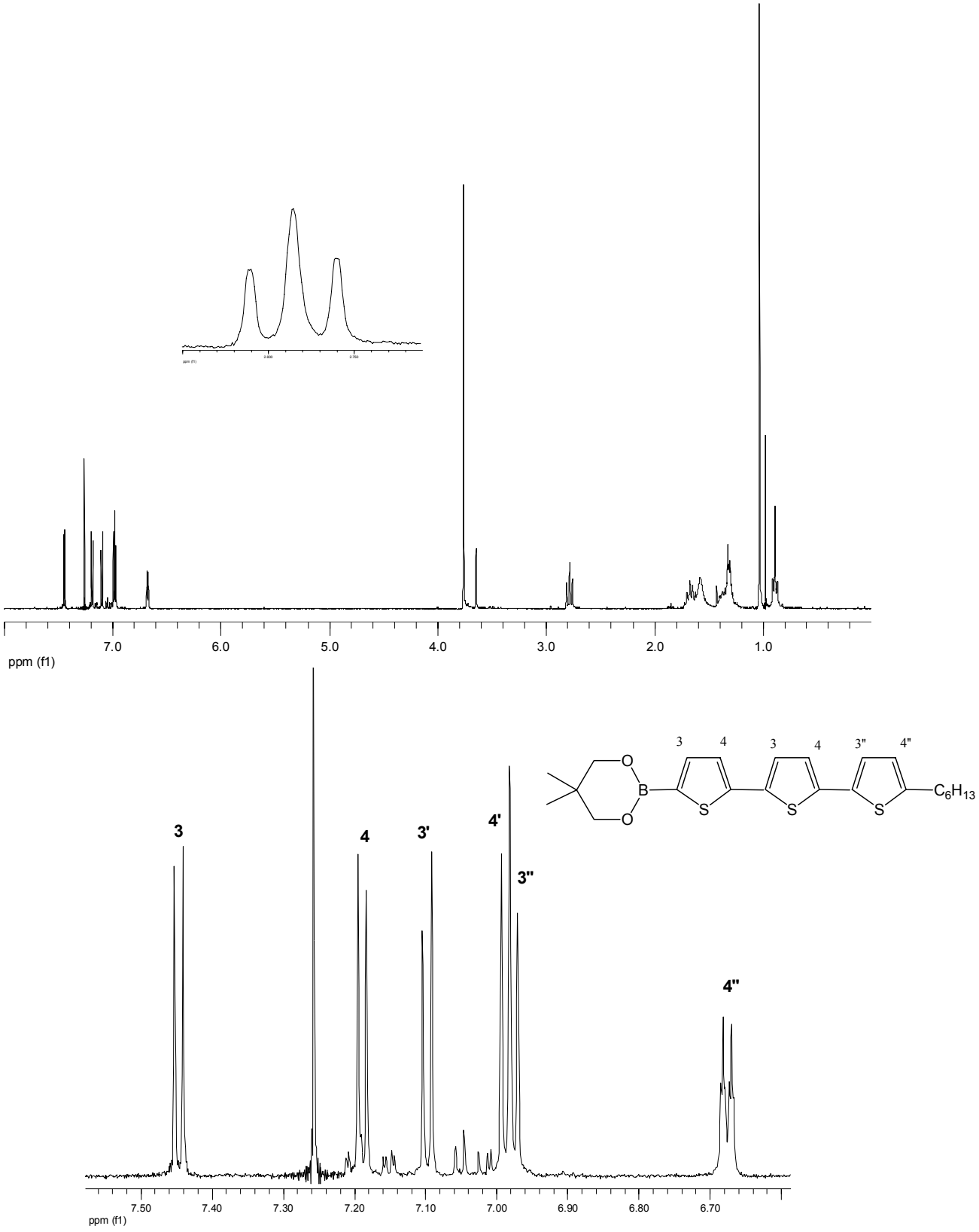

Figure 6.7. ^{1}H NMR spectrum (300 MHz, $CDCl_3$) of **28**.

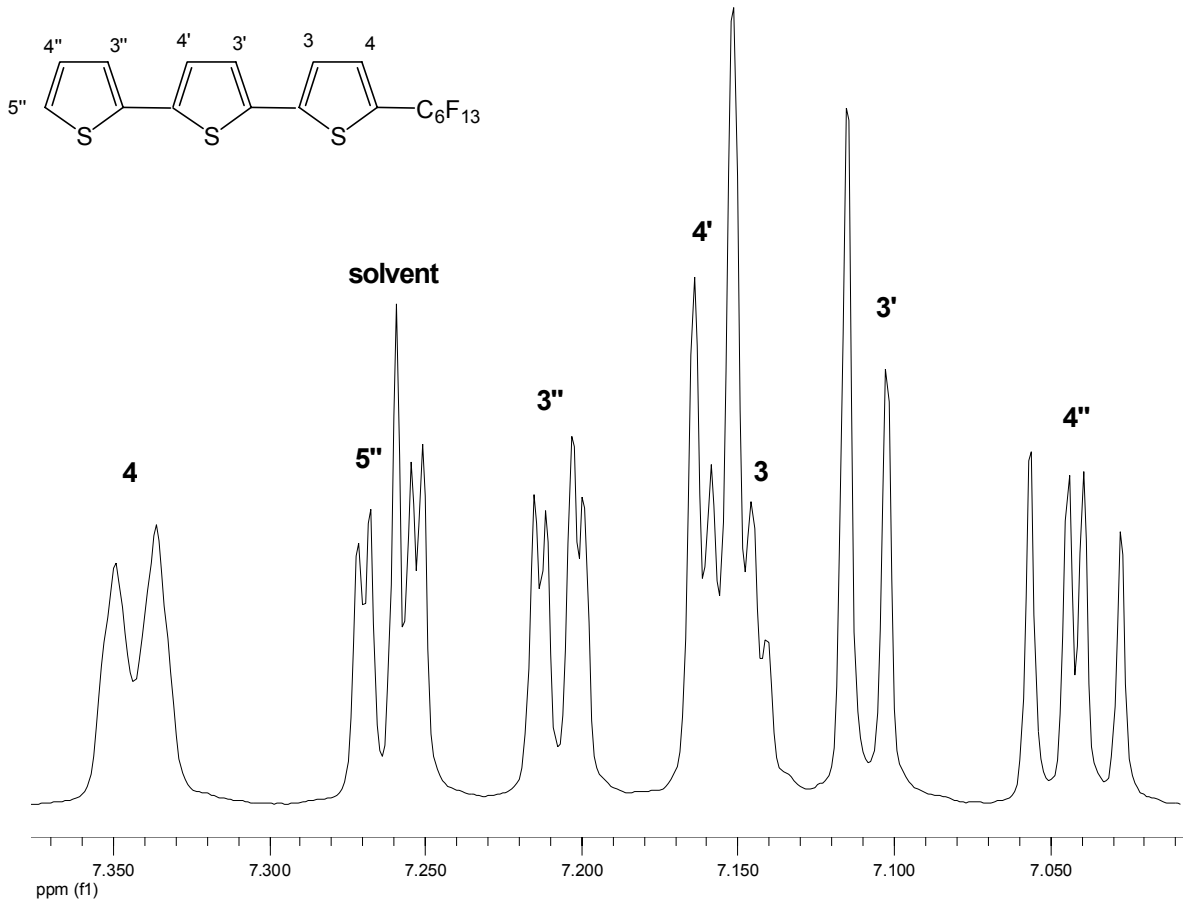

Figure 6.8. ^{1}H NMR spectrum (300 MHz, $CDCl_3$) of **30**.

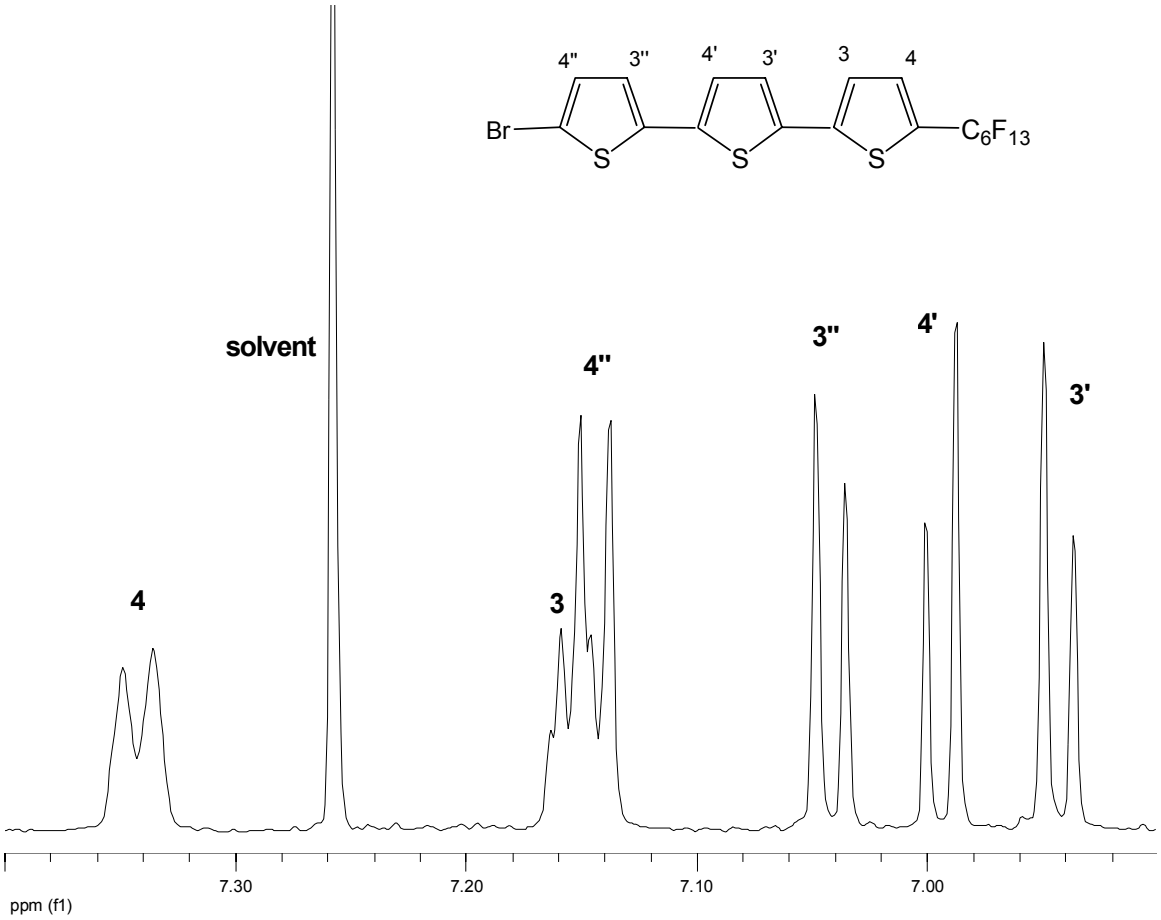

Figure 6.9. ^{1}H NMR spectrum (300 MHz, $CDCl_3$) of **32**.

UV-vis absorption and fluorescence in solution

A dilute solution of **F_6-6T-H_6** in toluene at 80 °C absorbs with a maximum at 435 nm and emits yellow fluorescence at a maximum of 521 nm with a shoulder at 550 nm, Figure 6.10. This amphiphilic sexithiophene has very similar spectra in solution to those of F_6-6T-F_6 and H_6-6T-H_6, and all of three sexithiophenes have a similar HOMO-LUMO

gap (about 2.4 eV). This indicates that the ground and excited states of sexithiophenes are barely affected by the α,ω-substitution.[7]

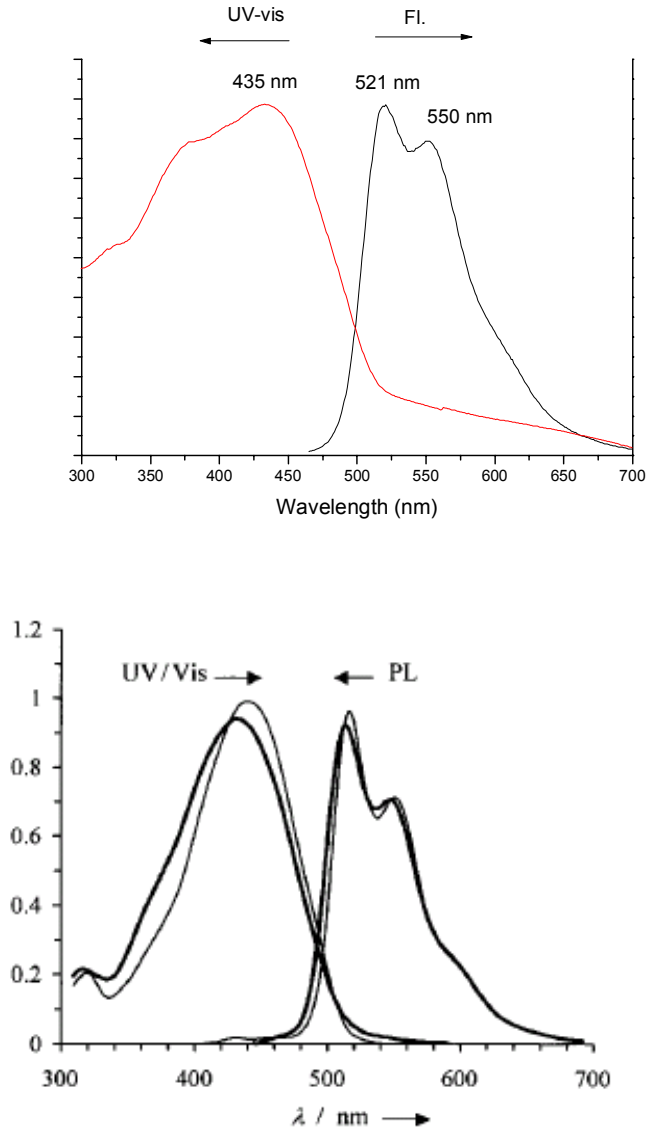

Figure 6.10. Top: UV-vis absorption and fluorescence spectra of **F_6-6T-H_6**, **33**, dilute solution in toluene at 80 °C; Bottom: UV-vis absorption and fluorescence spectra of **F_6-6T-F_6** (bold line) and **H_6-6T-H_6** (fine line), dilute solution in toluene at 80 °C. (Ref. 7)

Thermal analysis

The thermal properties of **F_6-6T-H_6** were investigated by differential scanning calorimetry (DSC) and thermal gravimetric analysis (TGA). The DSC of **F_6-6T-H_6** exhibits a distinct crystal-to-liquid-crystal (LC) transition at 298 °C (ΔH = 34.2 kJ/mol) and a weak LC-to-isotropic transition at 322 °C, Figure 6.11. The crystal-to-LC transition temperature of **F_6-6T-H_6** is between that of the symmetrically substituted sexithiophenes: F_6-6T-F_6 (292 °C) and H_6-6T-H_6 (300 °C). The LC-to-isotropic transition temperature of **F_6-6T-H_6** is higher than that of both F_6-6T-F_6 (309 °C) and H_6-6T-H_6 (308-313 °C).[7,12] These three substituted sexithiophenes all exhibit mesophase formation by virture of the amphiphilic structure consisting of the rigid sexithiophene core and more flexible alkyl and fluoroalkyl chains. The similar thermal behavior of these analogs indicates the strong π-π interactions of conjugated backbones is preserved no matter with terminal alkyl or fluoroalkyl chains. However, **F_6-6T-H_6** shows the highest melting points (~10 °C higher than F_6-6T-F_6 and H_6-6T-H_6), which indicates that introducing the polyphiphilicity by substitution of both fluroalkyl and alkyl chains further enhance the stability of the assembled structure.

The TGA of **F_6-6T-H_6** shows smooth weight loss upon heating under N_2 at atmosphere pressure, with 1% weight loss at 297 °C and 5% weight loss at 324 °C (Figure 6.12), which is much higher than F_6-6T-F_6 and H_6-6T-H_6 (1% weight loss at around 240 °C). However, **F_6-6T-H_6** has significant amount of residue (~35%), which is due to decomposition under atmosphere pressure. This result indicates **FH-6T-H** is a quite stable compound and its volatility is still under investigation, which will be

optimized to prepare thin films through vacuum sublimation, to solve the crystal structure and finally to do the device testing.

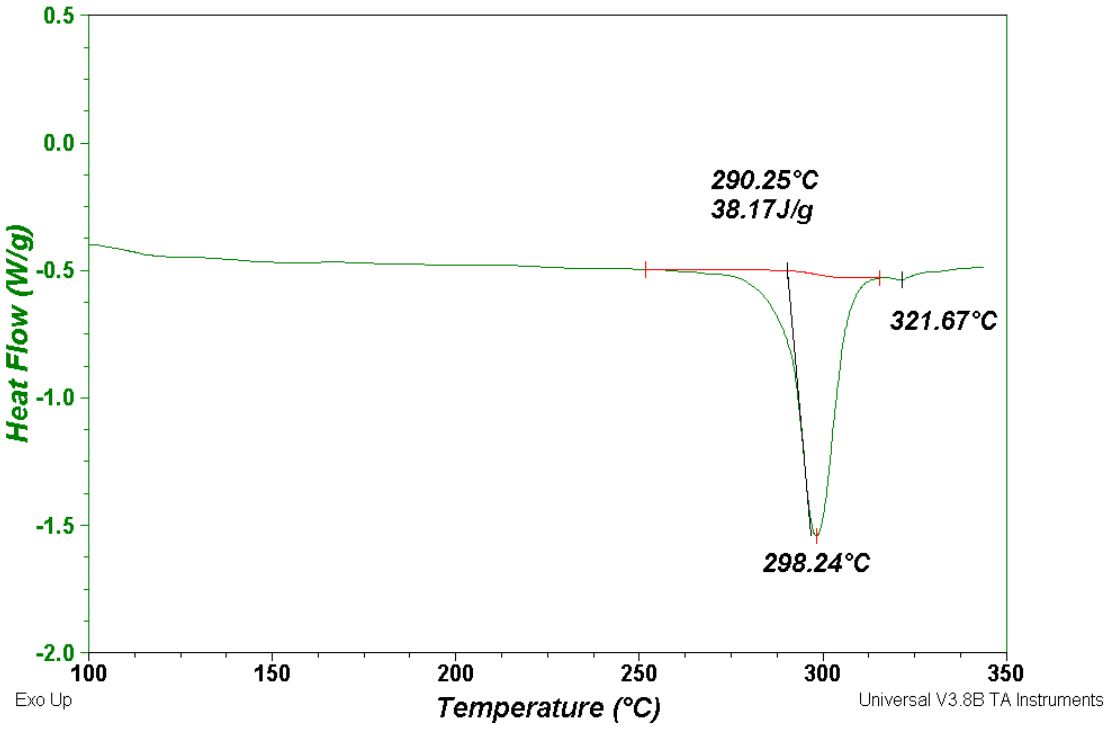

Figure 6.11. DSC of **F_6-6T-H_6** (20 °C/min, N_2).

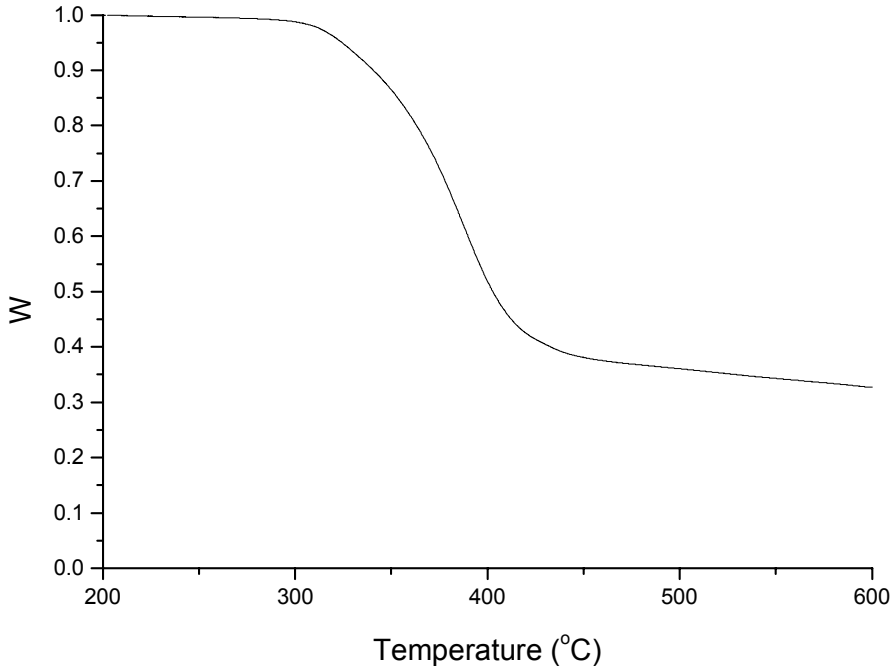

Figure 6.12. TGA of **F_6-6T-H_6** (1.5 °C/min, N_2).

Electrochemistry

CV of a dip-coated film of **F_6-6T-H_6** (0.1 M Bu_4NPF_6/CH_2Cl_2, carbon working electrode, relative to Ag/AgCl) is shown in Figure 6.13. The scans to positive potential give a large oxidative peak at 1.14 V (1.36 V vs SCE), and two small reductive peaks, E_1 = 0.74 V, E_2 = 1.00 V (E_1 = 0.97 V, E_2 = 1.22 V, vs SCE). The scans to negative potential give a reversible reduction wave at E_1 = -1.02 V, and an irreversible wave at E_2 = -1.78 V (E_1 = -1.24 V, E_2 = -2.00 V, vs SCE). Compared with the other two sexthiophenes, F_6-6T-F_6 and H_6-6T-H_6 (Table 6.1.), **F_6-6T-H_6** has the oxidation potential

between DFH-6T and DH-6T. This can be explained by a decrease in HOMO energy with more fluoroalkylation. However, **F_6-6T-H_6** has the lowest reduction potential. While this cannot be explained in terms of electronic effects of substitutents, it may arise from more ordered packing in solid state and intermolecular effects on the redox properties of conjugated oligomers.

Table 6.1. Oxidation and reduction potentials vs SCE of sexithiophenes.

Compound	Oxidation		Reduction	
	E_1 (V)	E_2 (V)	E_1 (V)	E_2 (V)
F_6-6T-F_6[a]	1.06	1.22	-1.42	-1.65
F_6-6T-H_6	0.97	1.22	-1.24	-2.00
H_6-6T-H_6[a]	0.87	1.09	-1.78	-2.01

a. From ref. 9.

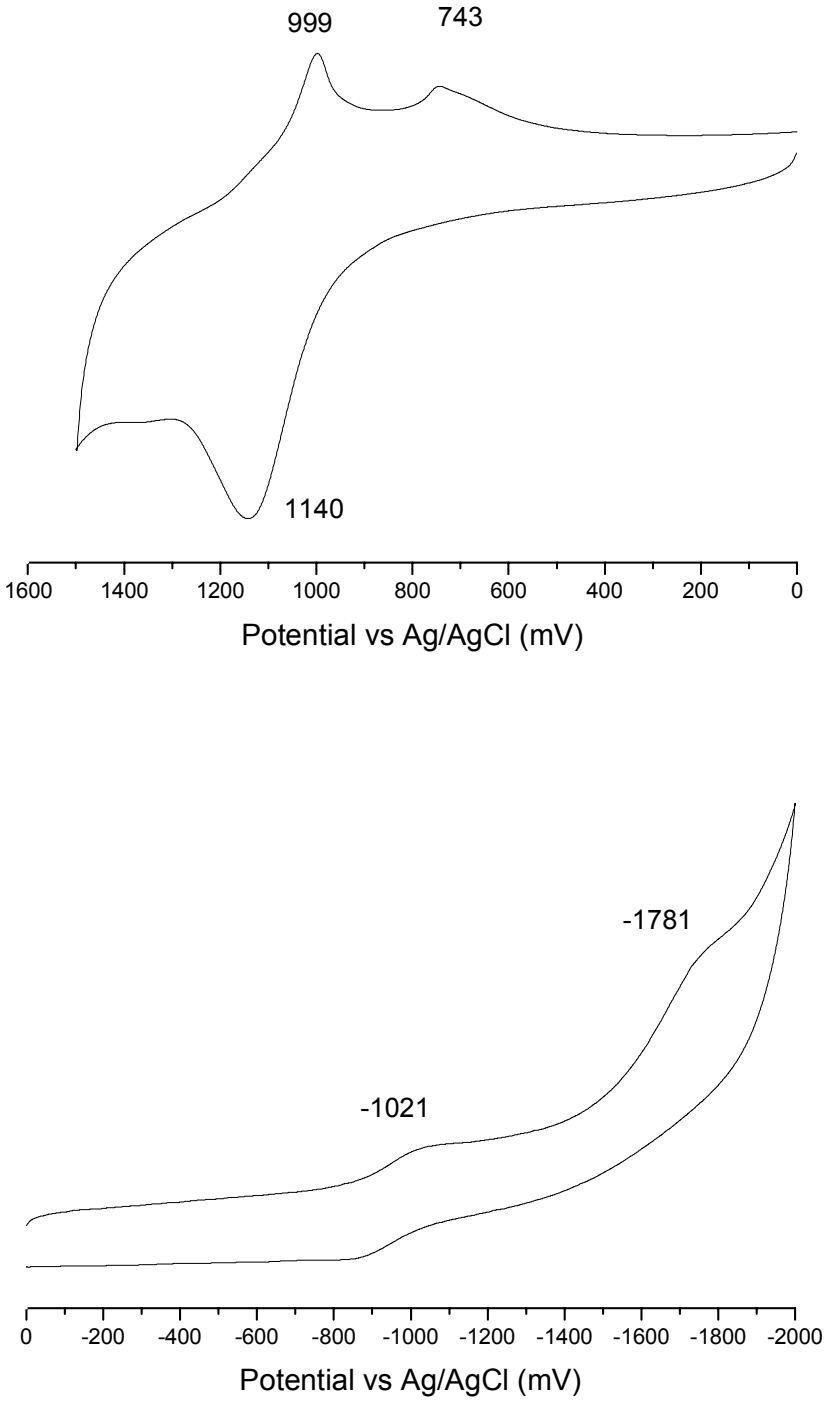

Figure 6.13. Cyclic voltammetry of **F_6-6T-H_6**dip-coated onto an electrode surface (0.1 M Bu_4NPF_6/CH_2Cl_2, carbon working electrode): top: 0 to +1600 mV; bottom, 0 to -2000 mV, Ag/AgCl as reference electrode.

Conclusion

In conclusion, an efficient route was developed to prepare α-hexyl-ω-perfluorohexyl sexithiophene, **F_6-6T-H_6**. The photophysics of **F_6-6T-H_6** in solution indicates the ground and excited states of sexithiophenes are not particularly sensitive to α,ω-substitution. The thermal analysis of **F_6-6T-H_6** suggests that it has a more stable assembled structure, compared with F_6-6T-F_6 and H_6-6T-H_6. Studies of the crystal structure and the device performance of **F_6-6T-H_6** should be performed.

References

1. Akimichi, H.; Waragai, K.; Hotta, S.; Kano, H.; Sakaki, H. *Appl. Phys. Lett*. **1991**, *58*, 1500.

2. Garnier, F.; Yassar, A.; Hajiloui, R.; Horowitz, G.; Deloffre, F.; Servet, B.; Ries, S.; Alnot, P. *J. Am. Chem. Soc.* **1993**, *115*, 8716.

3. Wurthner, F. *Angew. Chem., Int. Ed.* **2001**, *40*, 1037.

4. Katz, H. E.; Lovinger, A. J.; Johnson, J.; Kloc, C.; Siegrist, T.; Li, W.; Lin, Y.–Y.; Dodabalapur, A. *Nature* **2000**, *404*, 478.

5. Bao, Z.; Lovinger, J.; Brown, J. *J. Am. Chem. Soc.* **1998**, *120*, 207.

6. Laquindanum, J. G.; Katz, H. E.; Dodabalapur, A.; Lovinger, A. J. *J. Am. Chem. Soc*. **1996**, *118*, 11331.

7. Facchetti, A.; Deng, Y.; Wang, A.; Koide, Y.; Sirringhous, H.; Marks, T. J.; Friend, R. H. *Angew. Chem., Int. Ed*. **2000**, *39*, 4547.

8. Marks, T. J.; Facchetti, A.; Sirringhous, H.; Friend, R. H. *WO Patent 0209201*, **2002**.

9. Facchetti, A.; Mushrush, M.; Katz, H. E.; Marks, T. J. *Adv. Mater*. **2003**, *15*, 33.

10. Hong, X. M.; Katz, H. E.; Lovinger, A. J.; Wang, B.-C.; Raghavachari, K. *Chem. Mater*. **2001**, *13*, 4686.

11. Katz, H. E.; Johnson, J.; Lovinger, J.; Li, W. *J. Am. Chem. Soc*. **2000**, *122*, 7787.

12. Katz, H. E.; Dodalabapur, A.; Torsi, L.; Elder, D. *Chem. Mater*. **1995**, *7*, 2238.

CHAPTER VII

EQUILIBRIUM OF DICATIONS AND RADICAL CATION DIMERS IN STACKED CONJUGATED OLIGOMERS: 2D MODELS OF SPINLESS INTERCHAIN CHARGE TRANSFER IN DOPED CONDUCTING POLYMERS

Introduction

Organic semiconductors are extensively studied for potential applications in optical and electronic devices. However, current organic semiconductor materials cannot compete with the inorganic semiconductors in terms of performance. The heterogeneous nature of polymeric organic semiconductors limit interchain electronic communication, and hinders charge migration leading to low charge mobility. Although many methods have been used to introduce order to conducting polymers, the study of the interchain charge transfer mechanism is not well-developed. To identify the nature of the charge carries in doped conducting polymer and further explore interchain charge transfer we set out to design 2D-ordered organic semiconductors.

The polaron/bipolaron model for charge carriers in doped conjugated polymers serves to explain the observed paramagnetism at low levels of doping and diamagnetism at higher doping levels in materials with non-degenerate ground states. The polaronic versus bipolaronic nature of the charge carriers and their possible interconversion at

intermediate doping levels remains a subject of discussion.[1,2] The creation of a spinless bipolaron (B^{2+}) from two polarons ($P^{+\cdot}$) is driven by the energy difference of these two species and the balance between electron-phonon and electron-electron interactions. In theory, both of these species could coexist in the case where the polaron and bipolaron formation energies become comparable.[3,4]

Many well-defined oligomeric compounds have been used as models to study the nature of the charge carriers in conjugated polymers. One electron oxidation of a conjugated oligomer generates a monocation radical, with two subgap electronic transitions and an ESR signal. The removal of a second electron gives the corresponding dication, which show only one subgap transition and no ESR signal.[5,6,7] Thus, radical cations have been proposed as model polarons, and dications as bipolarons. Theoretical calculations agree with these results.[8,9] However, studies of oxidized conjugated polymers often show two strong subgap transitions, and the absence of an ESR signal, or a very weak ESR signal.[10,11,12,13] Therefore, the charge carriers in doped conjugated polymers cannot be just simply addressed as either only the polaron or only bipolaron.

Extensive studies of radical cations of π-conjugated oligomers have shown that they form π-dimers in solution at low temperatures or in poor solvents. This is a general finding for many conjugated oligomers, including oligothiophenes,[14,15,16,17,18,19] oligo(thienylene vinylene),[20] oligopyrroles,[21,22] mixed thiophene-pyrrole oligomers,[23] and oligo(p-phenylene vinylenes).[24] These π-dimers show two subgap absorptions, which is characteristic to radical cations. However, these π-dimers are also ESR silent. Thus, the discovery and characterization of π-dimers provide further understanding of the nature of charge carriers in doped conjugated polymers.

Some conjugated radical cations, such as diphenylpolyenes,[25] end-capped bithiophenes and bipyroles,[26,27] form σ-dimers instead of π-dimers. These σ-dimers have also been used to explain the weak ESR signal and the hysteresis between charging and discharging of conjugated polymers.

The dications of long oligothiophenes (nT, n≥12) are spinless and have two subgap absorptions, the same as polythiophenes.[28] This behavior has been explained as two polarons located on the same chain. The Coulomb repulsion outweighs the energy gain of creating a bipolaron, so two polarons stay apart from each other. It has also been found the radical cations of 12T disproportionate into neutral oligomers and dications. The similar disproportionation reaction was also observed for tetrathiafulvalene derivatives (TTF), in which dissolution of the radical cation salt only gives the neutral and the dicationic states.[29]

In order to extend the analysis of well-defined cationic oligomers into the second dimension, Salhi and Collard[30,31] and others[32,33] have described the synthesis and electrochemical characterization of oligothienyl-substituted paracyclophanes.[34,35] These studies indicate there is efficient π-π communication between the two benzene rings of paracyclophane, although they are not conjugated with each other.

Here we describe a new conjugated oligomer in which two oligomers stack on a top each other through a paracyclophane. We demonstrate that the bis(radical cation) and dication-neutral forms of the permanently stacked oligomers are in equilibrium with one another by an inter-oligomer disproportionation, using the electrochemistry, absorption spectroscopy and ESR. This further establishes a possible role for radical cation π-dimers in the charge transport mechanism of doped conjugated polymers.

Experimental

General methods

All reagents were obtained from commercial sources and used without further purification unless stated otherwise. Tetrahydrofuran (THF) and diethyl ether were dried over sodium benzophenone ketyl prior to distillation under nitrogen. Methylene chloride was dried over calcium hydride prior to distillation under nitrogen. Column chromatography was performed on silica gel (40 mesh, 60Å, Baker). Thin layer chromatography was performed on 3 × 5 cm plates of silica gel (0.2 mm thick, 60 F_{254}) on an aluminum support (EM Separations). All ^{1}H NMR spectra were collected on a Varian Gemini 300 MHz instrument using $CDCl_3$ as the solvent unless otherwise specified. Chemical shifts are reported relative to tetramethylsilane. ^{13}C NMR spectra were obtained at 75.5 MHz. IR analysis was performed on a Nicolet 520 FTIR spectrometer. UV-vis analysis was performed with a Perkin-Elmer Lambda 19 spectrometer. Fluorescence spectra were collected with a Spex Fluorolog Fluometer 1681 0.22m Spectrometer. Electron ionization or chemical ionization mass spectrum was performed using a VG Analytical 70-SE instrument with a L-250J Data System Analyzer Matrix assisted laser desorption/ionization (MALDI) was performed using an Applied Biosystems with a 4700 Proteomics Analyzer.

Electrochemical experiments were performed using a BAS 100B electrochemical analyzer in three-electrode cell equipped with a 2.0 mm^2 gold or platinum or graphite disk working electrode, a platinum wire counter electrode, and a saturated calomel electrode (SCE). Electrolyte tetra-*n*-butylammonium tetra(perfluorophenyl)borate was

prepared by metathesis of $Li[B(C_6F_5)_4].2Et_2O$ with $[NBu_4]Br$ and recrytallized from 2: 1 mixture of CH_2Cl_2/Et_2O

ESR spectra were recorded on a Bruker ER-200S RC X-band EPR Spectrometer equipped with microwave bridge with balanced mixer detection, a microwave power of 6.3 mW, magnetic field modulation 1 G, and time constant of 30 ms.

3-Octylthiophene was prepared by the Kumada coupling of 3-bromothiophene and 1-octylmagnesium bromide catalyzed by $Ni(dppp)Cl_2$. 2-Bromo-3-octylthiophene was made by bromination of 3-octylthiophene with NBS.

Synthesis

***pseudopara*-Dibromo[2.2]paracyclophane (34).** A solution of bromine was prepared by stirring of Br_2 (2.6 mL, 50 mmol) in 67 mL CCl_4 and 50 mL CH_2Cl_2 for 30 min. Iron filings (0.11 g, 2.0 mmol) were added to a solution of paracyclophane (5.0 g, 24 mmol) in a mixture of 20 mL CCl_4 and 60 mL CH_2Cl_2. The mixture was heated to reflux and the pre-made Br_2 solution was added dropwise over 4 h. The reaction mixture was cooled slowly to room temperature and stirred for another 30 min. The mixture was washed with saturated aqueous $NaHCO_3$ (2×100 mL), H_2O (100 mL) and brine (100 mL), and dried over $MgSO_4$. The solvent was removed under reduced pressure and the residue was recrystallized twice from a mixture solvent of $CHCl_3$ and Et_2O (around 6:1) to give **34** (1.96 g, 22%), as a white powder solid. -^{1}H NMR (300 MHz, $CDCl_3$) δ 7.14 (dd, 2 H, J = 4.8, 19.2), 6.51 (d, 2 H, J = 4.8), 6.44 (d, 2 H, J = 19.2), 3.49 (m, 2 H), 3.15 (m, 2 H), 2.88 (m, 4 H).

3,3'-Dioctyl-2,2'-bithiophene (35).[36] A mixture of magnesium filings (1.46 g, 60.0 mmol) in 60 mL dry THF was heated to maintain a mild reflux. 2-Bromo-3-octythiophene (11.0 g, 40.0 mmol) was added in dropwise and the mixture was heated at reflux for 4 h. The mixture was cooled to 0 °C and a solution of 2-bromo-3-octylthiophene (12.1 g, 44.0 mmol) and Ni(dppp)Cl_2 (1.30 g, 2.40 mmol) in 200 mL dry Et_2O was added via canular. The reaction mixture was stirred at room temperature overnight and quenched with ice cold aqueous HCl (100 mL conc. HCl and ~150 g ice). The organic layer was separated, washed with 10% aqueous H_2SO_4 (100 mL), H_2O (100 mL), 5% aqueous $NaHCO_3$ (100 mL) and brine (100 mL), and dried over $MgSO_4$. The solvent was removed under reduced pressure and vacuum distillation gave **35** (7.18 g, 46%), as a colorless liquid. -^{1}H NMR (300 MHz, $CDCl_3$) δ 7.28 (d, 2 H, *J* = 5.1), 6.96 (d, 2 H, *J* = 5.1), 2.49 (t, 4 H, *J* = 7.8), 1.47 (m, 4 H), 1.25 (m, 20 H), 0.88 (t, 6 H).

5-Bromo-3,3'-dioctyl-2,2'-bithiophene (36). A solution of 3,3'-dioctyl-2,2'-bithiophene (5.85 g, 15.0 mmol) and NBS (2.67 g, 15.0 mmol) in 100 mL DMF was stirred at –10℃ for 4 h. The mixture was poured into H_2O (100 mL) and extracted with hexane (3×100 mL). The combined organic portions were dried over $MgSO_4$. The solvent was removed and the crude product was purified by column chromatography (silica/hexane) to give **36** (6.06 g, 86%), as a yellow liquid. -^{1}H NMR (300 MHz, $CDCl_3$) δ 7.29 (d, 1H, *J* = 5.5), 6.94 (d, 1H *J* = 5.5 Hz), 6.91 (s, 1H), 2.48 (t, 2H, *J* = 7.8 Hz), 2.42 (t, 2H, *J* = 7.8 Hz), 1.50 (m, 4H), 1.22 (m, 20H), 0.86 (m, 6H). MS (EI): M^+ = 468.

5-(2,5-Dimethylphenyl)- 3,3'-dioctyl-2,2'-bithiophene (37). 2-Bromo-*p*-xylene (2.22 g, 12.0 mmol) was added dropwise to magnesium turnings (0.440 g, 18.0 mmol) in 40 mL dry THF and the mixture was heated at reflux for 3 h to give a solution of 1-(2,5-

dimethylphenyl)magnesium bromide. The Grignard reagent was transferred via a cannula to a solution of 5-bromo-3,3'-dioctyl-2,2'-bithiophene, **36** (4.33 g, 9.23 mmol) and Ni(dppp)Cl_2 (0.15 g, 0.28 mmol, 3 mol%) in 80 mL dry THF and the solution was heated to reflux overnight. The mixture was quenched with ice/water (100 mL H_2O with ~100 g ice), extracted with hexane (3×100 mL), and dried over $MgSO_4$. The solvent was removed under reduced pressure and the residue was purified by column chromatography (silica/hexane) to give **37** (4.00 g, 88%), as a yellow liquid. -^{1}H NMR (300 MHz, $CDCl_3$) δ 7.29 (d, 1H, *J* = 5.5), 7.26 (d, 1H, *J* = 1.9), 7.15 (d, 1H, *J* = 8.1), 7.04 (dd, 1H, *J* = 8.1, 1.9), 6.97 (d, 1H *J* = 5.5 Hz), 6.91 (s, 1H), 2.55 (t, 2H, *J* = 7.8 Hz), 2.51 (t, 2H, *J* = 7.8 Hz), 2.43 (s, 3H), 2.34 (s, 3H), 1.54 (m, 4H), 1.22 (m, 20H), 0.84 (m, 6H). IR (NaCl): 2960, 2927, 2855, 1460, 815, 729 cm^{-1}. MS (EI): M^+ = 494.

5-(2,5-Dimethylphenyl)- 3,3'-dioctyl-5'-tributylstannyl-2,2'-bithiophene (38). A solution of *n*-butyllithium (1.76 mL, 2.5 M solution in hexane, 4.40 mmol) was added to a solution of 5-(2,5-dimethylphenyl)-3,3'-dioctyl-2,2'-bithiophene, **37** (1.98 g, 4.00 mmol) in 60 mL of dry THF at –78℃ under argon. After stirring for 10 min, tributyltin(IV) chloride (1.19 mL, 4.40 mmol) was added and the reaction mixture was allowed to warm to room temperature, and was stirred for 3 h. Et_2O (100 mL) and brine (100 mL) were added to the reaction mixture and the aqueous portion was extracted with Et_2O (3×100 mL). The organic phases were combined and dried over Na_2SO_4. The solvent was removed to afford **29** (3.10 g, 99%), as a yellow liquid. -^{1}H NMR (300 MHz, $CDCl_3$) δ 7.26 (d, 1H, *J* = 1.9), 7.15 (d, 1H, *J* = 8.1), 7.05 (dd, 1H, *J* = 8.1, 1.9), 7.04 (s, 1H), 6.92 (s, 1H), 2.55 (m, 4H), 2.44 (s, 3H), 2.34 (s, 3H), 1.56 (m, 4H), 1.22 (m, 20H), 0.82 (m, 6H). IR (NaCl) 2960, 2927, 2855, 1460, 762 cm^{-1}. MS (FAB): M^+ = 783.

Bis[5-(2,5-dimethylphenyl)- 3,3'-dioctyl-2,2'-bithienyl]-[2.2]paracyclophane (39). A solution of 5-(2,5-dimethylphenyl)- 3,3'-dioctyl-5'-tributylstannyl-2,2'-bithiophene, **38** (3.10 g, 4.00 mmol), pseudopara-dibromo[2.2]paracyclophane, **34** (0.368 g, 1.00 mmol) and $Pd(PPh_3)_4$ (0.116 g, 0.10 mmol) in 30 ml dry DMF was stirred for 10 min under argon protection, and then heated at 100℃ for 20 h. The mixture was poured into H_2O (60 mL) and extracted with CH_2Cl_2 (3×100 mL). The combined organic portions were washed thoroughly with 10% aqueous KF solution (5 × 100 mL) and dried over $MgSO_4$. The solvent was removed under reduced pressure and flash column chromatography (silica/30:1 hexane/Et_2O) gave a mixture of **39** and byproduct. (0.95g, viscous yellow liquid). This crude product (40 mg) was further purified by reverse phase HPLC (THF/H_2O) to afford pure **39** as a viscous yellow liquid (34 mg, 68%). -^{1}H NMR (300 MHz, $CDCl_3$) δ 7.31 (d, 2H, *J* = 1.9), 7.18 (d, 2H, *J* = 8.1), 7.07 (dd, 2H, *J* = 8.1, 1.9), 6.99 (s, 2H), 6.97 (s, 2H), 6.82 (dd, 2H, *J* = 8.1, 1.9), 6.67 (d, 2H, *J* = 1.9), 6.59 (d, 2H, *J* = 8.1), 3.83 (m, 2H), 2.96 (m, 6H), 2.64 (m, 8H), 2.48 (s, 6H), 2.37 (s, 6H), 1.65 (m, 8H), 1.24 (m, 40H), 0.84 (m, 12H). ^{13}C NMR (300 MHz, $CDCl_3$) δ = 143.6, 143.0, 142.8, 142.4, 140.3, 137.2, 135.6, 135.2, 134.1, 133.4, 132.9, 131.0, 129.8, 129.0, 128.8, 128.6, 128.3, 128.0, 34.8, 34.7, 32.3, 31.2, 29.9, 29.7, 29.6, 23.1, 21.3, 14.6. IR (NaCl) 2967, 2907, 2848, 1947, 1446, 1414, 1262, 1104, 1032, 874, 808, 703, 670. HRMS (MALDI): 1192.7013 (observed), 1192.7015 (calculated), Δ = 0.20 ppm.

5,5'-Dibromo-3,3'-dioctyl-2,2'-bithiophene (40).[37] NBS (3.41 g, 19.2 mmol) was added in a solution of 3,3'-dioctyl-2,2'-bithiophene (3.74 g, 9.59 mmol) in dry DMF (40 mL) under N_2 at -15℃ and the mixture was slowly warmed to room temperature. The mixture was stirred for 6 h and poured into H_2O (100 mL). The mixture was extracted

with hexane (3×100 mL) and the combined organic portions were dried over $MgSO_4$. The solvent was removed under reduced pressure, and the crude product was purified by column chromatography (silica/hexane) to give **34** (3.82 g, 72%), as a yellow liquid. -^{1}H NMR (300 MHz, $CDCl_3$) δ 7.2-7.3 (m, 2H), 7.13 (dd, *J*=1.5, 8 Hz, 1H), 7.08 (d, *J*=3.6 Hz, 1H), 6.84 (d, *J*=3.6 Hz, 1H), 2.40 (s, 6H). MS (EI): M^+ = 268.

5,5'-Bis(2,5-dimethylphenyl)-3,3'-dioctyl-2,2'-bithiophene (41). 2-Bromo-*p*-xylene (2.78 g, 15.0 mmol) was added to a mixture of magnesium turnings (0.546 g, 22.4 mmol) and 50 mL dry THF, and the mixture was heated at reflux for 3 h to give a solution of 1-(2,5-dimethylphenyl)magnesium bromide. The Grignard reagent was transferred via a cannula to a solution of 5,5'-bromo-3,3'-dioctyl-2,2'-bithiophene, **40** (3.15 g, 5.76 mmol) and Ni(dppp)Cl_2 (0.19 g, 0.34 mmol, 3 mol%) in 90 mL dry THF, and the solution was heated to reflux overnight. The mixture was added to ice/water (100 mL H_2O with ~100 g ice), extracted with hexane (3×100 mL), and the combined organic extracts were dried over $MgSO_4$. The solvent was removed under reduced pressure and the residue was purified by column chromatography (silica/hexane) to give **41** (2.76 g, 80%), as a yellow liquid. -^{1}H NMR (300 MHz, $CDCl_3$) δ 7.30 (s, 2H), 7.16 (d, *J*=9 Hz, 2H), 7.06 (d, *J* =6 Hz, 2H), 6.94 (s, 2H), 2.63 (t, *J*=6 Hz, 4H), 2.46 (s, 6H), 1.7-1.6 (m, 4H), 1.4-1.2 (m, 16H), 0.90 (t, 6H); IR (NaCl): 2948, 2912, 2856, 1649, 1400, 910, 700 cm^{-1}. HRMS (FAB): 598.36377 (observed), 598.36670 (calculated), Δ = 4.9 ppm.

Results and Discussion

Synthesis

The synthesis of unstacked oligomer **41** is shown in Figure 7.1. Kumada coupling of 2-bromo-3-octylthiophene and 2-(3-octylthienyl)magnesium bromide gives 3,3'-dioctyl-2,2'-bithiophene. Bromination of 3,3'-dioctyl-2,2'-bithiophene with two equivalents of NBS yields 5,5'-dibromo-3,3'-dioctyl-2,2'-bithiophene, **40**. Kumada coupling of 5,5'-dibromo-3,3'-dioctyl-2,2'-bithiophene, **40**, and (2,5-dimethylphenyl)magnesium bromide yields 5,5'-bis(2,5-dimethylphenyl)-3,3'-dioctyl-2,2'-bithiophene, **41**, the unstacked model compound.

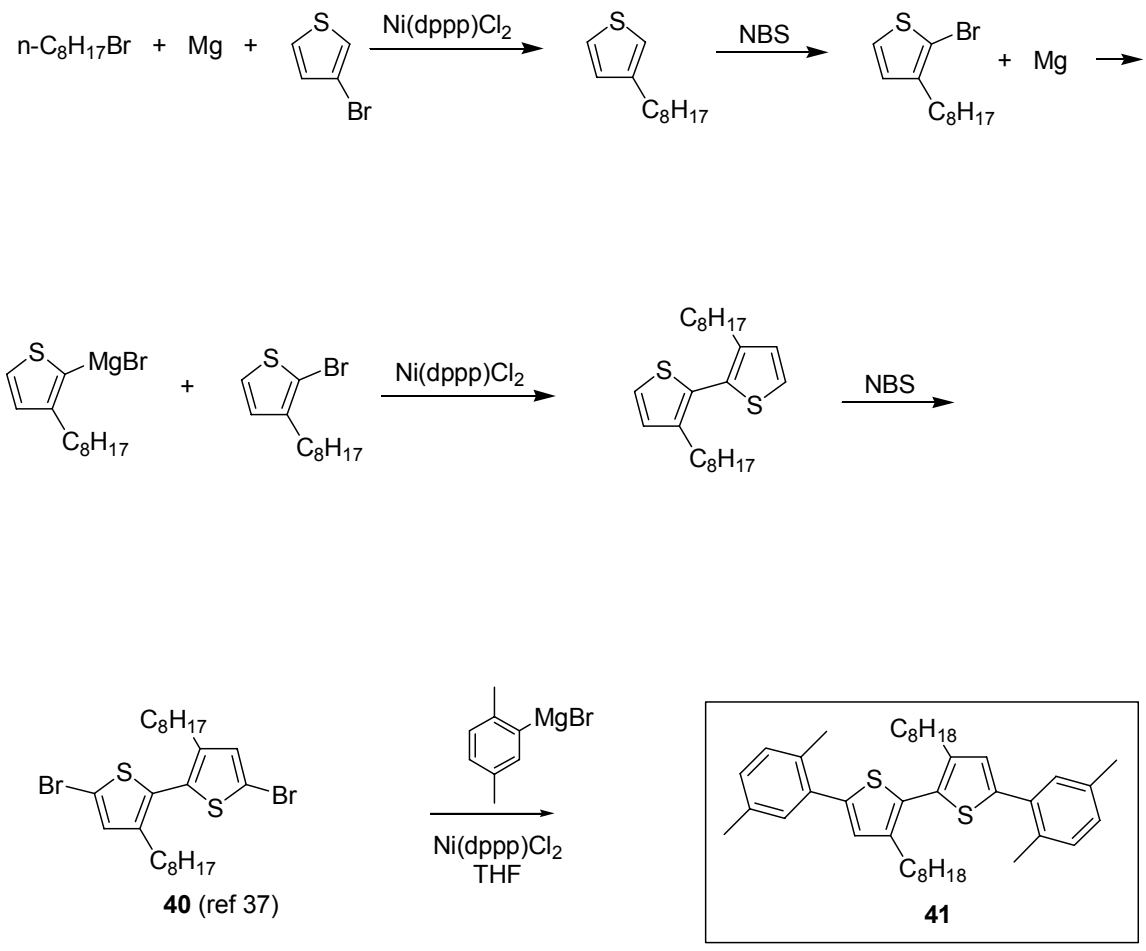

Figure 7.1. Synthesis of **41** (unstacked model compound).

The synthesis of stacked analogue, **39**, in which the conjugated oligomers are stacked atop each other through a paracyclophane, is shown in Figure 7.2. Bromination of 3,3'-dioctyl-2,2'-bithiophene, **35**, with one equivalent of NBS affords 5-bromo-3,3'-dioctyl-2,2'-bithiophene, **36** (^{1}H NMR, Figure 7.3.). Kumada coupling of (2,5-dimethylphenyl)magnesium bromide and **36** yields 5-(2,5-dimethylphenyl)-3,3'-dioctyl-

2,2'-bithiophene, **37** (^{1}H NMR, Figure 7.4.). Lithiation of **37** followed by reaction with tributyltin(IV) chloride gives the corresponding stannyl reagent, **38** (^{1}H NMR, Figure 7.5.), which undergoes Stille coupling with *pseudopara*-dibromo[2.2]paracyclophane, [38] **34**, to give bis[5-(2,5-dimethylphenyl)-3,3'-dioctyl-2,2'-bithienyl]-[2.2]paracyclophane, **39**, the stacked model. The Stille cross-coupling was not very clean. It gave the desired product, in which the coupling took place twice on the same cyclophene core. It also gave the side product, which only coupled once. The product and byproduct are both non-polar and could not separate by the flash chromatography even with the most non-polar solvents, such as cyclohexane, hexane, or petroleum ether. The product was purified by a preparative HPLC with a reverse phase column using a mixture of THF and H_2O as eluent. The identity of the purified compound was confirmed by ^{1}H-NMR (Figure 7.6.), ^{13}C-NMR (Figure 7.7.), and HRMS (by MALDI).

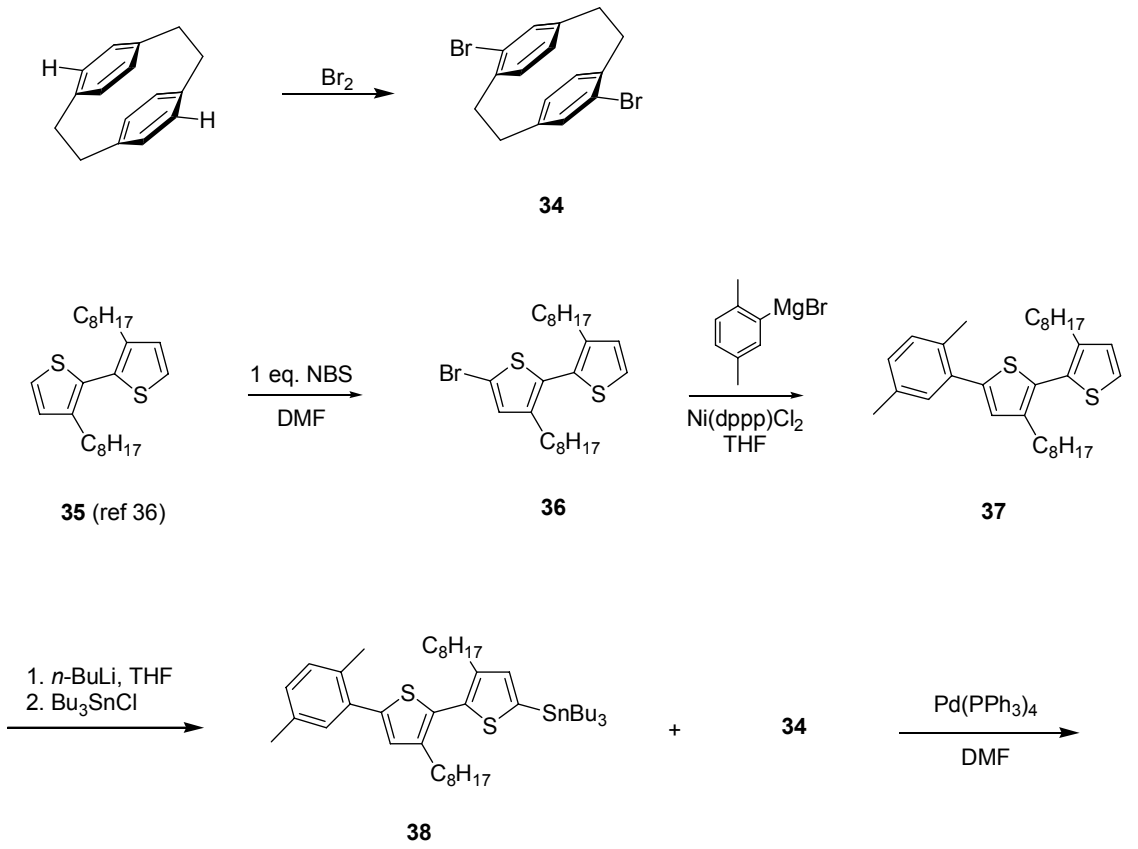

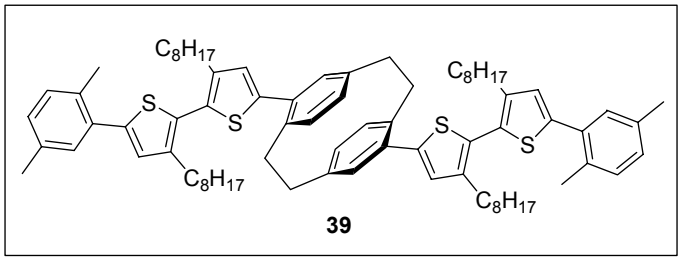

Figure 7.2. Synthesis of **39** (stacked model compound).

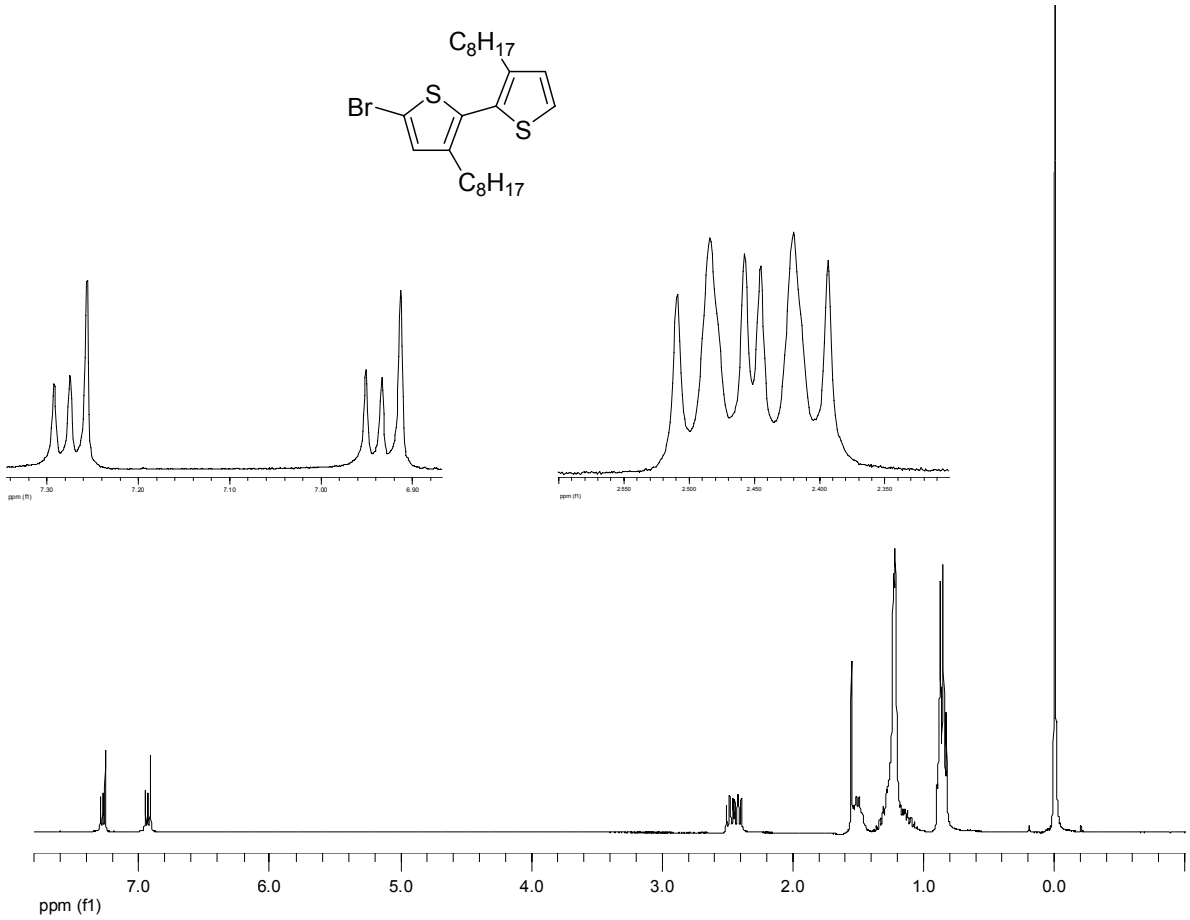

Figure 7.3. ^{1}H NMR spectrum (300 MHz, $CDCl_3$) of compound **36**.

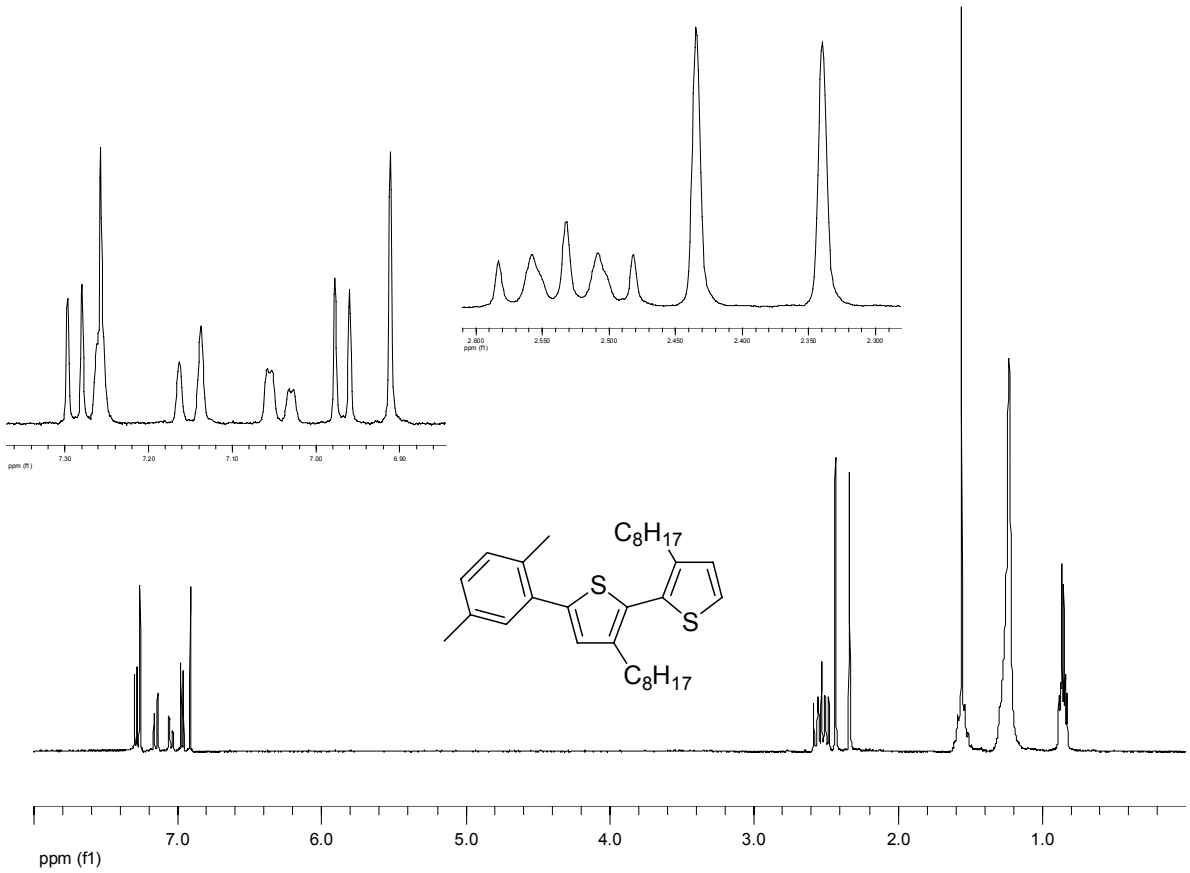

Figure 7.4. ^{1}H NMR spectrum (300 MHz, $CDCl_3$) of compound **37**.

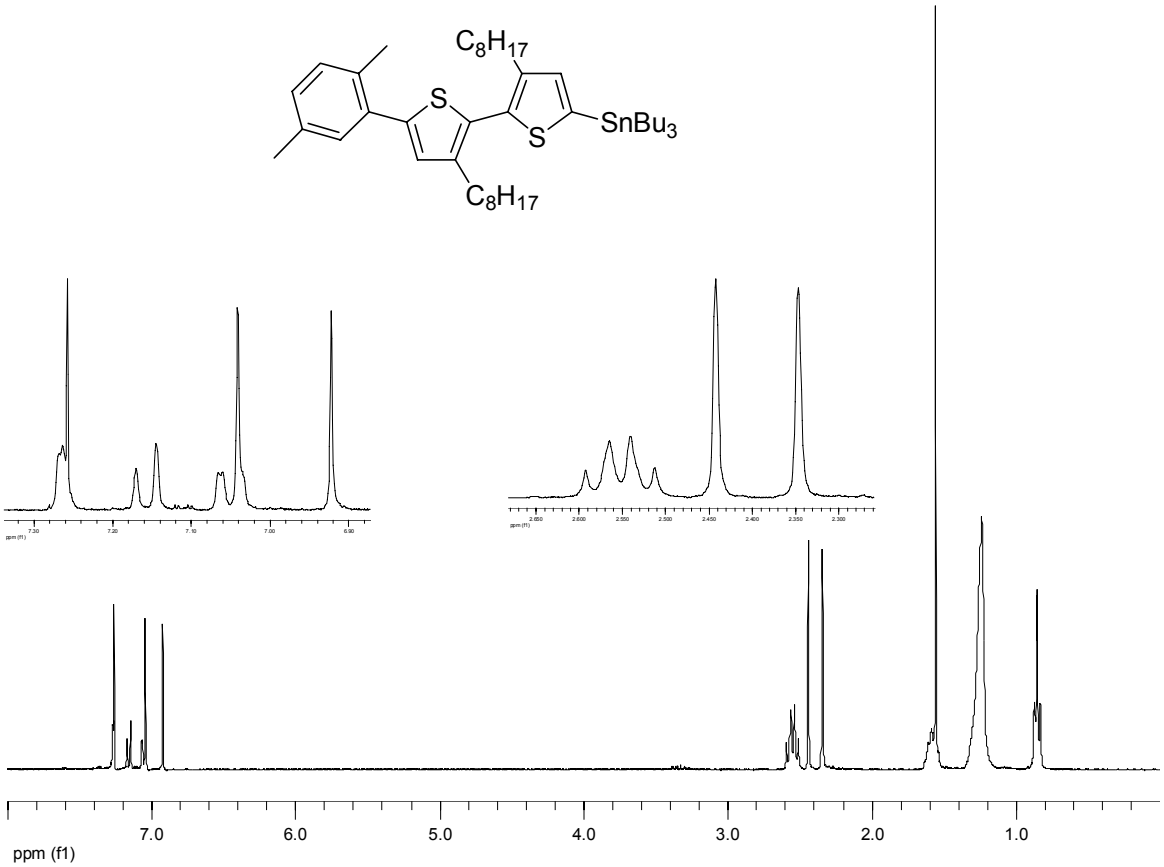

Figure 7.5. ^{1}H NMR spectrum (300 MHz, $CDCl_3$) of compound **38**.

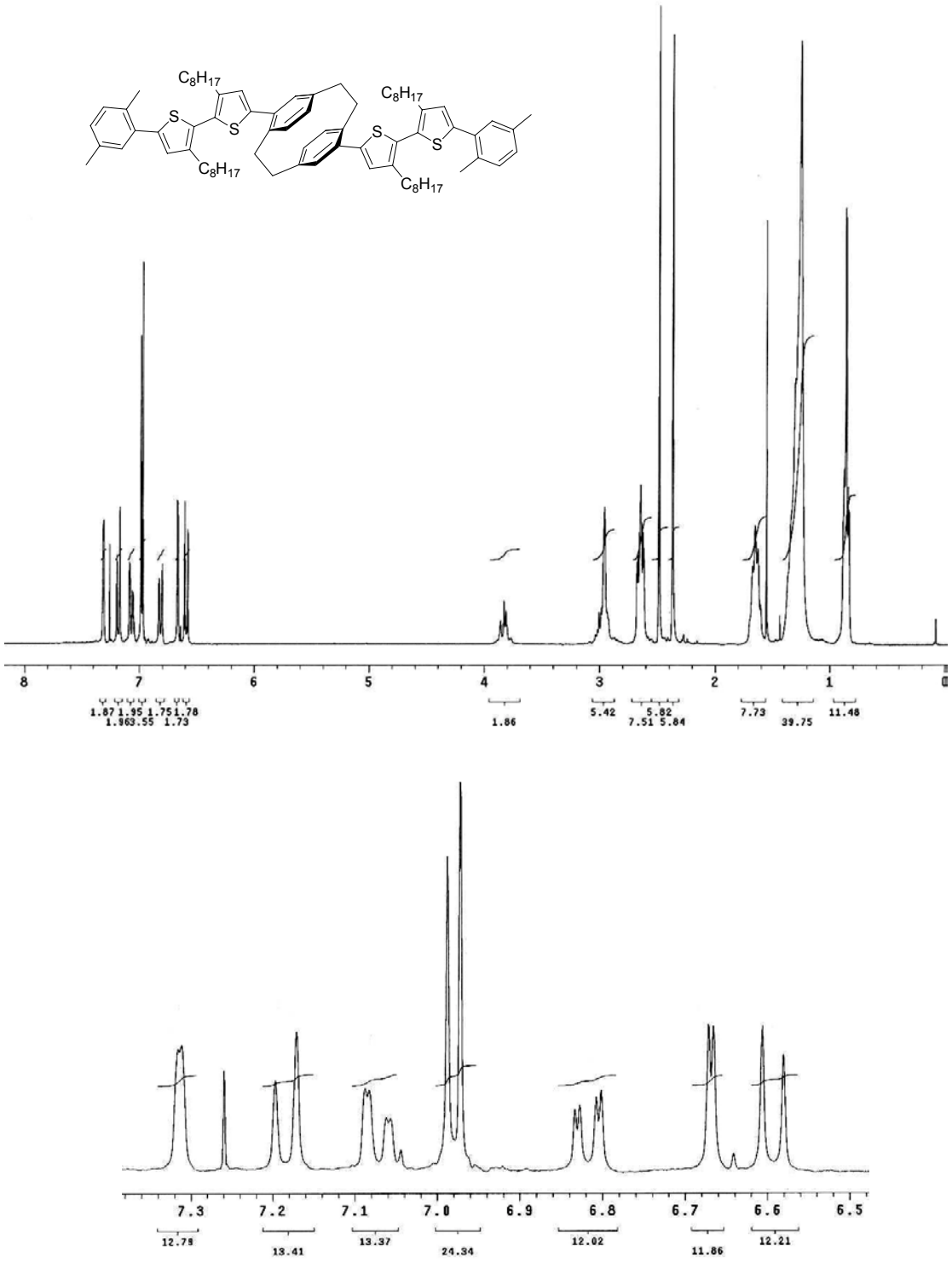

Figure 7.6. ^{1}H NMR spectrum (300 MHz, $CDCl_3$) of compound **39**.

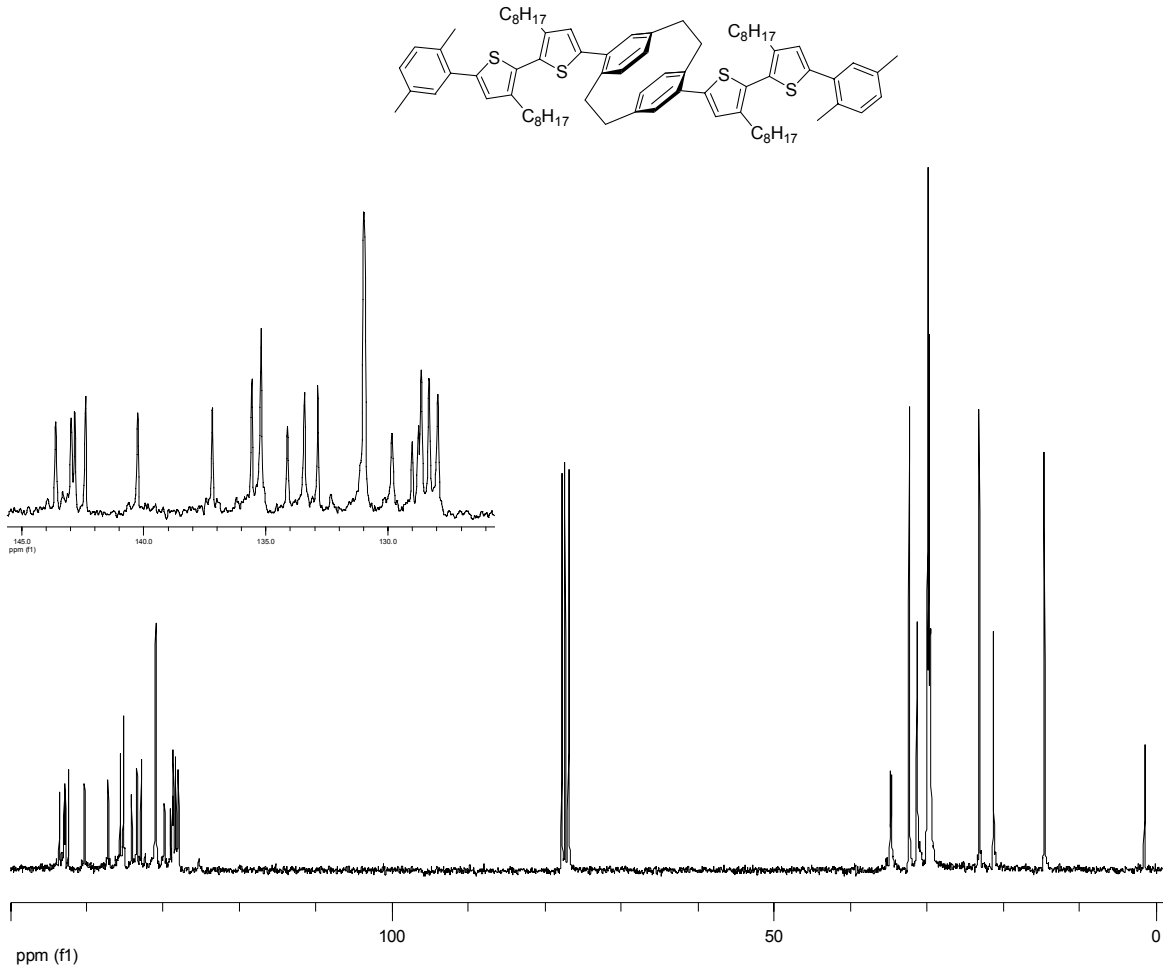

Figure 7.7. ^{13}C NMR spectrum (300 MHz, $CDCl_3$) of compound **39**.

Photophysics of the neutral state

The unstacked model compound **41** is a four-ring conjugated oligomer (e.g., xylene-thiophene-thiophene-xylene). The stacked model compound **39** contains two of the same four-ring conjugated oligomers stacked on the top of each other through the cyclophane core. The cyclophane core has two benzene rings linked through two ethylene bridges, so the two benzene rings are not conjugated to each other directly. However, the small face-to-face distance between these two benzene rings allows the two conjugated oligomers to communicate with each other, which has been confirmed by the electrochemistry and photophysics.[30,31]

The unstacked model compound **41** absorbs with a maximum at 307 nm and emits with a maximum at 431 nm. The stacked model compound **39** absorbs with a maximum at 319 nm and emits with two maxima at 441 and 469 nm, Figure 7.8. The absorption and emission spectra of the stacked model compound **39** are both red shifted (~ 10 nm), relative to the unstacked model compound **41**. Salhi and Collard reported the influence of paracyclophane π-stacks on the redox and optical properties of a broken conjugated polythiophene. The unstacked model compound **41** and the stacked model compound **39** are the unstacked repeating unit and the stacked repeating unit of that polymer, Table 7.1. Consistent with the red shift of the monomer relative to the polymer in absorption and emission spectra, the paracyclophane π-stack shows the same trend for the unstacked model compound **41** and the stacked model compound **39**, Table 7.1. The red shift in both ground state and excited state can be ascribed to the effect of π-stacking of another four-ring conjugated oligomer via the cyclophane structure at the termini of the four-ring conjugated oligomer. This has the effect of increasing delocalization, reduce the energy

difference between HOMO and LUMO, and thereby leading to the red shifted absorption and emission.

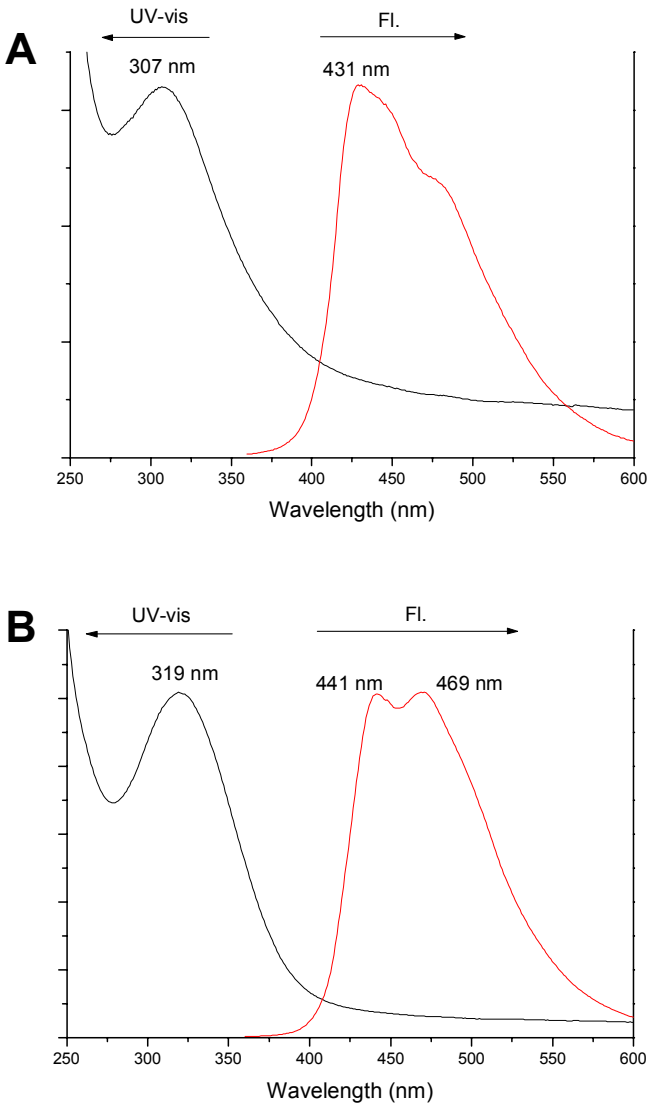

Figure 7.8. (A): UV-vis and fluorescence spectra of the unstacked model, compound **41**; (B): UV-vis and fluorescence spectra of the stacked model, compound **39.**

Table 7.1. Characteristics of the unstacked model **41**, stacked model **39** and the polymer.

	E_{ox} [a] (V)	Absorbance [b] λ_{max} (nm)	Fluorescence [b] λ_{max} (nm)
41	+1.29, +1.67	307	431
39	+1.27, +1.39, +1.84, +2.00	319	441, 469
Polymer[d]	+1.00 [c]	380	525

[a] c =1 mM in CH_2Cl_2 with 0.1 M Bu_4NPF_6, v = 100 mVs^{-1} on a gold electrode, all values relative to SCE. [b] 10^{-5} M solution in $CHCl_3$. [c] $E_{1/2}$, thin film deposited electrochemically on ITO glass. [d] data of the polymer from ref. 31.

Salhi and Collard also reported the enhancement of the quantum yield from the monomer to the polymer. We did not observe the same enhancement here. Fluorescence quantum yields (ϕ) were determined in $CHCl_3$ solutions by using coumarin 460 (Exiction, Dayton, Ohio; ϕ = 0.99 in CH_3CN) as a standard: compound **41**, 0.058; compound **39**, 0.057.

Redox behavior of compounds **41** and **39**

The unstacked model compound **41** should undergo the first oxidation (E_1) to form the radical cation $\mathbf{41}^{+\cdot}$, then the second oxidation (E_2) to for the dication $\mathbf{41}^{2+}$. The stacked model compound **39** should undergo the first oxidation (E_{1a}) to form the radical cation/neutral $\mathbf{39}^{+\cdot/0}$, a second oxidation (E_{1b}) to form the double charge species, a third oxidation (E_{2a}) to form the radical cation/dication $\mathbf{39}^{+\cdot/2+}$, and a fourth oxidation (E_{2b}) to form the dication/dication $\mathbf{39}^{2+/2+}$. However, unlike the other three states, the identity of the doubly charged species is ambiguous. It could exist as either the bis(radical cation)

$\mathbf{39}^{+\cdot/+\cdot}$, or as the dication/neutral $\mathbf{39}^{2+/0}$. The bis(radical cation) $\mathbf{39}^{+\cdot/+\cdot}$ is a good model for a polaron π-dimer, one polaron stacking on another polaron of the adjacent polymer chain. The dication/neutral $\mathbf{39}^{2+/0}$ is a good model for a bipolaron in the conjugated polymer matrix, a bipolron stacking with the neutral backbone of an adjacent polymer chain. We set out to identify the nature of the double charged species to gain a better understanding of the nature of the charge carriers in the doped conjugated polymers. The conversion (or possible equilibrium) between the bis(radical cation) $\mathbf{39}^{+\cdot/+\cdot}$ and the dication/neutral $\mathbf{39}^{2+/0}$ serves as a model for interchain charge transfer in the doped conjugated polymers, Figure 7.9.

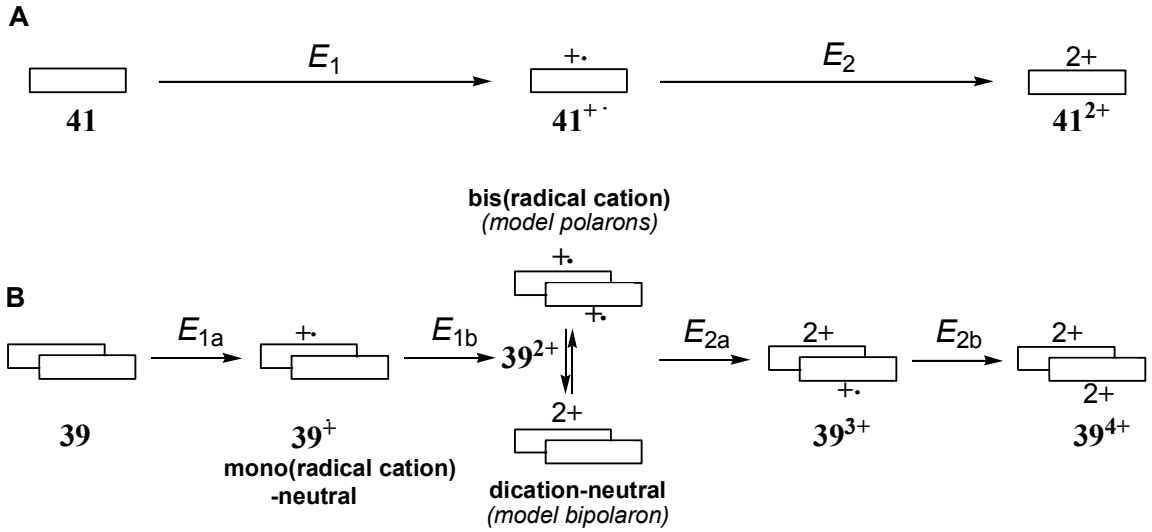

Figure 7.9. Oxidation states of unstacked oligoarene **41** (A) and stacked analog **39** (B), including a proposed equilibrium between bis(radical cation) and dication-neutral forms of $\mathbf{39}^{2+}$ which serve as models for radical cation π-dimer and bipolaron, respectively.

The stacked model compound **39** is thus a good model compound to explore the nature of the charge carriers and the interchain charge transfer mechanism in the doped conjugated polymers. We used electrochemistry, UV-vis-NIR spectroscopy and ESR to study the doubly charged state of **39** in an attempt to provide answers to the questions above.

Electrochemistry with the small-anion electrolyte Bu_4NPF_6

Salhi and Collard reported the splitting of only the first oxidation wave of oligothienyl-substituted cyclophanes into two single-electron processes as the result of π-stacking.[30] Further elongation of the oligoarene conjugation length allows us to study the splitting of both the first and second oxidation waves and build up the suitable model for charge carriers in solid conjugated polymers. In addition, we can study the interchain electron transfer. The stacked model compound **39** has a longer conjugation length than Salhi's compounds (four arenes *vs* three) and therefore has a lower second oxidation potential. Long alkyl chains impart solubility.

The cyclic voltammetry (CV) of compounds **41** and **39** show the influence of π-stacking on the redox behavior of the oligothienyl-substituted paracyclophanes. With Bu_4NPF_6 as the electrolyte, CV of unstacked model **41** shows two sharp reversible oxidation waves for the oxidation **41** to the radical cation (polaron, $\mathbf{41}^{+\bullet}$), and then to the dication (bipolaron, $\mathbf{41}^{++}$), at E_1 = + 1.07 V and E_2 = + 1.45 V, respectively, Figure 7.10. Differential pulse voltammetry (DPV) is of **41** in the same electrolyte also gave two well resolved peaks, Figure 7.11.

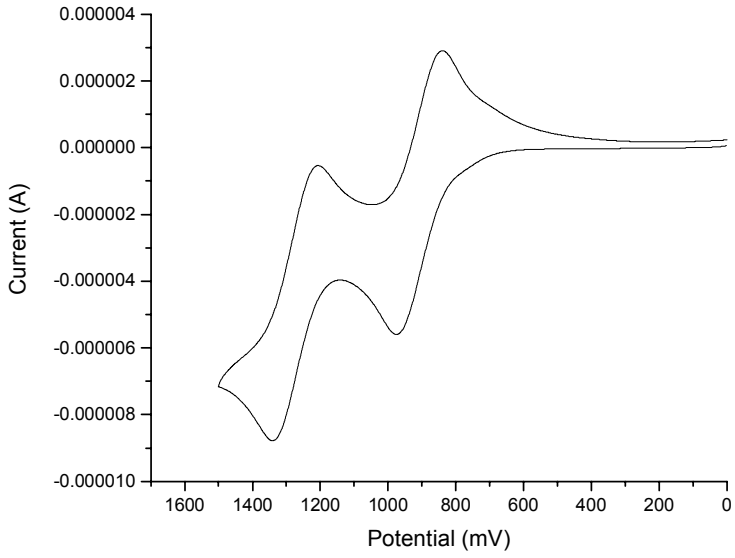

Figure 7.10. Cyclic voltammograms of **41**, 3 mM in CH_2Cl_2 containing 0.1 M Bu_4NPF_6, v = 100 mV/s on a gold electrode, Ag/AgCl reference electrode.

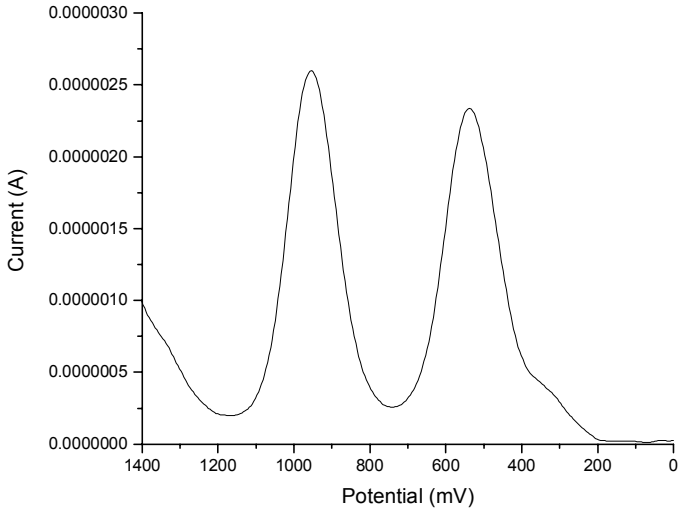

Figure 7.11. Differential pulse voltammogram of **41**, 3 mM in CH_2Cl_2 containing 0.1 M Bu_4NPF_6, v = 100 mV/s on a gold electrode, pulse amplitude = 25 mV, pulse width = 50 ms, pulse period = 200 ms, Ag/AgCl reference electrode.

With the same electrolyte, the CV of **39** also shows two two-electron oxidation waves but both of them display significant broadening, Figure 7.12. The DPV of **39** shows splitting of each wave into two distinct one-electron waves at E_{1a} = + 1.05 V, E_{1b} = + 1.17 V, E_{2a} = + 1.62 V, E_{2b} = + 1.78 V. Thus, splitting between the first and second oxidation amounts to 25 mV, and between the third and fourth oxidation it is 160 mV, Figure 7.13.

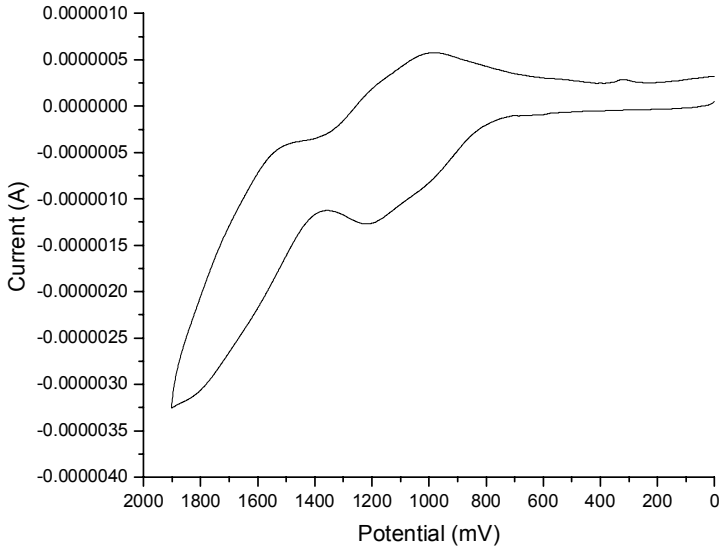

Figure 7.12. Cyclic voltammograms of **39**, 3 mM in CH_2Cl_2 containing 0.1 M Bu_4NPF_6, v = 100 mV/s on a gold electrode, Ag/AgCl reference electrode.

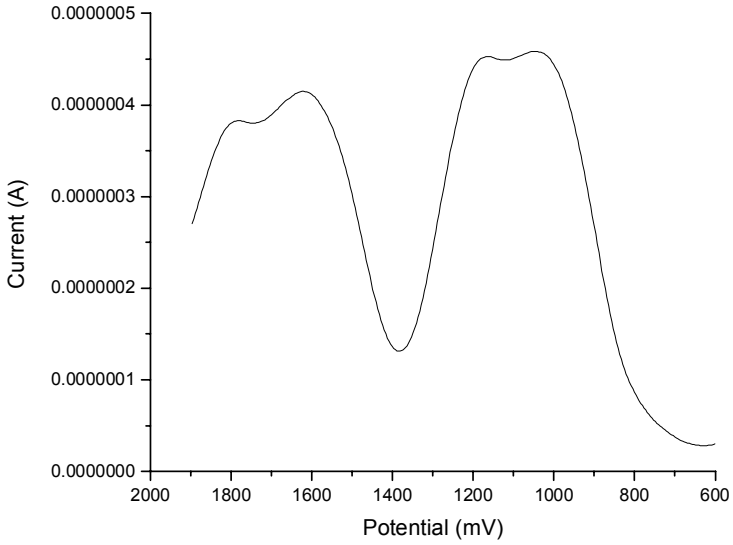

Figure 7.13. Differential pulse voltammogram of **39**, 3 mM in CH_2Cl_2 containing 0.1 M Bu_4NPF_6, v = 100 mV/s on a gold electrode, pulse amplitude = 25 mV, pulse width = 50 ms, pulse period = 200 ms, Ag/AgCl reference electrode.

Compound **39** is a cofacial "dimer" composed of two conjugated tetraarenes of the unstacked model compound **41**, with stacking of the terminal benzene rings in the form of a cyclophane. These splittings can be explained by the effect of π-stacking the arene in the cyclophane, Figure 7.14. In neutral state, each conjugated oligomer acts as an electron-donor to the other cofacially held oligomer through π-stacking. This accounts for **39** undergoing its first oxidation at a lower potential than the unstacked model compound **41** ($E_{1a} < E_1$). After removal of one electron from **39**, the positively charged arm then serves as a electron-withdrawing group as far as the other neutral arm is concerned. This means that $\mathbf{39}^{+./0}$ undergoes further oxidation at a higher potential. The mono-charged arms act as electron-withdrawing group to the other mono-charged oligomer of the

dication $\mathbf{39}^{+\cdot/+\cdot}$, and makes it harder to remove another electron to form $\mathbf{39}^{+\cdot/2+}$ than oxidation of unstacked oligomeric radical cation $\mathbf{41}^{+\cdot}$ to form dication $\mathbf{41}^{2+}$**.** The electron-withdrawing effect through π-stacking leads to $E_{2a} > E_2$. The fourth oxidation of **39** is to oxidize the mono-charged arm of $\mathbf{39}^{+\cdot/2+}$ to form $\mathbf{39}^{2+/2+}$. Since the double-charged arm is an even stronger electron-withdrawing group, this oxidation process takes place at a higher potential than for the unstacked mono-charged oligomer $\mathbf{41}^{+\cdot}$ to form $\mathbf{41}^{2+}$, Figure 7.15.

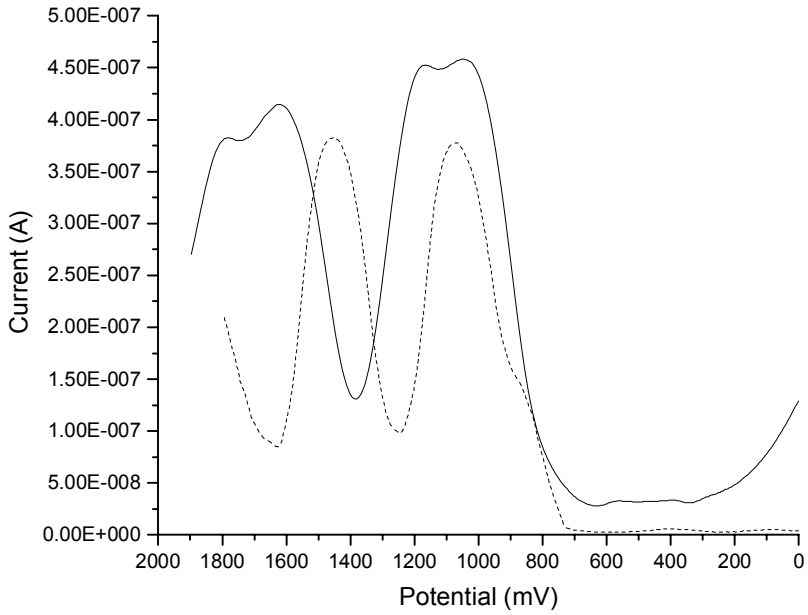

Figure 7.14. Differential pulse voltammograms of **41** (---) and **39** (—), 3 mM in CH_2Cl_2 containing 0.1 M Bu_4NPF_6, v = 100 mV/s on a gold electrode, pulse amplitude = 25 mV, pulse width = 50 ms, pulse period = 200 ms, Ag/AgCl reference electrode.

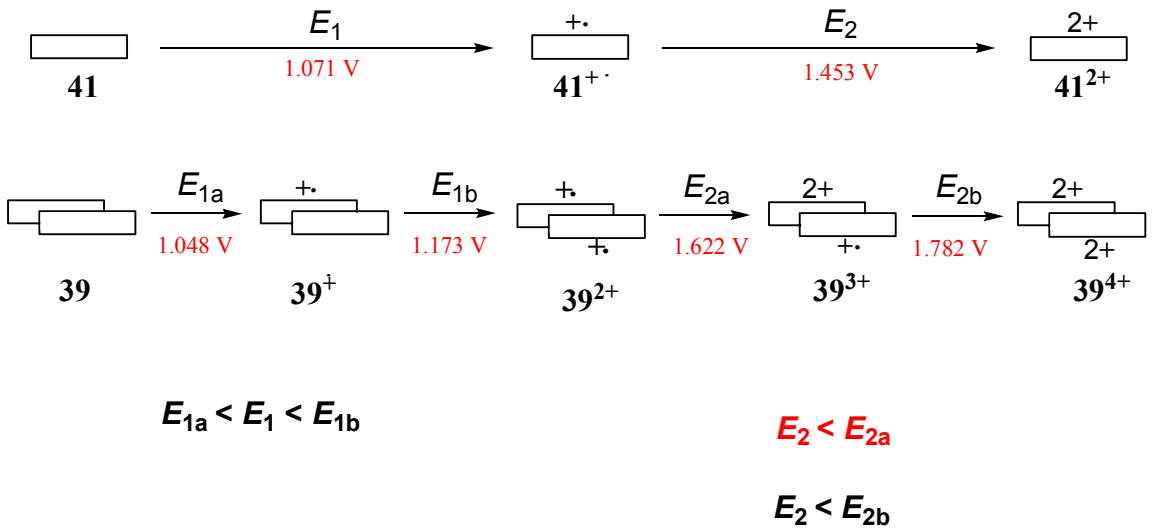

Figure 7.15. Electrochemical oxidation process of compound **41** and **39** with Bu_4NPF_6 electrolyte.

Electrochemistry with the bulky anion electrolyte $Bu_4NB(C_6F_5)_4$

Compared with the small anions such as PF_6^- and BF_4^-, the bulky anion $[B(C_6F_5)_4]^-$ has ion-pairs only weakly with highly charged cations.[39, 40] This improves the solubility of highly charged cations, and allows the charges to delocalize more freely over the organic conjugated molecule.

Using $Bu_4NB(C_6F_5)_4$ as the electrolyte, the CV of compounds **41** and **39** show the influence of weak ion-pairing on the redox behavior of the oligothienyl-substituted paracyclophanes. Both of the CV (Figure 7.16.) and DPV (Figure 7.17.) of the unstacked model **41** show two reversible redox waves, E_1 = + 1.18 V and E_2 = + 1.66 V, Compared to the use of a small, tight-binding anion, both oxidation potentials are increased. The increases difference between the oxidation potential with PF_6^- and $[B(C_6F_5)_4]^-$ are 104 mV for the first oxidation and 202 mV for the second oxidation.

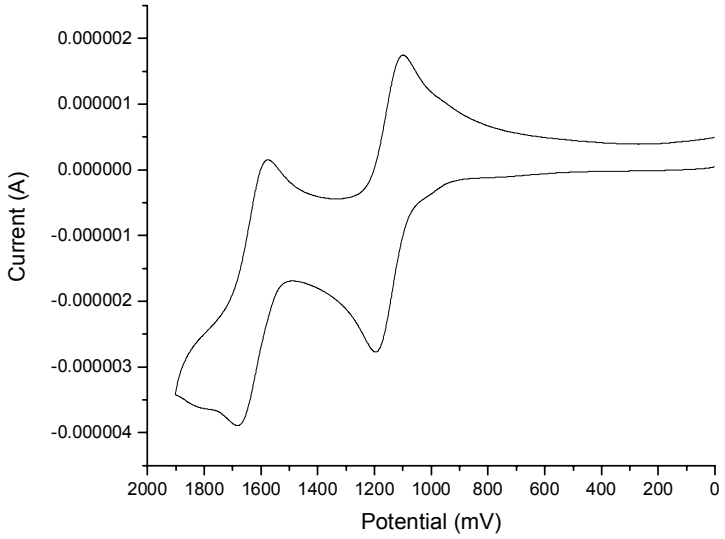

Figure 7.16. Cyclic voltammograms of **41**, 3 mM in CH_2Cl_2 containing 0.1 M $Bu_4NB(C_6F_5)_4$, v = 100 mV/s on a gold electrode, Ag/AgCl reference electrode.

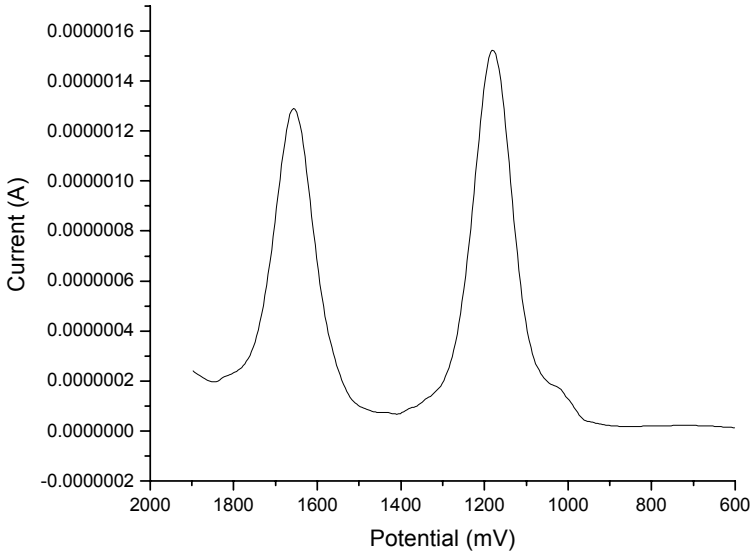

Figure 7.17. Differential pulse voltammogram of **41**, 3 mM in CH_2Cl_2 containing 0.1 M $Bu_4NB(C_6F_5)_4$, v = 100 mV/s on a gold electrode, pulse amplitude = 25 mV, pulse width = 50 ms, pulse period = 200 ms, Ag/AgCl reference electrode.

As with PF_6^-, the CV (Figure 7.18.) and DPV (Figure 7.19.) of **39** show four one-electron oxidation waves at E_{1a} = + 1.11 V, E_{1b} = + 1.18 V, E_{2a} = + 1.61 V, E_{2b} = + 1.78 V. Splitting between the first and second oxidations (70 mV), and between the third and fourth oxidations (177 mV) are larger than noted with PF_6^-. The bulky anion leads to a better separation of those two groups of peaks.

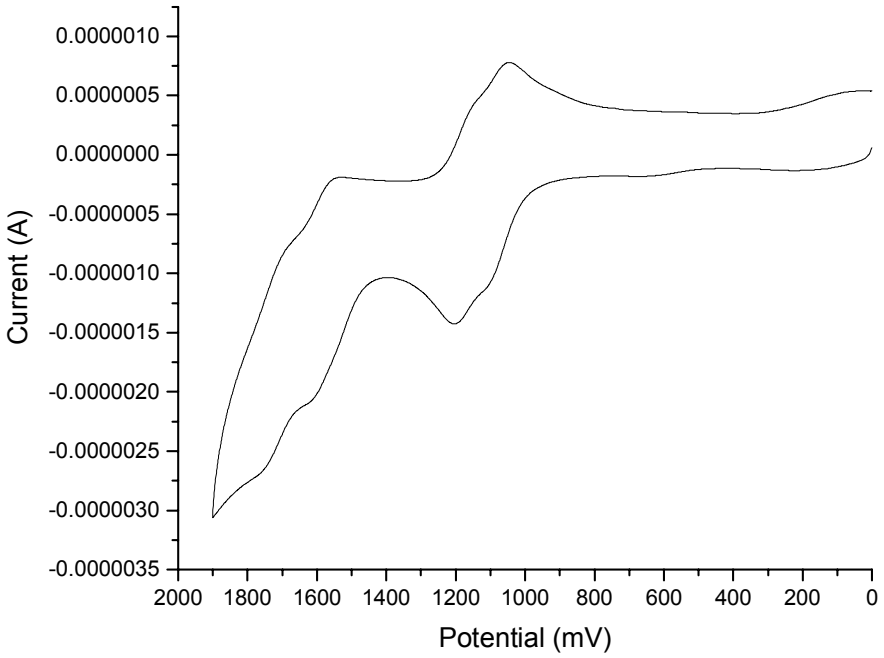

Figure 7.18. Cyclic voltammograms of **39**, 3 mM in CH_2Cl_2 containing 0.1 M $Bu_4NB(C_6F_5)_4$, v = 100 mV/s on a gold electrode, Ag/AgCl reference electrode.

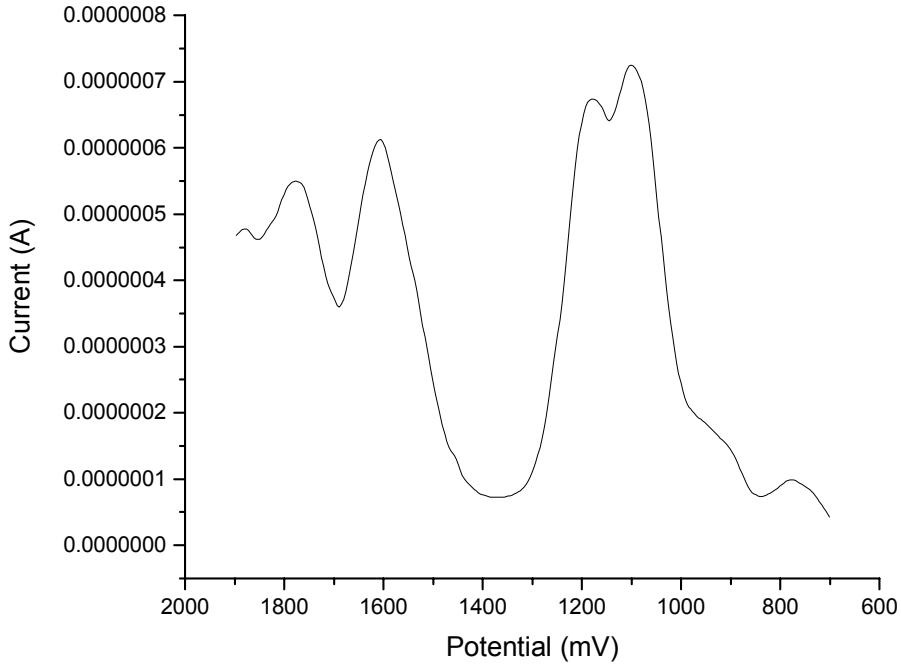

Figure 7.19. Differential pulse voltammogram of **39**, 3 mM in CH_2Cl_2 containing 0.1 M $Bu_4NB(C_6F_5)_4$, v = 100 mV/s on a gold electrode, pulse amplitude = 25 mV, pulse width = 50 ms, pulse period = 200 ms, Ag/AgCl reference electrode.

The same electronic effect as we ascribe in the small-anion electrolyte experiments can be used to explain $E_{1a} < E_1 < E_{1b}$ and $E_{2b} > E_2$, by the electron-donating effect of the stacked neutral oligomer and the electron-withdrawing effect of the stacked charged oligomer, Figure 7.20.

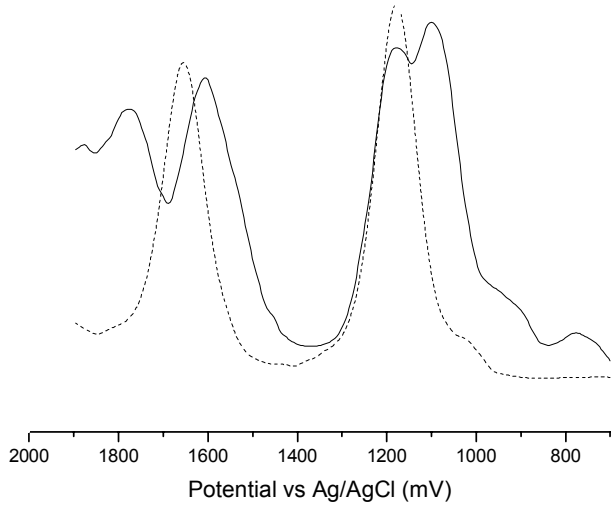

Figure 7.20. Differential pulse voltammograms of **39** (—) and **41** (---): 3 mM in CH_2Cl_2 containing 0.1 M $Bu_4NB(C_6F_5)_4$, v = 100 mV/s, pulse amplitude = 25 mV, width = 50 ms, period = 200 ms. Gold working electrode, Ag/AgCl reference electrode.

However, instead of the observed $E_{2a} > E_2$ in the small-anion experiments, the bulky-anion experiments gave the reverse $E_{2a} < E_2$, Table 7.2.

Table 7.2. Oxidation potentials of compound **41** and **39**.

Electrolyte		Bu_4NPF_6		$Bu_4NB(C_6F_5)_4$	
Compound		41	39	41	39
E_1 (V)	E_{1a}(V)	+1.07	+1.05	+1.18	+1.11
	E_{1b}(V)		+1.17		+1.18
E_2 (V)	E_{2a}(V)	+1.45	+1.62	+1.66	+1.61
	E_{2b}(V)		+1.78		+1.78

We propose the following explanation for this observation. The product of these oxidations is the triple charged species $\mathbf{39}^{+\cdot/2+}$. On the other hand, the starting material, the double charged species, has two possible electronic structures, $\mathbf{39}^{+\cdot/+\cdot}$ and $\mathbf{39}^{2+/0}$. If the third oxidation is to oxidize $\mathbf{39}^{2+/0}$, instead of $\mathbf{39}^{+\cdot/+\cdot}$, this process actually is oxidizing the neutral oligomer with a very strong electron-withdrawing group (i.e., a stacked dication), instead of oxidizing the mono-charged oligomer with a weaker electron-withdrawing group (i.e., a stacked radical cation). The neutral species, of course, has a lower oxidation potential than the cationic species. Even with a stacked dication, the stacked neutral oligomer is easier to oxidize compared with the oxidation of the mono-charged species $\mathbf{41}^{+\bullet}$ to give $\mathbf{41}^{2+}$, so $E_{2a} < E_2$, Figure 7.21.

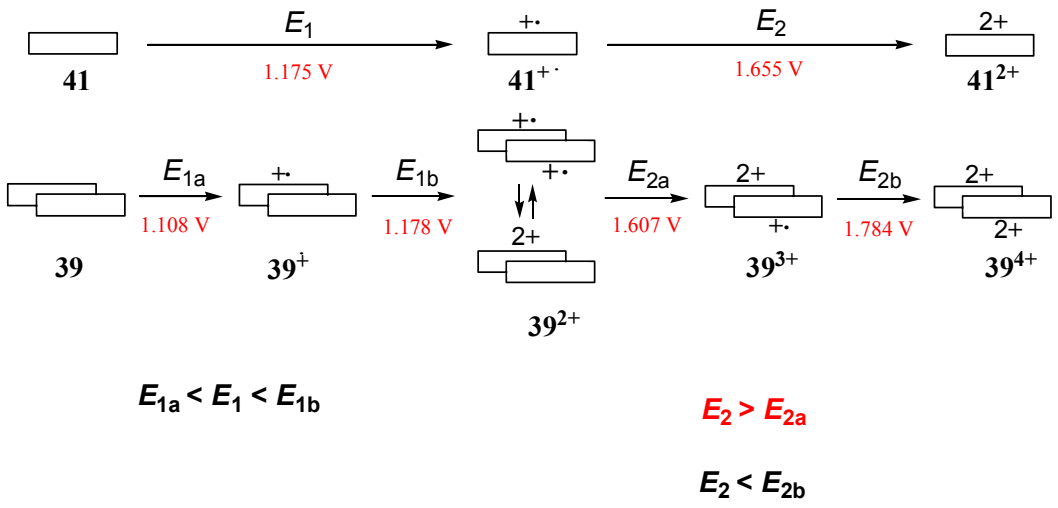

Figure 7.21. Electrochemical oxidation process of compound 41 and 39 with $Bu_4NB(C_6F_5)_4$ electrolyte.

The origin of $\mathbf{39}^{2+/0}$

How is $\mathbf{39}^{2+/0}$ formed? Is it the product from oxidation of the radical cationic stacked oligomer $\mathbf{39}^{+\cdot/0}$, or is it formed by oxidation of the neutral stacked oligomer of to give $\mathbf{39}^{+\cdot/+\cdot}$, followed by a disproportion reaction? Careful comparision of the relationship of E_1, E_2 and E_{1b} suggests $\mathbf{39}^{2+/0}$ is converted from $\mathbf{39}^{+\cdot/+\cdot}$, Table 7.2.

The second oxidation of **39** (E_{1b}) must correspond to oxidation of $\mathbf{39}^{+\cdot/0}$ to $\mathbf{39}^{+\cdot/+\cdot}$, the oxidation of a neutral oligmer (stacked with a radical cation), and the oxidation potential is comparable to that of the first oxidation of **41** (E_1). If the second oxidation of **39** (E_{1b}) was from $\mathbf{39}^{+\cdot/0}$ to $\mathbf{39}^{2+/0}$, oxidation of a radical cationic oligomer to form the dicationic oligomer, E_{1b} should be comparable to the second oxidation of **41** (E_2). The experimental data show, with both small and bulky anions, E_{1b} is comparable to E_1, and much smaller than E_2. This suggests that $\mathbf{39}^{+\cdot/+\cdot}$ is formed by oxidation and that $\mathbf{39}^{2+/0}$ is formed from interoligomer electron transfer within $\mathbf{39}^{+\cdot/+\cdot}$, Figure 7.22.

This results the question: why is this result observed for the bulky-anion experiments?

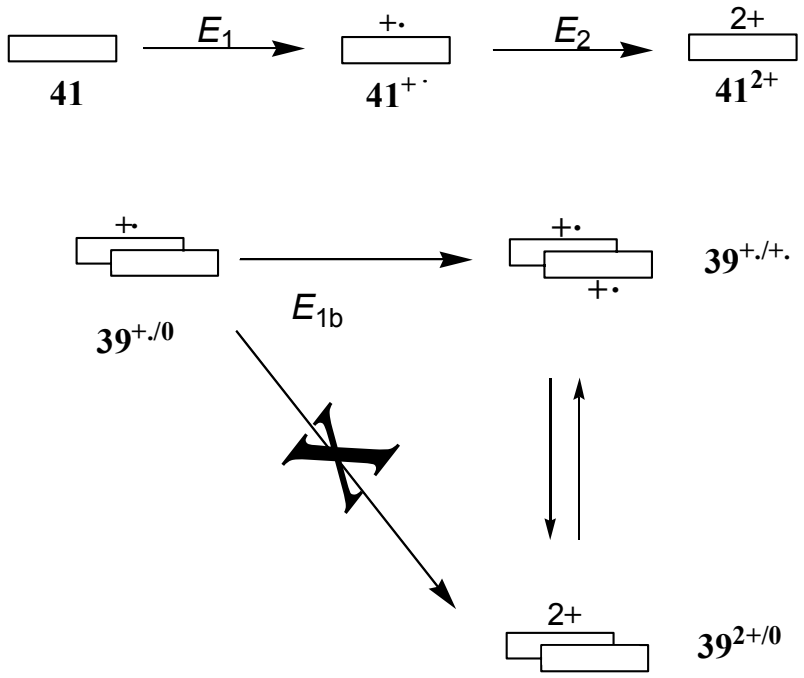

Figure 7.22. The origin of $\mathbf{39^{2+/0}}$

Why is $\mathbf{39^{2+/0}}$ formed in the presence of bulky anions?

The "bipolaron-neutral" state $\mathbf{39^{2+/0}}$ and the "polaron-polaron" state $\mathbf{39^{+\cdot/+\cdot}}$ are related to one another by an interoligomer disproportionation. The effect of π-stacking through cyclophane allows for electronic communication between two arms. This π-stacking effect leads to the potential for electron transfer and the possibility to delocalize the charge through the whole molecule, instead of just in one arm, and allows two radical cations to combine and form the dication.

This charge transfer process is more predominant in the presence of the bulky, weakly coordinating anion. In the presence of PF_6^-, the small anion forms a tight ion-pair with the radical cation. This "pins" the positive charge on the conjugated oligomer in the

"polaron-polaron" state $\mathbf{39}^{+\bullet/+\bullet}$. For the bulky anion ion-pairing is very loose providing mobility to the positive charges and electron transfer via the cyclophane leads to formation of a dication, which is favored by the combination of two radicals to cancel the spin, Figure 7.23.

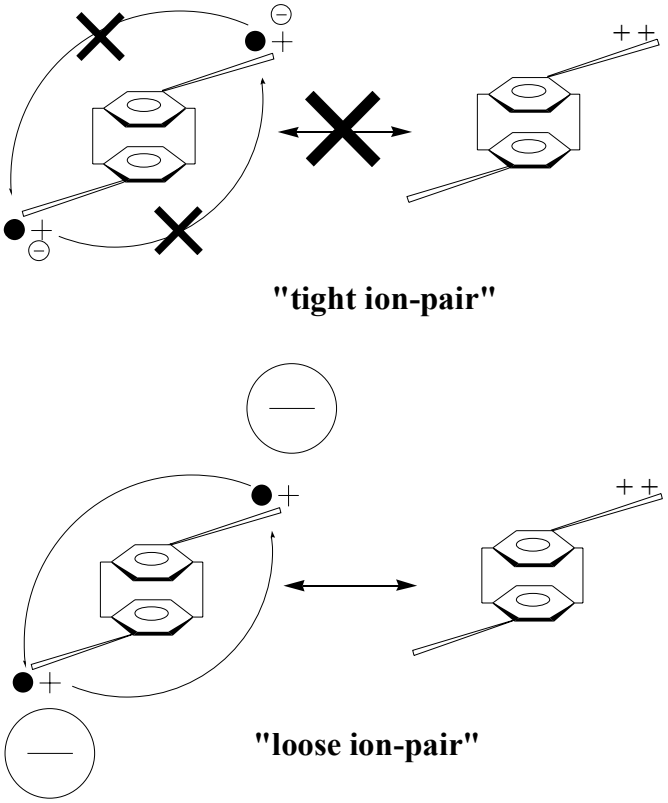

Figure 7.23. The effect of the counter ion sizes on the electron (charge) transfer

This experiment is a good model for the interchain electron transfer of *p*-doped conducting polymers. It mimics the process by which two polarons combine to form a bipolaron. In our system, the stacking arrangement is fixed covalently allowing us to investigate the interchain π-π communication in solution.

Spectroscopic characteristics of the stacked radical cation and dication – electrochemical oxidation

The electrochemistry above is indirect evidence for the existence of $\mathbf{39}^{2+/0}$ and a rationale that $\mathbf{39}^{2+/0}$ is formed by disproportionation of $\mathbf{39}^{+\cdot/+\cdot}$. However, further direct evidence is needed to address the existence of $\mathbf{39}^{2+/0}$ and its possible equilibrium with $\mathbf{39}^{+\cdot/+\cdot}$. Theoretical calculation suggests the radical cation has two subgap electronic transitions and the dication shows only one subgap transition.[8] Thus, in the absorption spectrum, the radical cation should have one absorption in UV-vis region an the other absorption in NIR region; the dication should have only one absorption in UV-vis region, which should be blue-shifted relative to that of the radical cation.[9]

The absorption spectra of the three oxidation states of the unstacked model **41** were determined by spectroelectrochemistry. The neutral form of **41** is colorless (λ_{max} = 308 nm), with no absorption in the range of 400 to 1600 nm. Electrochemical oxidation (bulk electrolysis, +1200 mV) of **41** to the radical cation, $\mathbf{41}^{+\cdot}$, provides a violet solution with one peak in the visible region (λ_{max} = 538 nm) and another peak in the near-IR region (λ_{max} = 913 nm), consistent with other reports of the absorption spectra of oligothienyl radical cations.[41,42] The dication $\mathbf{41}^{2+}$, formed at higher potentials (+1600 mV), gives a pink solution and only shows one absorption in visible region (λ_{max} = 521

nm), blue shifted by 17 nm relative to the radical cation, in accord with Bredas' INDO-SCI calculations on oligothiophenes,[9] Figure 7.24.

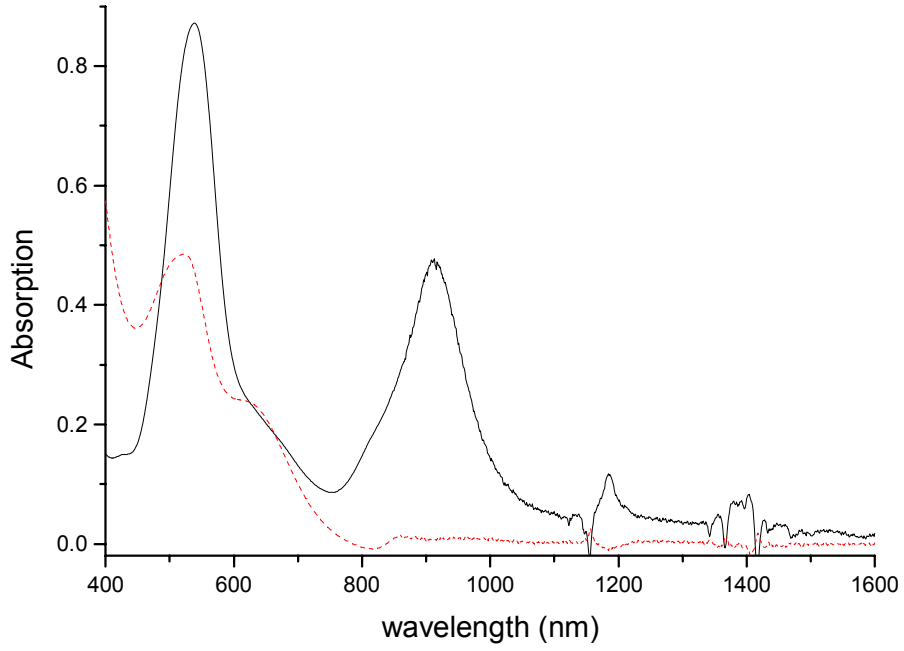

Figure 7.24. UV-vis-NIR spectra of $\mathbf{41}^{+\cdot}$ (—), 1.0 mM with bulk electrolysis at +1200 mV; $\mathbf{41}^{2+}$ (---), 1.0 mM with bulk electrolysis at +1600 mV.

Electrochemical oxidation (bulk electrolysis, +1400 mV) of **39** shows two oxidation states with radical cation characteristics. Upon removing one electron per molecule, $\mathbf{39}^{+\cdot}$ shows characteristic radical cation absorption with two major peaks (λ_{max} = 568 nm, 993 nm). Upon removing the second electron, $\mathbf{39}^{2+}$ shows a red shifted UV-vis

peak (λ_{max} = 597 nm) and a sligtly blue shifted NIR peak (λ_{max} = 984 nm), which is consistent with the shifts of radical cation π-dimers of oligothiphenes in solution relative to the isolated oligomers, Figure 7.25.

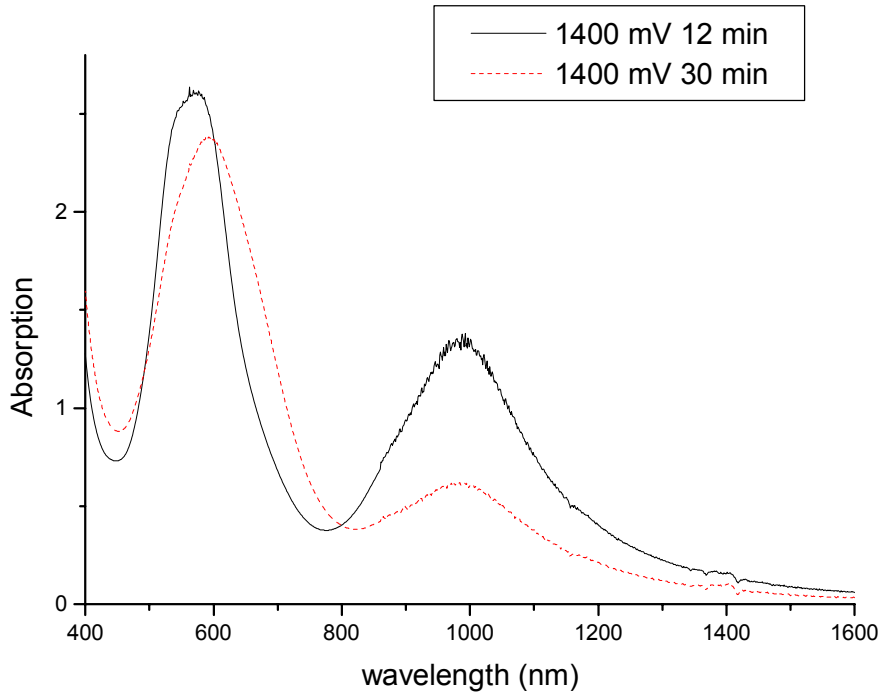

Figure 7.25. UV-vis-NIR spectra of $\mathbf{39}^{+\cdot}$ (—), 3.0 mM with bulk electrolysis at +1400 mV for 12 minutes; $\mathbf{39}^{2+}$ (---), 3.0 mM with bulk electrolysis at +1400 mV for 30 minutes.

Chemical oxidation with $FeCl_3$ in CH_2Cl_2

Further insight into the absorbance spectra of stacked and unstacked analogs **39** and **41** was obtained by titration with a chemical oxidant, iron(III) chloride. The oxidation potential of $FeCl_3$ in CH_2Cl_2 is +1.22 V versus Ag/AgCl,[43] which provides us with access to the radical cations of oligothiophenes (T_n) with the following stoichiometry:

$$T_n + 2\ FeCl_3 \rightarrow T_n^{+\cdot} + FeCl_4^- + FeCl_2$$

Addition of $FeCl_3$ to a solution of unstacked tetraarene **41** in CH_2Cl_2 leads to the formation of a violet solution with absorbance peaks which match those of the radical cation formed by electrochemical oxidation. Upon addition of small amounts of $FeCl_3$ (<10 mol%) to a solution of the stacked analog, **39**, the UV-vis-NIR spectrum shows absorbances with peaks at 556 nm and 994 nm which we ascribe to $\mathbf{39}^{+\cdot}$, a species with a cation radical stacked with a neutral oligomer, Figure 7.26. These peaks are both red shifted slightly from the values of the unstacked radical cation $\mathbf{41}^{+\cdot}$ due to the influence of the cofacially held neutral arene. Similar spectral peaks were observed upon electrochemical oxidation at +1400 mV. With four equivalents of $FeCl_3$, the spectrum consists of a single absorbance in the near-IR region (λ_{max} = 907 nm), and a broad absorption in the visible region that can be fit to two peaks with λ_{max} of 505 and 587 nm, Figure 7.27. Based on the stoichiometry, we assign these new peaks to the two forms of the stacked dication. Since all reported oligothienyl radical cations display a prominent absorbance in the near-IR region and a red shifted peak in the visible region relative to

unstacked radical cationic oligomers, we assign the peaks at 587 and 907 nm to the bis(radical cation) form, $\mathbf{39}^{+\cdot/+\cdot}$, of the stacked dication. Based on the blue-shift of the other peak (λ_{max} = 505 nm) relative to the radical cation forms ($\mathbf{39}^{+\cdot}$ and $\mathbf{39}^{+\cdot/+\cdot}$), and the blue shift of the unstacked model dication $\mathbf{41}^{2+}$ relative to $\mathbf{41}^{+\cdot}$, we assign this new peak to the dication-neutral, $\mathbf{39}^{2+/0}$. Further doping, with addition of up to six equivalents of oxidant, results in no further change in the spectrum since the oxidation potential of $FeCl_3$ is not sufficiently high to further oxidize the stacked arene to the tri- or tetracation, Figure 7.28.

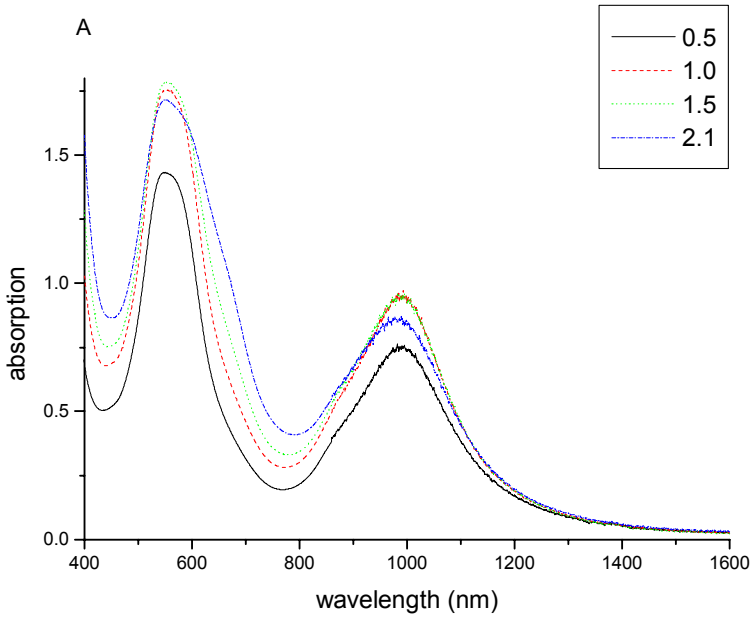

Figure 7.26. UV-vis-NIR spectra of 1 mM **39** in CH_2Cl_2 doped with 0.5, 1.0, 1.5 and 2.1 equivalents of $FeCl_3$.

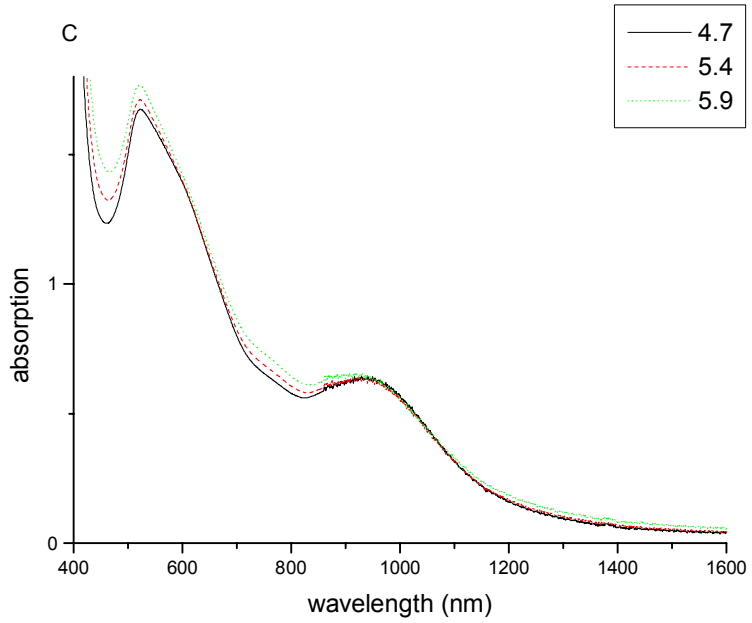

Figure 7.27. UV-vis-NIR spectra of 1 mM **39** in CH_2Cl_2 doped with 4.7, 5.4 and 5.9 equivalents of $FeCl_3$.

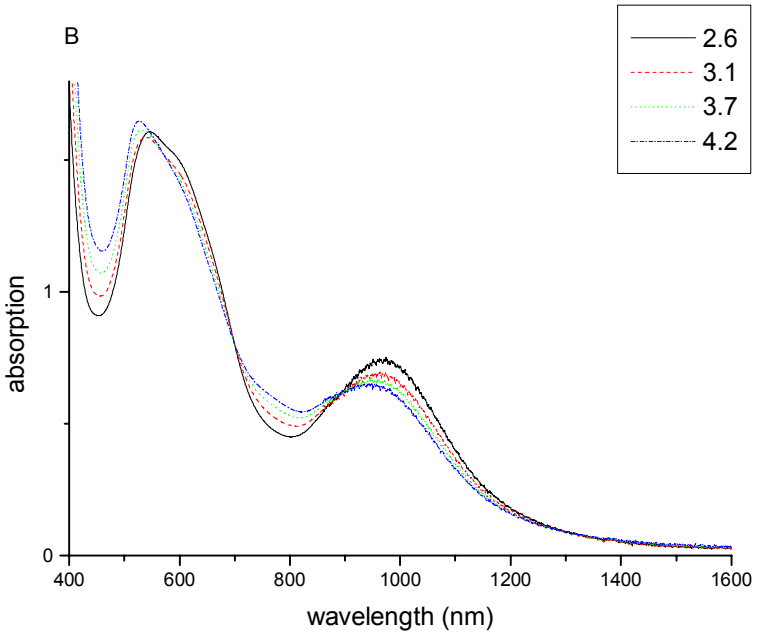

Figure 7.28. UV-vis-NIR spectra of 1 mM **39** in CH_2Cl_2 doped with 2.6, 3.1, 3.7 and 4.2 equivalents of $FeCl_3$.

With less than four equivalents of oxidant, the radical cation-neutral ($\mathbf{39}^{+\cdot}$), and the bis(radical cation) and dication-neutral forms of the stacked dication all coexist, Figure 7.29. One isosbestic point is observed in the near-IR region, indicating the conversion of two types of radical cation which absorb in this region: the radical cation-neutral ($\mathbf{39}^{+\cdot}$) and the bis(radical cation) form, $\mathbf{39}^{+\cdot/+\cdot}$, of the dication. Two isosbestic points are observed in the visible region, consistent with the presence of three species which absorb in this region: the mono(radical cation)-neutral ($\mathbf{39}^{+\cdot}$), and the bis(radical cation) ($\mathbf{39}^{+\cdot/+\cdot}$) and dication-neutral ($\mathbf{39}^{2+/0}$) forms of the dication.

Thus, the UV-vis-NIR spectra indicate the bis(radical cation) ($\mathbf{39}^{+\cdot/+\cdot}$) and dication-neutral ($\mathbf{39}^{2+/0}$) species coexist after removing two electrons from **39**.

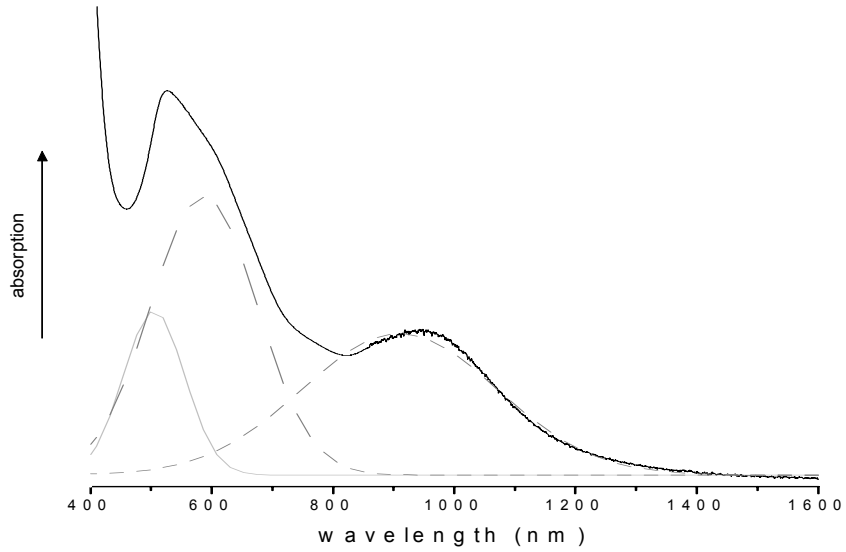

Figure 7.29. UV-vis-NIR spectrum of 1 mM **39** in CH_2Cl_2 doped with 4.2 equivalents of $FeCl_3$ and deconvolution into contributions arising from the bis(radical cation) , $\mathbf{39}^{+\cdot/+\cdot}$, and dication-neutral , $\mathbf{39}^{2+/0}$, forms of the stacked dication.

Chemical oxidation with $NOSbF_6$ in CH_2Cl_2

Another oxidant, $NOSbF_6$, was also used to oxidize the stacked model compound **39**. Compared to $FeCl_3$, the use of $NOSbF_6$ provides a more distinct peak in the visible region of the spectrum because the oxidant itself does not absorb this region. The oxidation potential of $NOSbF_6$ is high enough to remove the third electron from **39**, so the oxidation process is not limited to the formation of the dication.

$NOSbF_6$ has subtle solubility in CH_2Cl_2. Addition of $NOSbF_6$, in the first 30 minutes, results in a decrease in the intensity of the absorption peak for the neutral **39** (λ_{max} = 322 nm). At the same time, the two absorptions of $\mathbf{39}^{+\cdot}$ (λ_{max} = 562 nm, 997 nm) become prominent with more oxidant getting into the solution, Figure 7.30. This is consistent with the conversion of **39** to form $\mathbf{39}^{+\cdot}$ with one equivalent of $NOSbF_6$.

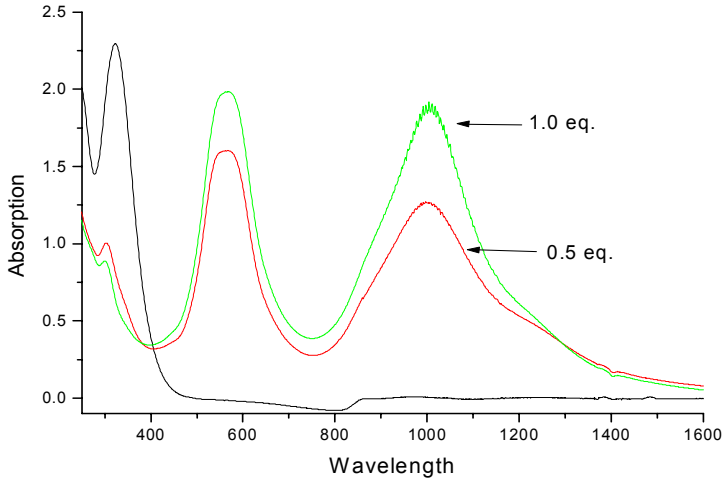

Figure 7.30. UV-vis-NIR spectraof 1 mM **39** in CH_2Cl_2 neutral and doped with $NOSbF_6$ within 30 minutes.

Between 30 to 120 minutes, similar with the results from $FeCl_3$ experiment, two isosbestic points in the UV-vis region and one isosbestic point in the NIR region are observed. One isosbestic point in the NIR region (895 nm) indicates two radical species in equilibrium with each other, $\mathbf{39}^{+\cdot}$ and $\mathbf{39}^{+\cdot/+\cdot}$. Two isosbestic points in the UV-vis region (531 nm, 628 nm) suggest three species which absorb in this region coexist, $\mathbf{39}^{2+/0}$, $\mathbf{39}^{+\cdot}$ and $\mathbf{39}^{+\cdot/+\cdot}$, Figure 7.31. This result confirms the coexistence of $\mathbf{39}^{2+/0}$ and $\mathbf{39}^{+\cdot/+\cdot}$. However, more than 2.0 equivalents of $NOSbF_6$ can remove the third electron to form the triple-charged species, Figure 7.32.

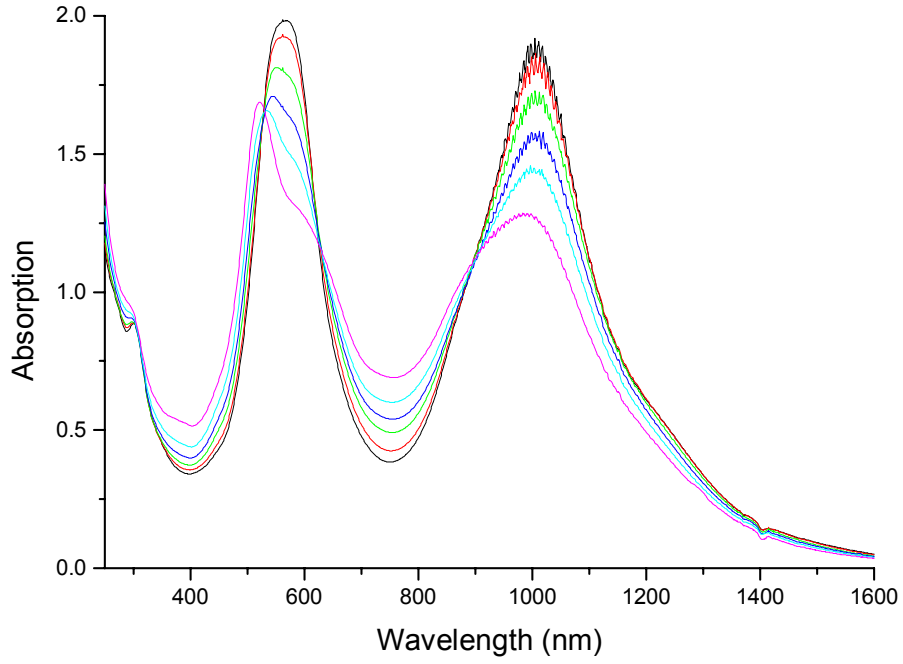

Figure 7.31. UV-vis-NIR spectraof 1 mM **39** in CH_2Cl_2 doped with $NOSbF_6$ from 30 minutes to 120 minutes.

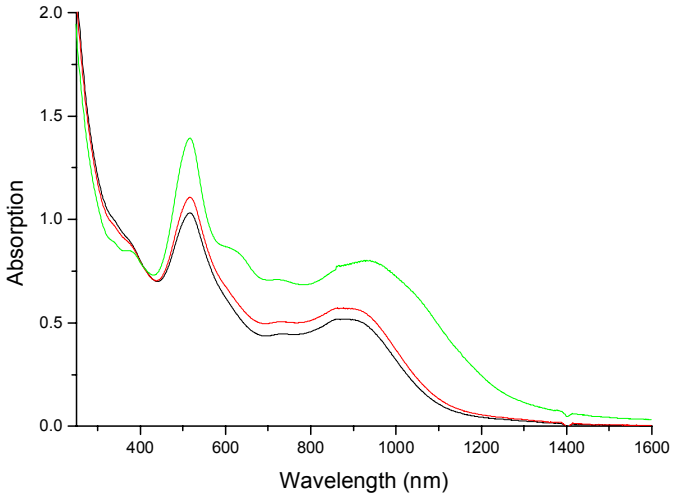

Figure 7.32. UV-vis-NIR spectroscopy of 1 mM **39** in CH_2Cl_2 doped with $NOSbF_6$ over 135 minutes.

Equilibrium of $\mathbf{39}^{2+/0}$ and $\mathbf{39}^{+\cdot/+\cdot}$ (temperature control)

The temperature-dependence of the spectra of the stacked dication indicates that the bis(radical cation) and dication-neutral forms are in equilibrium. After cooling a solution of the stacked dication in CH_2Cl_2 (generated by addition of 4 equivalents of $FeCl_3$) to -70°C, the solution was warmed gradually and UV-vis-NIR spectra were collected. Since the salt (39^{2+} with $FeCl_4^-$) precipitates out at low temperature, the concentration of the solution increases upon warming. Thus, all the spectra were normalized with the absorption of $\mathbf{39}^{2+/0}$ (505 nm). At lower temperatures, the absorption of $\mathbf{39}^{+\cdot/+\cdot}$ in the UV-vis region (587 nm) is prominent. Upon warming the intensity of this peak decreases; accordingly, the absorption of $\mathbf{39}^{+\cdot/+\cdot}$ in the NIR region (907 nm) are decreasing consistently, Figure 7.33. This observation is corresponding to a shift in the

equilibrium between the dication-neutral form $\mathbf{39}^{2+/0}$ and the bis(radical cation) form. $\mathbf{39}^{+\cdot/+\cdot}$, which $\mathbf{39}^{+\cdot/+\cdot}$ is favored at lower temperatures.

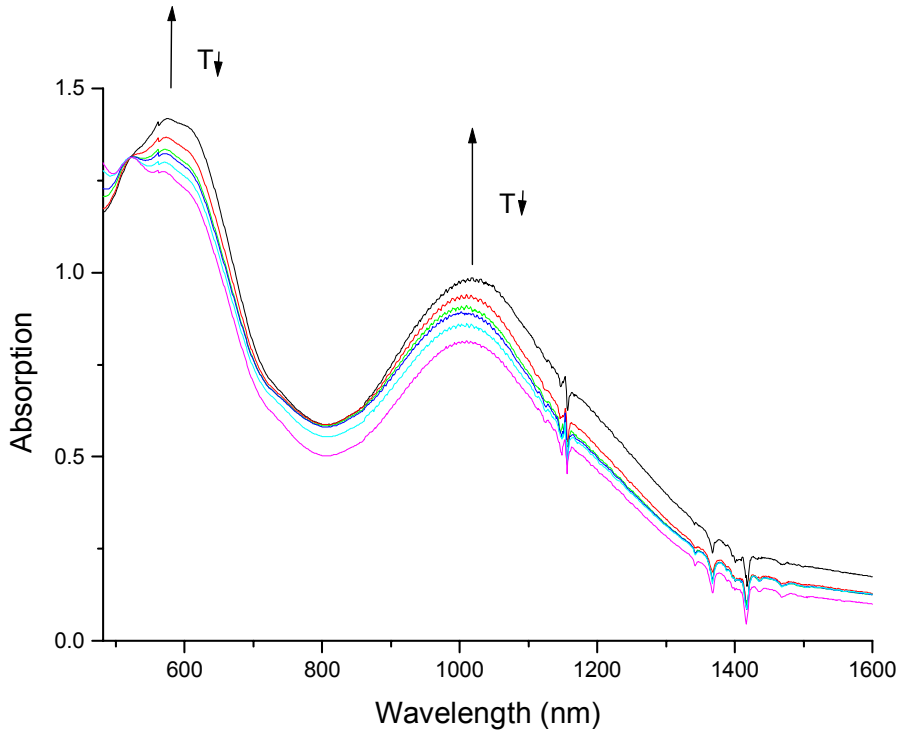

Figure 7.33. UV-vis-NIR spectra of 1 mM **39** in CH_2Cl_2 doped with 4.0 equivalents of $FeCl_3$ under various temperatures, every 10°C from –70 °C to –10 °C.

Equilibrium of $\mathbf{39}^{2+/0}$ and $\mathbf{39}^{+\cdot/+\cdot}$ (solvent control)

The solvent-dependence of the spectra of the stacked dication also indicates that the bis(radical cation) and dication-neutral forms are in equilibrium. Anhydrous CH_3CN

was added in a solution of the stacked dication in CH_2Cl_2 (generated by addition of 4 equivalents of $FeCl_3$) and the UV-vis-NIR spectra were collected. With more CH_3CN, the NIR peak continuously decreases, Figure 7.34. This result corresponds to a shift in the equilibrium from the radical species $\mathbf{39}^{+\cdot/+\cdot}$ to the non-radical species $\mathbf{39}^{2+/0}$. A polar solvent, such as CH_3CN, favors the multiple-charged species $\mathbf{39}^{2+/0}$.

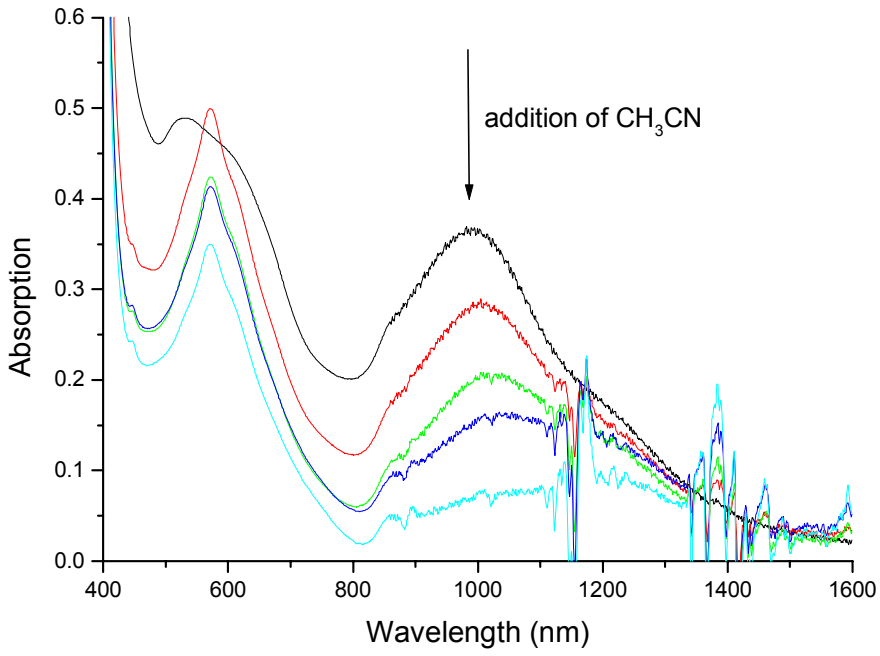

Figure 7.34. UV-vis-NIR spectra of 1 mM **39** in CH_2Cl_2 doped with 4.0 equivalents of $FeCl_3$ upon addition of CH_3CN, 0 to 17%.

Chemical oxidation with $FeCl_3$ in CH_3CN

Since the polarity of the solvent can shift the equilibrium of the two doublly-charged species, we also explored the oxidation in CH_3CN. This gives rise to a set of completely different UV-vis-NIR spectra, Figure 7.35. Increasing the amount of oxidant from 0.5 to 4.0 equivalents results in a decrease in the intensity of NIR peak. With 4.0 equivalents of oxidant, the NIR peak almost disappears, which indicates the disappearance of radical cation species. Why and how the oxidation process is different in CH_2Cl_2 and CH_3CN is still under investigation. One possible reason is the oxidation potential of the model compound or the oxidation potential of oxidant is changed in CH_3CN. Or it is due to the favorable formation of $\mathbf{39}^{2+/0}$ in polar solvent.

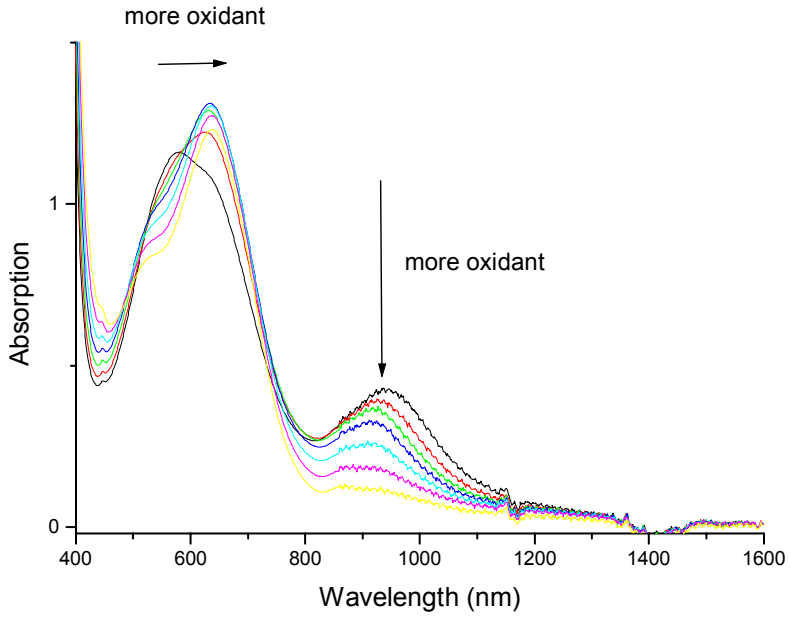

Figure 7.35. UV-vis-NIR spectra of 1 mM **39** in CH_3CN doped with 0.5, 1.0, 1.5, 2.0, 2.5, 3.0, 3.5 and 4.0 equivalents of $FeCl_3$.

Charge transfer between oligomers: **41** versus **39**

The equilibrium between the two forms of the stacked dication, in which the two subunits cannot diffuse apart, is an intramolecular analog of the disproportionation of radical cations observed previously for substituted bithiophenes in polar solvents,[44] Figure 7.36. We also observe the solvent-dependent intermolecular disproportionation of the unstacked model **41**. Whereas electrochemical oxidation of **41** in CH_2Cl_2 at +1200 mV provides a solution for which the UV-vis-NIR spectrum is consistent with the formation of radical cation. Electrochemical oxidation of **41** in a 1:1 mixture of CH_2Cl_2 and CH_3CN at +1200 mV leads to the same radical cation absorption spectra, with an additional shoulder (621 nm). We ascribe this shoulder is due to the absorption of the π-dimer of the radical cations, consistent with the shift of the absorption of many conjugated oligomers.

Interestingly, electrochemical oxidation of **41** in CH_3CN at + 1200 mV gives the same absorption spectrum as from electrochemical oxidation of **41** in CH_2Cl_2 at + 1600 mV, a potential high enough to remove two electrons. This spectrum has only one absorption (511 nm) in the UV-vis region and no NIR absorption. This indicates the formation of the dication $\mathbf{41}^{2+}$, Figure 7.36. However, + 1200 mV in CH_3CN is not a high enough potential to remove the second electron directly. We ascribe this to the formation of the dication $\mathbf{41}^{2+}$ by disproportionation of two $\mathbf{41}^{+\cdot}$, Figure 7.36. Radical cations $\mathbf{41}^{+\cdot}$ are generated at + 1200 mV, and the polar solvent, CH_3CN favors the formation of the π-dimer of the radical cations $\mathbf{(41}^{+\cdot}\mathbf{)_2}$, which undergoes an intermolecular disproportionation to form a dication $\mathbf{41}^{2+}$ and a neutral **41** species. This is the intermolecular analogue of the conversion between $\mathbf{39}^{2+/0}$ and $\mathbf{39}^{+\cdot/+\cdot}$, Figure 7.37.

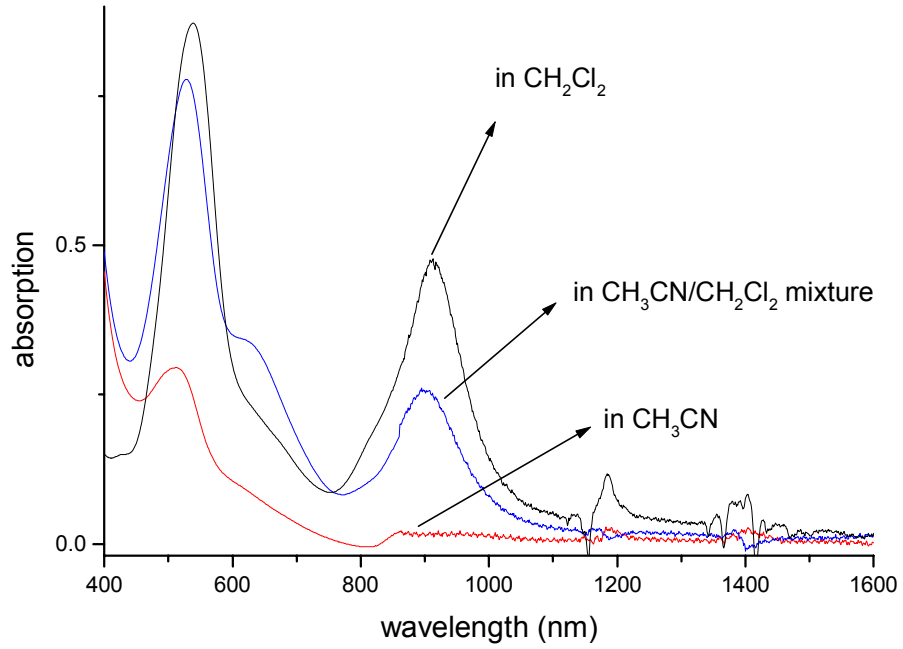

Figure 7.36. UV-vis-NIR spectra of 1.0 mM **41** with bulk electrolysis at +1200 mV, in CH_2Cl_2, in 1:1 CH_2Cl_2/CH_3CN and in CH_3CN.

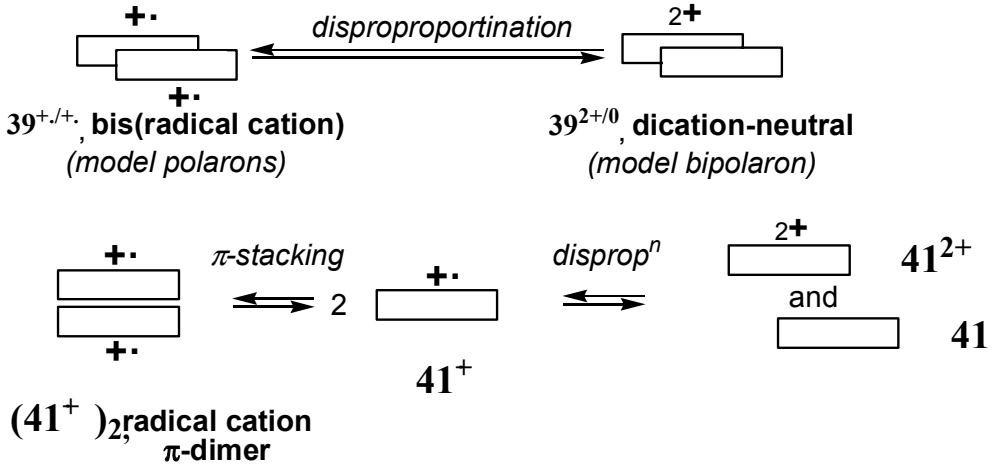

Figure 7.37. Comparison of models for polarons and bipolarons: **39**, covalently stacked oligomers; **41**, linear oligomers.

ESR study of the oxidation process of **39**

Electron spin resonance spectra of a solution prepared by titration of **39** in CH_2Cl_2 with $FeCl_3$ indicate the emergence of a paramagnetic species (g = 2.0023) with up to two equivalents of oxidant, i.e., with formation of the radical cation $\mathbf{39}^{+\cdot}$. The signal decreases in intensity upon addition of up to four equivalents, i.e., formation of the dication, $\mathbf{39}^{2+}$, which might exist as either the bis(radical cation) $\mathbf{39}^{+\cdot/+\cdot}$ (i.e., model of polaron dimer) or dication-neutral $\mathbf{39}^{2+/0}$ (i.e., model of bipolaron), Figure 7.38. With even more oxidant, a very weak spin signal still exists.

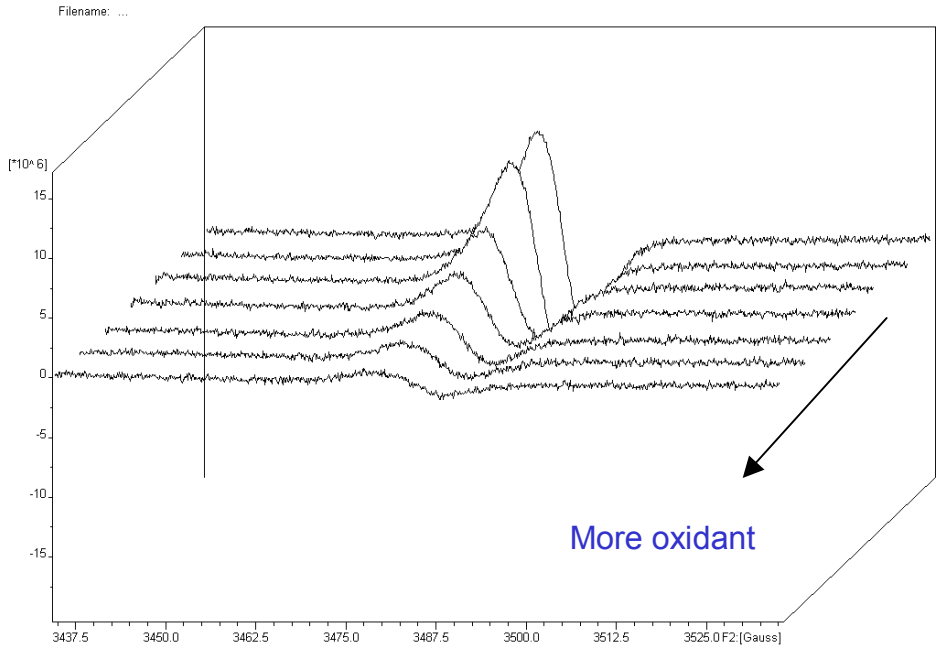

Figure 7.38. ESR upon titration of **39** in CH_2Cl_2 with 2.0 to 4.0 equivalent $FeCl_3$

The studies on oxidized conjugated polymers show the absence of or a very weak ESR signal. The ESR studies of the stacked model compound **39** suggest the coexistence of both polaron dimer and bipolaron leads no ESR signal or a very weak ESR signal, which is consistent with the observation for polymer films.

Nature of charge carriers and a model of inter-chain charge transfer mechanism

For a long time, the nature of the charge carrier in doped conjugated polymers was regarded either as polaron or bipolaron. In the 1990s, Miller and others suggested that a polaron dimer could be another alternative. In this project, the studies of the electrochemistry, UV-vis-NIR spectra and ESR of the stacked model compound **39** suggest the bis(radical cation) $\mathbf{39}^{+\cdot/+\cdot}$ and the dication-neutral $\mathbf{39}^{2+/0}$ coexist and are in equilibrium with each other. Thus the nature of the charge carrier in doped conjugated polymers could rely on the interconversion of those species.

In textbooks, the hopping of the charge carriers is used to explain the interchain charge transfer in doped conjugated polymers. How and why the charge carriers can be hopping from one polymer chain to another is not very clear. In this project, it is observed that the charge carriers can disproportionate between two stacked oligomers with the equilibrium of the bis(radical cation) $\mathbf{39}^{+\cdot/+\cdot}$ and the dication-neutral $\mathbf{39}^{2+/0}$. Thus we propose a new interchain charge transfer in doped conjugated polymers, which is the interchain disproportionation of polaron dimers and bipolarons, Figure 7.39.

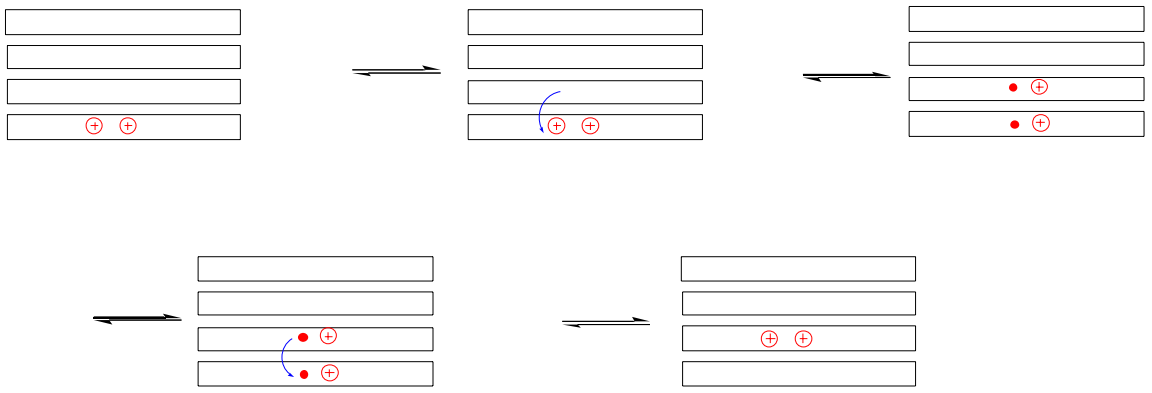

Figure 7.39. A model of inter-chain charge transfer mechanism in doped conducting polymers

Conclusion

In conclusion, the bis(radical cation) form of the stacked dication, $\mathbf{39}^{+\bullet/+\bullet}$, serves as a covalently-linked analog of radical cation π-dimers which have been proposed by Miller as possible charge carriers in p-doped conjugated polymers. The spinless stacked dication-neutral form, $\mathbf{39}^{2+/0}$ is a model for bipolarons in conjugated polymers. The coexistence of these two forms further suggests that both may serve as charge carriers. Interconversion between these forms by disproportionation mimics a possible mechanism for charge migration in doped conjugated polymers.

References

1. Furukawa, Y. *J. Phys. Chem.* **1996**, *100*, 15644.

2. Tol, A. J. W. *Chem. Phy*. **1996**, *208*, 73.

3. Nowak, M. J.; Rughooputh, S. D. D. V.; Hotta, S.; Heeger, A. J. *Macromolecules*, **1987**, *20*, 965.

4. Colaneri, N.; Nowak, M.; Spiegel, D.; Hotta, S.; Heeger, A. J. *Phys. Rev. B*, **1987**, *36*, 7964.

5. Fichou, D.; Xu, B.; Horowitz, G.; Garnier, F. *Synth. Metals* **1991**, *41-43*, 463.

6. Fichou, D.; Horowitz, G.; Garnier, F. *Synth. Metals* **1990**, *39*, 125.

7. Fichou, D.; Horowitz, G.; Xu, B.; Garnier, F. *Synth. Metals* **1990**, *39*, 243.

8 . Cornil, J.; Brédas, J. L. *Adv. Mater*. **1995**, *7*, 295.

9. Cornil, J.; Beljonne, D.; Brédas, J. L. *J. Chem. Phys.* **1995**, *103*, 842.

10. Su, W. P.; Schrieffer, J. R.; Heeger, A. J. *Phys. Rev. Lett*. **1979**, *42*, 1698.

11. Fesser, K.; Bishop, A. R.; Campbell, D. K. *Phys. Rev. B* **1983**, *27*, 4804.

12. Brédas, A. J.; Street, G. B. *Acc. Chem. Res*. **1985**, *18*, 309.

13. Patil, O. A.; Heeger, A. J.; Wudl, F. *Chem. Rev*. **1988**, *88*, 183.

14. Hill, M. G.; Mann, K. R.; Miller, L. L.; Peneau, J. F. *J. Am. Chem. Soc.* **1992**, *114*, 2728.

15. Yu, Y.; Gunic, E.; Zinger, B.; Miller, L. L. *J. Am. Chem. Soc.* **1996**, *118*, 1013.

16. Baüerle, P.; Segelbacher, U.; Maier, A.; Mehring, M. *J. Am. Chem. Soc.* **1993**, *115*, 10217.

17. Baüerle, P.; Segelbacher, U.; Gaudl, K. U.; Huttenlocher, D.; Mehring, M. *Angew. Chem., Int. Ed*. **1993**, *32*, 76.

18. Zotti, G.; Schiavon, G.; Berlin, A.; Pagani, G. *Chem. Mater.* **1993**, *5*, 430.

19. Hapiot, P.; Audebert, P.; Monnier, K.; Pernaut, J. M.; Garcia, P. *Chem. Mater*. **1994**, *6*, 1549.

20. Apperloo, J. J.; Raimundo, J. M.; Frere, P.; Roncali, J.; Janssen, R. A. J. *Chem. Eur. J.* **2000**, *6*, 1698.

21. van Haare, J. A. E. H.; Groenendaal, L.; Havinga, E. E; Janssen, R. A. J.; Meijer, E. W. *Angew. Chem., Int. Ed.* **1996**, *35*, 638.

22. van Haare, J. A. E. H.; van Boxtel, M.; Jassen, R. A. J. *Chem. Mater*. **1998**, *10*, 1166.

23. Prakka, J. P.; Jeevarajan, J. A.; Jeevarajan, A. S.; Kispert, L. D.; Cava, M. P. *Adv. Mater*. **1996**, *8*, 54.

24. Sakamoto, A.; Furukawa, Y.; Tasumi, M. *J. Phys. Chem. B* **1997**, *101*, 1726.

25. Smie, A.; Heinze, J. *Angew. Chem., Int. Ed*. **1997**, *36*, 363.

26. Tschuncky, P.; Heinze, J.; Smie, A.; Engelmann, G.; Kobmehl, G. *J. Electroanal. Chem.* **1997**, *433*, 223.

27. Merz, A.; Kronberger, J.; Dunsch, L.; Neudeck, A.; Petr, A.; Parkanyi, L. *Angew. Chem., Int. Ed.* **1999**, *38*, 1442.

28. van Haare, J. A. E. H.; Havinga, E. E.; van Dongen, J. L. J.; Janssen, R. A. J.; Cornil, J.; Brédas, J. L. *Chem. Eur. J.* **1998**, *4*, 1509

29. Frere, P.; Allain, M.; Elandaloussi, E. H.; Levillain, E.; Sauvage, F. X.; Riou, A.; Roncali, J. *Chem. Eur. J.* **2002**, *8*, 784

30. Salhi, F.; Lee, B.; Metz, C.; Bottomley, L. A.; Collard, D. M. *Org. Lett*. **2002**, *4*, 3195.

31. Salhi, F.; Collard, D. M. *Adv. Mater*. **2003**, *15*, 81.

32. Guyard, L.; Audebert, P. *Electrochem. Commun.* **2001**, *3*, 164.

33. Guyard, L.; Nguyen Dinh An, M.; Audebert, P. *Adv. Mater.* **2001**, *13*, 133

34. In addition, Bazan has published extensively on the influence of stacking on the photophysics of *neutral* conjugated oligomer-substituted paracyclophanes: Bartholomew, G. P.; Bazan, G. *Acc. Chem. Res.* **2001**, *34*, 30; Bartholomew, G. P.; Bazan, G. *J. Am. Chem. Soc.*. **2002**, *124*, 5183.

35. Cofacial and other close-packed arrangements of neutral and charged arenes are, of course, important to numerous other processes and classes of molecule, e.g., Sun, D.; Rosokham, S. V.; Kochi, J. K. *J. Am. Chem. Soc.* **2004**, *126*, 1388.

36. Hutten, P. F.; Gill, R. E.; Herrenma, J. K.; Hadziioannous, G. *J. Phys. Chem*. **1995**, *99*, 3218.

37. Xu, J.; Ng, S. C.; Chan, H. S. O. *Tetrahedron Lett*. **2001**, *42*, 5327.

38. Reich, H. J.; Cram, D. J. *J. Am. Chem. Soc*. **1969**, *91*, 3527

39. LeSuer, R. J., Geiger, W. E. *Angew. Chem.. Int. Ed.* **2000**, *39*, 248

40. Barriere, F., Camire, N., Geiger, W. E., Mueller-Westerhoff, U. T., Sanders, R. *J. Am Chem. Soc*. **2002**, *124*, 7262

41. Levillain, E.; Roncali, J. *J. Am. Chem. Soc*. **1999**, *121*, 8760.

42. Guay, J.; Kasai, P.; Diaz, A.; Wu, R.; Tour, J. M. *Chem. Mater*. **1992**, *4*, 1097.

43. Guay, J.; Kasai, P.; Diaz, A.; Wu, R.; Tour, J. M. Dao, L. H. *Chem. Mater*. **1992**, *4*, 1097.

44. Frère, P.; Allain, M.; Elandaloussi, E. H.; Levellain, E.; Sauvage, F. X.; Riou, A.; Roncali, J. *Chem. Eur. J.* **2002**, *8*, 784.

Chapter VIII

FUTURE WORK

As a continuation to this work, some novel fluorinated polythiophenes are proposed, which may give a more stable n-type polythiophene materials with high electron mobility. On the other hand, the new stacking system is also proposed, which is easier to synthesis and also possible to give a well-defined 2D conducting structure.

Fluorinated substitution: from single bond to double bond, to cyclic structure

The studies on fluorinated substitution to conjugated polymers, especially polythiophenes, were initiated by the synthesis and polymerization of 3-(semifluoroalkyl)thiophenes.[1] Hong and Collard then reported that semifluoroalkyl side chains allow for control over the supramolecular organization of conjugated polymers.[2,3,4] In this thesis, we describe the preparation of three new fluorinated polythiophenes, poly(3-(perfluoroalkyl)thiophene)s, poly(3-alkyl-*alt*-3-(perfluoroalkyl)thiophene)s and poly(3-(1,1-difluoroalkyl)thiophene)s and their novel electronic and photonic properties. All these polymer structures are based on the saturated fluorinated substituents.

The study of the unsaturated fluorinated substitution of thiophenes is limited to 2-(1,2,2-trifluorovinyl)thiophene.[5] Early studies of the synthesis of 1,2,2-trifluorostyrene

gave low yield,[6,7] or require expensive fluorinated starting materials.[8] Recently a cheap fluorinated starting material CF_3CFH_2 (HFC-134a) has been used to prepare 1,2,2-trifluorostyrene with high selectivity at high yield.[9] Subsequently, the substitution of one of the fluorine atoms on the C2 position of 1,2,2-trifluorostyrene with alkyl chains has been achieved.[10] Based on this literature, a synthesis of 3-(1,2-difluoro-1-alkenyl)-thiophene is proposed, Figure 8.1. CF_3CFH_2 is treated with 2 equivalents of LDA, followed by the transmetallation with $ZnCl_2$ to give the active species, CF_2=CFZnCl, which reacts with 3-iodothiophene to give 3-(1,2,2-trifluorovinyl)thiophene. This can further react with an alkyllithium reagent to give 3-(1,2-difluoro-1-alkenyl)-thiophene. These will serve as monomers for polymerization. The double bond in these monomers may hinder the organometallic polymerization, and the high oxidation potential of monomers may also hinder the oxidative polymerization. To lower the oxidation potential, a synthesis of terthiophenes with 1,2-difluoro-1-alkenyl substitution on the central ring is proposed in Figure 8.2.

1,2,2-Trifluorostyrene undergoes cyclic dimerization to give a selective *cis* subsituted cyclic dimer. Defluorination forms form a double bond between two benzene rings, which gives a conjugated fused ring system.[11] The dimerization of 2-(1,2,2-trifluorovinyl)thiophene is easy to achieve by heating and gives high yield.[12] Based this literature, a synthesis of fused thiophenes with fluorinated cyclic structure is proposed, Figure 8.3. The resulting monomer can be polymerized by either oxidative or organometallic polymerization to give a promising n-type conjugated polymer, which has both an efficient electron-poor and very rigid planar backbone. This might be expected to give ahigh electron mobility.

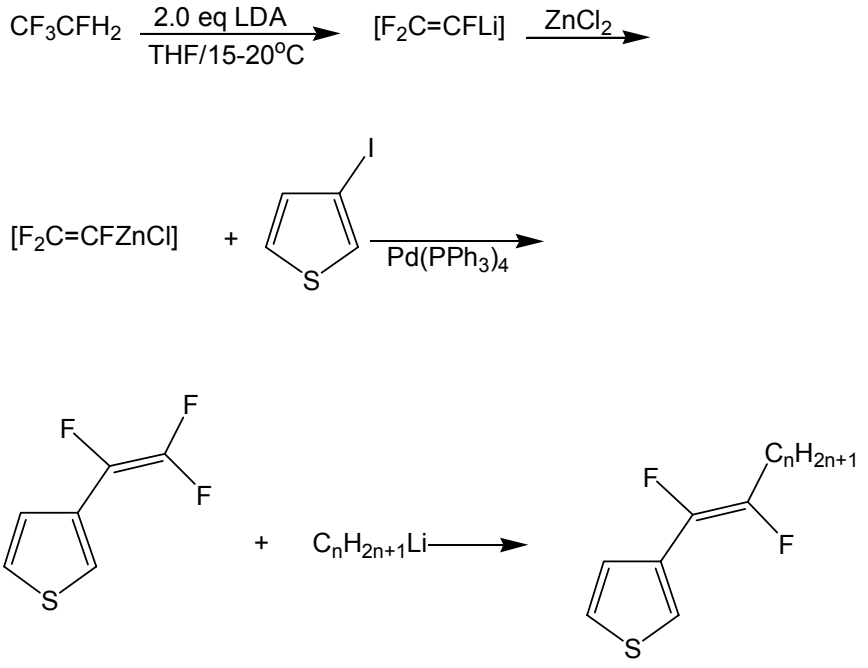

Figure 8.1. Synthesis of thiophene monomers with fluorinated double bond.

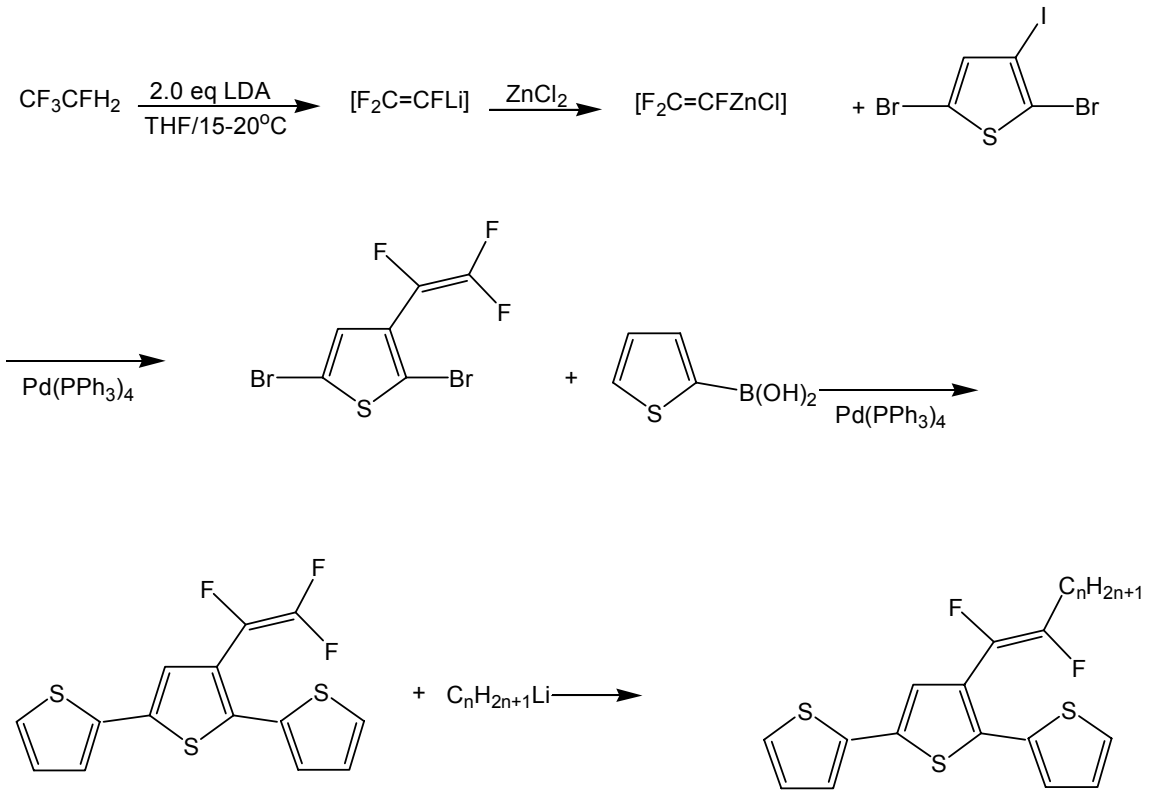

Figure 8.2. Synthesis of terthiophenes with fluorinated double bond.

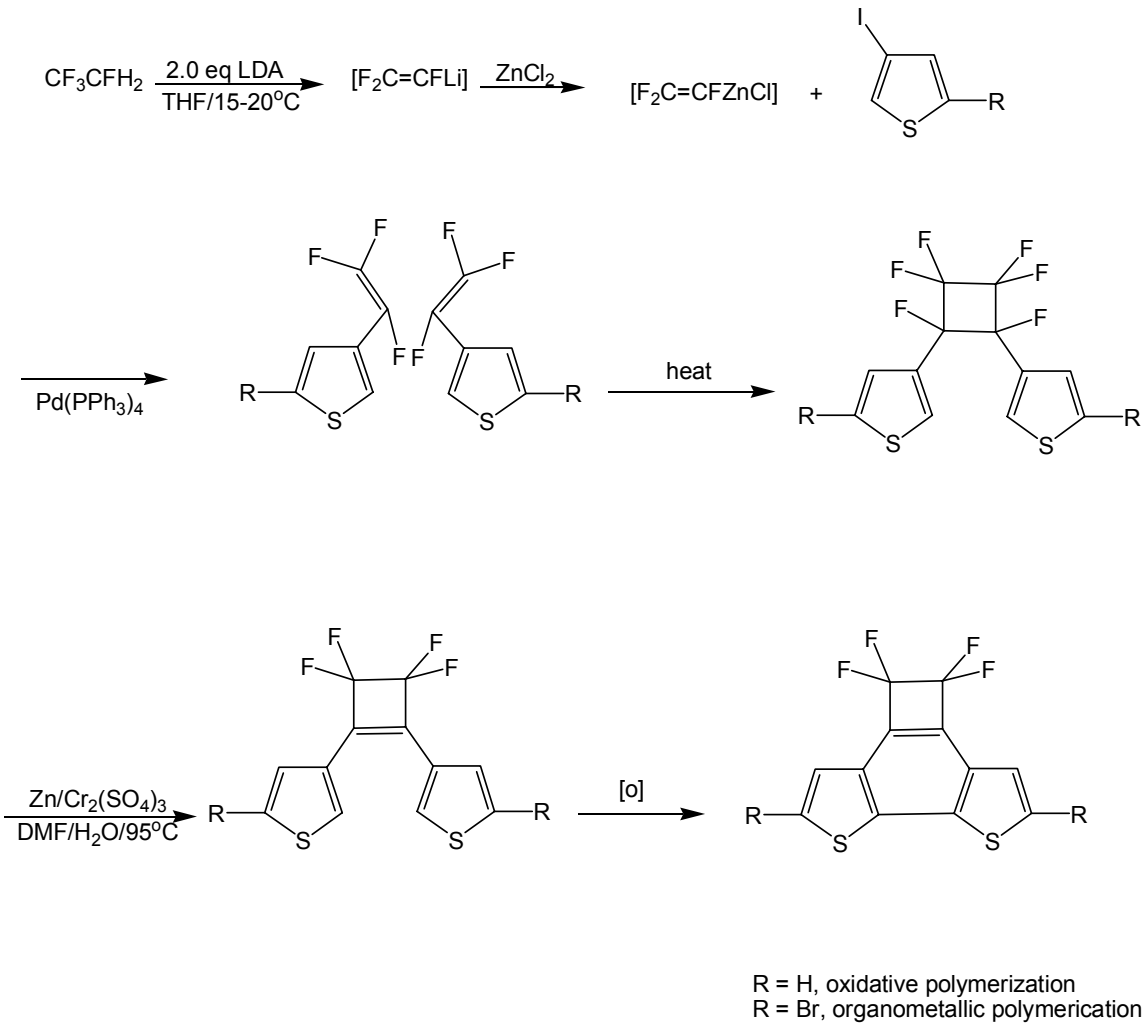

Figure 8.3. Synthesis of fused thiophenes with fluorinated cyclic structure.

Stacking oligothiophenes with pentaerythritol

Although various architectures have been used to stack conjugated oligomers and to achieve a 2-D conducting structure, the synthesis of these stacking structures are quite complicated. A simple and efficient way to prepare the stacked conjugated oligomers is required to make materials for devices application. Recently, a simple way to control π-π stacking of aromatic rings through pentaerythritol was reported.[13] Different from other pentaerythritol derivatives, the four aromatic rings linked by a pentaerythritol core pack in a quasi-parallel fashion, rather than a planar or tetrahedral conformation. This quasi-parallel conformation facilitates the π-π interaction between rings with a distance of 3.6 to 3.9Å This structural model could be applied to stack oligothiophenes. For example, the bithiophenes can be linked to pentaerythritol through 2-positions. The stacked oligomers can be further polymerized to give a 2D conjugated polymer with broken conjugation, Figure 8.4. The thiophenes also can be linked to pentaerythritol through 3-positions, which gives a 2D conjugated polymer, Figure 8.5.

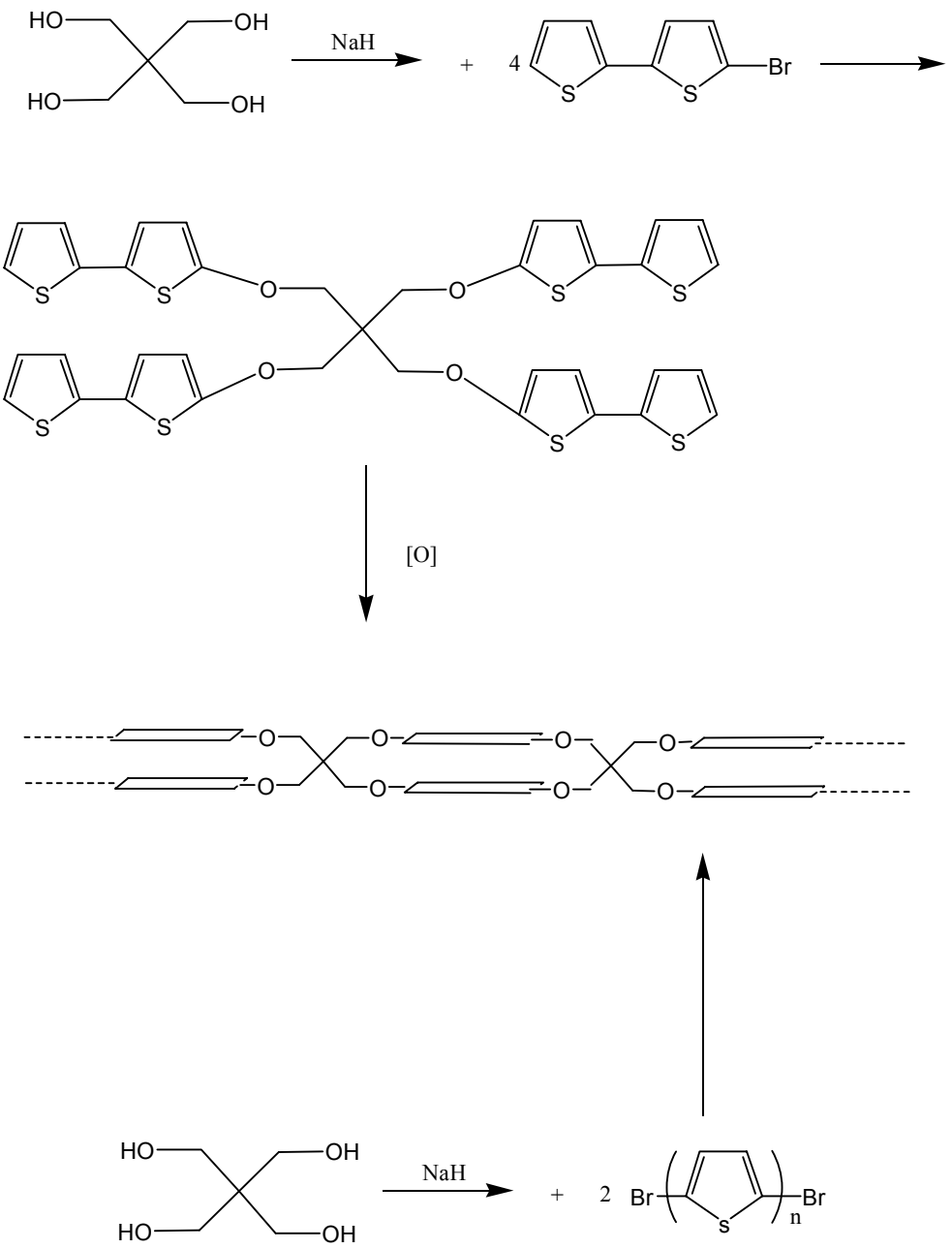

Figure 8.4. Synthesis of stacked (parallel) thiophene oligomers with pentaerythritol.

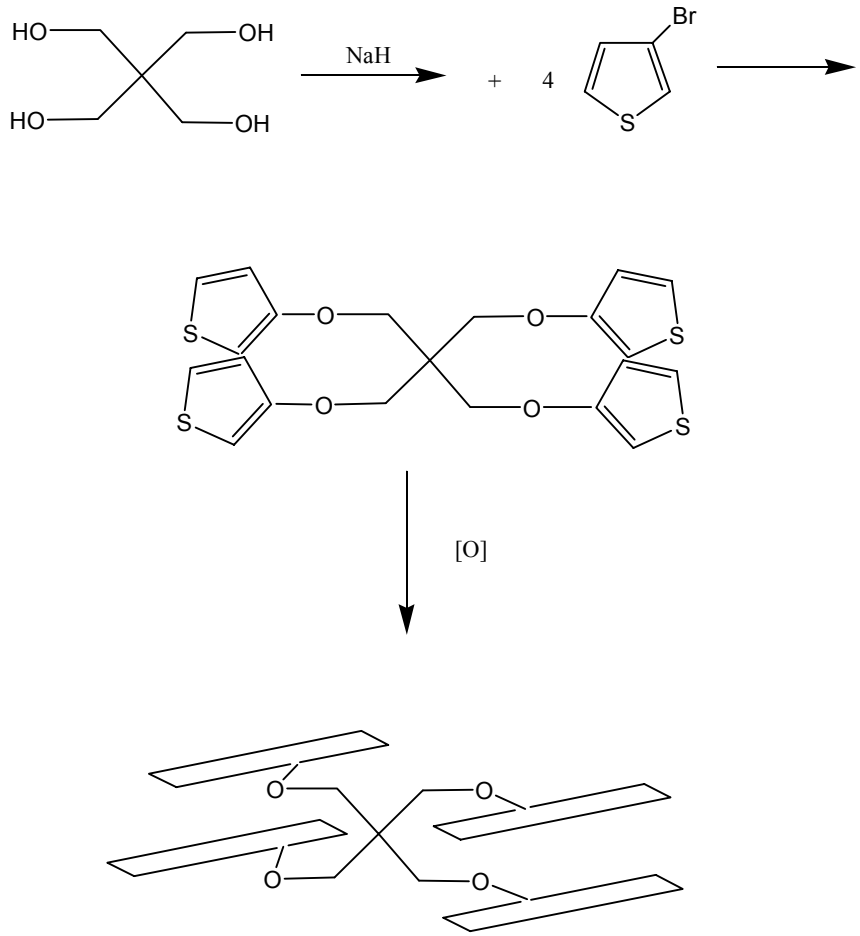

Figure 8.5. Synthesis of stacked (perpendicular) thiophene oligomers with pentaerythritol.

References

1. Büchner, W.; Garreau, R.; Lemaire, M.; Roncali, J.; Garnier, F. *J. Electroanal. Chem. Interfacial Electrochem.* **1990**, *277*, 355; Büchner, W.; Garreau, R.; Roncali, J.; Lemaire, M. *J. Fluorine Chem.* **1992**, *59*, 301; Robitaille, L.; Leclerc, M. *Macromolecules* **1994**, *27*, 1847; Leclerc, M.; Robitaille, L.; Bergeron, J.Y.; Callender, C.L. *Polym. Prepr.* **1994**, *35(1)*, 305.

2. Hong, H.; Tyson, J. C.; Middlecoff, J. S.; Collard, D. M. *Macromolecules* **1999**, *32*, 4232.

3. Hong, X. M.; Collard, D. M. *Macromolecules* **2000**, *33*, 3502.

4. Hong, X.; Tyson, J. C.; Collard, D. M. *Macromolecules* **2000**, *33*, 6916.

5. Gillet, J. P.; Sauvetre, R.; Normant, J. F. *Synthesis* **1986**, *7*, 538.

6. Prober, M. *J. Am. Chem. Soc.* **1953**, *76*, 968.

7. Dixon, S. J. *J. Org. Chem.* **1956**, *21*, 400.

8. Heinze, P. S.; Burton, D. J. *J. Org. Chem.* **1988**, *53*, 2714.

9. Anilkumar, R.; Burton, D. J. *Tetrahedron Lett.* **2002**, *43*, 2731.

10. Talavalaeva, T. V.; Petrii, O. P.; Timofeyuk, G. V.; Zimin, A. V.; Kocheshkov, K. A. *Dokl. Chem*. **1964**, *154*, 79.

11. Bartlett, P. D.; Cohen, G. M. *J. Am. Chem. Soc.* **1973**, *95*, 7923.

12. Tellier, F.; Sauvetre, R.; Normant, J. F.; Dromzee, Y.; Jeanin, Y. *J. Organomet. Chem.* **1987**, *331*, 281.

13. Caronna, T.; Liantonio, R.; Logothetis, T. A.; Metrangolo, P.; Pilati, T.; Resnati, G. *J. Am. Chem. Soc.* **2004**, *126*, 4500.

APPENDIX A

ATTEMPTS TO MAKE 3-(PERFLUOROALKYL)THIOPHENES WITH SHORTER CHAIN LENGTHS

3-Trifluoromethylthiophene was synthesized according to the literature in very low yields (~15%).[1] Further modification (high concentration, a more stable perfluoroalkylation reagent) to improve the yields gives a 8:2 mixture of 3-trifluoromethyl- and 3-pentafluoroethylthiophene at a reasonable yield. The formation of 3-pentafluoroethylthiophene requires pentafluoroethyl radical, which does not directly come from starting materials. The pentafluoroethyl radical is formed from the reaction of a difluoromethyl carbene (.CF_2.) with a trifluoromethyl anion (CF_3^-). This mixture is difficult to separate. 2,5-Dibromo-3-perfluorobutylthiophene was prepared and isolated at a very low yield (<10%) using a method modified from literatures,[2] Figure A.1.

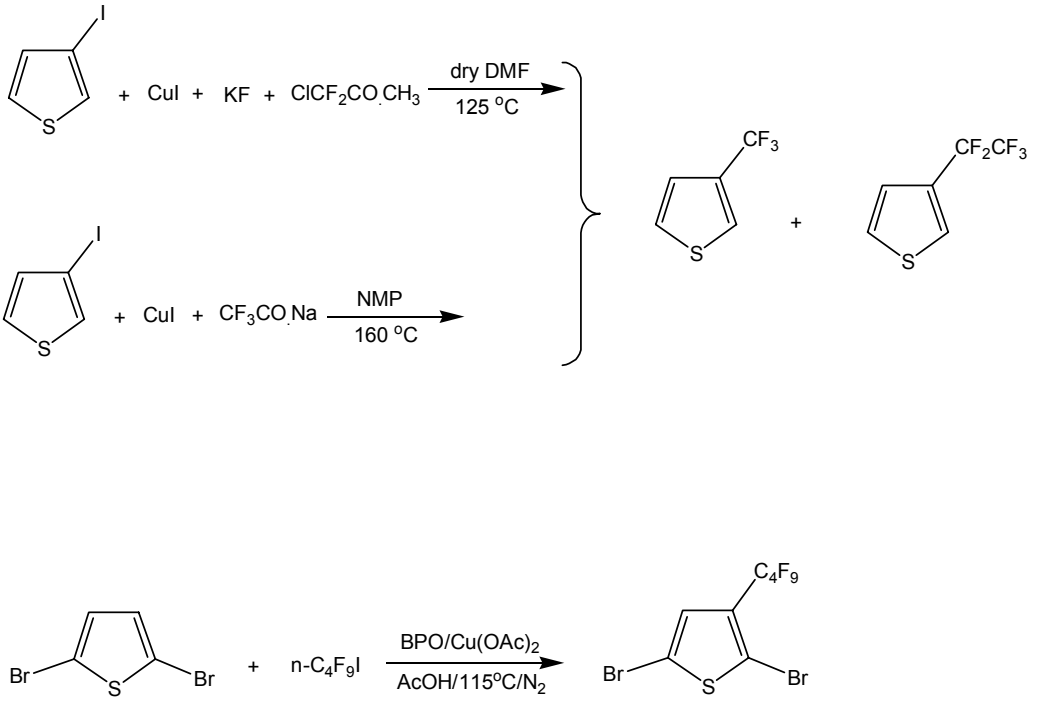

Figure A.1. Synthesis of 3-(perfluoroalkyl)thiophene with shorter chain length

References

1. Leroy, J.; Rubinstein, M.; Wakselman, C. *J. Fluorine Chem*. **1985**, *27*, 291.

2. Yoshida, M.; Yoshida, T.; Kamigata, N.; Kobayashi, M. *Bull. Chem. Soc. Jpn.* **1988**, *61*, 3549.

APPENDIX B

PREPARATION OF TETRA-N-BUTYLAMONIUM TETRA(PERFLUOROPHENYL)BORATE

$$Li[B(C_6F_5)_4].2Et_2O + n\text{-}Bu_4NBr \rightarrow n\text{-}Bu_4NB(C_6F_5)_4 + LiBr$$

A solution of n-Bu_4NBr (2.55 g, 7.91 mmol) in 5 mL MeOH was added dropwise in a solution of $Li[B(C_6F_5)_4].2Et_2O$ (5.00 g, 5.75 mmol) in 10 mL MeOH. The mixture was stirred for 1 h and H_2O (5 mL) was added dropwise to precipitate the product. The mixture was placed in a refrigerator overnight. The mixture was filtered and the solid was washed with ice-cold MeOH (5 mL). The solid was allowed to dry in air and then dissolved in excess dry CH_2Cl_2 (~ 15 mL). The CH_2Cl_2 solution was stirred with anhydrous $MgSO_4$ for 2 h, and then filtered. The solvent was removed under reduced pressure to give the crude product (5.62 g). The crude product was dissolved in 55 mL CH_2Cl_2 and Et_2O (30 mL) was added slowly in the solution. The solution was placed in a refrigerator overnight to allow crystals to grow. The crystals was filtered out, rinsed with hexane, and allowed to dry in air to give n-$Bu_4NB(C_6F_5)_4$ (4.41 g, 69%), as a white crystalline solid.

VITA

Ling Li was born in Yunnan Province, China in 1977 and then moved to Dujiangyan in Sichuan Province, China and was grown up there. With major in Chemistry, he received Bachelor Degree of Science from Peking University in Beijing in 1999, with a Bachelor thesis on the synthesis of mesogen-jacketed liquid crystalline polymer. In the fall of 1999, he started to study in the Ph.D. program of School of Chemistry and Biochemistry in Georgia Institute of Technology. His researches focus on the synthesis and characterization of the novel conducting polymeric materials, including fluoroalkylated polythiophenes and stacked oligothiophenes as models for interchain charge transfer in conducting polymers. He received his Degree of Philosophy in the summer of 2004.